Testing Methodology for Resilient Modulus of Base Materials

by

Soheil Nazarian, Ph.D., P.E.

Rafael Pezo, Ph.D.

and

Miguel Picornell, Ph.D.

Research Project 0-1336

APPLICATION OF RESILIENT MODULUS TESTS
TO TEXAS BASE MATERIALS

Conducted for

Texas Department of Transportation
in cooperation with
Federal Highway Administration

The Center for Geotechnical and Highway Materials Research
The University of Texas at El Paso
El Paso, TX 79968-0516

Research Report 1336-1
July 1996

TECHNICAL REPORT STANDARD TITLE PAGE

1. Report No.	2. Government Accession No.	3. Recipient's Catalog No.
TX-94 1336-1		

4. Title and Subtitle	5. Report Date
Testing Methodology for Resilient Modulus of Base Materials	July 1996
	6. Performing Organization Code

7. Author(s)	8. Performing Organization Report No.
Nazarian, S., Pezo R., and Picornell P.	Research Report 1336-1

9. Performing Organization Name and Address	10. Work Unit No.
Center for Geotechnical and Highway Materials Research. The University of Texas at El Paso El Paso, Texas 79968-0516	11. Contract or Grant No. Study No. 0-1336

12. Sponsoring Agency Name and Address	13. Type of Report and Period Covered
Texas Department of Transportation P.O. Box 5051 Austin, Texas 78763	Report Sept. 1, 1992-Aug 31, 1995
	14. Sponsoring Agency Code

15. Supplementary Notes

Research Performed in Cooperation with TxDOT and FHWA
Research Study Title: APPLICATION OF RESILIENT MODULUS TESTS TO TEXAS BASE MATERIALS

16. Abstract

The main objective of this report is to describe a proposed resilient modulus testing procedure which has been developed for the Texas Department of Transportation. This procedure contains the main characteristics of the AASHTO T294-92 procedure with several exceptions. The loading sequence is modified to avoid subjecting the specimens to high deviatoric stresses at low confining pressures. The conditioning cycles are eliminated and replaced by grouting the specimen to the platens to minimize disturbance to the specimen during stage testing. The effects of end restraint on the measured deformations are minimized by using a gage length equal to the middle one-third of the specimen. To avoid well-known problems with mounting LVDT's on the specimen, non-contact probes are utilized to measure the deformations. To maximize the amount of information gained from testing, the lateral deformations are measured with non-contact probes to determine the Poisson's ratio.

Based on tests on synthetic and base materials from different parts of Texas, the methodology proposed here seems to yield more accurate and repeatable results. In addition, compared to the AASHTO protocol, the preparation and setup of the specimen are more convenient and less time-consuming.

17. Key Words	18. Distribution Statement
Pavement Design, Modulus, Laboratory Testing, Flexible Pavements, Resilient Modulus	No restrictions. This document is available to the public through the National Technical Information Service, 5285 Port Royal Road, Springfield, Virginia 22161

19. Security Classif. (of this report)	20. Security Classif. (of this page)	21. No. of Pages	22. Price
Unclassified	Unclassified	86	

Form DOT F 1700.7 (8-69)

The contents of this report reflect the view of the authors, who are responsible for the facts and the accuracy of the data presented herein. The contents do not necessarily reflect the official views or policies of the Texas Department of Transportation or the Federal Highway Administration. This report does not constitute a standard, specification, or regulation.

NOT INTENDED FOR CONSTRUCTION, BIDDING, OR PERMIT PURPOSES

Soheil Nazarian, Ph.D., P.E. (69263)
Rafael Pezo, Ph.D.
Miguel Picornell, Ph.D.

Acknowledgements

The authors would like to give their sincere appreciation to Mr. Harold Albers of the TxDOT Materials and Test Division for his ever-present support. Thanks are also due to the laboratory personnel of the 23 districts that provided their assistance by promptly completing the survey and providing materials for laboratory tests.

The research assistants on this project were Sriram Melarkode, Kelvin Kroeker and Jaime Rojas.

The analytical work presented in Chapter 4, was conducted by Mr. Juaquin Urbina at no cost to the project. The financial funds for this portion of the project was provided by the National Science Foundation under the program entitled "Research Career for Minority Scholars."

Abstract

Resilient moduli of base and subgrade materials are important parameters in the new pavement design method adopted by AASHTO and many state agencies. Several testing protocols for determining the resilient modulus of subgrade soils have been evaluated and proposed. Unfortunately, less effort has been focused on developing protocols for base materials.

The main objective of this report is to describe a proposed resilient modulus testing procedure which has been developed for the Texas Department of Transportation. This procedure contains the main characteristics of the AASHTO T294-92 procedure with several exceptions. The loading sequence is modified to avoid subjecting the specimens to high deviatoric stresses at low confining pressures. The conditioning cycles are eliminated and replaced by grouting the specimen to the platens to minimize disturbance to the specimen during stage testing. The effects of end restraint on the measured deformations are minimized by using a gage length equal to the middle one-third of the specimen. To avoid well-known problems with mounting LVDT's on the specimen, non-contact probes are utilized to measure the deformations. To maximize the amount of information gained from testing, the lateral deformations are measured with non-contact probes to determine the Poisson's ratio.

Based on tests on nine synthetic specimens and nine different base materials from different parts of Texas, the methodology proposed here seems to yield more accurate and repeatable results. In addition, compared to the AASHTO protocol, the preparation and setup of the specimen are more convenient and less time-consuming.

Executive Summary

Conducting resilient modulus tests on base materials has become more common in recent years. As a result, AASHTO has adopted three new methodologies for resilient modulus testing of granular materials in the last few years. The newest procedure (AASHTO T294-92), which basically reflects the procedure suggested by SHRP, is significantly more convenient to perform when compared to the initial procedure adopted by AASHTO (e.g. AASHTO T274). However, some aspects of the testing methodology are still being investigated and modified.

The main objectives of the study reported herein are: 1) to critically assess the strengths and weaknesses of the AASHTO procedure as related to base materials, and 2) to develop a procedure which would avoid the possible weaknesses of that protocol.

In general, the AASHTO protocol was found to be reasonable. However, several modifications were suggested. These modifications are related to: 1) the loading sequence, 2) specimen conditioning, 3) the measurement of the axial deformation, and 4) the determination of Poisson's ratio.

The proposed modifications and theoretical or practical justifications for them are reported in detail. In addition, the results from laboratory tests performed using synthetic specimens and base materials collected from different districts in Texas are summarized. The modified methodology provides more accurate and repeatable measurement of the resilient modulus.

Implementation Statement

All the required equipment has been purchased or manufactured at UTEP and transferred to TxDOT. The testing methodology has been drafted and tested on numerous synthetic and actual base specimens. In our opinion, this test methodology should be immediately implemented on trial basis, so that the possible logistical and practical problems with the protocol can be addressed.

Table of Contents

List of Tables

List of Figures

Chapter 1

Introduction

Problem Statement

The successful design of new pavements and prediction of the remaining life of the existing roads depend on proper characterization of pavement materials. The new design methods (e.g., the 1986 AASHTO Pavement design guide) require the use of resilient modulus tests for determining stiffness parameters, and constitutive behavior of pavement components, such as subgrade, subbase and base.

The characterization of subgrade materials with resilient modulus tests was the subject of a project carried out at the Center for Transportation Research (CTR) and The University of Texas at El Paso (UTEP). As a part of that project, CTR developed guidelines for testing primarily cohesive soils (Pezo et al., 1992) and UTEP developed a procedure to test predominantly granular materials (Feliberti et al., 1992). Based on an extensive testing program, these procedures were found to be repeatable and easy to perform. However, these procedures had to be expanded, so that base materials can be more conveniently characterized. The available AASHTO standard procedures (AASHTO T-274 and its later modifications T-292 and T-294) are rather sketchy.

This projects major goals as follows: 1) to develop a reliable methodology for resilient modulus testing of base materials, 2) to outline a procedure for combining field and laboratory results in the design, and finally, 3) to install a new M_R testing system in the laboratories of Materials and Test Division of TxDoT, in Austin, Texas. The first item is discussed in this report. The second item will be the subject of the next report. The third goal has been achieved, but does not require a report.

Objectives

The first purpose of this study was to develop a reliable methodology for resilient modulus testing of base materials. In order to achieve this purpose, the following steps were taken:

1. performed an information search with regards to the behavior of granular materials under dynamic loading and the state of the art in resilient modulus testing;

2. improved existing resilient modulus testing protocol, so that base materials could be tested more reliably and easily;

3. evaluated the system, so that its reliability in testing base materials could be determined;

4. compared the results from resilient modulus tests with other laboratory and analytical methods to validate the procedures and recommended guidelines;

5. evaluated the effects of moisture content and density on the resilient modulus of base materials; and

6. developed empirical relationships expressing resilient modulus, as a function of confining pressure, deviatoric stress, axial strain and bulk stress, so that they could be used in the routine design of pavements.

Organization

As an introduction Chapter 2 contains a review of various literatures. Chapter 3 describes the methodology adopted for the testing of base materials. In Chapter 4, the results from finite element analyses on models representing base materials are compared with experimental results to validate the testing system. The calibration and evaluation of the testing system with synthetic specimens are contained in Chapter 5. The selection process for obtaining base materials from various locations in Texas is described in Chapter 6. The M_R test results and constitutive models representing different materials are introduced in Chapter 7. Chapter 8 contains a discussion of the results. Chapter 9, which concludes this report, contains the summary, and conclusion of this research effort.

Chapter 2

Review of Literature

In this chapter, a brief review of the fundamentals of the resilient modulus testing and the state-of-practice in performing these tests are incorporated. The results from a comprehensive literature search related to this topic can be found in two other TxDoT reports, Pezo et al. (1992) and Feliberti et al. (1992). For the sake of brevity, that information is not reflected here.

Introduction

The resilient modulus of subgrade and base materials are typically determined in a repeated load triaxial test. The test is performed by placing a specimen in a cell and applying repeated axial load. After subjecting the specimen to all around confining pressure, measurements are taken of the recoverable axial deformation and the applied load. The resilient modulus is calculated from

$$M_R = \sigma_d / \epsilon_a \tag{2.1}$$

Parameter σ_d, the axial deviatoric stress, is

$$\sigma_d = P / A_i \tag{2.2}$$

where P is the applied load and A_i is the original cross-sectional area of the specimen. Parameter ϵ_a, the resilient axial strain, is calculated from

$$\epsilon_a = \Delta L / L_i \tag{2.3}$$

where ΔL is recoverable axial deformation along a gage length, L_i. The Poisson's ratio ν is calculated from

$$\nu = \epsilon_l / \epsilon_a \tag{2.4}$$

Parameter ϵ_l, the lateral strain is calculated from

$$\epsilon_l = \Delta d / d_i \tag{2.5}$$

where Δd is the recoverable lateral deformation measured at the specimen's mid-height and d_i is the original diameter of the specimen.

As described by Baladi (1989), the total deformation of any pavement material subjected to cyclic load can be the sum of three independent deformations as illustrated in Figure 2.1. They are as follows:

1. Time-independent elastic deformation recoverable upon the removal of the load, ED,

2. Time-dependent visco-elastic deformation recoverable after the removal of the load, VD, and

3. Plastic deformation due to the load-unload cycle, irrecoverable and is dependent on load intensity and rate, loading period, PD.

The deformation ED is a measure of the instantaneous resilient modulus; deformation VD is a measure of visco-elastic properties/modulus, and deformation PD is a measure of creep and fatigue characteristics of the material.

Parameters Affecting Resilient Modulus

A large number of parameters affect the resilient response of a base material under repeated loading. The most important factor is perhaps the type of material (fine-grained vs granular). Reviewed in this section are the most significant and pertinent factors, which include the following: loading condition, compaction, soil index properties, soil gradation, and soil moisture suction.

Loading Condition

The most significant factor that affects the resilient modulus of soils is the state of stress. The resilient behavior of fine-grained soils is more dependent on the deviatoric stress than on the confining pressure. Thompson (1989) indicated that field resilient modulus was typically associated with a repeated deviator stress of 42 KPa, and that unconfined compression tests would yield relatively accurate estimate of the resilient modulus.

In the case of coarse-grained or granular materials, confining pressure has greater effect on the resilient response than deviatoric stress (Seim, 1989). The resilient modulus of a granular material increases with an increase in confining pressure (Hicks and Monismith, 1981; and Thompson, 1989).

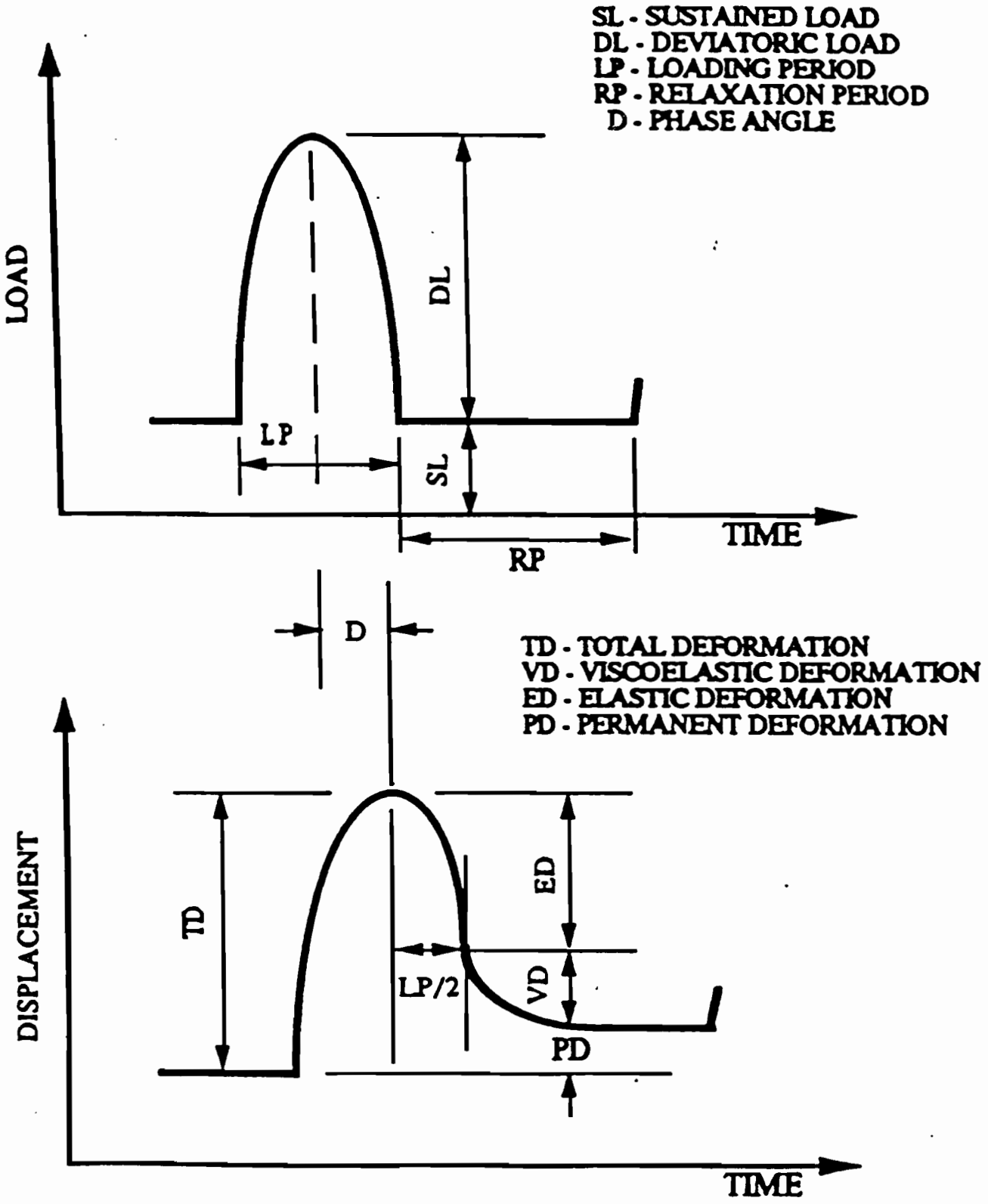

Figure 2.1 - Schematic of Load and Displacement Time Histories from a Resilient Modulus Test

Compaction

The resilient response of a material is affected by the degree of compaction, degree of saturation, moisture content, and method of compaction.

Thompson (1989) stated that for a given degree of saturation, soils compacted to the maximum dry density yield higher resilient moduli. Thompson and Lagrow (1988) proposed "moisture adjustment" factors to adjust resilient modulus values for moisture contents in excess of the optimum.

Resilient moduli obtained are higher on the dry side of optimum than on the wet side. (Seed et al., 1962; Tanimoto and Nishi, 1970; Thompson and Robnett, 1979).

If allowed to rest before testing, the specimens compacted at higher degree of saturation exhibit a significant increase in strength due to thixotropic effects (Mitchell, 1960; Seed et al., 1962). The effect of thixotropy is significant on specimens compacted on the wet side, as compared to the dry side of the optimum (Tanimito and Nishi, 1970). As such, the degree of saturation plays a major role in the resilient response of granular materials subjected to repeated loading.

The other primary compaction factor, which influences the resilient response, is the method of compaction employed. It is purported that specimens prepared under static compaction yield higher resilient modulus than those prepared under kneading compaction (Seed et al., 1962 and 1967; Elliot and Thornton, 1988). Also, the moduli measured on specimens prepared with the static compaction are less repeatable, as compared to specimens prepared using kneading compaction (Seim, 1989). If the Proctor method is used, the resilient moduli lie between the moduli obtained from specimens prepared with the static and kneading compaction methods (Seim, 1989).

Soil Index Properties

The soil properties, which have an effect on the resilient response of soils, are liquid limit, plasticity index, group index, silt content, specific gravity, and organic content (Thompson, 1989). Thompson (1989) also states that the properties that tend to contribute to low resilient moduli are low plasticity, low group index, high silt content, low clay content, low specific gravity, and high organic contents. Thompson and Robnett (1979) and Thompson and Lagrow (1988) have proposed resilient modulus based on soil index properties stated above.

Soil Gradation

Hicks and Monismith (1981) stated that the resilient modulus of a partially crushed aggregate decreased with an increase in fine content, while the modulus increased for the crushed aggregate with increasing fines content. Thompson (1989) stated that for a given gradation, crushed materials provide an increase in resilient moduli.

Freeze-Thaw and Soil Moisture Suction

The resilient behavior of fine-grained soils is greatly affected by freeze-thaw action. A substantial increase in resilient deformation will occur, due to a small number of freeze-thaw cycles, even without a change in moisture content (Bergan and Fredlund, 1973; Culley, 1970; Chamberlain, 1973; Bergan and Monismith, 1973; Bergan and Culley, 1973; Robnett and Thompson, 1976).

Resilient modulus is a function of confining pressure, deviatoric stress, and matrix suction (Fredlund et al., 1975 and 1977). A linear relationship exists between resilient modulus and soil moisture suction (Dehlen, 1969; and Finn et al., 1972).

Resilient Modulus Tests

In 1986, AASHTO incorporated the resilient modulus of base and subgrade in pavement design in place of soil support values. The AASHTO Guide prescribed a standard method of testing for resilient modulus of subgrade Soils (AASHTO T274-82). In 1989, a workshop on the state of practice on resilient modulus testing took place at the Oregon State University. The main purpose of this workshop was to evaluate the resilient modulus testing procedures, where numerous authors described their experiences. The various findings are as follows.

Thompson (1989) stated that the state highway agencies were experiencing considerable difficulty in establishing the appropriate resilient modulus inputs into the AASHTO design procedure of 1986.

Huddleston and Zhou (1989) concluded that by using the AASHTO T-274, results found the greatest amount of variability was with the granular base material.

Ho (1989) concluded that stress conditioning done in AASHTO T-274 could be too severe for Florida subgrade soils. In addition, testing at low deviatoric stresses (7 KPa and 14 KPa) might yield unrealistically high resilient modulus values.

Jackson (1989) criticized the preparation procedure and test sequence adopted in AASHTO T-274 as difficult.

Dhamrait (1989) stated that the Illinois DOT had developed their own testing procedure. It differed from the AASHTO T-274 in that the specimen conditioning and testing sequences were performed without confining pressure and with a lower number of stress applications.

Cochran (1989) documented the experience of Minnesota DOT with the resilient modulus test. He stated that the results from laboratory and field tests did not compare favorably.

These problems with the AASHTO T-274 have brought about many improvements in the testing setup and procedure by various agencies and researchers. For the TxDoT, improvements to the resilient modulus testing method for primarily non-granular materials have been recommended by Pezo et al. (1992). The main conclusions were that a diligent effort is required in the installation and use of a resilient modulus testing system. A strong contact between the specimen and each end cap is very important for repeatable modulus estimates. Pezo et al. also described an improved testing configuration which has been implemented in the TxDoT laboratory.

Feliberti et al. (1992) at UTEP found that the procedure proposed by Pezo et al. is appropriate for cohesive materials, but not applicable to granular materials. Feliberti et al. recommended a new procedure for conducting resilient modulus tests on granular materials.

Constitutive Models

Two constitutive models are traditionally used for describing the results of resilient modulus tests. Both these models are adopted by both AASHTO and SHRP. For coarse-grained materials, the most-widely used relationship is:

$$M_R = k_1 \theta^{k2} \tag{2.6}$$

where k_1 and k_2 are material constants, and θ is the bulk stress (first stress invariant).

For cohesive materials, the constitutive model most commonly used is:

$$M_R = k_1 \sigma_d^{k2} \tag{2.7}$$

where σ_d is the deviatoric stress.

Both Pezo et al. and Feliberti et al. have recommended improved constitutive models to describe the test results, which were somewhat similar. Pezo et al. indicated that M_R tests are performed to measure resilient axial strains, ϵ_a, induced under different levels of deviatoric stress, σ_d, and confining pressure, σ_c, and that the resilient moduli are simply calculated values. The resilient axial strain is the parameter that should be considered as the dependent variable, and not the resilient modulus, thus, they proposed first developing the following regression model:

$$\epsilon_a = 10^a \sigma_d^b \sigma_c^c \tag{2.8}$$

where a, b and c are material constants. Based on Equation 2.8, they derived two models:

$$M_R = k_1 \sigma_d^{k2} \sigma_c^{k3} \tag{2.9}$$

and

$$M_R = k_1 \epsilon_a^{k2} \sigma_c^{k3} \quad (2.10)$$

Once again, parameters k_1 through k_3 are statistically-determined coefficients.

Feliberti et al. (1992) indicated that the two parameters, state of stress and strain level, significantly contribute to the stiffness (modulus). As such, the two traditional models are not complete. The model proposed for granular materials, considers directly the effects of the state of stress (bulk stress), but ignores the effects of strain amplitude. On the other hand, the model proposed for the cohesive soils, considers directly the effects of strain level (deviatoric stress), but virtually ignores the effect of the state of stress. Feliberti et al. studied two models of the form:

$$M_R = k_1 \theta^{k2} \epsilon_a^{k3} \quad (2.11)$$

and

$$M_R = k_1 \sigma_c^{k2} \epsilon_a^{k3} \quad (2.12)$$

In both models, the strain level is considered a direct parameter. However, in the first model (Equation 2.11), bulk stress represents the state of stress, and in the second model (Equation 2.12), the effects of the state of stress are included through the confining pressure.

Although, these models look similar in format, each one has its unique characteristics. Pezo et al. indicated that Equations 2.9 and 2.10 are the constitutive models to use when describing the non-linear behavior of either cohesive and cohesionless materials. Whereas, Feliberti et al. indicated that Equation 2.11 best described the behavior of granular materials, while Equation 2.12 best described the behavior of cohesive materials.

State-of-Practice

In the last four years, AASHTO proposed two different procedures T292-91 and T294-92 for resilient modulus of soils. A separate testing procedure for base materials has been proposed in AASHTO T294-92.

The testing procedure for the resilient modulus of base materials as prescribed in AASHTO T294-92 consists of preparing 150 mm x 300 mm specimens in a split mold with a vibratory compactor with the vibration time to be decided "based on experience". A rubber membrane is placed either before or after compaction. To place the membrane, vacuum is applied, so that the membrane fits inside the mold, and the soil is then compacted.

Before testing, the specimen is conditioned under a confining pressure of 105 KPa by applying 1000 repetitions of an axial deviator stress of 105 KPa. A haver-sine load pulse consisting of a 0.1 second load followed by a 0.9 second rest period is used.

The test protocol follows the sequence shown in Table 2.1, using the same type of loading waveform as in the case of specimen conditioning. The load applied to the specimen is monitored by an external load cell placed above the top of the triaxial chamber. The resilient axial deformation is measured externally with two spring loaded LVDT's placed outside the triaxial chamber immediately below the load cell. The problems with the new AASHTO procedure and proposed remedies are discussed in the next chapter.

It should be mentioned that a national study funded by the FHWA is under way at The Georgia Institute of Technology and its subcontractors (NCHRP Project 1-28). However, the results from that study were not available during the conduction of this research.

Table 2.1 - Testing Sequence for Type 2 Soils Proposed by AASHTO

Sequence No.	Confining Pressure (KPa)	Deviator Stress (KPa)	Number of Load Applications
0	42	28	1000
1	42	14	100
2	42	28	100
3	42	42	100
4	42	56	100
5	42	70	100
6	42	14	100
7	21	28	100
8	21	42	100
9	21	56	100
10	21	70	100
11	0	14	100
12	0	28	100
13	0	42	100
14	0	56	100
15	0	70	100

Chapter 3

Testing Procedures

Introduction

This chapter describes the problems and limitations of the existing AASHTO T-292 procedure for the resilient modulus testing of base materials. Also, described is a new testing methodology which eliminates or minimizes some of the limitations in the existing procedure.

Problems with Existing Procedure

One of concerns with the AASHTO procedure is the sequence of loads applied to the specimen (see Table 2.1). Rada and Witczak (1981) suggested that the primary resilient response of granular materials are influenced by stress state.

Hicks and Monismith (1971) also suggested that the resilient moduli of untreated granular materials are primarily affected by the stress level. They have also stated that granular materials possess distinctly nonlinear stress-strain behavior, where the resilient modulus increases with confining pressure.

Chen et al. (1993) studied the variability of resilient modulus due to testing procedures. They stated that the stress sequence in the T294-92 procedure has stiffening and strengthening effects on the specimen, as the stress level increases from low to high.

Houston et al. (1993) indicated the importance of balancing the deviatoric stress and confining pressure in the loading sequence. They also indicated that some of the load sequences in the AASHTO procedure may subject the specimen to excessive stress levels.

Nazarian and Feliberti (1993) stated that the specimen disturbance, due to large deviatoric stresses applied at low confining pressures, might lead to excessive deformations of the specimens, especially when the specimen has a low modulus. They also observed that several specimens failed during the testing program before completing all of the loading steps. As the resilient modulus test is a stage test, the specimens should not fail during testing, nor significantly change its properties between different loading steps.

The AASHTO procedure suggests the application of 100 repetitions of deviatoric stress at every stage of testing. According to Ho (1989), this may result in the overestimation of the modulus. Pezo (1991) recommends a maximum of 25 loading repetitions at different stress states during testing.

In summary, all these studies point towards selecting the loading sequence with caution to maximize the quality of the results obtained from the laboratory testing.

One important factor to consider is the conditioning of specimens before testing. AASHTO procedure requires 1000 conditioning cycles to provide a uniform contact at the platens and to eliminate any additional movement at these points. Pezo et al. (1992) initiated the use of grouting of the test specimens to the end platens instead of the conditioning cycles.

According to Pezo et al. (1992) specimen conditioning is an unnecessary process for properly grouted specimens. In their opinion, specimen conditioning does not serve its purpose which is primarily to provide intimate contact between the specimen and end platens. Moreover specimen conditioning involves high confining pressures and deviatoric stresses which may affect the resilient modulus, because of the changes in stress history of soil prior to testing. Nazarian and Feliberti (1993) and Kim and Drabkin (1994) also supported this suggestion.

The grouting of the specimen to the top and bottom platens affects the axial deformation of a specimen during the resilient modulus tests, especially close to the top and the bottom of the specimen. Therefore, for accurately determining the resilient modulus, the axial deformations can no longer be measured using the full length of the specimen. The reason for this is that relatively large shear stresses are developed in the specimen in the vicinity of the grout.

The effects of grouting on the modulus of a specimen was quantified in a theoretical and experimental study described in Chapter 4. In that study, the axial and lateral deformations of a specimen grouted to the top and bottom platens were numerically determined using a finite element code. The numerical results were confirmed by extensive laboratory tests on synthetic specimens. The effects of grouting on the measured resilient moduli were determined, as a function of the location of sensors.

In the AASHTO procedure, the deformations are measured externally with two spring loaded LVDT's. Kim and Drabkin (1994) state that for materials with higher stiffness the external deformation measurements may result in an underestimation of the resilient moduli. Burczyk et al. (1993) confirm these findings. Pezo et al. (1991) adopted two LVDT's inside the triaxial

chamber for the measurement of axial deformations. Karasahin et al. (1993) have used LVDT's, as well as, hoops carrying strain gages for measuring axial and lateral deformations, respectively. These were fixed to studs compacted into the edge of the specimen at one-fourth and three-fourth height for the axial and radial strain measurements. Kamal et al. (1993) have also adopted a similar type of arrangement.

All these studies concur that measuring the deformation of a specimen should be done inside the cell and preferably on the specimen. However, practically speaking, one of the main reasons for not measuring the deformations on the specimens has been the extreme difficulties with proper placement of measurement devices (such as LVDT's) on the specimens.

Hicks and Monismith (1971) and many other investigators indicate that small changes in Poisson's ratio can result in significant changes in the response of pavement structure. As such, the measurement of Poisson's ratio is important. Measuring the lateral deformation, as well as, permanent deformation is quite desirable during the resilient modulus test of base specimens in the laboratory.

Based on this discussion several changes were incorporated and evaluated in the procedure defined below.

1. Grouting of the specimen was incorporated, and as such, the conditioning sequence was removed.

2. The loading sequence was altered to avoid high deviatoric stresses at low confining pressures.

3. Deformations were measured internally using non-contact probes.

4. To minimize the errors in measuring the deformation of the specimen (due to shear stresses developed because of grouting), the axial measurements were made at the middle 1/3 of the specimen.

5. To determine Poisson's ratio, lateral deformation was simultaneously measured in the mid-height of the specimen using non-contact probes.

Proposed Procedure

In this section, the proposed procedure for determining resilient modulus of base materials is described. As mentioned above, an attempt was made to account for the limitations in AASHTO procedure by making alterations and modifications in the specimen preparation, testing system, specimen conditioning, and testing sequence. A draft testing protocol is included in Appendix A.

Specimen Preparation

Proper specimen preparation is of utmost importance. Based upon our experience, if the membrane is placed before compaction there is a likelihood of tearing or dilating it during compaction by the bigger particles present in the base material. The compaction with the vibratory compactor is somewhat inconvenient. Obtaining uniform specimens with it is also of concern.
In the presently-proposed process (see Figure 3.1), the specimen is prepared in a cylindrical split mold. The dimensions of the mold are 150 mm x 300 mm with an extension of 30 mm at the bottom for placing the end platen. The provision for the bottom end platen is needed for the ease of grouting. A standard Proctor hammer, weighing 24.5 KN and having a fall of 25 mm, is used for compacting the base material. In order to maintain the standard compactive effort, the number of layers were increased to six. Seim (1989) states that if the Proctor compaction method is employed, the resilient moduli and its variability are reasonable and between those obtained from static and kneading compacted specimens.

The material required for preparing a specimen is homogenized at the desired moisture content by adding the required water, thoroughly mixing, and storing for one day. The bottom end platen is covered with grout and is placed in the mold. The material is compacted in six equal layers each of 50 mm thickness. Each layer is subjected to 25 blows with the hammer. After compacting, the excess material protruding out of the mold collar is removed with a blade. The top platen is then grouted to the specimen. The flatness of the top plate is checked and adjusted with a level. The mold is disassembled. A rubber membrane is placed around the specimen using a membrane expander and vacuum. The membrane is sealed to the top and bottom end platens with O-rings.

Testing System

Shown in Figure 3.2 is the resilient modulus testing system used at UTEP, which is similar to that delivered to TxDoT. It consists of a closed-loop hydraulic system capable of repeated dynamic loading up to a shortest duration of 10 milliseconds. The details of the system can be found in Feliberti et al. (1992).

A haver-sine loading waveform with a loading duration of 0.1 seconds and rest period of 0.9 seconds is used in accordance with the recommendations of AASHTO. The loading frame of this system carries a triaxial cell, in which the specimen is placed. As shown in Figure 3.3, the triaxial cell consists of a base plate, a top plate, an acrylic tube for holding confining pressure, and a piston which passes through a central hole in the top plate for the application of the load. A load cell with a capacity 25 KN is centered over the specimen outside the triaxial cell for monitoring the applied loads.

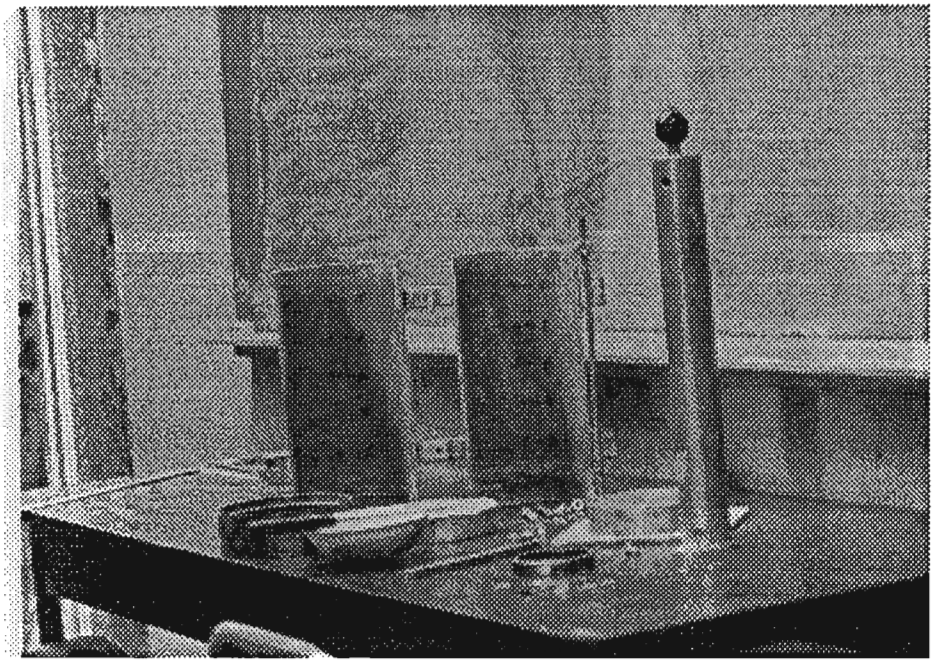

Figure 3.1 - Setup Used for Preparing Specimens

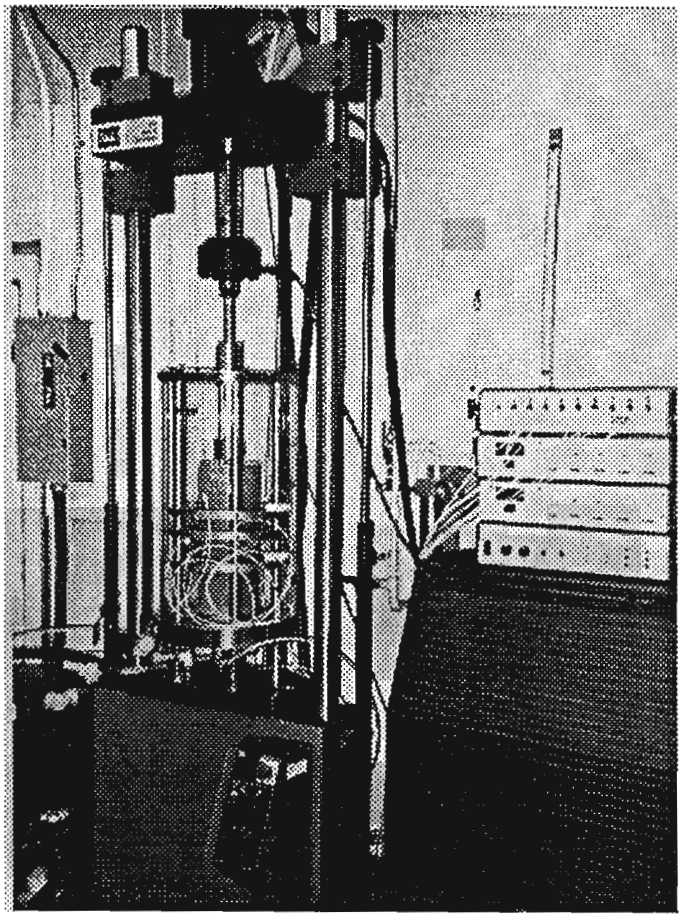

Figure 3.2 - Resilient Modulus Testing System

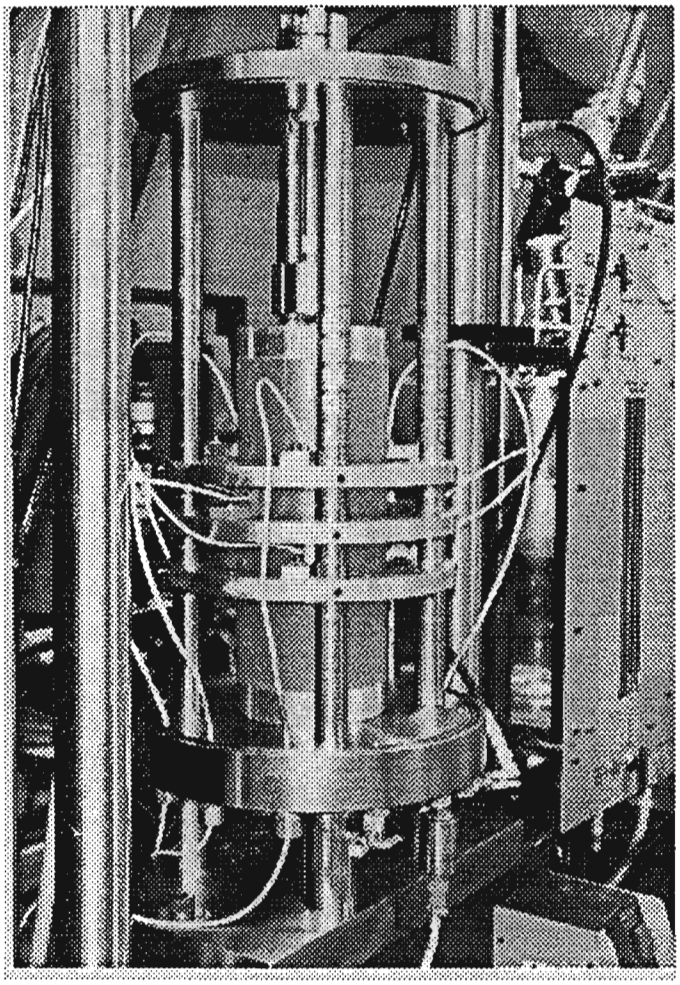

Figure 3.3 - Triaxial Cell Used in This Study

The confining pressure is either applied by subjecting the specimen to vacuum or by compressed air pressure inside the acrylic tube surrounding the specimen.

The specimen along with the various deformation sensors are shown in Figure 3.4. The axial deformations are measured along the middle one-third of the specimen with six voltage proximeters. Three proximeters are installed at about 100 mm from the bottom of the specimen and the other three about 100 mm from the top. At each level, the three proximeters are located at 120° intervals. The axial deformation is calculated as the average of the differences between the deformations measured at the two levels. In addition, the variation between the deformations measured at each 120° are carefully monitored to ensure that the specimen is uniformly deformed under the applied axial load. The lateral deformations are also measured with the proximeters, which are fixed at the mid-height of the specimen at 180° interval.

The proximeters can measure deformations up to 0.75 mm. Steel angles and flats, which serve as targets for the proximeters, are installed on the specimen to measure axial and lateral deformations, respectively. Small pieces of steel angels are placed inside the specimen during compaction. A strong magnet is then used to fix the target to the specimen over the membrane. An extensive study shows that this set-up has minimal effects on measuring the deformations.

The deformations along the full length of the specimen can also be measured by either installing the proximeters facing the top end platen of the specimen, or by mounting a LVDT above the triaxial cell.

The signals from the load cell, the six proximeters for axial deformation measurement, and the two proximeters for lateral deformation measurement, are acquired, saved, and displayed using a data acquisition system.

A typical output from one test is shown in Figure 3.5. The top two records correspond to the load cell and the LVDT. The third through fifth records (from the top) are the voltage outputs of the top proximeters. Similarly, the sixth through eighth records are the outputs from the bottom proximeters. Finally, the bottom two records corresponds to the lateral deformations measured with the bottom proximeters. The sampling rate used in the acquisition of data is 512 samples/second for each sensor, which ensures that the main features of the data are accurately captured and identified.

The saved data is automatically reduced using a program developed for this purpose which reports the deviatoric stress, axial strain, lateral strain, resilient modulus, and Poisson's ratio.

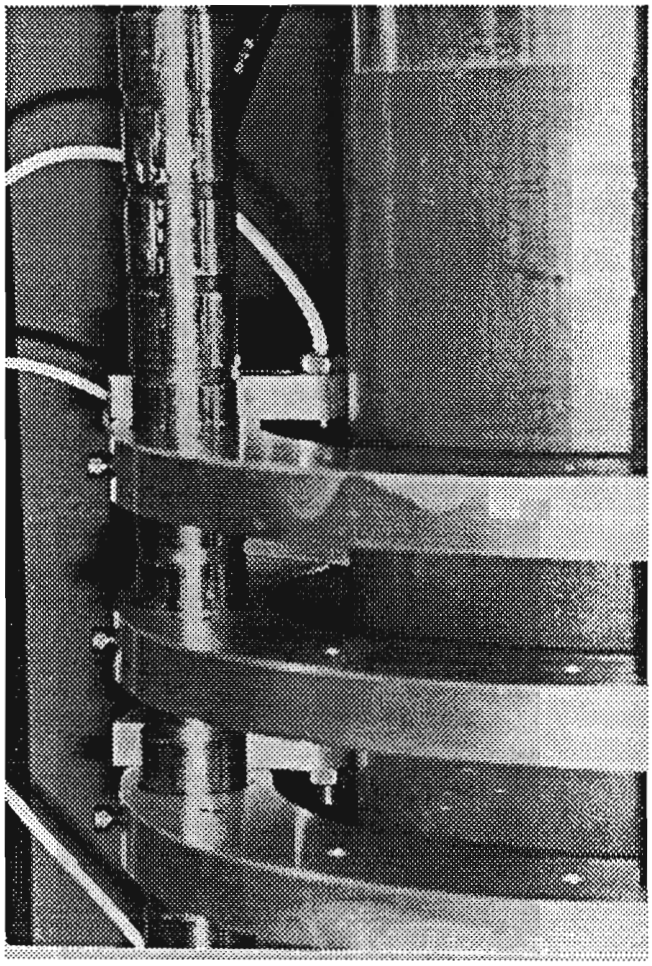

Figure 3.4 - Specimen and Associated Sensors Mounted in Place

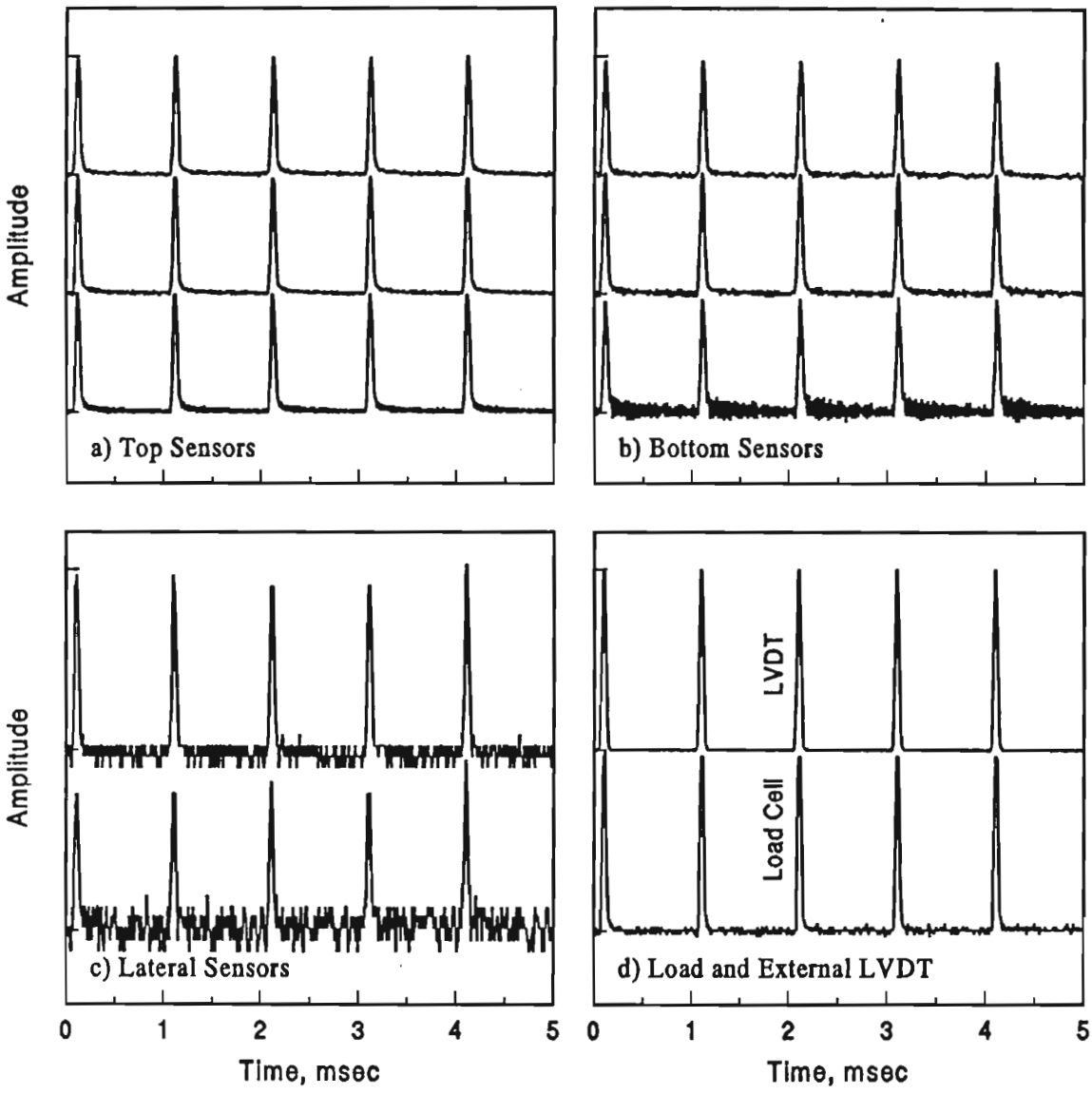

Figure 3.5 - Typical Displacement and Load Output from the Data Acquisition System

Testing Sequence

The resilient modulus tests consist of applying various deviatoric stresses at different confining pressures. At each level, the confining pressure is allowed to stabilize in the specimen for 10 minutes, before the application of the deviatoric stress.

Table 3.1 shows the loading sequence used to perform test. Comparisons were made between 25 and 5 stress repetitions for numerous specimens, the differences in resilient moduli were not significant (less than 3 percent). As such, five cycles of loading was adopted at every stage of testing to optimize testing time, and to minimize the degradation of the specimen.

From the measured axial and lateral displacements at a particular deviatoric stress and confining pressure, the resilient modulus and Poisson's ratio of the specimen can be determined using Equations 2.1 through 2.6.

Table 3.1 - Proposed Testing Sequence for Base Materials

Sequence No. no	Confining Pressure	Deviator Stress (KPa)	Number of Load Applications
1	35	35	5
2	35	70	5
3	35	105	5
4	70	35	5
5	70	70	5
6	70	105	5
7	70	140	5
8	105	35	5
9	105	70	5
10	105	105	5
11	105	140	5
12	105	210	5

Post Testing Steps

After the resilient modulus testing is complete, the specimen can be failed under static loading (if desired). The specimen is then removed from the equipment. The two ends contaminated with the hydrostone mix are removed. The specimen is then divided into three pieces. Each piece is weighed and placed in the oven for 24 hours, so that the water content can be measured.

Reduction of Data

Once the resilient modulus test is complete, the data is reduced. Typical output records from all sensors are shown in Figure 3.5. Since large amounts of data are collected for each test, a computer program was developed to automatically calculate the resilient modulus and Poisson's ratio.

The reduction program, called REDUCE.FOR, is a user-friendly program. It generates a comprehensive output file for each loading step. Each output file contains the name of the file, the loading sequence, resilient axial strain, lateral strain, resilient modulus, and Poisson's ratio for five consecutive cycles. As an example, the output file obtained from the data shown in Figure 3.5 is shown in Figure 3.6. This file can be utilized for a thorough examination of the results.

A summary file containing the average values, as well as, the coefficients of variation for a particular loading sequence is also generated. The file, as shown in Figure 3.7, contains the resilient axial strain, the resilient lateral strain, the applied deviatoric stress and confining pressure, the average resilient modulus, and the average Poisson's ratio. This file can be easily used to develop a constitutive model.

Figure 3.6 - Typical Summary File Generated for One Specimen

File Name	Stress	Cv	Lateral Strain	Cv	Axial Strain	Cv	Modulus	Cv	Poission's Ratio	Cv
c31f50.d	44.47	0.1	.265E-03	0.9	0.573E-03	0.6	77638	0.6	0.46	1.0
c31f40.d	35.52	0.1	.208E-03	0.7	0.455E-03	1.0	78009	1.0	0.46	0.6
c3if30.d	26.65	0.1	.156E-03	1.5	0.345E-03	0.8	77254	0.8	0.45	1.4
c3if20.d	17.73	0.1	.103E-03	2.7	0.234E-03	1.2	75617	1.1	0.44	2.9
c31f15.d	13.27	0.1	.769E-04	2.1	0.178E-03	0.8	74728	0.8	0.43	2.9
c31f10.d	08.71	0.4	.510E-04	3.2	0.121E-03	1.6	72147	1.7	0.42	4.2
c3if5.d	04.31	0.9	.255E-04	4.6	0.727E-04	3.9	59291	3.9	0.35	2.7
c31f2.d	01.69	1.2	.163E-04	7.6	0.303E-04	10.7	56493	10.5	0.54	13.0

Chapter 4

Numerical Investigation of Test Set-up

Introduction

As indicated in the previous chapter, uneven surface contacts, pores, or gaps between the specimen and end platens are not desirable in the resilient modulus testing. Small movements or unevenness at the ends of stiff materials can lead to uneven transmission of the applied loads; hence, mis-estimation of the moduli. This problem can be avoided by carefully grouting the specimen to the end platens (Pezo, 1991).

This chapter contains the results of a numerical investigation performed to assess the effects of grouting on the determination of the stiffness properties. The modulus and Poisson's ratio of cylindrical specimens with a variety of length-to-diameter ratios (L/D) were numerically determined, and compared to the original (input) values.

Another objective of this investigation was to determine the appropriate locations for accurately measuring the axial deformations of a specimen in the resilient modulus tests. The anticipated error are also quantified, when other configurations are uses. There are several implication of this exercise; for example, TxDOT can readily prepare specimens which are 150 mm in diameter and 200 mm in length. Such dimensions yield a L/D of 1.33, that is much more different than the ratio commonly used in triaxial tests (L/D = 2). The errors associated with this size specimens can be estimated.

Approach

To simulate the above experimental conditions, a finite element analysis (FEA) program, ALGOR, was used. To simulate the effect of grouting, the top nodes of the specimen were restrained to motion in the radial directions and the bottom nodes were restrained from motion in radial and vertical directions.

The appropriate finite element mesh was obtained by varying the mesh size from coarse (25 mm) to fine (1.25 mm) and checking the convergence and accuracy of results. The final model used throughout this study had square axisymmetrical elements, approximately 1.25 mm in dimensions.

A uniform axial stress of 70 KPa was placed along the top nodes, to simulate the triaxial test performed in the laboratory. A nominal modulus of elasticity of 75 MPa and Poisson's ratio of 0.49 were assigned to the specimen. These values were used because of their resemblance to the properties of one of the synthetic specimens used in the experimental validations. The specimen's diameter was maintained at 150 mm. The length-to-diameter ratio (L/D) varied between 1.3 and 5.

The vertical displacements were recorded to evaluate the different gage lengths that could be used to test actual specimens. Gage length is defined as the centered distance within the specimen mid-length where its axial deformations are measured during testing. The following nominal gage lengths were considered: L, L/2, L/3, L/4 and L/5. Using the numerical outputs of each case, the modulus and Poisson's ratio were calculated in the same fashion they are calculated in the laboratory (see Equations 2.1 through 2.5). The use of only one load level, and one modulus of elasticity would not affect the generality of the results discussed next, since the material was assumed to be linearly elastic.

As customary, the axial strains were calculated as the difference in vertical displacement between the top and bottom measuring points, divided by the gage length. This axial strain along with the applied stress were used to calculate the modulus of the material (see Equations 2.1 through 2.3). The Poisson's ratio was also calculated by first dividing the lateral displacement of the node located at mid-height, by the specimen radius to determine the lateral strain, and then by dividing the lateral strain by the axial strain (see Equations 2.4 and 2.5).

The resulting values obtained in this manner were then compared to the properties originally input into the models. Such comparison was expressed in terms of a ratio — herein referred to as the offset ratio. Accordingly, the offset ratio for the modulus was defined as the ratio of the modulus of elasticity corresponding to a specific gage length and to a specific specimen dimensions (L/D) over the modulus originally assigned to the model. In a similar fashion, the normalized Poisson's ratio was defined. A comparison of Equations. 2.1 and 2.4 indicates that the offset ratios calculated for either the modulus or Poisson's ratio should be identical. As such, only one set of offset ratios, which should be applicable both to the values of Poisson's ratio and modulus, are reported here.

Presentation of Results

Table 4.1 and Figure 4.1 exhibit the offset ratios obtained from this approach. To generalize the results, the gage length measurements, which use the axial deformations, are normalized with respect to the total length of the specimen. This normalized length is called the "gage length ratio (GLR)".

From the numerical results shown in Table 4.1 and Figure 4.1, the offset ratio increases as the gage length ratio also increases. Practically speaking, measuring the axial deformation closer to the end platens (i.e. using greater GLR's) will result in an overestimation of the modulus of elasticity and the Poisson's ratio of the material. Conversely, the closer the measurement points to the center of the specimen are, the more accurate the stiffness parameter measurements will be. For a typical specimen, the offset ratio is almost equal to 1, where the length-to-diameter ratio is about 2, and if the gage length ratios is about 0.5 and lower. At least theoretically, the gage length ratios of less than 0.5 should be used to avoid inaccuracies in the measurements of the stiffness parameters.

Table 4.1 - Variation in Estimated Modulus or Poisson's Ratio with Length-to-Diameter and Gage length

Gage Length Ratio[1]	Offset Ratio[2]					
	L/D = 1.3	L/D = 1.5	L/D = 2.0	L/D = 3.0	L/D = 4.0	L/D = 5.0
1	1.24	1.22	1.15	1.09	1.07	1.05
0.5	1.08	1.06	1.02	1	1	1
0.33	1.05	1.04	1.01	1	1	1
0.25	1.05	1.04	1.01	1	1	1
0.2	1.04	1.03	1.01	1	1	1

[1] Gage Length Ratio = (the distance between two points along the specimen used for measuring axial deformation / (the length of specimen)

[2] Offset Ratio = Estimated Modulus (or Poisson's ratio) / Assumed Modulus (or Poisson's ratio)

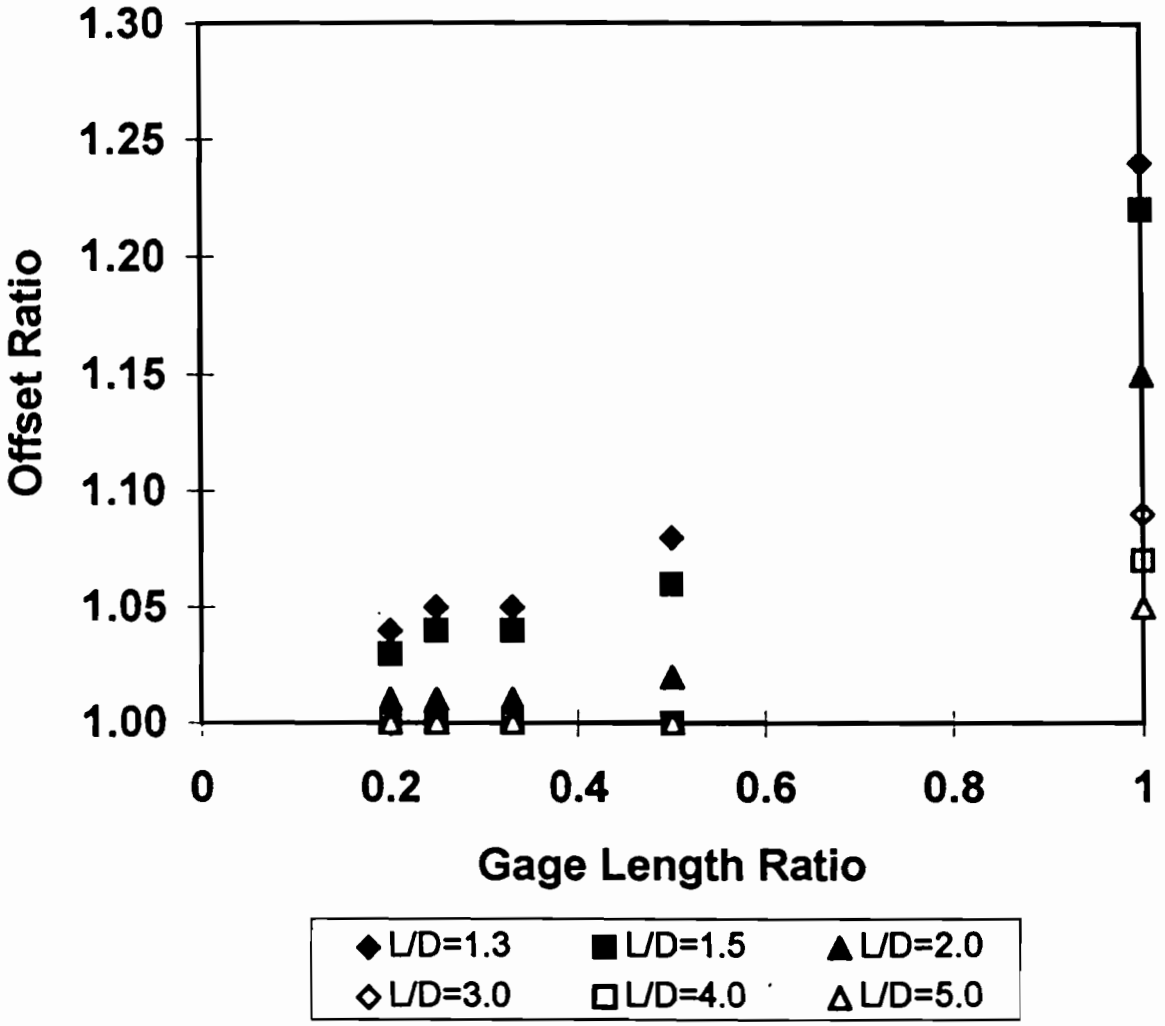

Figure 4.1 - Influence of Gage Length Used for Axial Deformation Measurements and Specimen Dimensions on Estimated Stiffness Parameters

Parameters The variation in modulus with gage length ratio can be attributed to the development of shear stresses in the vicinity of the top and the bottom caps, due to grouting. In other words, grouting will impede the development of axial deformations at the ends of the specimen, because of the shearing action. As a result, the axial strains are not constant along the length of the specimen; thus, the modulus of elasticity and Poisson's ratio estimates are affected, especially if the gage length includes the end zones. In addition, as explained by Bishop (1954) and many other researchers and practitioners during the last four decades such estimates are affected by the specimen dimensions.

An attempt was also made to relate the offset ratio to the length-to-diameter ratio and gage length ratio (GLR) using an statistical approach. Practically speaking, the errors involved in performing tests with different configurations can be easily calculated with this relationship without having to go through a lengthy and laborious process. After checking the normality and proper transformation of the data, the following regression equation was developed:

$$OR = 0.930 * e^{0.15/(L/D) + 0.09 * Sin\text{-}1(GLR)} \quad (4.1)$$

where, OR is the offset ratio. The coefficient of determination, R^2, and the standard error of the estimate, SEE, are 0.88 and 0.02, respectively, indicating a moderately well fit.

Although Equation 4.1 is an approximation of a theoretical analysis, it has practical implications. For instance, the modulus of elasticity and Poisson's ratio will be overestimated by about 15 percent if a decision is made to test specimens with a L/D ratio equal to 2 and to monitor the axial deformations with respect to the total length of the specimens (GLR = 1).

Conversely, if the decision is made to use specimens with a L/D ratio equal to 4/3 and to monitor the axial deformations along the total length of the specimens (to simplify the specimen set-up and to use available equipment), the modulus and Poisson's ratio can be overestimated by as much as 25 percent.

The experimental verification and validation of some results presented in Table 4.1 were accomplished by first testing three synthetic (calibration) specimens with different stiffness, and then, by testing actual specimens of base materials. The results are discussed in the next section.

For practical use, a gage length ratio of 0.333 on specimens with L/D = 2.0 was selected and recommended for the resilient modulus testing. This configuration seems to be a reasonable compromise, between accuracy in determining the modulus and Poisson's ratio (less than one percent theoretical error as per Table 4.1) and practicality in mounting of sensors and targets in the laboratory.

Verification of Numerical Results

Three synthetic specimens made of poly-urethane elastomer resin were used in this study. Stokoe et al. (1990) described in detail the composition and overall behavior of this type of material. The specimens used were stiffer and larger than those used by Stokoe et al., so that they resemble base specimens better.

The hardness grades of the base layers used were 90A "soft", 50D "medium" and 70D "hard." Each sample, which was manufactured with a diameter of 150 mm and a height of 1,000 mm, was cut into three equal pieces for a total of nine specimens. Special attention was paid to the surface of the specimen to ensure the flatness, smoothness and parallelism.

The specimens that resemble a soft base are referred to as specimens A-1, A-2, and A-3, medium base as specimens B-1, B-2 and B-3, and hard base as specimens C-1, C-2 and C-3.

Static compression test was first performed on each specimen. All tests were conducted with the specimens grouted to the end platens with a hydrostone paste that was allowed to cure for 1 hour. All tests were performed at a zero confining pressure and a temperature of 22°C.

The static compression tests consisted of gradually increasing the load on the specimen. The stress on the specimen was increased from 0 KPa to 96 KPa over a period of 15 minutes. In addition, the applied force was maintained for 1 minute, at axial stresses of about 35 KPa, 70 KPa and 96 KPa. The load, axial deformations, and lateral deformations were recorded throughout the test.

For each specimen, the axial and lateral deformations were measured at 25-mm intervals along the length of the specimen. Gage length ratios of 1, 0.83, 0.67, 0.53, 0.36 and 0.20 were considered. These tests were carried out on randomly-selected specimens A-1, B-1 and C-2.

Tables 4.2 through 4.4 contain the summary of the results. The results of interest are the offset ratios. For the three deviatoric stresses shown in the tables, the moduli and Poisson's ratios are quite repeatable. Further evaluation of the results will be discussed in the next chapter.

To closely compare the numerical and experimental results, Finite Element Analysis was used to numerically model the behavior of the three synthetic specimens. Table 4.5 contains the parameters input into the finite element models. The actual height, diameter and density of each specimen were used. The average values for the Young's modulus and Poisson's ratio corresponding to the gage length of 64 mm (GLR = 0.20) measured in the laboratory were also input to the program.

The numerical outputs and the experimental measurements are compared in Figures 4.2 through 4.4 for the three specimens. The axial and lateral deformations along the length of the specimens are shown for each specimen. For all three specimens, the lateral and axial deformations from

Table 4.2 - Test Results from Tests on Soft Specimen A-1

Deviatoric Stress (KPa)	Gage Length (mm)	Axial Strain (%)	Lateral Strain (%)	Young's Modulus (MPa)	Poisson's Ratio	Gage Length Ratio	Offset Ratio
35	64	0.1066	0.0518	32.3	0.49	0.20	1.00
35	114	0.1019	0.0518	33.8	0.51	0.36	1.05
35	165	0.0967	0.0518	35.6	0.54	0.53	1.10
35	216	0.0920	0.0518	37.4	0.56	0.67	1.16
35	267	0.0907	0.0518	38.0	0.57	0.83	1.18
35	318	0.0899	0.0518	38.3	0.58	1.00	1.19
70	64	0.2132	0.1028	32.3	0.48	0.20	1.00
70	114	0.2038	0.1028	33.8	0.50	0.36	1.05
70	165	0.1834	0.1028	36.6	0.56	0.53	1.13
70	216	0.1840	0.1028	37.5	0.56	0.67	1.16
70	267	0.1814	0.1028	38.0	0.57	0.83	1.18
70	318	0.1821	0.1028	37.8	0.56	1.00	1.17
98	64	0.2984	0.1435	32.3	0.48	0.20	1.00
98	114	0.2853	0.1435	33.8	0.50	0.36	1.05
98	165	0.2627	0.1435	36.7	0.54	0.53	1.13
98	216	0.2576	0.1435	37.4	0.56	0.67	1.16
98	267	0.2539	0.1435	38.0	0.57	0.83	1.18
98	318	0.2499	0.1435	38.6	0.57	1.00	1.19

Table 4.3 - Test Results from Tests on Medium Specimen B-1

Deviatoric Stress (KPa)	Gage Length (mm)	Axial Strain (%)	Lateral Strain (%)	Young's Modulus (MPa)	Poisson's Ratio	Gage Length Ratio	Offset Ratio
35	64	0.0520	0.0243	66.2	0.47	0.20	1.00
35	114	0.0494	0.0243	69.7	0.49	0.36	1.05
35	165	0.0437	0.0243	78.8	0.55	0.53	1.19
35	216	0.0429	0.0243	80.3	0.56	0.67	1.21
35	267	0.0423	0.0243	81.4	0.57	0.83	1.23
35	318	0.0422	0.0243	81.6	0.57	1.00	1.23
70	64	0.1140	0.0542	60.4	0.48	0.20	1.00
70	114	0.1092	0.0542	63.1	0.50	0.36	1.05
70	165	0.0965	0.0542	71.4	0.56	0.53	1.18
70	216	0.0988	0.0542	69.7	0.55	0.67	1.15
70	267	0.0924	0.0542	74.6	0.58	0.83	1.23
70	318	0.0930	0.0542	74.1	0.58	1.00	1.23
98	64	0.1566	0.0754	61.6	0.48	0.20	1.00
98	114	0.1517	0.0754	63.6	0.50	0.36	1.04
98	165	0.1343	0.0754	71.8	0.56	0.53	1.17
98	216	0.1278	0.0754	75.5	0.59	0.67	1.23
98	267	0.1263	0.0754	76.4	0.60	0.83	1.25
98	318	0.1254	0.0754	76.9	0.60	1.00	1.25

Table 4.4 - Test Results from Tests on Hard Specimen C-2

Deviatoric Stress (KPa)	Gage Length (mm)	Axial Strain (%)	Lateral Strain (%)	Young's Modulus (MPa)	Poisson's Ratio	Gage Length Ratio	Offset Ratio
35	64	0.0140	0.0066	246.1	0.47	0.20	1.00
35	114	0.0134	0.0066	257.1	0.49	0.36	1.05
35	165	0.0133	0.0066	259.0	0.50	0.53	1.05
35	216	0.0131	0.0066	263.0	0.50	0.67	1.07
35	267	0.0131	0.0066	263.0	0.50	0.83	1.07
35	318	0.0127	0.0066	271.3	0.52	1.00	1.11
70	64	0.0284	0.0136	242.6	0.48	0.20	1.00
70	114	0.0276	0.0136	249.6	0.49	0.36	1.03
70	165	0.0259	0.0136	266.0	0.52	0.53	1.10
70	216	0.0249	0.0136	276.7	0.55	0.67	1.14
70	267	0.0241	0.0136	285.9	0.56	0.83	1.18
70	318	0.0236	0.0136	291.9	0.58	1.00	1.20
98	64	0.0393	0.0185	245.4	0.47	0.20	1.00
98	114	0.0375	0.0185	257.2	0.49	0.36	1.05
98	165	0.0355	0.0185	271.7	0.52	0.53	1.11
98	216	0.0344	0.0185	280.4	0.54	0.67	1.14
98	267	0.0338	0.0185	285.4	0.55	0.83	1.16
98	318	0.0329	0.0185	293.2	0.56	1.00	1.20

Table 4.5 - Parameters Used in Finite Element Analysis

Specimen	Height (mm)	Diameter (mm)	Density (Kg/m^3)	Young's Modulus (MPa)	Poisson's ratio
A-1	318	150	1121	32	0.48
B-1	318	150	1204	63	0.48
C-2	318	150	1271	245	0.47

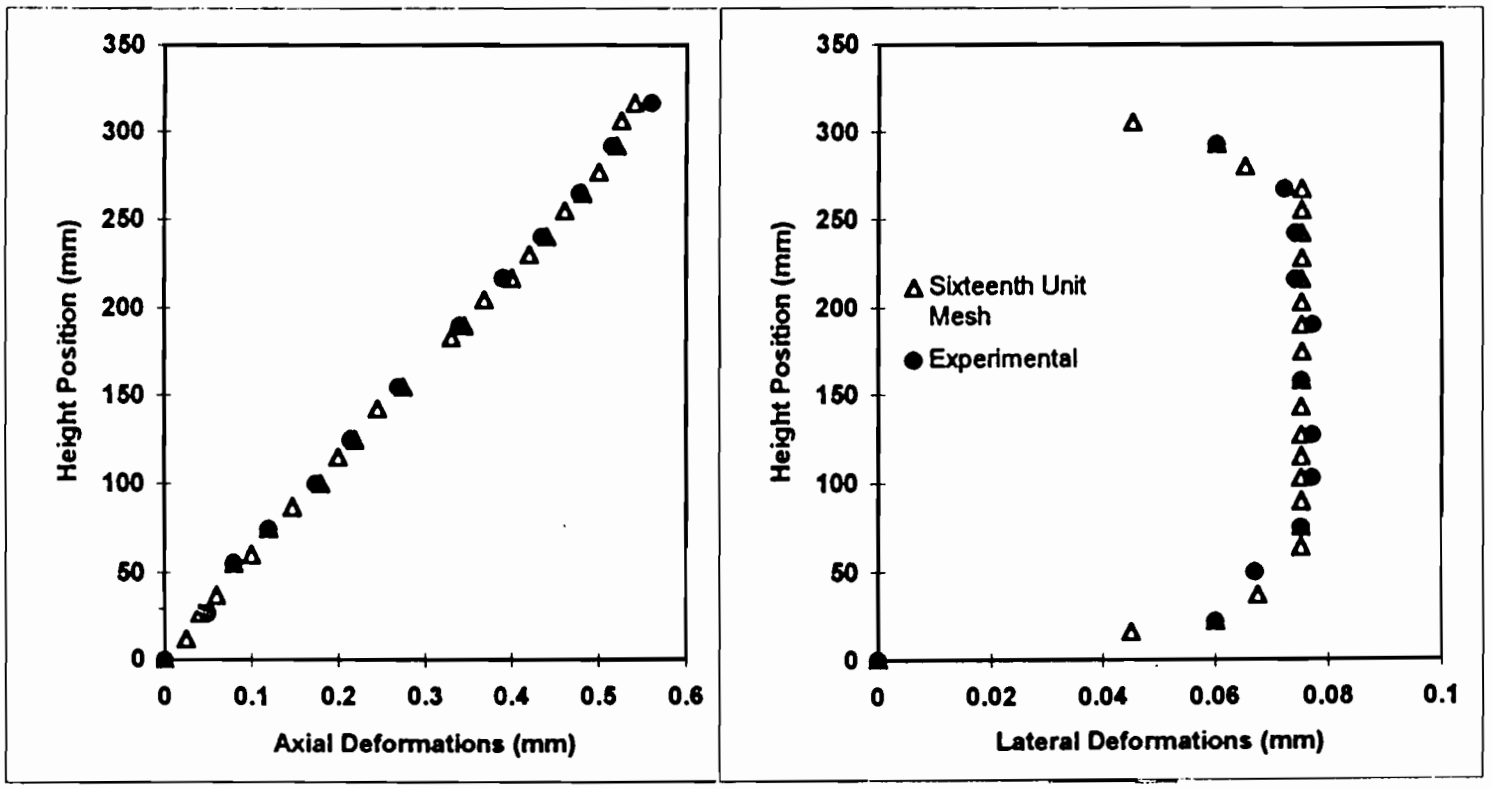

Figure 4.2 Comparison of Experimental and Numerical Results from a Soft Synthetic Specimen due to an Axial Stress of 10 KPa

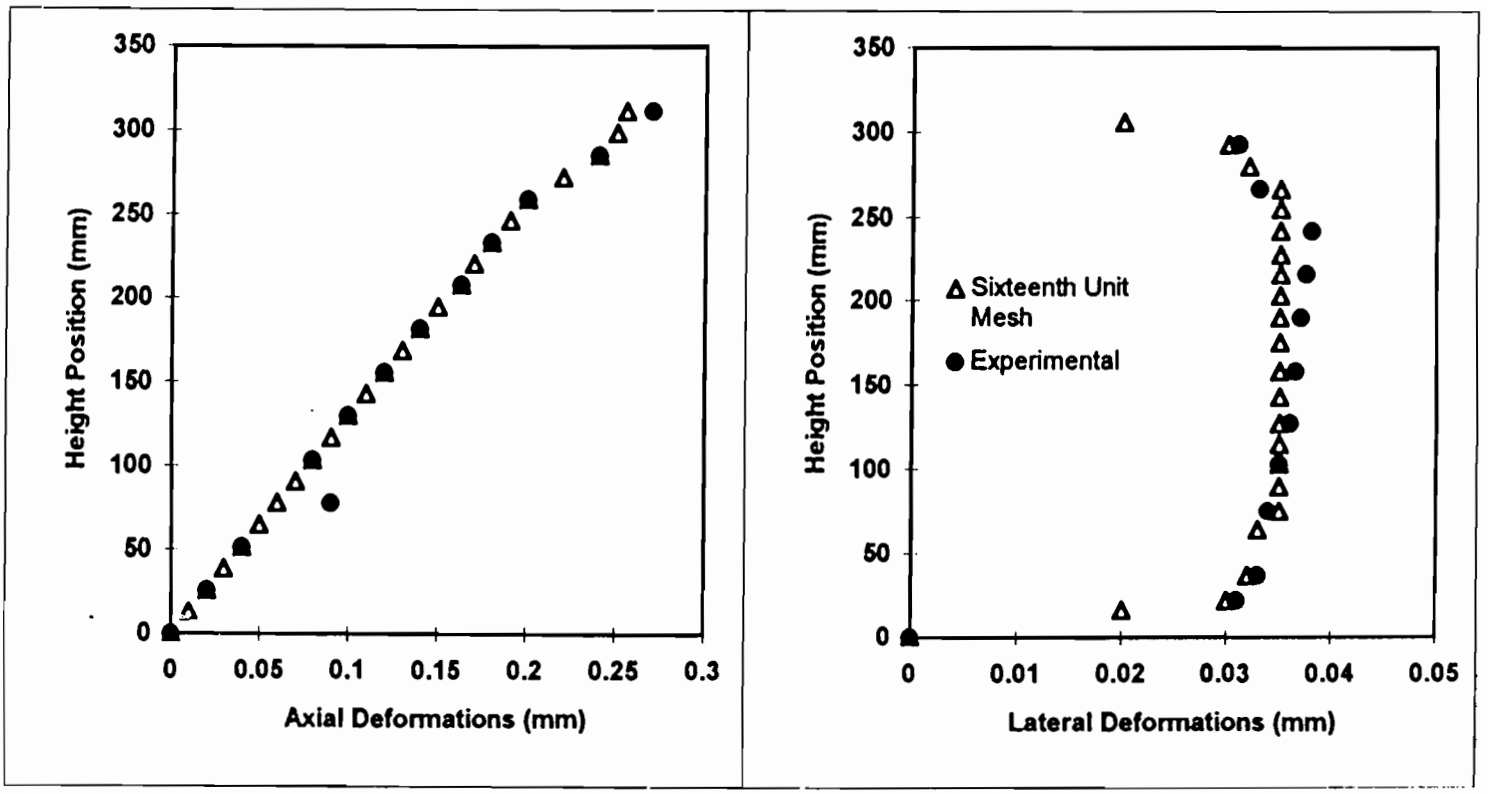

Figure 4.3 Comparison of Experimental and Numerical Results from a Medium Synthetic Specimen due to an Axial Stress of 10 KPa

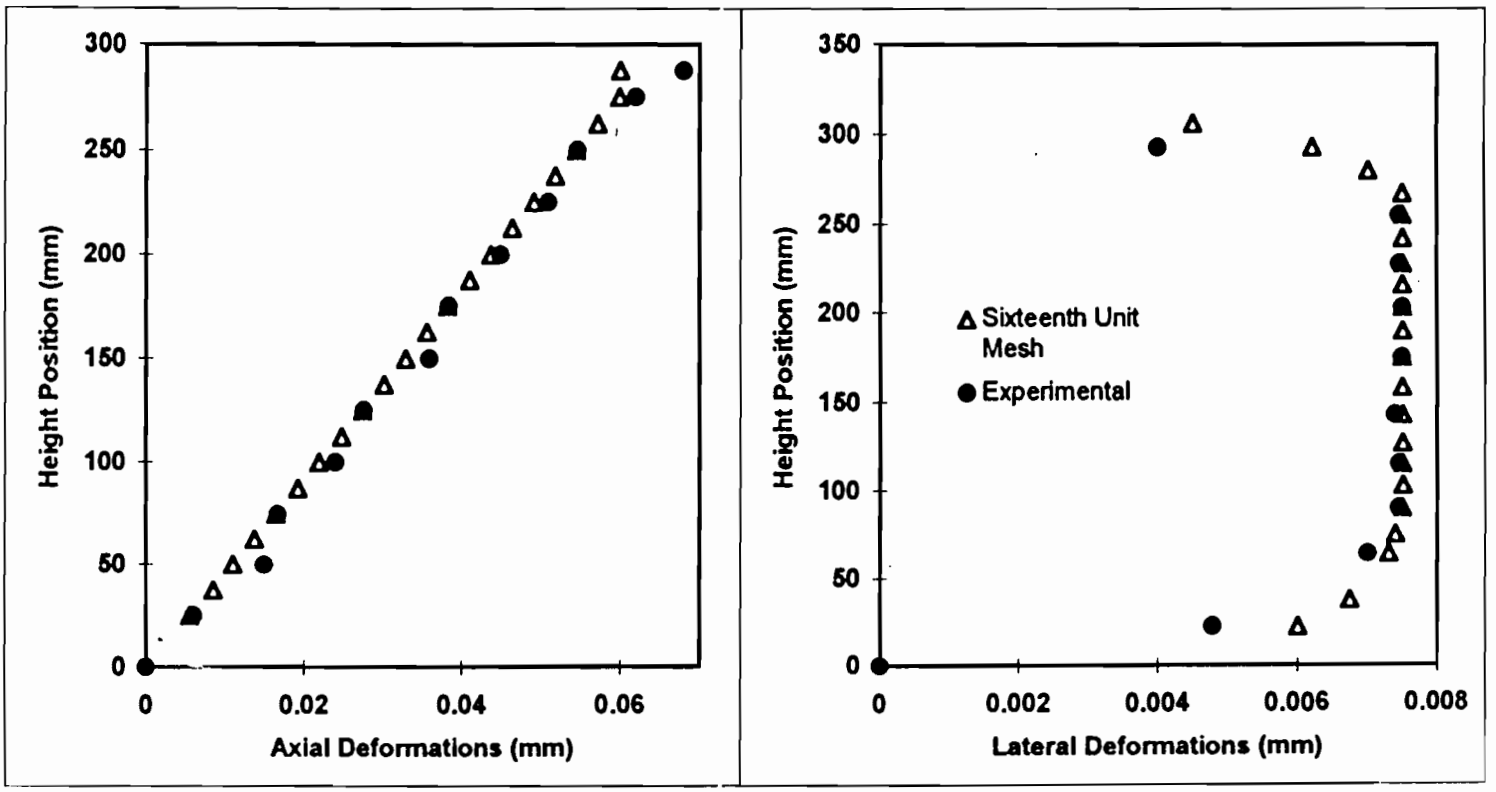

Figure 4.4 Comparison of Experimental and Numerical Results from a Hard Synthetic Specimen due to an Axial Stress of 10 KPa

the numerical and experimental results follow one another well. The only exceptions are the data points that are close to the top and bottom platens. These comparisons present encouraging agreements between the theory and practice with respect to the behavior of synthetic specimens subjected to a static load.

Even though the resilient modulus test is a dynamic test, the implications of this analysis are believed to be analogous. Further analyses by Urbina et al. (1995) and Stokoe et al. (1990) confirm this inference.

An alternative way to compare the numerical and laboratory results is to compare the variation in offset ratio with the gage length ratio (GLR). At any given deviatoric stress, the offset ratios were calculated by dividing the modulus at each gage length by the modulus at a gage length of 64 mm (GLR = 0.2).

The offset ratios from the numerical analyses and laboratory tests are compared in Figure 4.5. Since all laboratory tests were carried out on specimens with length-to-diameter ratio (L/D) of 2.1, the numerical results from L/D = 2 are only shown in the figure.

As such, these experimental results confirm the fact that axial measurements needs to be taken at a gage length of, at least, the middle-third portion of the specimen, and not at its entire length. However, if the entire length of the specimen is used for convenience purposes or other reasons, the stiffness parameters will be to some degree overestimated.

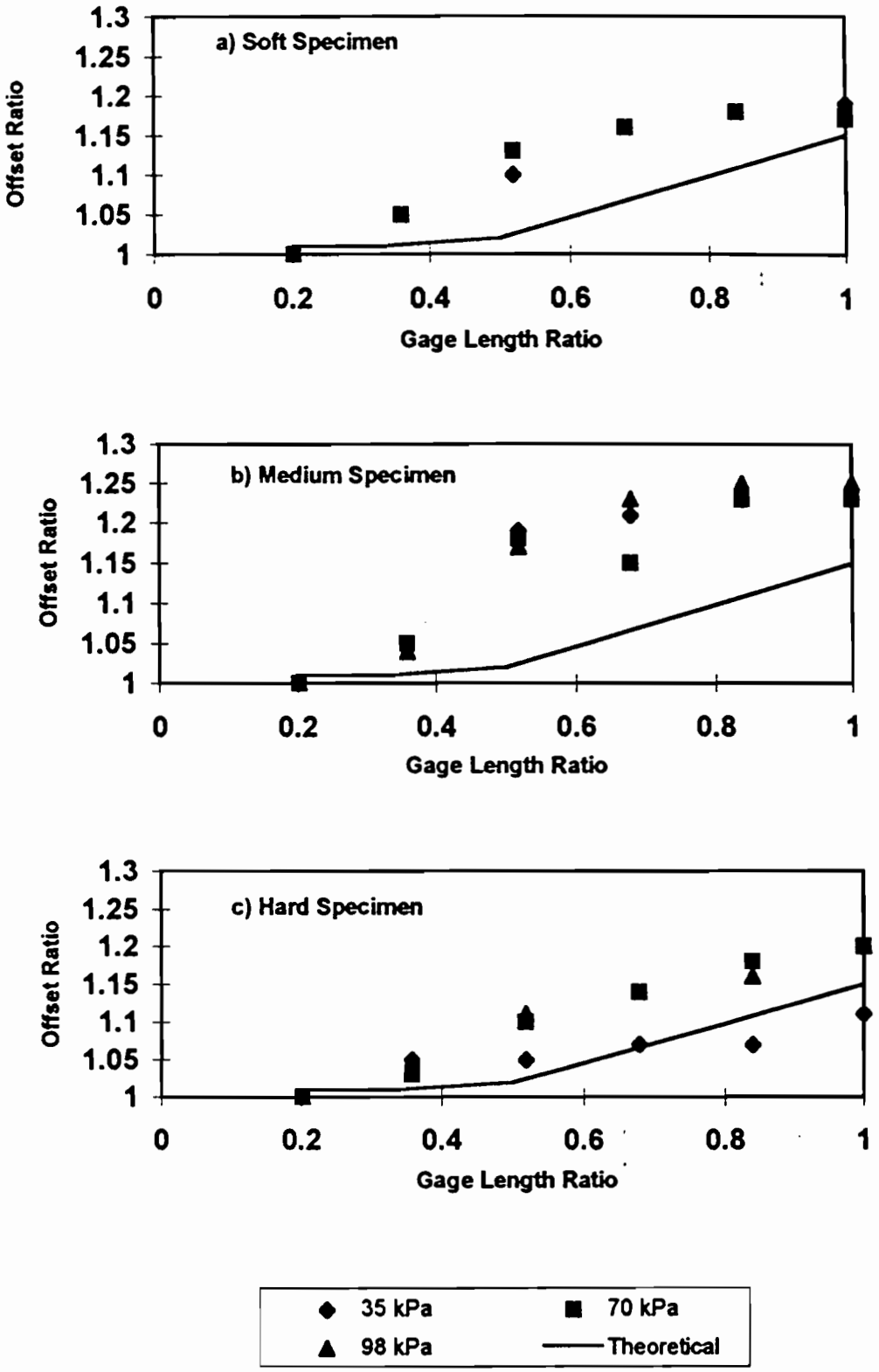

Figure 4.5 Comparison of Theoretical and Experimental Offset Ratios

Chapter 5

Evaluation of Proposed Testing System

Introduction

Before testing actual base specimens, nine synthetic specimens were tested to calibrate the device and to evaluate its performance. This chapter discusses the results obtained from static, resilient modulus and free-free resonant column tests on these specimens.

As indicated before, a rod of about 1 m of each material was purchased. From each rod, three specimens were cut. The nine synthetic specimens were named A1, A2, A3 (soft), B1, B2, B3 (medium), and C1, C2, and C3 (hard). Since all three specimens at a particular stiffness level were cut from a longer specimen, they should be of very similar composition and properties. The properties of these specimens were discussed in the previous chapter.

Static Tests

Static compression tests were performed on the nine synthetic specimens. All tests were conducted with the specimens grouted to end platens. Hydrostone paste, that was allowed to cure for 1 hour, was used to grout the specimens. All tests were performed at zero confining pressure and at a temperature of 22° C.

The procedure followed for static tests was described in Chapter 4. The static compression test consisted of gradually increasing the load on the specimen from 0 KPa to 98 KPa over a period of 15 minutes. At stresses of 35 KPa, 70 KPa, and 98 KPa, the applied force was maintained constant for 1 minute. Axial deformations were measured with the proximeters. The targets for axial deformation measurements consisted of aluminum blocks that were glued to the specimen. The lateral deformations were also recorded during the entire test. The targets for lateral

deformation measurements were aluminum foils glued to the specimens. To evaluate the suggested protocol, only the results from the GLR of 0.33 are discussed in this section.

The variation in modulus with deviatoric stress for A1, A2, and A3 (soft) are shown in Figure 5.1. The modulus values obtained for the three specimens are quite similar; therefore, the tests can be considered repeatable. The maximum deviation from the average modulus was less than 3 percent. Typically, the differences in moduli of the three specimens were less than 2 percent.

The values of the Poisson's ratios are very similar for the three specimens. Basically for all three specimens, the Poisson's ratio is close to 0.50, and is independent of deviatoric stress.

The results from similar tests on the static specimens are shown in Figures 5.2 and 5.3, respectively. As in the case of the soft specimens, the results are quite repeatable and the moduli and Poisson's ratios from the three specimens yield very similar results.

In Table 5.1, the moduli and Poisson's ratios from static tests are summarized. Since the results were independent of deviatoric stress, only one modulus (corresponding to the average value from all experiments) is reported for a given set of specimens. The coefficient of variation corresponding to each parameter is also reported. The results once again confirms the repeatability of the test method.

Table 5.1 - Average Young's Moduli and Poisson's Ratios Measured on Synthetic Specimens

Specimen	Static Modulus		Poisson's Ratio	
	Average (MPa)	C.V. (percent)	Average	C.V. (percent)
Soft	34	1.1	0.50	1.2
Medium	66	2.5	0.50	1.3
Hard	258	2.9	0.49	1.1

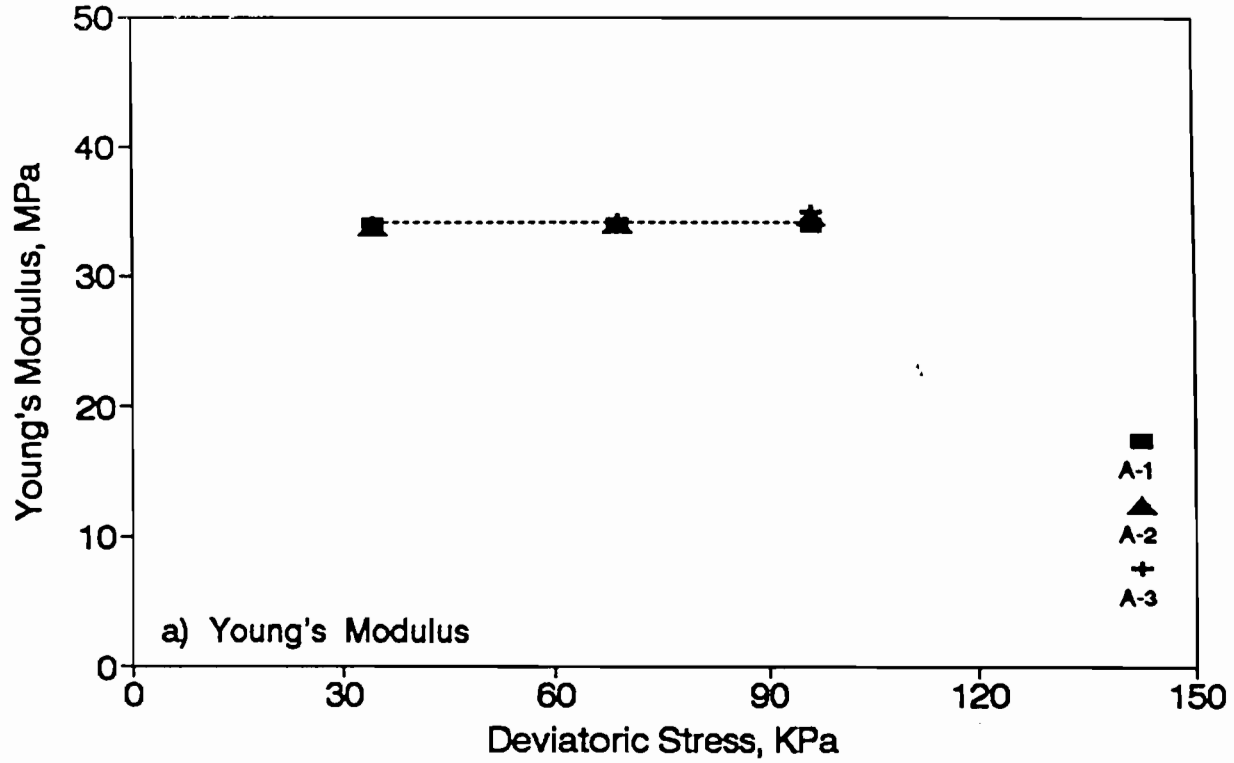

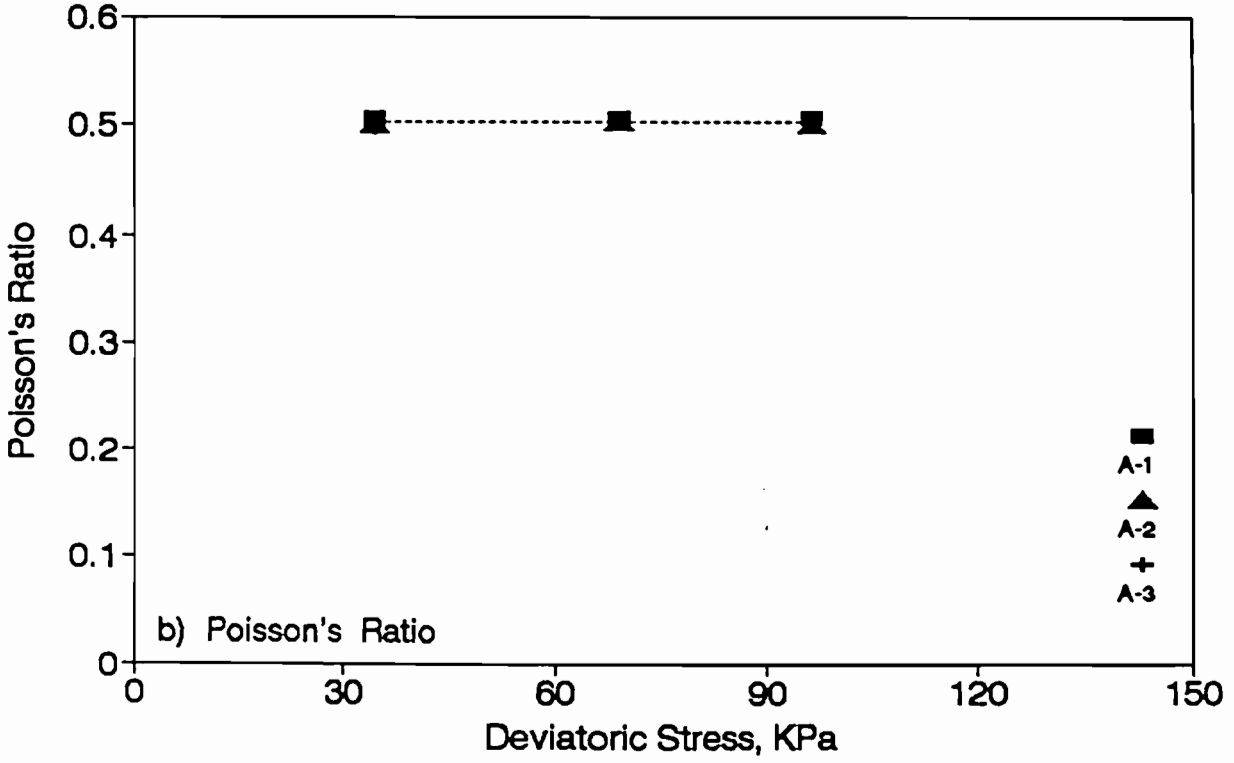

Figure 5.1 - Comparisons of Static Moduli and Poisson's Ratios from Three Soft Specimens

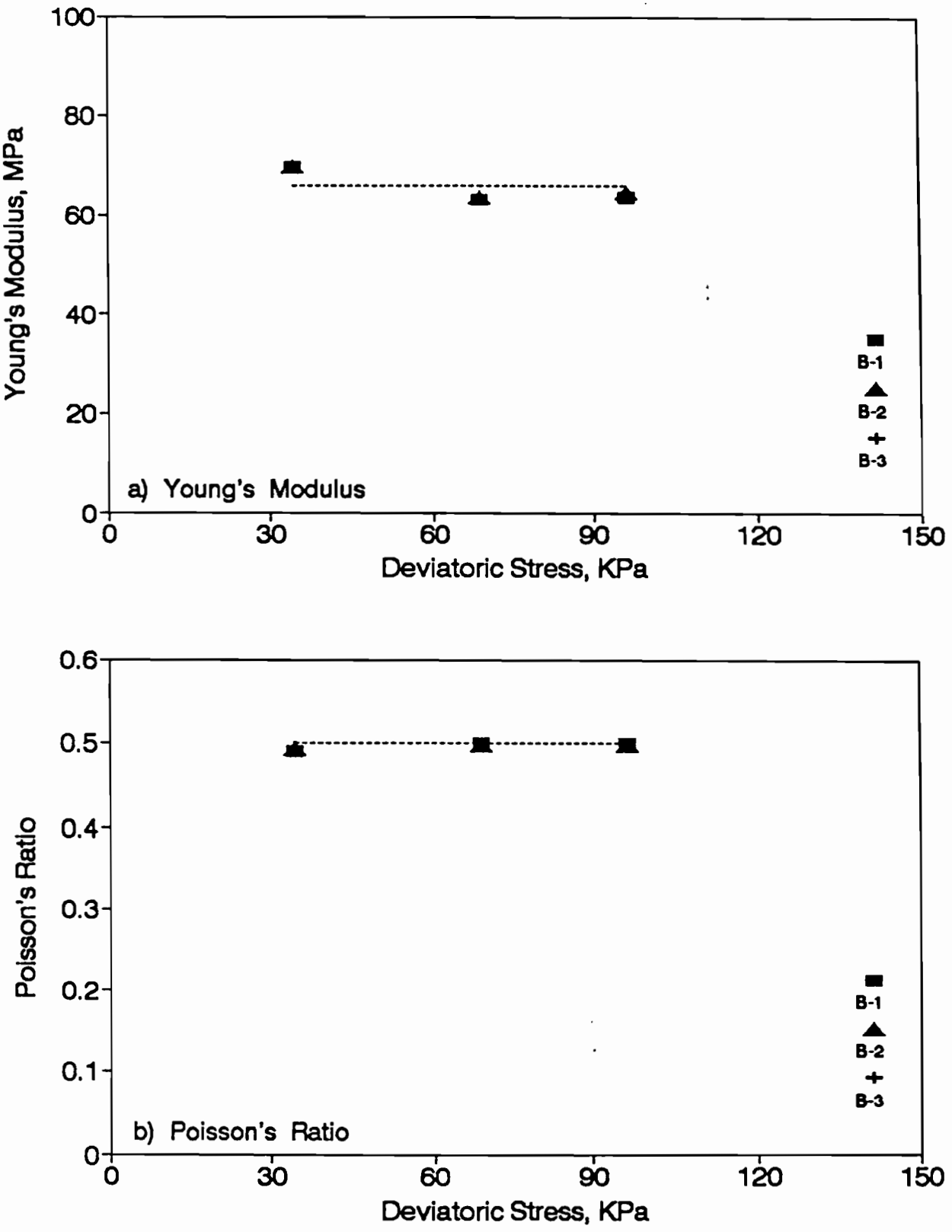

Figure 5.2 - Comparison of Static Moduli and Poisson's Ratios from Three Medium Specimens

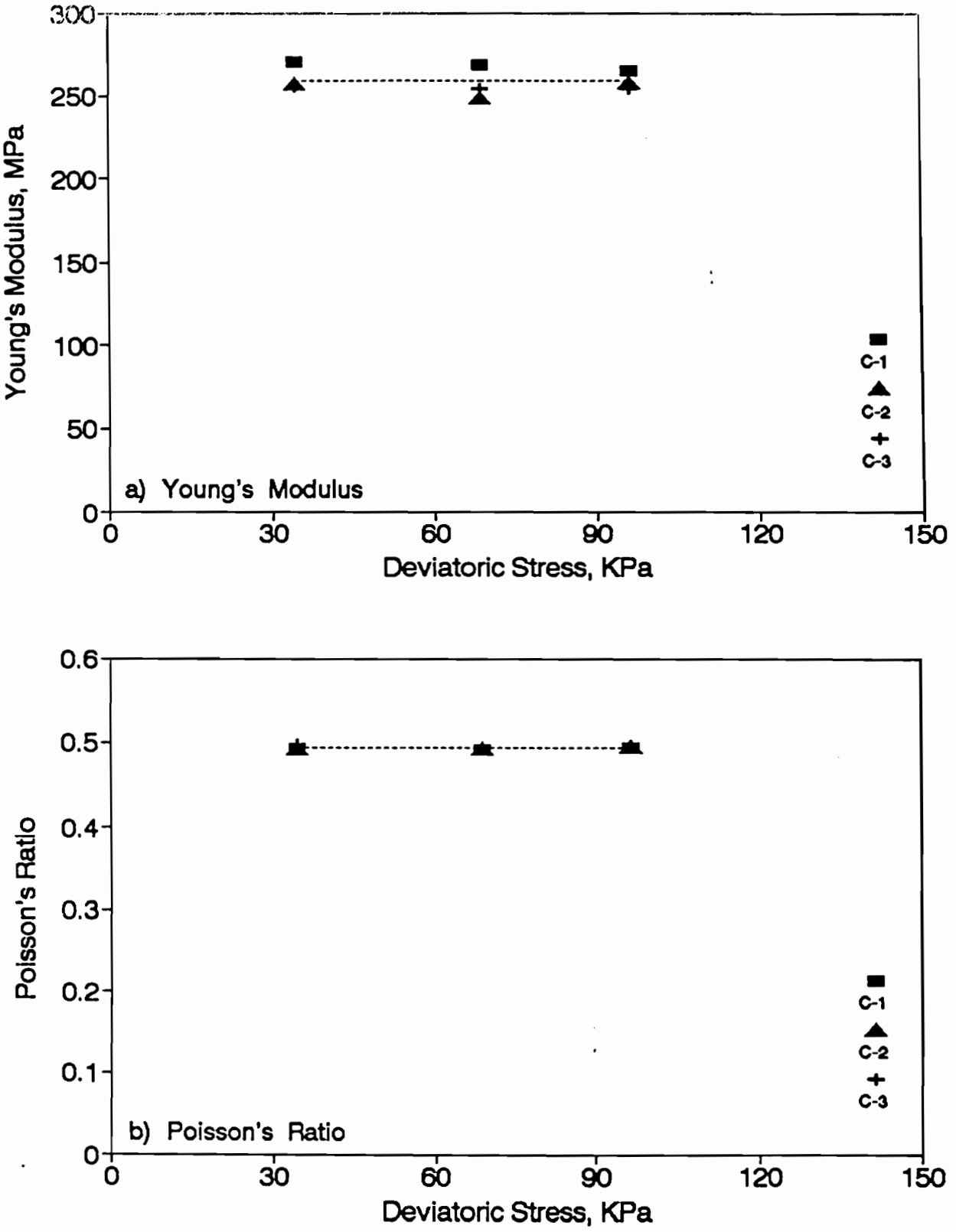

Figure 5.3 - Comparisons of Static Moduli and Poisson's Ratios from Three Hard Specimen

Resilient Modulus Tests

Also, performed on the nine synthetic specimens were resilient modulus tests. The temperature, confining pressure, and end conditions were the same as those adopted in static tests.

The resilient modulus test consisted of subjecting the specimen to different magnitudes of repeated loads. A haver-sine loading waveform of load pulse duration 0.1 seconds and a rest period of 0.9 seconds were adopted.

The nominal deviatoric stresses applied on each specimen were the following: 10 KPa, 20 KPa, 45 KPa, 70 KPa, 100 KPa, 150 KPa, 200 KPa, and 250 KPa. In this case the axial deformations were only measured at gage length ratios of 1.0, 0.33, and 0.2. On the other hand, the lateral deformations were measured at the mid-height of the specimen. The targets for axial and lateral deformation measurements were installed in the same manner as done for the static tests.

The variations in resilient moduli and Poisson's ratios with deviatoric stress for the three soft specimens are shown in Figure 5.4. As expected, all three specimens yield very similar results. Once again, the resilient modulus and Poisson's ratio are independent of deviatoric stress. This is in agreement with the results obtained by Stokoe et al. (1991) on similar synthetic specimens.

Similar results but for the medium and hard specimens are included in Figures 5.5 and 5.6, respectively. Once again, the results are quite repeatable and follow the patterns discussed for the soft specimens.

Given in Table 5.2 is the relevant statistical information related to the stiffness and Poisson's ratio of the three specimens. The results are quite repeatable, since in all cases the coefficients of variation are less than 3.2 percent.

Table 5.2 -Average Resilient Moduli and Poisson's Ratios Measured on Synthetic Specimens at GLR L/3

Specimen	Resilient Modulus		Poisson's Ratio	
	Average (MPa)	C.V. (percent)	Average	C.V. (percent)
Soft	59	1.9	0.48	3.2
Medium	127	1.6	0.46	2.2
Hard	565	0.7	0.46	1.3

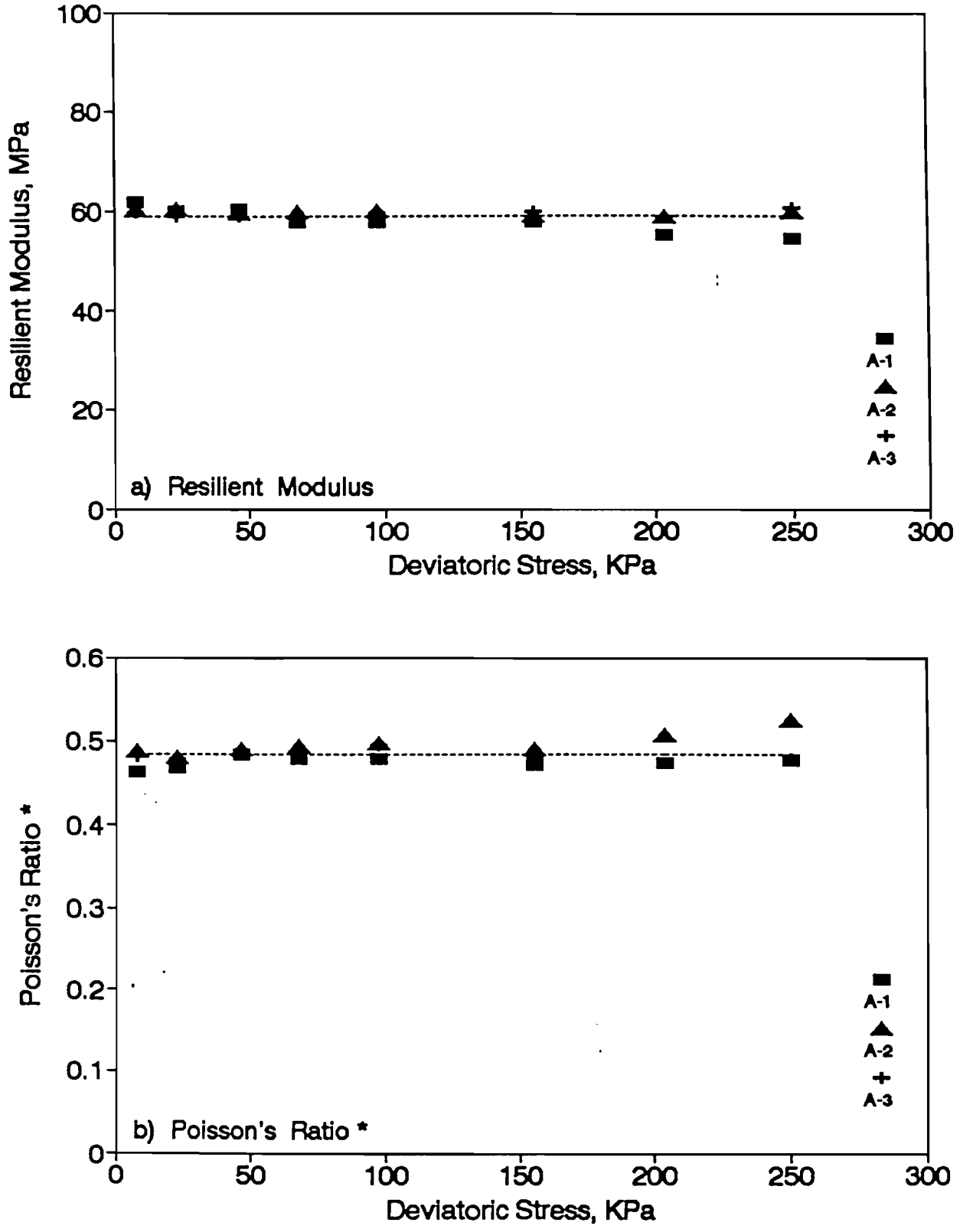

Figure 5.4 - Comparisons of Resilient Moduli and Poisson's Ratios from Three Soft Specimens

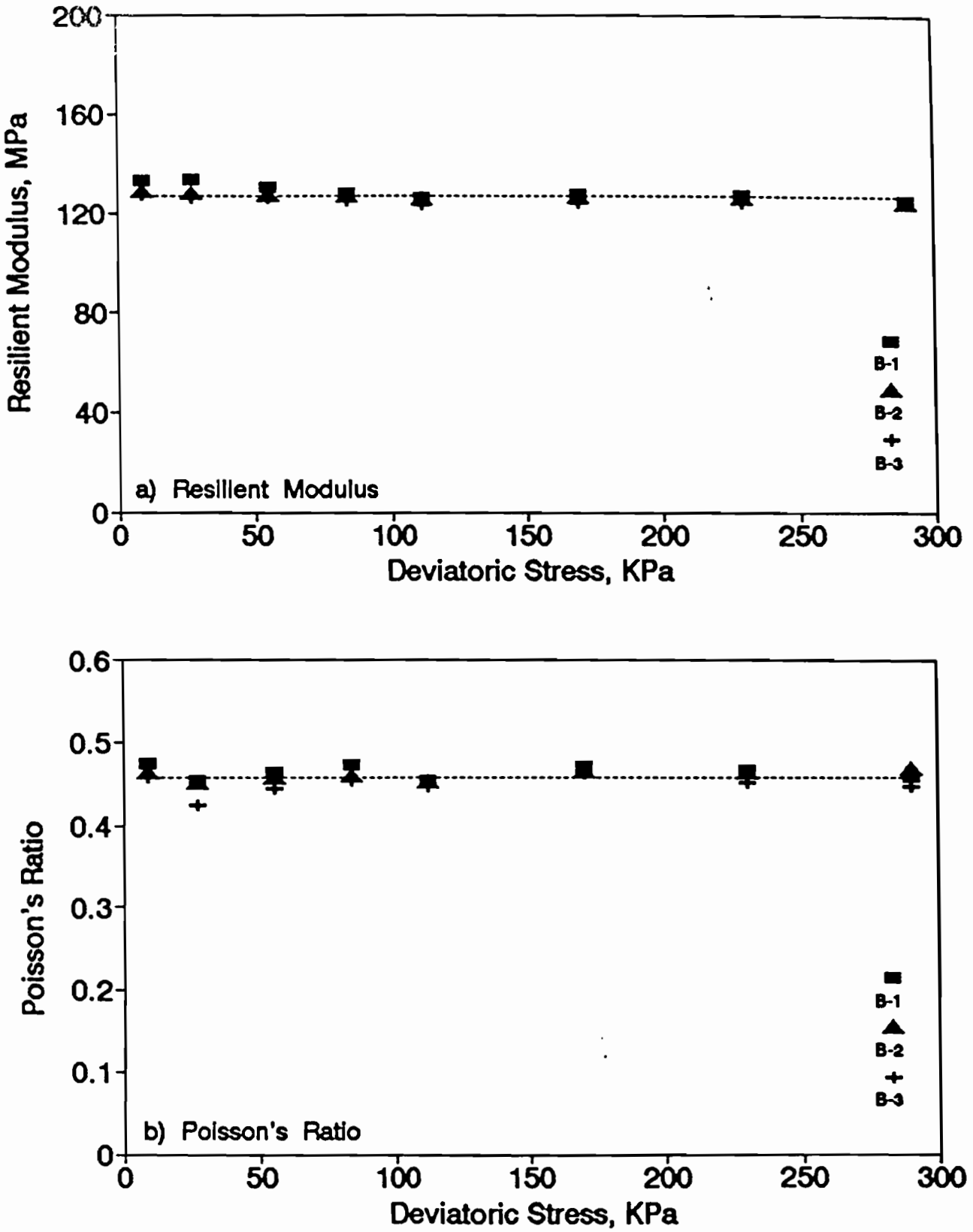

Figure 5.5 - Comparison of Resilient Moduli and Poisson's Ratios from Three Medium Specimens

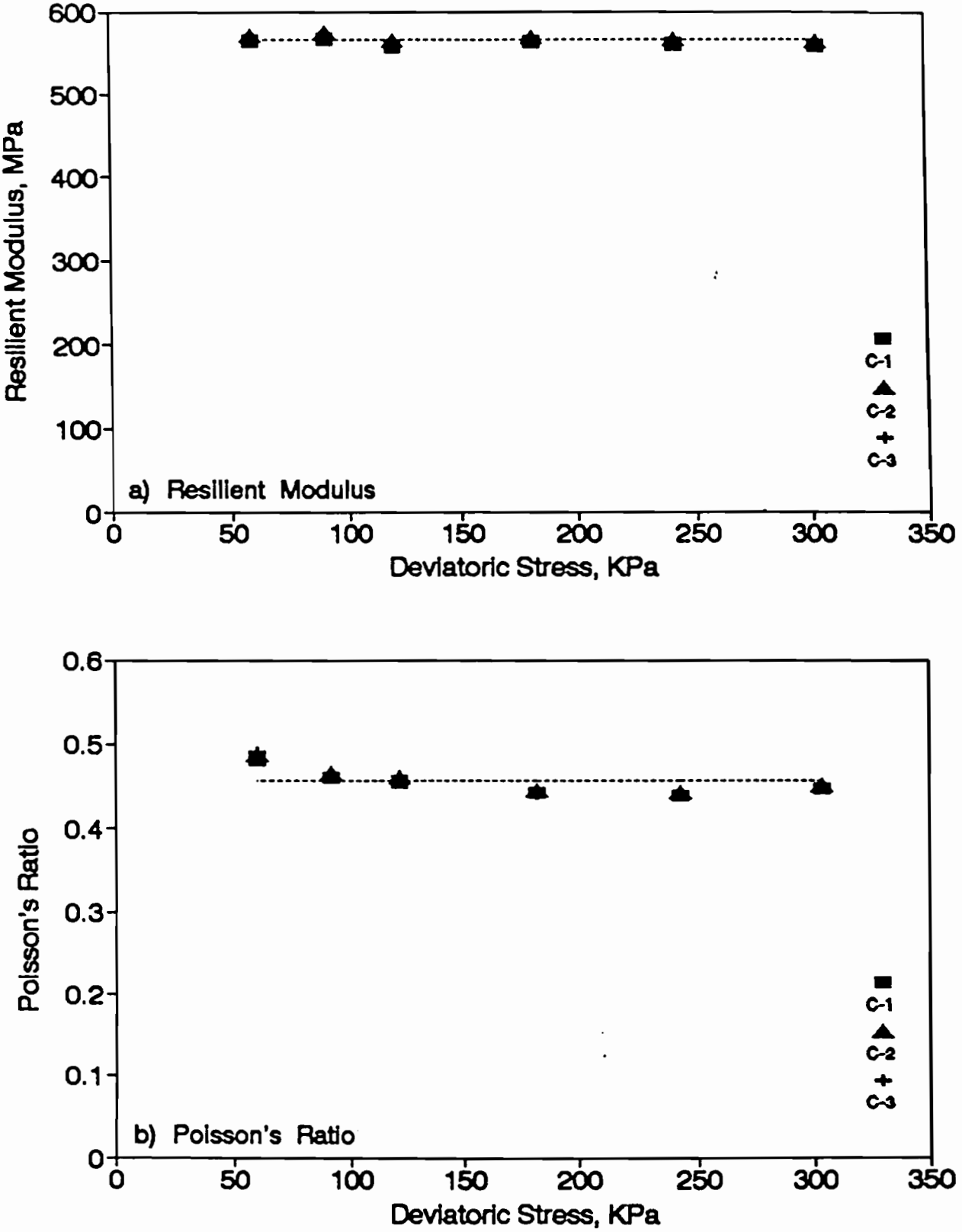

Figure 5.6 - Comparison of Resilient Moduli and Poisson's Ratios from Three Hard Specimens

Resonant Column Tests

Also performed on the nine synthetic specimens were Free-Free resonant column tests. The test setup is schematically shown in Figure 5.7. Both the shear and Young's moduli of the material can be measured. The specimen is suspended from two very thin piano wires, as shown in the figure.

An accelerometer, oriented in the axial direction, is mounted on the specimen to measure Young's modulus. The opposite side of the specimen is then impacted with a hammer instrumented with a load cell. The impact will induce compression waves, which will reflect from the two ends of the specimen. The initial and reflected waves are sensed by the accelerometer. The time-histories from the load cell and the accelerometer are measured and captured. Spectral analyses are then performed on the two time-histories, so that the fundamental resonant frequency associated with the reflection of can be obtained. Typical spectral functions measured on a specimen is shown in Figure 5.8. In Figure 5.8a, the fundamental compressional resonant frequency is clearly marked.

The Young's modulus, E, is determined from (Richart et al., 1970):

$$E = \frac{\gamma}{g} (2 f_c L)^2 \tag{5.1}$$

where L = the length of the specimen, f_c = the fundamental natural frequency related to compression waves, γ = the weight of the specimen, and g = acceleration of gravity.

Similarly, the tests can be performed to determine the shear modulus of the specimen. In order to do this, the setup described above requires two modifications. First, the accelerometer has to be oriented in the radial direction. Second, a piece of metal has to be glued to the end of the specimen as an anvil for the instrumented hammer. The hammer will impact the anvil radially, so that torsional waves are generated in the specimen. The procedure is identical to that described for determining Young's modulus, except for these two minor modifications.

The shear modulus, G, is determined from:

$$G = \frac{\gamma}{g} (2 f_t L)^2 \tag{5.2}$$

The only difference between Equations 5.1 and 5.2 is that f_c, the fundamental compressional resonant frequency, is replaced with f_t, the fundamental torsional resonant frequency. Typical spectral functions from torsional tests on the same specimen is shown in Figure 5.8b. Once again, the fundamental torsional frequency is clearly marked on the figure.

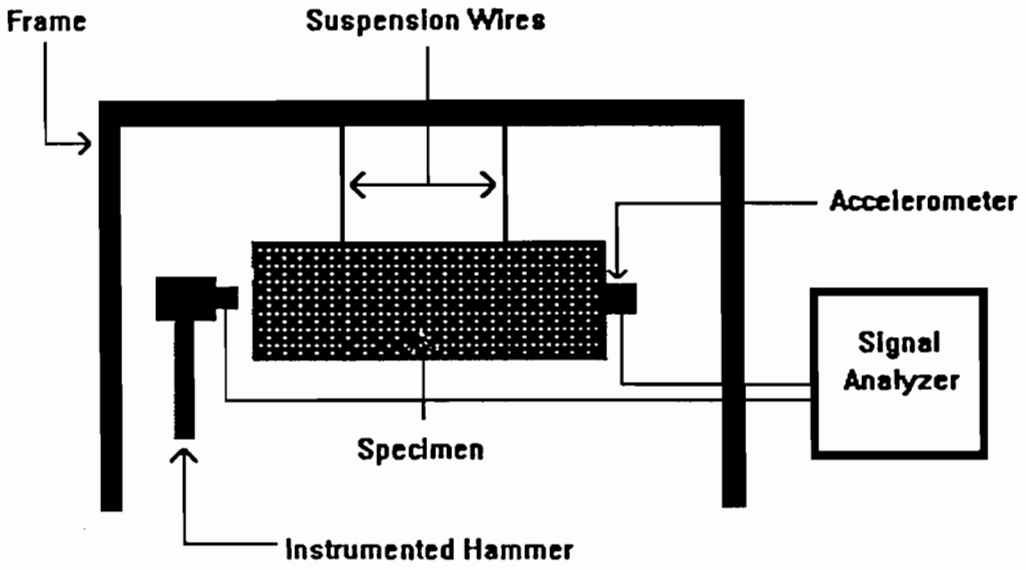

Figure 5.7 - Resonant Column Test Setup

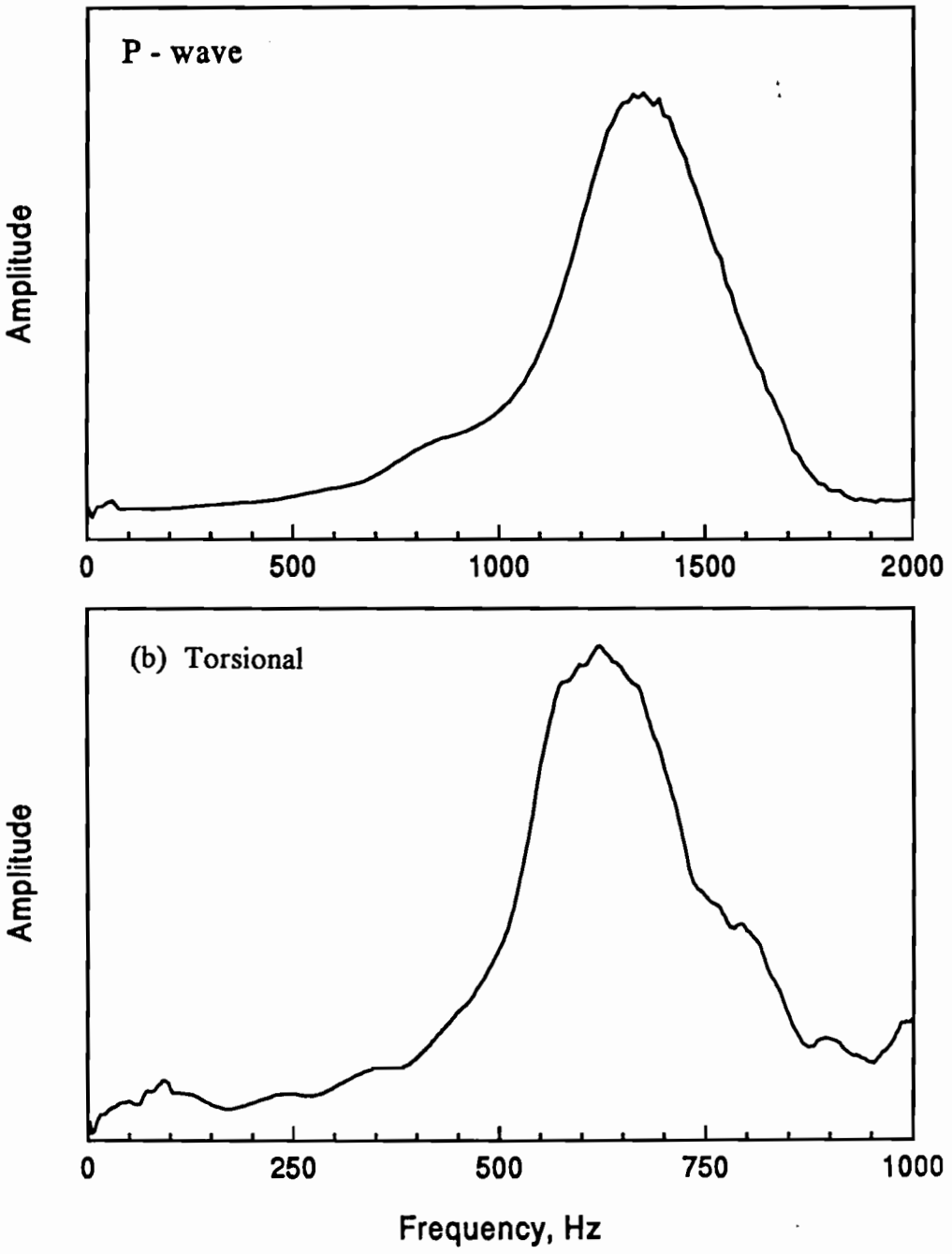

Figure 5.8 - Spectral Functions from Free - Free Resonant Column Tests

Once the shear and Young's moduli are measured, Poisson's ratio, ν, can be calculated from:

$$\nu = \left(\frac{E}{2G} - 1\right) \tag{5.3}$$

Shown in Table 5.3 are three specimens with similar stiffness, the shear and Young's moduli are virtually identical, indicating the extremely good repeatability in the test methodology. When the moduli from the three specimens with the same stiffness are compared, the coefficients of variations are typically less than 1 percent.

Table 5.3 - Average Young's Moduli and Poisson's Ratios Measured on Synthetic Specimens with Free-Free Resonant Column Tests

Specimen	Modulus		Poisson's Ratio	
	Average (MPa)	C.V. (percent)	Average	C.V. (percent)
Soft	70	0.8	0.47	2.3
Medium	219	0.7	0.50	1.1
Hard	916	0.0	0.50	0.0

Comparison of Results from Different Tests

Compared in Figure 5.9 are the variations in modulus values obtained from the three tests with frequency of excitation for the soft, medium and hard specimens. The results from the static tests are arbitrarily plotted at a frequency of 0.1 (to approximate zero Hz). The moduli from the resilient modulus tests are plotted at a frequency of 10 Hz—an approximate frequency corresponding to the reciprocal of the duration of the loading pulse. For resonant column tests, the actual frequencies were measured, and therefore, the moduli are plotted at the appropriate frequencies.

As reported by Stokoe et al. (1991), the synthetic specimens behave in a visco-elastic manner — i.e. modulus varies with frequency. This type of behavior is clearly exhibited in the synthetic specimens tested in this study.

Young's moduli obtained from the resonant column tests are higher than those obtained from resilient modulus tests. This can be attributed to the higher frequencies of excitation in these tests as compared to resilient modulus tests. Similarly, the results from the static tests are much lower than those measured from the resilient modulus tests. In general, a linear relationship exists between the modulus and the logarithm of frequency of testing, for all three specimens. This finding concurs with those of Stokoe et al. (1991).

The values of Poisson's ratio obtained from the three methods are quite similar. The Poisson's ratios of all three specimen are more or less about 0.5. This results is also in concurrence with findings of Stokoe et al.

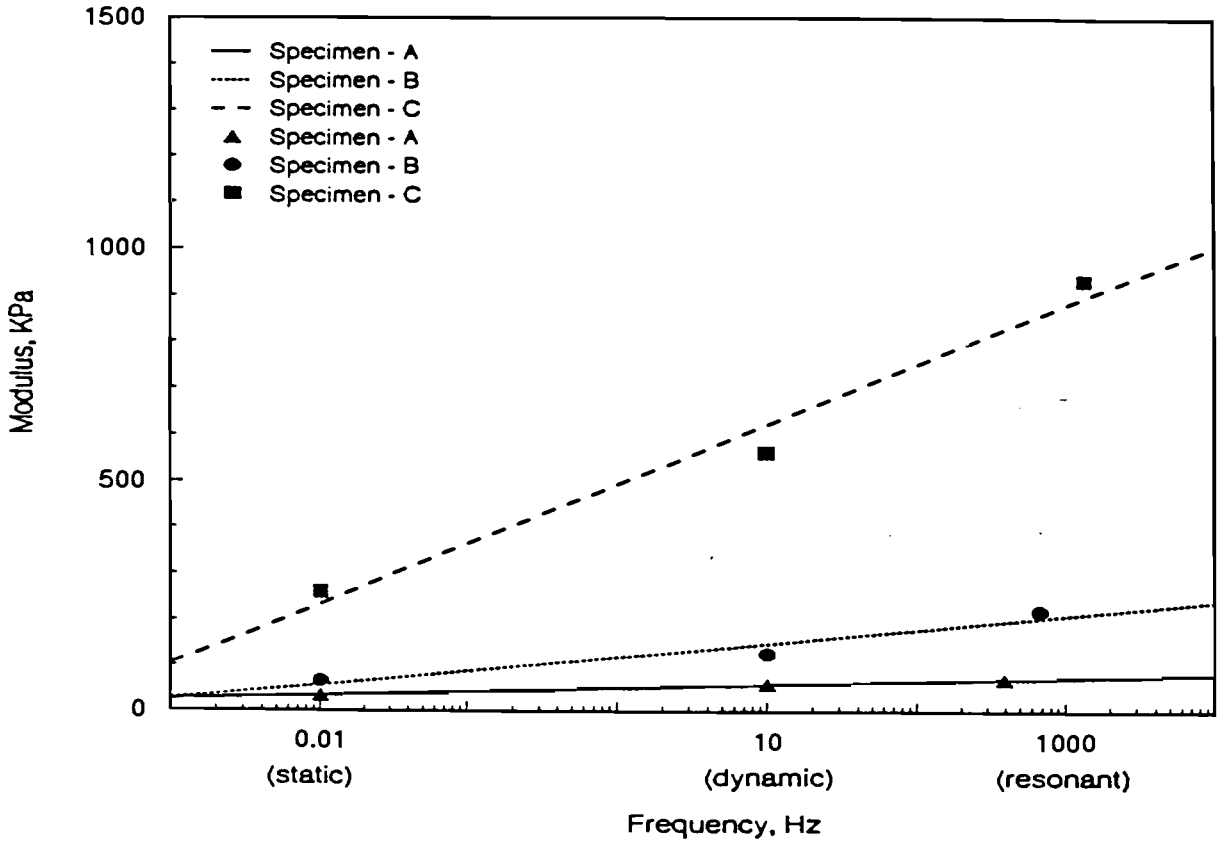

Figure 5.9 - Comparison of Moduli Obtained with Static, Resilient Modulus and Resonant Column Tests

Chapter 6

Testing of Base Materials

The process used to select the representative base materials is described in this chapter. Also included is the index properties of the selected base materials.

Material Selection

The first step in selecting the representative samples was to identify the most commonly used base materials in the state. The type, source and quantity of materials needed were identified based on this information.

To determine the types of base materials used in the state, a questionnaire was prepared and distributed to all district laboratory engineers. The questionnaire was prepared with the assistance of the Project Director and the staff of the El Paso District.

The final version of the questionnaire, shown in Appendix B, was mailed in October, 1992, to all districts. One district chose not to respond. The results from the other 23 districts were organized in a database and analyzed. The findings were as follows: out of approximately 80,000 miles of highway included in the survey, about 92 percent is flexible and 8 percent rigid.

As shown in Figure 6.1, approximately 74 percent of the bases are constructed from granular materials (i.e. limestone, iron-ore, gravel, caliche). The rest are either treated with lime (12 percent), cement (8 percent), or asphalt (5 percent).

Figure 6.2 shows the distribution of the granular materials in the state. Approximately one-half of the base materials are limestone. The other materials used include about 15 percent iron-ore, 11 percent caliche, and 7 percent gravel.

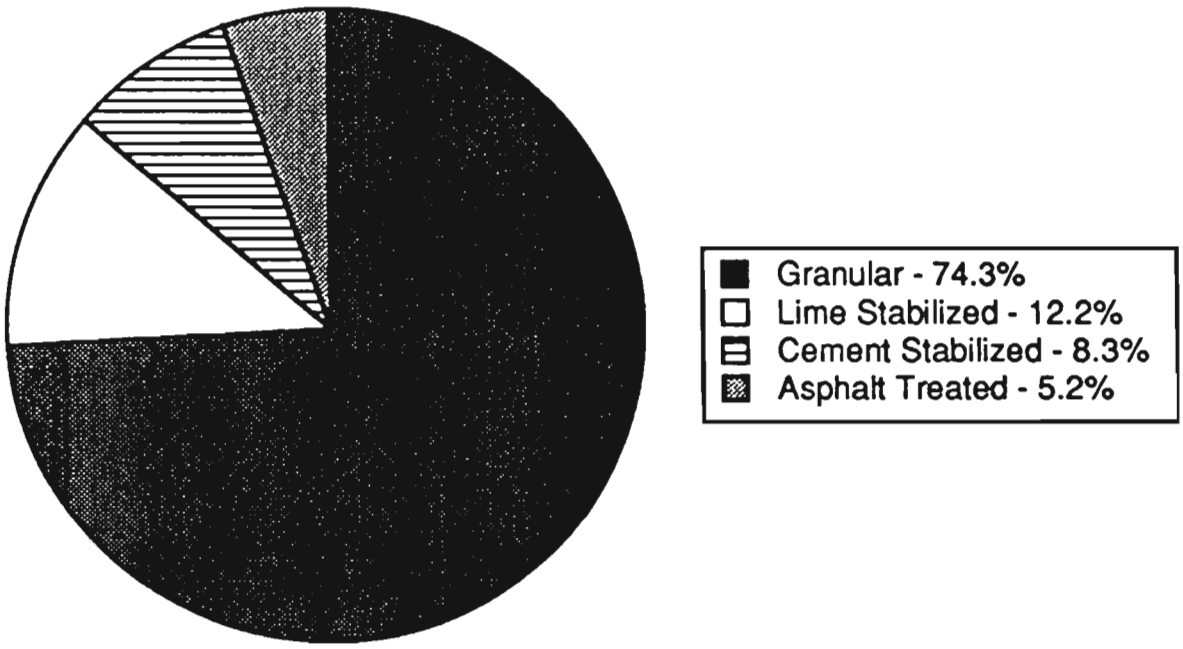

Figure 6.1 - Percentage of Base Material Types Used in Texas Highways.

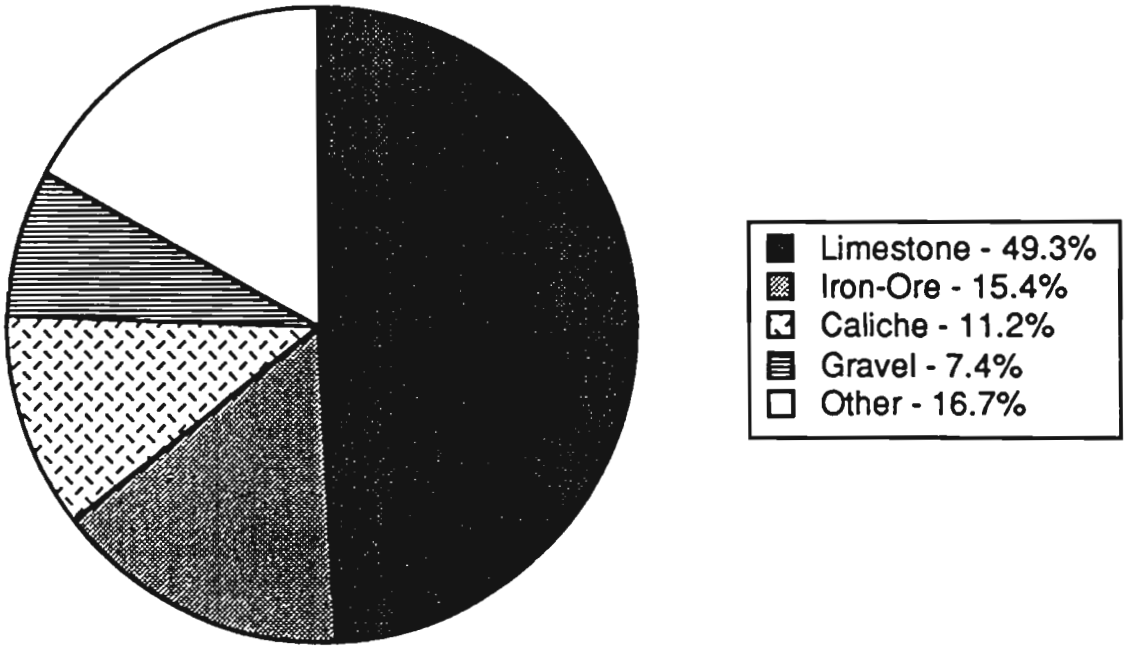

Figure 6.2 - Percentage of Granular Base Material Types used in Texas Highways.

Also identified were the variations in index properties of different granular base materials. These values are depicted in Table 6.1. As expected, some variations in all parameters were observed; however, in almost all cases the values are within ranges specified by TxDOT.

The primary parameter in selecting a material as base course depends on the availability of such material in the district. Also considered, especially when the base is supposed to be treated or stabilized, are other parameters, such as the traffic volume, pavement type and subgrade type.

Based upon the information gathered, ten base samples were requested from ten different districts, in which nine districts graciously provided the materials. The index properties of these materials are described in the next section. The materials provided consisted of five limestone, two caliche, one iron-ore and one gravel.

Table 6.1 Range of Properties of the Granular Base Materials

BASE	Max Particle Size (in)	Retain #4 (%)	Retain #40 (%)	Passing #200 (%)	LL (%)	PI (%)	Texas Triaxial	Wet Ball Mill (%)	OMC (%)	Actual Density (pcf)
Ash	1/5	45	65	N/A	17-25	2-8	2.8	34	13	108
Sandstone	1-1.75	35-60	65-75	71-75	18-30	2-14	1-2.7	23-43	7-10	123-136
Iron-ore	0.5-2.5	28-75	40-85	N/A	15-28	2-10	2.3-3	10	6-9	130-150
Gravel	1.5-1.75	30-75	60-80	N/A	15-40	5-14	3.3-3.7	41	5-11	125-142
Dolomite	1.75	45-75	60-85	N/A	N/A	12	N/A	50	5-8	130-138
Caliche	1-2	59-65	75-85	N/A	25-45	4-15	1-3	50	8-18	106-126
Limestone	1-1.75	40-75	60-90	76	12-40	0-16	1-3	5-50	4-11	123-148

Index Properties of Base Materials

Table 6.2 summarizes the results of index tests performed on the acquired base materials. The particle size distribution curves for all the base materials are shown in Figure 6.3. All the limestones are within the specifications for the Grade 4 base materials suggested by Tx-DOT. The gradation of all the other materials, also met the requirements, except for the iron-ore sample where the percentage retained on the No. 4 sieve was slightly below the minimum value given in the specifications.

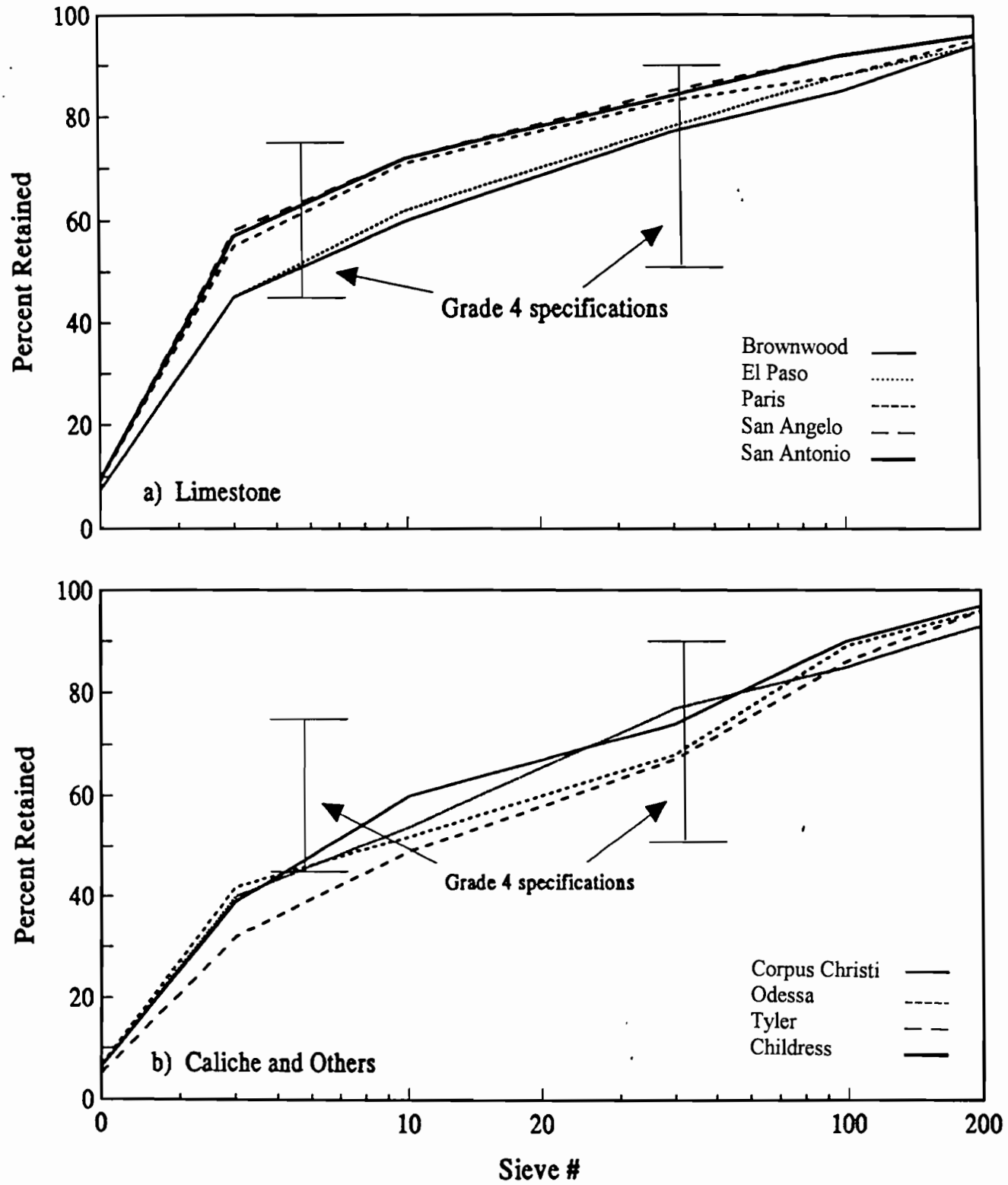

Figure 6.3 - Grain Size Distribution of Base Materials Obtained from Districts

Table 6.2 - Index Properties of Base Materials Used in This Study

Base	Retained #4 (%)	Retained #40 (%)	Retained #200 (%)	LL (%)	PI (%)	Optimum Moisture Content (%)	Dry Density Kg/m^3
Corpus Christi	38	73	4	33.0	10	17.8	16.6
San Angelo	57	85	4	14.6	2.1	6.5	22.9
Odessa	40	68	8	N/A	22.0	4.3	21.0
Brownwood	70	86	6	16.6	3.4	3.8	23.3
El Paso	52	79	7	24.0	8.0	5.4	22.9
Tyler	31	68	4	27.0	6.9	7.8	22.9
Childress	40	78	7	28.7	8.9	5.5	21.6
Paris	50	66	6	21.2	3.4	7.9	20.4
San Antonio	49	74	5	23,5	9.8	7.5	23.9

The Atterberg limits of the materials are exhibited in Figure 6.4. The liquid limits varied between 14.6 percent and 24.2 percent in the case of the limestones and varied between 2.1 percent and 9.8 percent in the plasticity index. The material from San Angelo was nearly non-plastic and the one from San Antonio was more plastic.

For the caliches, the material from Corpus Christi was more plastic than the sample from the Odessa District. The liquid limit and plasticity index of the Corpus Christi material is 33 and 10, respectively, while the Odessa material is 22 and 4.7, respectively.

The liquid limit and plasticity index for the iron-ore (Tyler) were 27.2 percent and 10 percent, respectively, and for the sand and gravel base (Childress) were 28.7 and 8.9 percent.

Out of the five limestones, three (Paris, San Angelo, and San Antonio) were well-graded, and the other two (Brownwood and El Paso) were clayey sands. The two caliches were classified as poorly graded clayey sands. The material from Odessa, also contained significant amount of silt. The other two materials (iron-ore, and sand and gravel) were also poorly graded clayey sands.

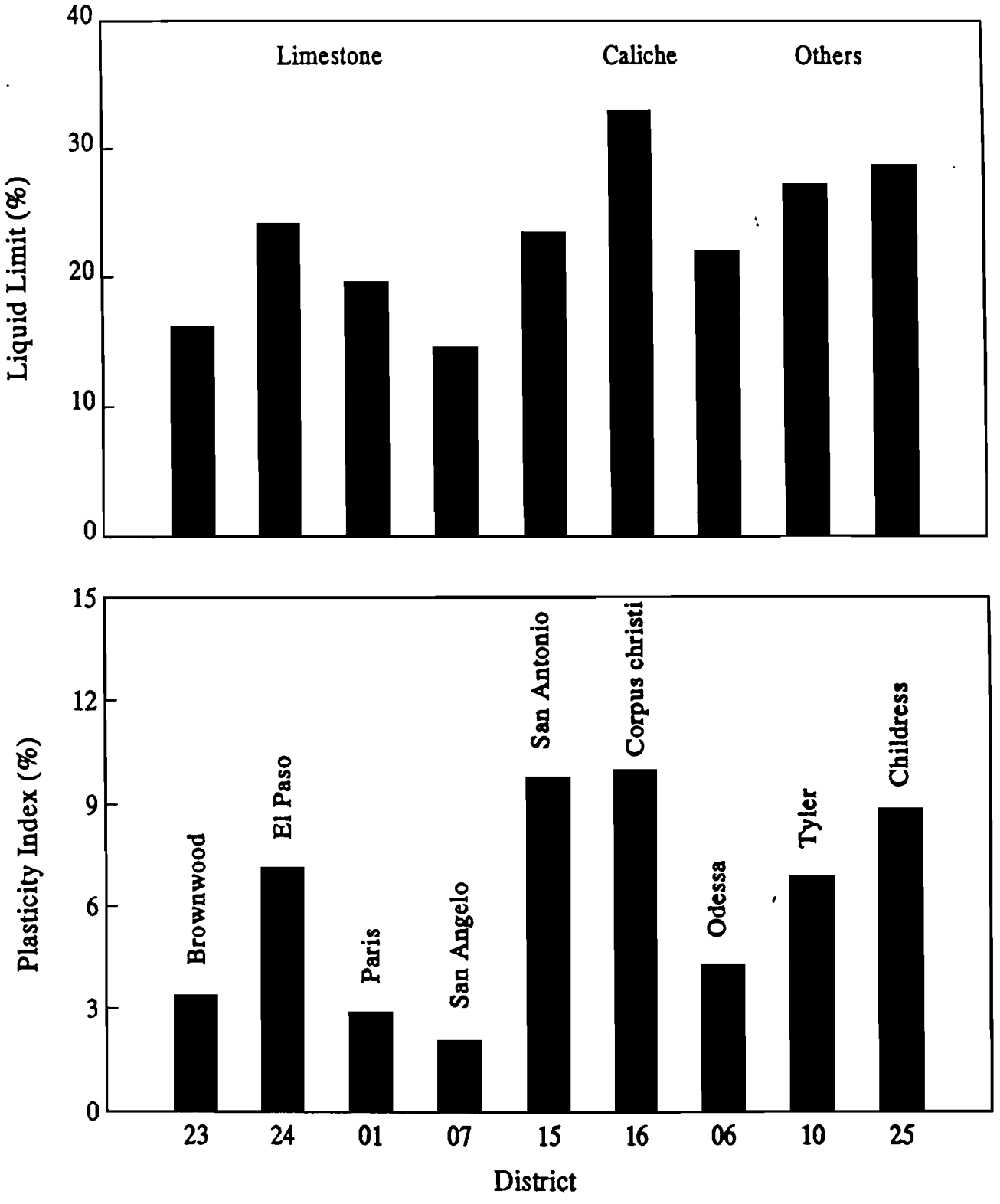

Figure 6.4 - Atterberg Limits of Base Materials Obtained from Districts

The optimum moisture contents and the corresponding dry densities are shown in Figure 6.5. The moisture content varied between 3.9 percent and 7.9 percent in the limestones. The material from Brownwood had the lowest value, and the materials from Paris and San Antonio had the highest values. The maximum dry densities of these materials varied between 20.4 KN/m^3 and 23.9 Kn/m^3. The material from Paris had the lowest density and the one from San Antonio had the highest.

In caliches, the material from Odessa had an optimum moisture content of 6.7 percent and the one from Corpus Christi 17.8 percent. The maximum dry density of the former was 21.0 Kn/m^3 and the latter was 16.6 Kn/m^3. The iron-ore material (Tyler) had a maximum dry density of 22.9 Kn/m^3 at an optimum moisture content of 7.8 percent. The sand and gravel base (Childress) had a maximum dry density of 21.6 Kn/m^3 at an optimum moisture content of 6.7 percent.

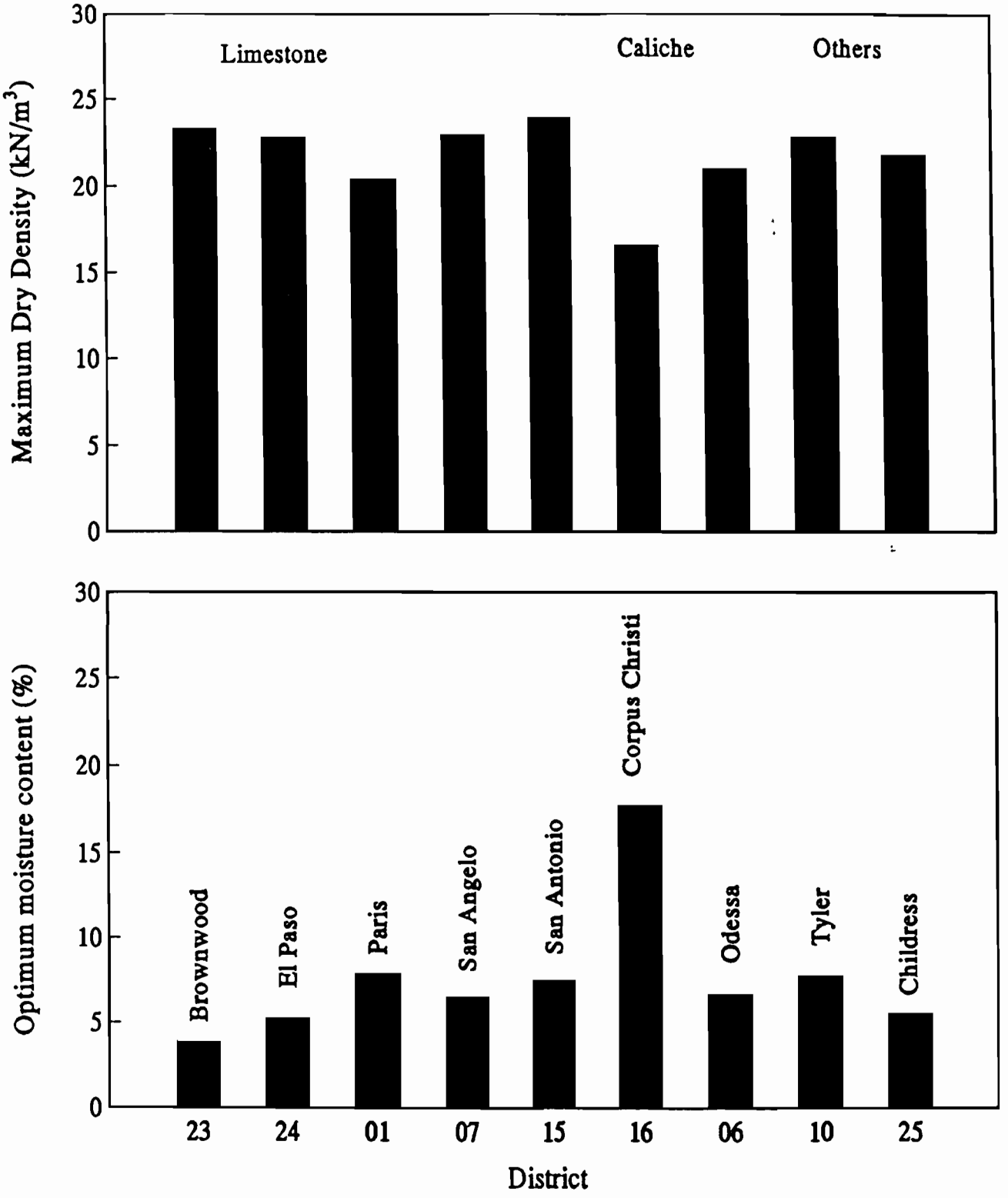

Figure 6.5 - Compactive Characteristics of Materials Used in This Study

Chapter 7

Resilient Modulus Tests

Resilient modulus tests were performed on all the base materials listed in Chapter 6, utilizing the procedure previously described in Chapter 3. A minimum of six specimens were tested from each sample — two specimens compacted at optimum moisture content, two dry of optimum and two wet of optimum. The specimens were tested at different moisture contents, so that the sensitivity of the moduli to moisture content could be determined. Replicate specimens were tested at each moisture content, so that the repeatability of the results could be verified. The results obtained from these tests are presented and briefly discussed below.

Presentation of Results

Shown in Figure 7.1 are variations in resilient modulus and Poisson's ratio of two similar limestone specimens with deviatoric stress and confining pressure. The modulus values are more or less independent of deviatoric stress, and highly dependent on confining pressure. This is the typical behavior expected from this type of material. Poisson's ratio of the specimen is fairly constant, and more or less about 1/3 independent of confining pressure or deviatoric stress. The two independent specimens yield very similar results, indicating the repeatability associated with the process.

Figure 7.2 shows the variations in resilient modulus and Poisson's ratio of sand and gravel specimen with deviatoric stress and confining pressure. Once again, the moduli are more or less independent of deviatoric stress. The modulus values almost increase linearly with the confining pressure. This is a behavior which is similar to that of the limestone specimens. However, the variation in modulus with confining pressure is less, when compared to the limestone. An increase in confining pressure can also be observed, with a small decrease in Poisson's ratio (from about 0.35 to 0.30). This can be attributed to the presence of fines in this material.

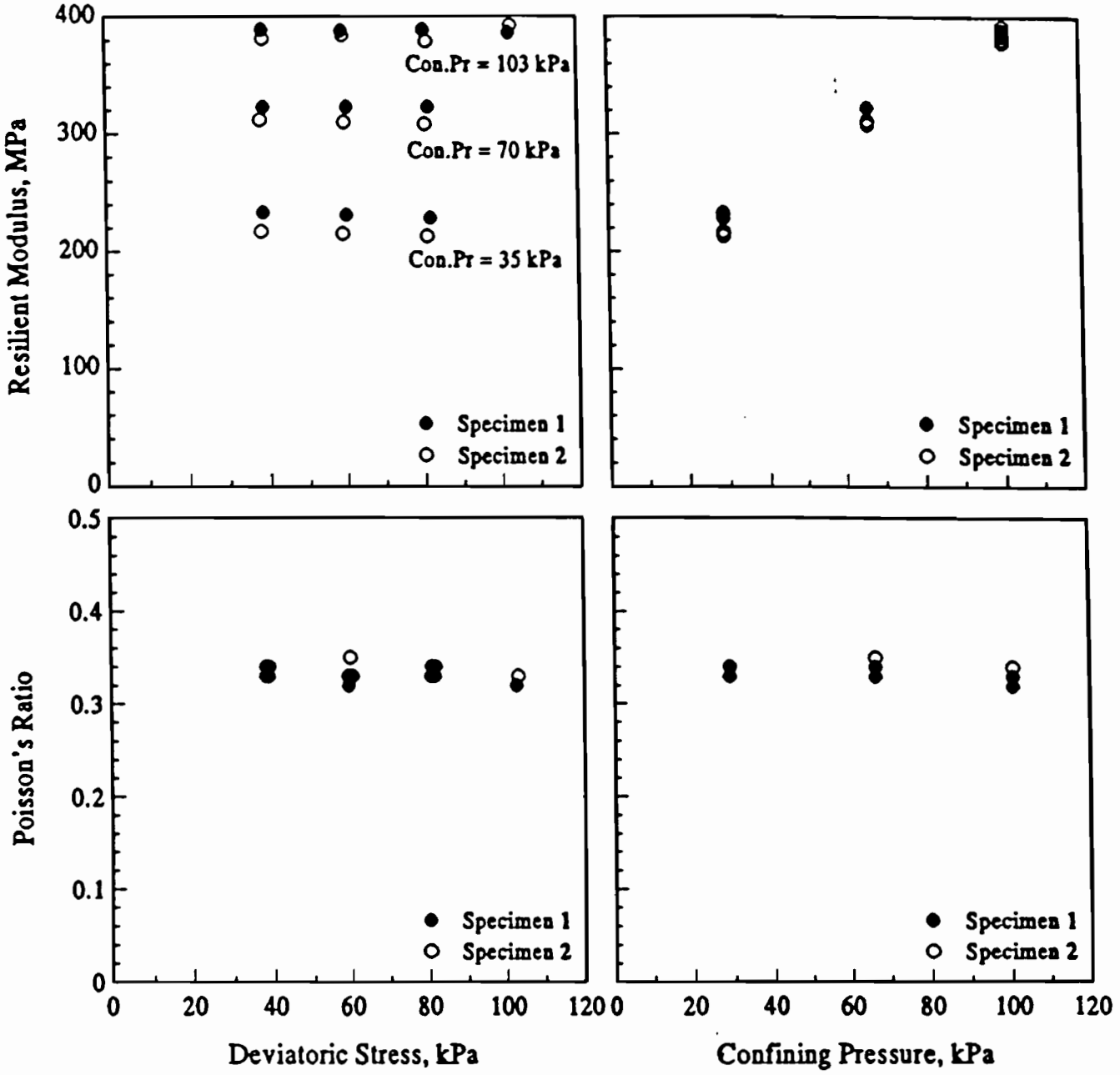

Figure 7.1 - Typical variation in Modulus and Poisson's Ratio with Deviatoric Stress and Confining Pressure for Limestone

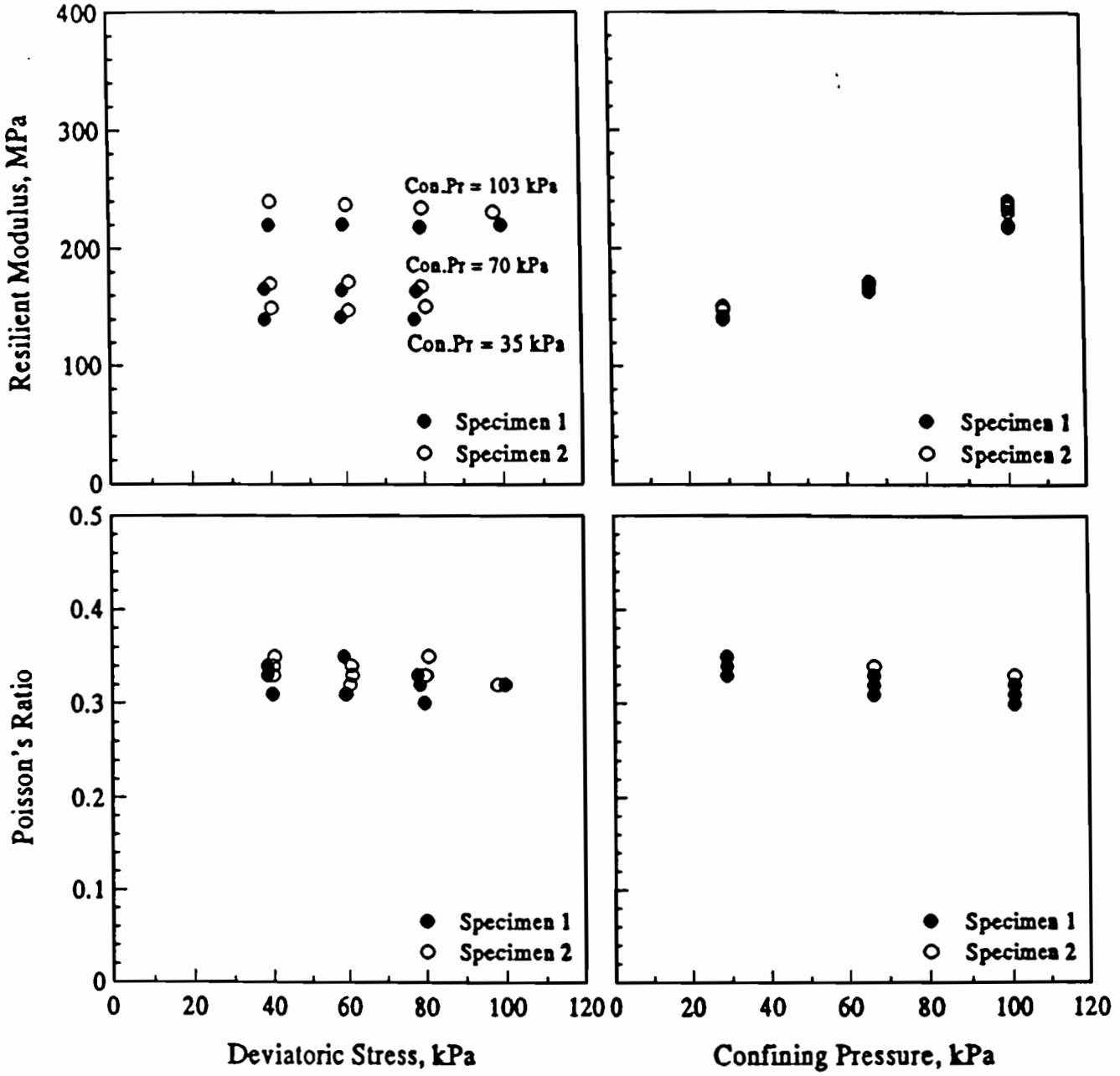

Figure 7.2 - Typical variation in Modulus and Poisson's Ratio with Deviatoric Stress and Confining Pressure for Sand and Gravel

As shown in Figure 7.3, the resilient modulus of the caliche can be considered independent of confining pressure and deviatoric stress. This is typical behavior expected from material containing high calcium-carbonate content. Similarly, the Poisson's ratio seems to remain constant at about 1/3 for all confining pressures and deviatoric stresses.

The variations in modulus and Poisson's ratio for all materials are included in Appendix C; however, the results are summarized below.

Included in Figure 7.4 are the resilient moduli and Poisson's ratios of the five limestone base materials as a function of confining pressure for the lowest deviatoric stress. The maximum variation in modulus with confining pressure could be observed in the case of the Brownwood specimen, while in the Paris specimen the minimum variation could be observed. At the highest confining pressure, the material from San Angelo had the highest modulus (430 MPa) and Paris had the lowest (320 MPa). At the lowest confining pressure, the material from San Angelo material was the stiffest (260 MPa) and the material from Brownwood exhibited the lowest modulus (150 MPa).

The Poisson's ratio does not vary much with the confining pressure for all materials. The largest variation was observed for samples from the Paris District, where it varied from 0.35 to 0.39. In general, a Poisson's ratio of 0.35 may be a good representative value for the limestones tested.

The resilient moduli and Poisson's ratios for the two caliche base materials are shown in Figure 7.5. These materials do not show any variation in stiffness with changes in confining pressure. Resilient modulus was 160 MPa for the Corpus Christi base, and was 240 MPa for the Odessa base. The Poisson's ratio of these materials did not vary with confining pressure. The values were 0.37 for the former and 0.35 for the latter.

The resilient moduli and Poisson's ratios of the other two base materials are also exhibited in Figure 7.5. The modulus and Poisson's ratio of iron-ore (Tyler) material do not vary with confining pressure. The values being 180 MPa and 0.3 respectively. The modulus of sand and gravel (Childress) varies from 110 MPa at a confining pressure of 29 KPa, to 180 MPa at a confining pressure of 101 KPa. The Poisson's ratio remained constant at about 0.3.

Figure 7.6 shows the moduli obtained from specimens compacted both dry and wet of optimum, normalized with the values obtained from the specimens compacted to optimum moisture content. The normalized values of specimens compacted dry of optimum varied between 0.50 and 0.85. In limestones, the numbers varied with confining pressure. For most bases, the lower numbers were observed at the lower confining pressures and the higher numbers at the higher confining pressures. Only in the case of Brownwood base the trend was the opposite.

In caliches, for specimens compacted dry of optimum the normalized values were 0.75 for Corpus Christi base and 0.5 for Odessa base. They did not vary with confining pressure as the moduli

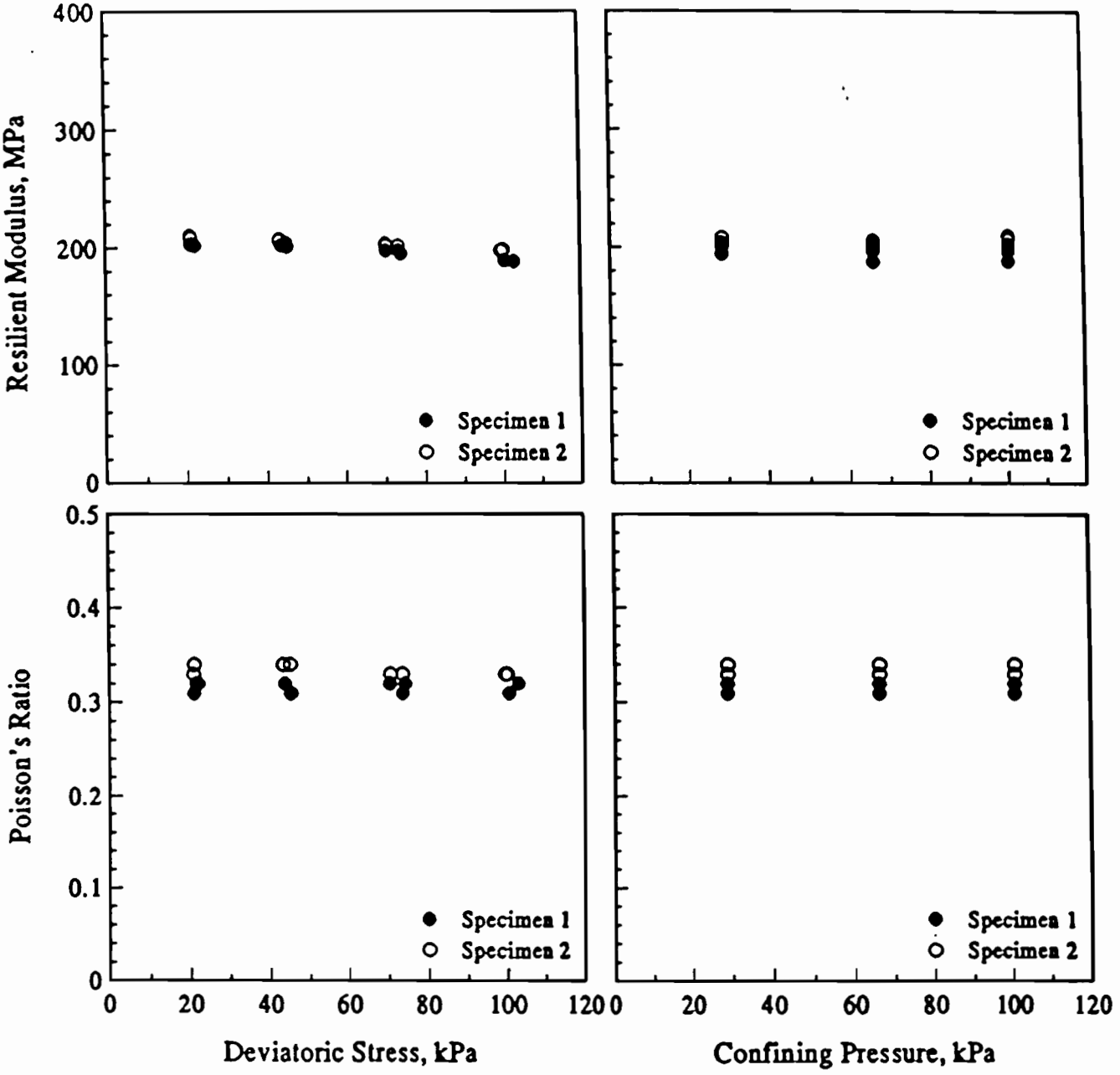

Figure 7.3 - Typical variation in Modulus and Poisson's Ratio with Deviatoric Stress and Confining Pressure for Caliche

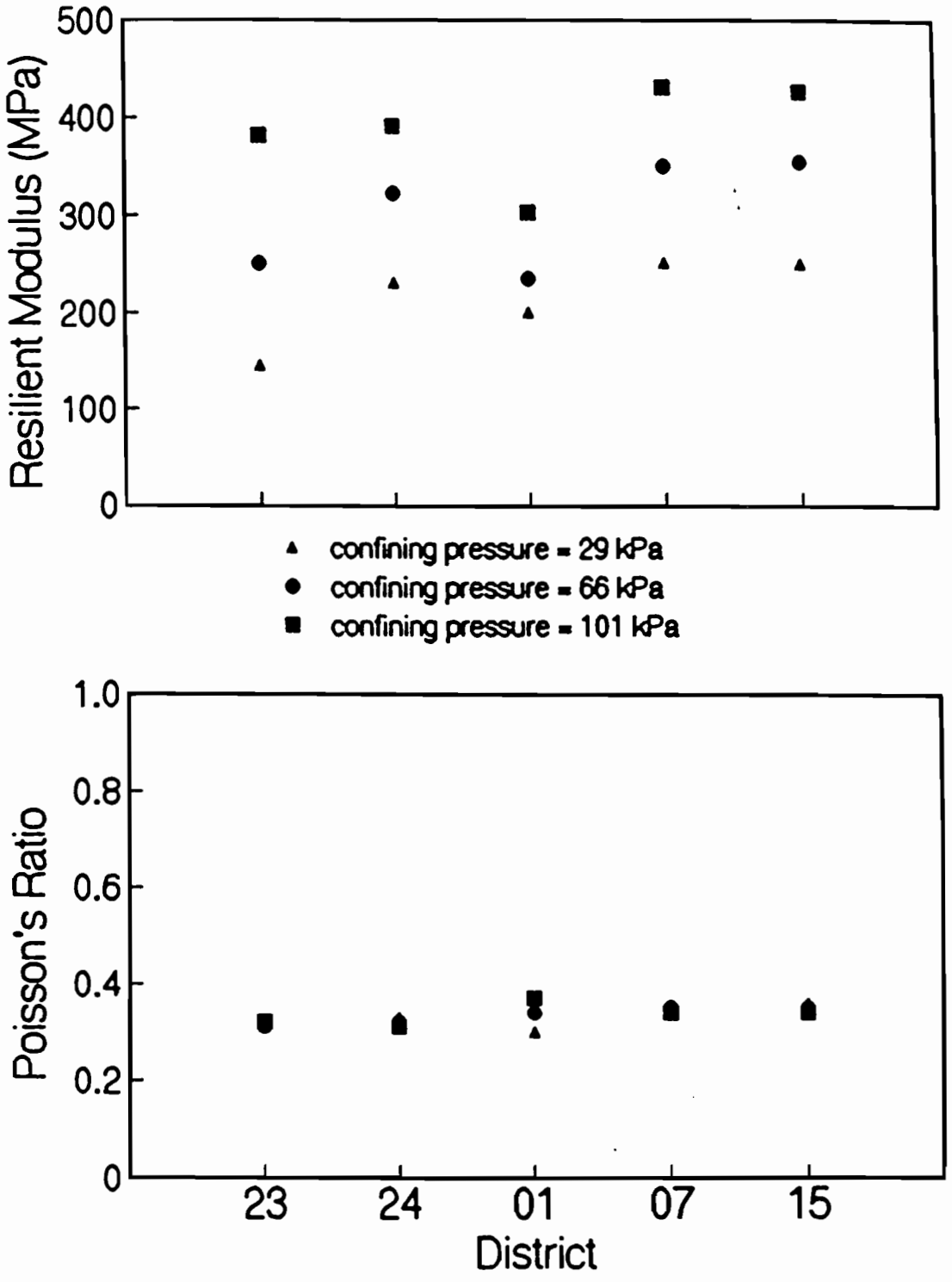

Figure 7.4 - Variations in Moduli and Poisson's Ratios of Different Limestone Bases

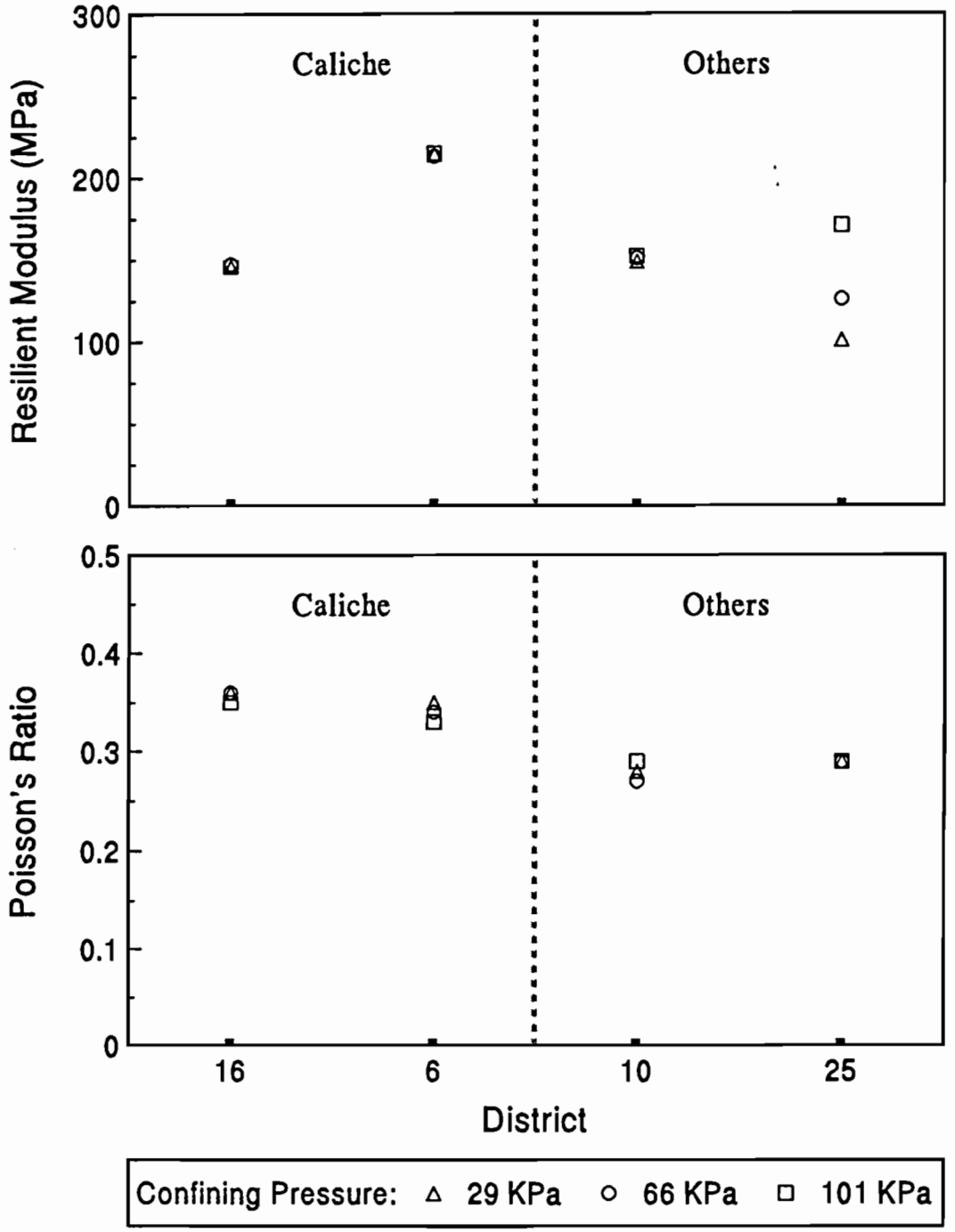

Figure 7.5 - Variations in Moduli and Poisson's Ratios of Other Bases

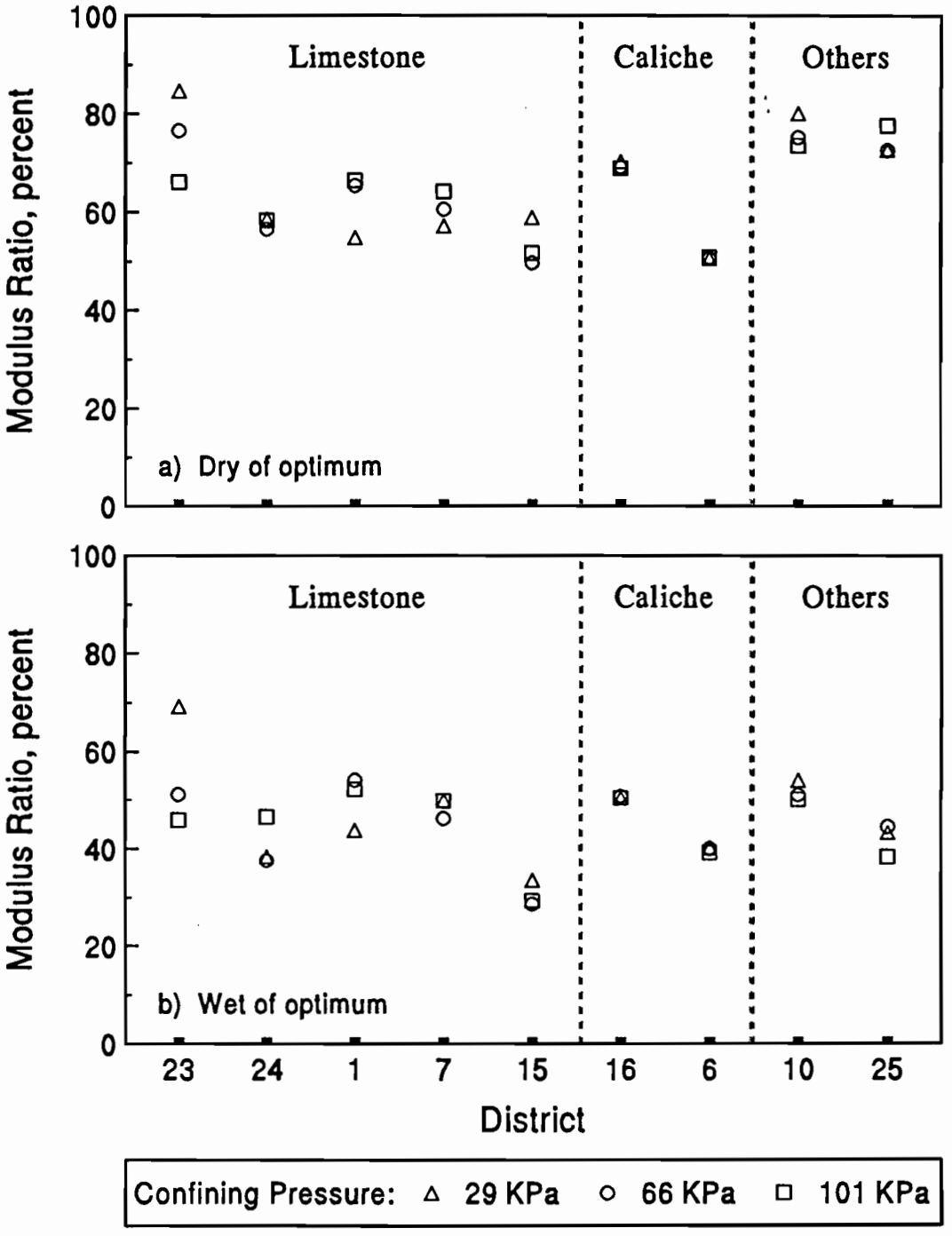

Figure 7.6 - Influence of Moisture Content on Moduli of Materials Tested

values. The values for iron-ore base varied slightly 0.75 at a confining pressure of 101 KPa to 0.8 at a confining pressure of 29 KPa. The values for sand and gravel (Childress) base varied slightly from 0.75 to 0.8, if the confining pressure varied from 101 KPa to 29 KPA.

The normalized values for specimens compacted wet of optimum varied between 0.3 and 0.7. In the case of specimens compacted dry of optimum, the trend was the same. Once again, the Brownwood base exhibited the opposite trend. The normalized modulus for the caliches were about 0.5 for the Corpus Christi base and 0.4 for the Odessa base with no variations at confining pressure. The values for the iron-ore (Tyler) varied from 0.48 to 0.50, when the confining pressure was decreased from 101 KPa to 29 KPa. The numbers for sand and gravel (Childress) varied from 0.40 to 0.43, when the confining pressure was decreased from 101 KPa to 29 KPa.

Even though no clear trends in the variations of modulus could be observed, it is clearly evident that the stiffness (modulus) of the base material (in some cases substantially) decreases, due to the materials being compacted with moisture contents other than optimum.

Constitutive Models

After the data was collected for each specimen, several alternative constitutive models were obtained. The conventional constitutive models (Equation 2.6) and the models suggested by Pezo et al. (Equation 2.9) and Feliberti et al. (Equation 2.12) were used.

Table 7.1 includes the model parameters and the quality of the fit for the conventional model applied to the results of the specimens tested at optimum water content. For each base sample, three sets of parameters are reported. The first two sets correspond to the results from the individual specimens tested. The third contains the average values from the two sets above.

For the limestones, the R^2 values vary between 0.76 and 0.95. Therefore, the model can be considered as acceptable for some of the samples. The model is quite inadequate for the caliches, and should not be used since the R^2 values are less than 0.2. The model is also not acceptable for the iron-ore sample, because in this case, the R^2 values are about 0.75. Finally, for the sand and gravel the model is marginal judged by the R^2 values which are about 0.85.

Tables 7.2 and 7.3 contain more comprehensive models suggested in Project 1177. The two models describe the data quite well. The R^2 values are above 0.99 for all soils, except the sand and grave, and even for the sand and gravel the R^2 values are above 0.94.

Based on the nine samples tested, it is difficult to judge which model is more appropriate, since the coefficients of determination very close to unity were obtained or almost all soils; therefore, hereafter the model suggested in Equation 2.9 will be considered.

The constitutive models for the specimens tested dry and wet of optimum water content exhibited similar trend. For the sake of brevity the corresponding tables are included in Appendix D.

Table 7.1 - Model Parameters for Constitutive Model Presented in Equation 2.6

Material	District	Specimen	Model Parameters*		R^2
			k1**	k2	
Limestone	23 Brownwood	1	3994	0.742	0.878
		2	3994	0.740	0.878
		Avg	3994	0.741	
	24 El Paso	1	16886	0.530	0.942
		2	11805	0.590	0.947
		Avg	14346	0.560	
	01 Paris	1	31819	0.370	0.762
		2	19696	0.310	0.869
		Avg	25758	0.340	
	07 San Angelo	1	29002	0.430	0.944
		2	13059	0.590	0.944
		Avg	21031	0.510	
	15 San Antonio	1	20357	0.510	0.949
		2	16305	0.550	0.947
		Avg	18331	0.530	
Caliche	16 Corpus Christi	1	155320	-0.020	0.064
		2	143711	-0.010	0.026
		Avg	149520	-0.015	
	06 Odessa	1	224780	-0.020	0.138
		2	225884	-0.020	0.170
		Avg	225332	-0.020	
Iron-Ore	10 Tyler	1	93707	0.100	0.776
		2	102531	0.070	0.741
		Avg	98119	0.085	
Sand and Gravel	25 Childress	1	14976	0.450	0.886
		2	14768	0.460	0.834
		Avg	29744	0.455	

* $M_R = k_1\theta^{k2}$ ** M_R, k_1 and θ are in KPa

Table 7.2 - Model Parameters for Constitutive Model Presented in Equation 2.9

Material	District	Specimen	Model Parameters			R^2
			k1	k2	k3	
Limestone	23	1	12548	0.022	0.711	0.999
		2	12548	0.020	0.710	0.999
		Avg	12548	0.021	0.711	
	24	1	58047	-0.010	0.420	0.999
		2	44670	0.000	0.460	0.999
		Avg	51359	-0.005	0.440	
	01	1	67205	-0.010	0.330	0.996
		2	39312	-0.010	0.430	0.999
		Avg	53259	-0.010	0.380	
	07	1	77417	0.000	0.340	0.996
		2	51330	-0.010	0.470	0.998
		Avg	64374	-0.005	0.405	
	15	1	67845	-0.010	0.400	0.999
		2	59695	-0.010	0.430	0.999
		Avg	63770	-0.010	0.415	
Caliche	16	1	155258	-0.040	0.020	0.999
		2	149874	-0.030	0.030	0.999
		Avg	152566	-0.035	0.025	
	06	1	231694	-0.040	0.000	0.999
		2	230308	-0.040	0.000	0.999
		Avg	231001	-0.040	0.000	
Iron-ore	10	1	128396	-0.030	0.080	0.999
		2	129040	-0.020	0.070	0.999
		Avg	128718	-0.025	0.075	
Sand and Gravel		1	39348	0.020	0.340	0.967
		2	42748	0.010	0.350	0.946
		Avg	41048	0.015	0.345	

Table 7.3 - Model Parameters for Constitutive Model Presented in Equation 2.12

Material	District	Specimen	Model Parameters			R^2
			k1	k2	k3	
Limestone	23	1	15577	0.023	0.727	0.999
		2	15577	0.020	0.720	0.999
		Avg	15577	0.022	0.724	
	24	1	53208	-0.010	0.420	0.999
		2	46633	0.000	0.460	0.999
		Avg	49921	-0.005	0.440	
	01	1	58970	-0.010	0.320	0.996
		2	42721	-0.010	0.440	0.999
		Avg	50846	-0.010	0.380	
	07	1	78295	0.000	0.340	0.996
		2	48634	0.000	0.460	0.998
		Avg	63465	-0.005	0.400	
	15	1	62112	-0.010	0.400	0.999
		2	56517	0.000	0.430	0.999
		Avg	59315	-0.005	0.415	
Caliche	16	1	98582	-0.040	0.010	0.999
		2	108453	-0.030	0.030	0.999
		Avg	103518	-0.035	0.020	
	06	1	142923	-0.040	0.000	0.999
		2	149271	-0.040	0.000	0.999
		Avg	146097	-0.040	0.000	
Iron-ore	10	1	94243	-0.030	0.080	0.999
		2	101413	-0.020	0.060	0.999
		Avg	97828	-0.025	0.070	
Sand and Gravel		1	49915	0.020	0.350	0.967
		2	48130	0.010	0.350	0.946
		Avg	49023	0.015	0.350	

The results of the resilient moduli obtained from all specimens were combined in one database to obtain the most general-purpose representative model. The factors considered in the model are as follows: 1) the liquid limit (LL), 2) relative density (DR), 3) moisture content (MC), and 4) plasticity index (PI), as well as, the deviatoric stress (σ_d), and confining pressure(σ_c). After extensive statistical analyses, the most favorable model was found to be in the form of

$$M_R = K_1 \, \sigma_d^{k2} \, \sigma_c^{k3} \tag{7.1}$$

where

$$K_1 = e^{a - b\,(LL) - c\,(MC) + d\,(DR)} \; PI^e \tag{7.2}$$

The advantage of this model is that it maintains the general form of the model used for individual specimens (i.e. Equation 2.9), while the characteristics of soils in terms of index properties are reflected in the constant parameter of the model (i.e. K_1).

When this model was applied to the moduli measured for all soil samples, the equation became

$$M_R = e^{5.425 - 0.065\,LL - 0.025\,MC} \; \sigma_d^{-0.059} \; \sigma_c^{0.310} \; PI^{0.44} \tag{7.3}$$

In the above equation, the index property that most influences the model, is the plasticity index, whilst the liquid limit and moisture content influence the modulus to a lesser extent. In terms of the state of stress, the confining pressure significantly affects the modulus, while the deviatoric stress has little effect.

Unfortunately, the R^2 value is about 0.6 for this relationship; therefore, the model is not representative of the data. A less general model should then be developed.

In the next step, three separate models were developed using the same general model defined in Equation 7.1. The three models correspond to the resilient moduli from data collected for specimens tested at optimum, at wet of optimum, and at dry of optimum water contents.

Included in Table 7.4 are the fit parameters for the three models, as well as, the coefficient of determination for each model. As for the general equation, the plasticity index has the most significant effect on the resilient modulus. This effect is less pronounced as the soil becomes wetter. The exponent for parameter PI (constant d in Table 7.4) decreases from 1.198 to 0.719 to 0.142 for specimens compacted dry of, at and wet of optimum moisture content, respectively.

Parameter a is more or less constant at about seven. The liquid limit contributes only slightly to the modulus. Constant b in Table 7.4, decreases from 0.15 to 0.11 to 0.07, as the soil becomes progressively wetter. The negative sign for this parameter indicates that as the liquid limit increases the modulus should decrease. This observation is in concurrence with the previous studies by other researchers, such as Thompson and Robnett.

The moisture content has a little affect, as well. The value of the constant c is more or less constant at about 0.02 or 0.03. Based on the sign of this parameter, as the moisture content increases the modulus should increase. This conclusion may not be true in all cases; therefore the parameter can be considered a mathematical convenience, rather than a physical phenomenon.

In terms of the state of stress, it seems that the deviatoric stress has a small affect on the modulus values. Constant k_2 is rather small and can probably be ignored. The exponent of confining pressure (k_3) is quite constant and is about 1/3. Based on many studies in earthquake geotechnical engineering laboratory testing, this value is quite reasonable.

The quality of fit is relatively good judging by the R^2 values. For the specimens tested wet and dry of optimum moisture contents, the R^2 values are about 0.82. For the specimens prepared at the optimum water content, this value is improved to about 0.89. Therefore, it seems that these relationships can be used at least as a first approximation.

Table 7.4 - Model Parameters for Equation 7.1

Water Content	Parameters Related to Index Properties K_1					Parameters Related to State of Stress		R^2
	a	b	c	d	e	k2	k3	
Dry of Optimum	7.465	-0.153	0.036	-0.068	1.198	-0.015	0.321	0.823
Optimum	7.531	-0.110	0.025	---	0.719	-0.009	0.319	0.895
Wet of Optimum	6.539	-0.072	0.021	0.229	0.142	-0.011	0.335	0.828

Table 7.5 includes a summary of the results, the average, standard deviation and the coefficient of variation of moduli for each soil and each moisture condition. These values can perhaps be used in the network pavement condition surveys. However, one should carefully consider the large coefficients of variation obtained for each type of base.

The average values are included in Figure 7.7. The moduli range from a high of 295 MPa measured for the limestone at an optimum moisture content, to a low of 65 MPa for the sand and gravel wet of optimum moisture content.

Table 7.5 and Figure 7.7 also contain the average values of the Poisson's ratios measured for different types of soil. The coefficients of variation associated with these materials are, by far less than those measured for moduli. For almost all bases, Poisson's ratios measured for the specimens prepared dry of optimum are slightly higher than those measured for the specimens prepared at or wet of optimum moisture contents. The latter two cases, the Poisson's ratio are more or less constant at about 0.30. The overall averages of the Poisson's ratios are 0.37, 0.31 and 0.30 for specimens prepared dry, at or wet of optimum water content, respectively.

As indicated before, the main intent of this report is to introduce the recommended procedures and testing protocol. In the next report, an extensive analysis of the results will be presented.

Table 7.5 - Average Stiffness parameters Measured for Different Types of Base

Base Type	Specimen Moisture*	Resilient Modulus, MPa			Poisson's Ratio		
		Average	Standard Deviation	C.V.	Average	Standard Deviation	C.V.
Lime-stone	Dry	219	87	39.8%	0.36	0.02	5.3%
	Optimum	295	86	29.2%	0.33	0.02	6.8%
	Wet	129	42	32.7%	0.29	0.03	11.5%
Caliche	Dry	94	3	2.9%	0.33	0.03	10.2%
	Optimum	174	28	16.0%	0.33	0.02	3.8%
	Wet	71	3	4.1%	0.28	0.02	2.9%
Iron-Ore	Dry	119	3	2.5%	0.38	0.01	2.5%
	Optimum	158	7	4.6%	0.25	0.01	3.9%
	Wet	71	2	3.1%	0.29	0.01	2.9%
Sand and Gravel	Dry	139	29	21.1%	0.41	0.01	2.9%
	Optimum	185	37	20.2%	0.33	0.01	4.4%
	Wet	65	12	17.8%	0.33	0.02	6.4%

* Dry and wet correspond to specimens with a moisture content of about 2% less than or more than optimum, respectively

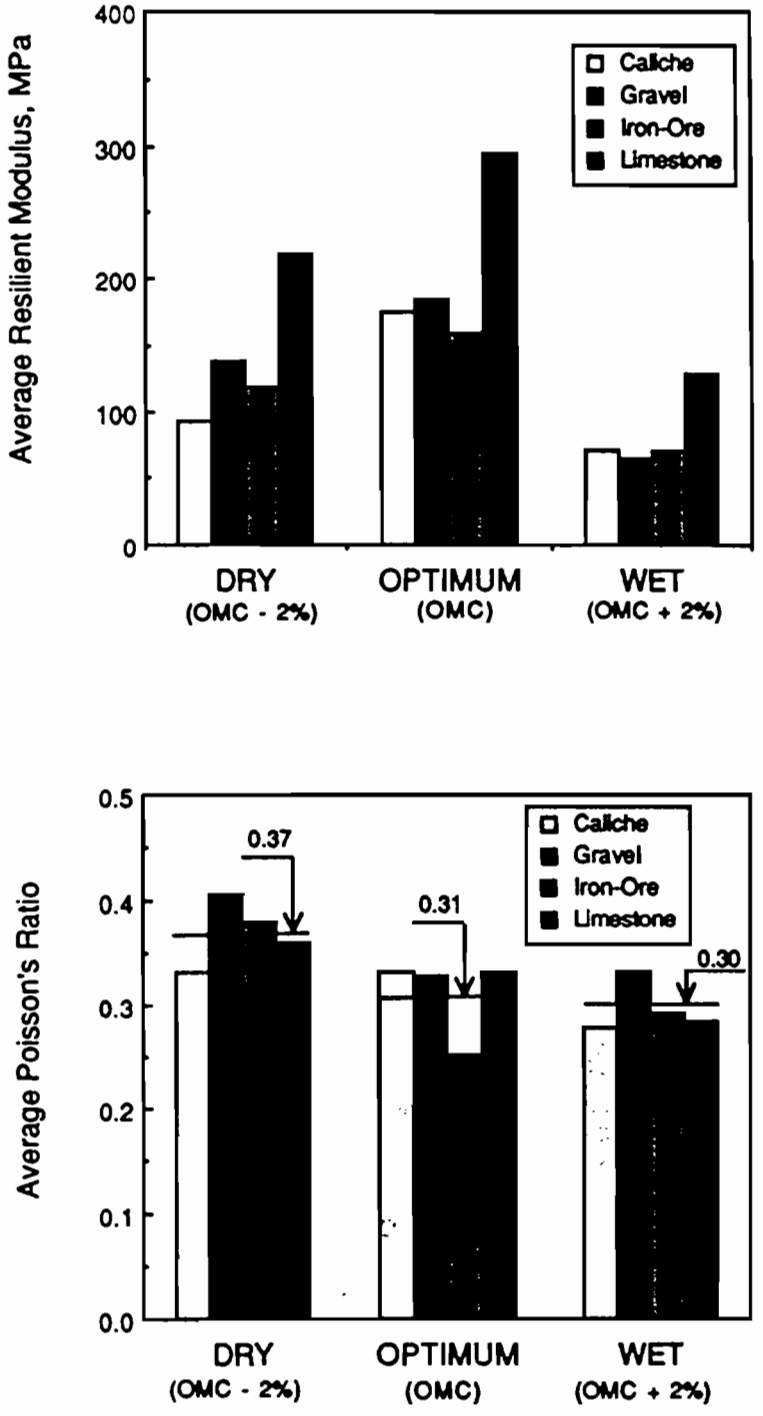

Figure 7.7 - Average Values of Moduli and Poisson's Ratios of each Base Material Tested

Chapter 8

Summary and Conclusions

AASHTO has adopted three new methodologies for resilient modulus testing of granular materials in the last few years. The newest procedure (AASHTO T294-92), which basically reflects the procedure suggested by SHRP, is significantly more convenient to perform, when compared to the initial procedure adopted by AASHTO (e.g. AASHTO T274). However, some aspects of the testing methodology are still being investigated and modified.

The main objectives of the study reported herein were: 1) to critically assess the strengths and weaknesses of the AASHTO procedure as related to base materials, and 2) to develop a protocol which would avoid the possible weaknesses of the previous protocol.

In general the AASHTO protocol was found to be reasonable; however several modifications were suggested. These modifications are related to: 1) the loading sequence, 2) specimen conditioning, 3) the measurement of the axial deformation, and 4) the determination of Poisson's ratio. Specifically, the following modifications are suggested:

- A new loading sequence is proposed, which may minimize the specimen disturbance.

- Instead of using load conditioning, grouting the specimen to the top and bottom platen may yield more repeatable results.

- If the specimen is grouted, measuring the moduli over the length of the specimen is not appropriate. The optimal point for measuring the axial deformations may be the middle one-third of the specimen.

- The deformations can be measured more accurately, repeatable and more conveniently when non-contact probes are used.

- Poisson's ratio of the specimen can be measured with ease using non-contact probes. The new set-up yields Poisson's ratios, that seem more realistic than those measured with other set-ups.

The proposed modifications and theoretical or practical justifications for them are reported in detail. In addition, the results from laboratory tests performed using synthetic specimens and base materials collected from different districts in Texas are summarized. The modified methodology provides more accurate and repeatable measurement of the resilient modulus.

References

1. Burczyk J., K. Ksaibati, R. Anderson-Sprecher, and M. Farrar, Factors Influencing the Determination of a Subgrade Resilient Modulus Value, *Presented at the 73rd Annual Meeting of the Transportation Research Board*, Washington, D.C., 1994.

2. Bergan A. T., and Culley R. W., Some Fatigue Considerations in the Design of Asphalt Concrete Pavements, *Symp. on Frost Action of Roads*, Organization for Economic Cooperation and Development, Oslo, Norway, pp. 33-77, 1973.

3. Bergan A. T., and Fredlund D. G., Characterization of Freeze-Thaw Effects on Subgrade Soils, *Symp. on Frost Action of Roads*, Organization for Economic Cooperation and Development, Oslo, Norway, pp. 119-143, 1973.

4. Bergan A.T., and Monismith C. L., Characterization of Subgrade Soils in Cold Regions for Pavement Design Purposes, *Hwy. Res. Record 431*, pp. 25-37, 1973.

5. Chamberlain E. J., A Model for predicting the influence of Closed System Freeze-Thaw on the Strength of Thawed Soils, *Symp. on Frost Action on Roads*, Organization for Economic Cooperation and Development, Oslo, Norway, pp. 94-97, 1973.

6. Chen D.H., M.M. Zaman, and J.G. Laguros, Resilient Moduli of Aggregate Materials: Variability Due to Testing Procedure and Aggregate Type, *Presented at the 73rd Annual Meeting of the Transportation Research Board*, Washington, D.C., 1994.

7. Cochran G. R., Minnesota Department of Transportation Experience with Laboratory MR Testing, *Workshop on Resilient Modulus Testing*, Oregon State University Corvallis, Oregon, March 1989.

8. Culley R. W., Effect of Freeze-Thaw Cycling on Stress-Stain Characteristics and Volume Change of a Till Subjected to Repetitive Loading, *Can. Geotech. J.*, Vol 8, No. 3, pp. 359-371, 1970.

9. Dehlen G. L., The Effect of Non-linear Response on the Behavior of Pavements Subjected to Traffic Loads, *doctoral dissertation*, University of California, Berkeley, 1969.

10. Dhamrait J. S., Illinois' Experience with Resilient Modulus, *Workshop on Resilient Modulus Testing*, Oregon State University, Corvallis, Oregon, March, 1989.

11. Elliot R. P., and Thornton S. I., Resilient Modulus and AASHTO Pavement Design, *Transp. Res. Record 1196*, pp. 116-124, 1988.

12 Feliberti M., Nazarian, S., and Srinivasan T., Critical Evaluation of Parameters Affecting Resilient Modulus Tests on Subgrades, *Res. Report 1177-2*, Volume 1, University of Texas at El Paso, El Paso, Texas, 1992.

13. Finn F. N., Nair K., and Monismith C. L., Application of Theory in the Design of Asphalt Pavements, *Third Int'l Conf. on the Structural Design of Asphalt Pavements*, Vol. 1, pp. 329-409, 1972.

14. Fredlund D. G., Bergan A. T., and Sauer E. K., Deformation Characterization of Subgrade Soils for Highway and Runways in Northern Environments, *Can. Geotech. J.*, Vol. 12, pp. 213-223, 1975.

15. Hicks G.R., and C.L. Monismith, Factors Influencing the Resilient Response of Granular Materials, *Highway Research Record 345*, National Research Council, Washington, D.C., pp. 15-31, 1981.

16. Ho R.K.H., Repeated Load Tests on Untreated Soils - A Florida Experience, *Workshop on Resilient Modulus Testing*, Oregon State University, Corvallis, Oregon, 1989.

17. Houston W.N., S.L.Houston, and T.W.Anderson, Stress State Considerations for Resilient Modulus Testing of Pavement Subgrades, *Transportation Research Record 1406*, National Research Council, Washington, D.C., 1993, pp. 124-132.

18. Huddleston I. J., and Zhou H., Round Robin Tests Results in Pavement Design, *Workshop on Resilient Modulus Testing*, Oregon State University, Corvallis, Oregon, 1989.

19. Jackson N.C., Thoughts on AASHTO T-274-82, Resilient Modulus of Subgrade Soils, WSDOT Materials Lab, Report No. 200, Workshop on Resilient Modulus Testing, Oregon State University, Corvallis, Orgeon, March, 1989.

20. Kamal M.A., A.R. Dawson, O.T. Farouki, D.A.B. Hughes, and A.A. Sha'at, Field and Laboratory Evaluation of the Mechanical Behavior of Unbound Granular Materials in Pavements, *Transportation Research Record 1406*, National Research Council, Washington, D.C., pp. 88-97, 1993.

21. Karasahin M., A.R. Dawson, and J.T. Holden, Applicability of Resilient Constitutive Models of Granular Material for Unbound Base Layers, *Transportation Research Record 1406*, National Research Council, Washington, D.C., pp. 98-107, 1993.

22. Kim D.S., and S. Drabkin, Accuracy Improvement of External Resilient Modulus (M_R) Measurements Using Specimen Grouting to End Platens, *Presented at the 73rd Annual Meeting of the Transportation Research Board*, Washington, D.C., 1994.

23. Mitchell J. K., Fundamental Aspects of Thixotraphy in Soils, *J. Soils Mech. Found. Engrg.*, ASCE, Vol. 86, pp. 19-52, 1960.

24. Nazarian S., and M.Feliberti, Methodology for Resilient Modulus Testing of Cohesionless Subgrades, *Transportation Research Record 1406*, National Research Council, Washington, D.C., 1993, pp. 108-115.

25. Pezo R.F., D.S. Kim, K.H. Stokoe II, and W.R. Hudson, A Reliable Resilient Modulus Testing System, *Transportation Research Record 1307*, National Research Council, Washington, D.C., pp. 90-98, 1991.

26. Pezo R. F., German C., Hudson W. R., and Stokoe K. H., Development of a Reliable Resilient Modulus Test for Subgrade and Non-Granular Subbase Materials for use in Routine Pavement Design, *Res. Report 1177-4f*, The University of Texas at Austin, Austin, Texas, 1992.

26. Rada G., and M.W. Witczak, Comprehensive Evaluation of Laboratory Resilient Moduli Results for Granular Material, *Transportation Research Record 810*, National Research Council, Washington, D.C., pp. 23-33, 1981.

27. Robnett Q. L., and Thomson M. R., Resilient Properties of Subgrade Soils, *Transportation Engineering Journal*, ASCE Vol. 105, No. TE1, pp. 71-89, 1979.

28. Seed H.B., Chan C. K., Lee C. E., *Resistance Characteristics of Subgrade Soils and Their Relation to Fatigue Failure in Asphalt Pavements*, International Conference on the Structural Design of Asphalt Pavements, August, 1962.

29. Seed H. B., Mitry F. G., Monismith C. L., and Chan C. K., Prediction of Flexible Pavement Deflections from Laboratory Repeated-Loads Tests, *NCHRP Report 35*, Highway Research Board, 1967.

30. Seim D.K., A Comprehensive Study on the Resilient Modulus of Subgrade Soils," *Workshop on Resilient Modulus Testing*, Oregon State University, Corvallis, Oregon, 1989.

31 Stokoe A., and Kim D. S., Deveopment of Synthetic Specimens for Calibration and Evaluation of Resilient Modulus Equipment, Transportation Research Board, 69th Annual Meeting, Washington, D. C., January, 1990.

32. Tanomota K., and Nishi M., On Resilence Characteristics of Some Soils Under Repeated Loading, *Soild and Foundations*, JSSMFE, Vol. 10, pp. 75-92, 1970.

33 Thompson M. R., Factors Affecting the Resilient Moduli of Soils and Granular Materials, Workshop on Resilient Modulus Testing, Oregon State University, Corvallis, Oregon, March, 1989.

34. Thompson M. R., and Robnett Q. L., Resilient Properties of Subgrade Soils, *Transportation Engineering Journal*, ASCE Vol. 105, No. TE1, pp. 71-89, 1976.

35. Urbina J., Pezo R. F., Nazarian S., and Picornel M., Parametric Investigation on the Stress and Strain distribution within Cylindrical Specimens Subjected to Triaxial Tests, *Submitted to ASCE Journal of Geotechnical Engineering for Publication.*

APPENDIX A

Draft Testing Protocol

DRAFT
STANDARD METHOD OF RESILIENT MODULUS TEST FOR UNBOUND GRANULAR BASE/SUBBASE MATERIALS

SCOPE

This test method provides a means for determining the Resilient Modulus, M_R, and Poisson's ratio, nu, of cylindrical specimens of granular base/subbase materials under conditions that represent a reasonable simulation of the physical conditions beneath flexible pavements subjected to moving wheel loads. The method provides for the measurement of recovered axial and lateral strains of specimens subjected to repetitive loadings. This test method is a modification of the standard method AASHTO T 294-92.

The properties determined with these procedures can be used in the available linear-elastic and non-linear elastic layered theories to calculate the physical response of pavement structures subjected to traffic loading. They can also be used in the design of pavements following the 1986- AASHTO Guide.

APPLICABLE DOCUMENTS:

- Test Method Tex-101-E, Preparation of Soil and Flexible Base Materials for Testing.
- Test Method Tex-103-E, Determination of Moisture Content in Soil Material.
- Test Method Tex-110-E, Determination of Particle Size Analysis of Soils.
- Test Method Tex-113-E, Laboratory Compaction Characteristics and Moisture-Density Relationship of Base and Cohesionless Sand
- Test Method Tex-117-E, Triaxial Compression Tests for Disturbed Soils and Base Materials.
- Test Method Tex-118-E, Triaxial Compression Test for Undisturbed Soils.

SUMMARY OF THE TEST METHOD

Repeated axial deviatoric forces of fixed magnitude, duration and frequency are applied to an appropriately prepared cylindrical specimen that is subjected to static confining pressures. During the load applications, the resilient axial and lateral deformations are measured to calculate the dynamic stiffness properties of the specimen, namely Resilient Modulus and Poisson's Ratio.

SIGNIFICANCE AND USE

The Resilient Modulus test provides a basic constitutive relationship between stress and strain of the pavement materials and a means of characterizing them under a variety of environmental and load conditions that simulate pavements subjected to moving wheel loads.

BASIC DEFINITIONS

1 P_{max} is the maximum applied axial load to the specimen consisting of the seating load and cyclic load (effect due to confining pressure is not included).

2 P_S is the seating load applied to the specimen to maintain a positive contact between the loading ram and the specimen top cap.

3 P_{cyclic} is the repetitive axial load (cyclic load) applied to the specimen.

4 σ_{max} is the axial stress applied to the specimen that consists of the seating load (P_S) and the cyclic load (P_{cyclic}) over the cross sectional area of the specimen. The confining stress is not included.

5 σ_S is the axial seating or contact stress; that is, the seating load over the cross sectional area of the specimen. It should be maintained at very small values.

6 σ_3 is the total radial stress; that is, the confining pressure in the triaxial chamber.

7 $\sigma_d=\sigma_{max} - \sigma_S$ is the deviatoric axial stress; that is, the maximum repetitive applied axial stress. It is also referred to as the cyclic axial stress.

8 Gage Length is the distance between the top and bottom transducers used to monitor the axial deformations. A gage length equal to one-third of the specimen length shall be used for all testing.

9 ε_a is the resilient axial strain induced by σ_d. This is defined as the resilient (recovered) axial deformation over the gage length.

10 ε_l is the resilient lateral strain also induced by σ_d. This is defined as the resilient (recovered) lateral or radial deformation measured at the mid-section of the specimen over its radius.

11 $M_R = \sigma_d/\varepsilon_a$ is the secant resilient modulus.

12 $nu = - \varepsilon_l/\varepsilon_a$ is the Poisson's ratio.

13 Load duration is the time interval during which the specimen is subjected to a deviatoric stress. A load duration of 0.1 second shall be used.

14 Cycle duration is the time interval between two consecutive applications of deviatoric stress. A cycle duration of 1 second shall be used.

15 Loading wave form is the haversine load pulse in which test specimens are loaded to simulate traffic loading in the laboratory.

APPARATUS

1 Triaxial Pressure Chamber: The pressure chamber is used to contain the test specimen and the confining fluid during the test (air is used as the chamber fluid). A triaxial chamber suitable for the use in resilience testing of granular materials is shown in Figure 1. The chamber is similar to most standard triaxial cells, except that it is somewhat larger to facilitate the internally mounted transducers.

2 Loading Device: the external loading device must possess a stiffness of at least 1,500 kN/mm. This property is actually estimated by placing a jack (or using the hydraulic actuator) between the two platens of the machine, applying several static loads and measuring it displacement.

The loading device shall be capable of providing varying repeated loads in fixed cycles of load and release. A closed-loop electro-hydraulic system is required for this operation. A havesine loading waveform consisting of a load duration of 0.10 seconds and a cycle duration of 1 second, as shown in Figure 2, should be applied to the specimen.

3 Load and Specimen Response Measuring Equipment:

a The axial load measuring device should be an electronic load cell that can either be placed inside the triaxial chamber, between the specimen top cap and the loading piston, or outside of it, that is between the actuator piston and the piston of the triaxial chamber.

The magnitude of friction between the piston and the top plate of the chamber will determine the need for one, or the other approach. Under the different conditions of confining pressure, up to 10 N of frictional force can be tolerated. A load cell of 25 kN in capacity and having an accuracy of ± 5 N is recommended for the testing of the specimens of 150-mm in diameter.

b Test chamber pressures shall be monitored with conventional pressure gages, manometers, or pressure transducers having a capacity of 350 kPa and an accuracy

of at least 0.5 kPa. The device used to monitor pressure should be regularly checked and periodically calibrated to ensure its proper performance.

c The deformation measuring devices consists of nine internal non-contant probes attached to aluminun rings that are fixed onto the columns inside the triaxial chamber, and one linear variable differential transformer (LVDT) installed on top of the testing frame. Six probes shall be used to monitor the axial deformation, whereas, three shall be used for monitoring the lateral deformations of the specimen. The external LVDT shall be used to monitor the movement of the hydraulic actuator.

The non-contact probes shall be installed 120 degrees apart of each other and should face their corresponding steel targets. The non-contact probes will have a linearity of output and with a maximum range of ± 2.0 mm. As such, a prudent gap between the non-contact probes and the targets shall be left in order to ensure that the probes will never go out of range during the entire test. A sketch of their installation is shown in Figure 1.

d Each one of the non-contact probes shall be wired, so that each transducer can be read and the results reviewed independently. Measured displacements shall be averaged for estimating the stiffness properties of the test specimen. They should be regularly checked and periodically calibrated to ensure their proper performance.

e The external LVDT shall be installed in the actuator to monitor its travel. The LVDT will have a linerity of ± 0.25 percent of full range output, a repeatability of ± 1 percent of full range, a minimum sensitivity of 2 mv/v (AC) or 5 mv/v (DC) and a maximum range of ± 25 mm.

f To minimize errors, the entire system should be calibrated periodically. The use of synthetic specimens of known properties is recommended to assess the accuracy and repeatability of the measurements.

g Suitable signal excitation, conditioning and recording equipment are required for simultaneous recording of axial load, air pressure and deformations. The signal shall be clean and free of noise (use shielded cables that are properly grounded).

Filtering the output signal during or after acquisition is discouraged. If filter is used, it should have a frequency greater that 30 Hz. A supplemental study should be made to insure that correct peak readings are obtained from the filtered data compared to the unfiltered data.

h A data acquisition board mounted inside a personal computer having computational and control capabilities should be used. A minimum sampling rate of 200 records per channel per second is recommended. However, a supplemental study is suggested to

establish the optimum number of data points to be used for each specific data acquisition system.

4. Specimen Preparation Equipment: A variety of equipment is required to prepare test specimens that are representative of field conditions. Typical equipment includes:

   a Split molds may be used to prepare specimens of 150-mm in diameter and 300 mm in length. For compaction, an automatic tamper (as specified in Tex-113-E) can be used-provided that the area of the rammer's striking face represents no more than 30 percent of the specimen area.

   b Miscellaneous: Other required equipment includes calipers, micrometer gauge, steel rule, rubber membranes 0.25-mm to 0.79-mm thick, rubber O-rings, a membrane expander, scales, moisture content cans, a water-bubble level, and hydrostone cement.

PREPARATION OF TEST SPECIMENS

1 Specimen Size: Specimen length-diameter ratio should not be less than two and not higher than three. Traditionally, minimum specimen diameter is defined as five times it nominal size[1]. As such, for granular base materials with nominal sizes as high as 30 mm, minimum diameter should be 150 mm and minimum specimen length is 300 mm.

2 Test specimen: all the specimens shall be prepared in the laboratory according toTex-101-E. Material shall be first collected according to Tex-400-A.

   a The water content and dry density of the compacted specimens shall not vary more than $\pm$0.5 percent and $\pm$2 percent from the specified water content and dry density for the base course, respectively.

   b For evaluation purposes, laboratory compacted specimens shall be prepared at *in situ* water content and at the *in situ* dry density. The compacting effort specified in Test Methods Tex-113-E can be used for compaction, as long as the specimens prepared are full representation of *in situ* conditions. To determine the *in situ* water content and *in situ* density of the base course, Test Method Tex-115-E or AASHTO T-238 and T-239 (nuclear method) can be used.

   c For design purposes, laboratory compacted specimens shall be prepared at the optimum moisture content and the maximum dry density determined as per Tex-113-E as determined by the pavement engineer.

---

[1] Nominal size is the particle size of the material corresponding to the 95 percent passing size.

d At least two replicate specimens that represent the desired conditions shall be prepared for testing. Nevertheless, if the pavement engineer feels it is necessary, replicate specimens can be more than two. Specimens can also be prepared at different water contents from the optimum and/or *in situ* water content. This may be required by the pavement engineer who aims at evaluating the variation of these stiffness properties of the pavement materials at the different seasonal conditions.

3 Compaction Method: Tex-113-E is the method of compaction recommended. Nevertheless, the plasticity index of the soil should be first determined in order to select the compacting effort (CE).

a After properly assembling the split mold, a bottom cap shall be placed in position before placing the material into the mold. In addition, a hydrostone paste shall be spread on top of the bottom cap to obtain a thickness no greater than 3 mm. to ensure a strong and uniform contact with the specimen.

b To compact the total volume of the soil (V), six layers are recommended to obtain a more uniform specimen, as well as, to facilitate the placement of the targets. the surface of each layer should be scarified before placing the next layer. Knowing the weight of the hammer (W) and the height of drop (H), the number of blows (N) per layer can be determined as follows:

$$N = \frac{CE \cdot V}{6 \cdot W \cdot H} \qquad (1)$$

c Three sets of three steel targets shall be inserted into the specimen during compaction. One set of targets shall be inserted after compacting the second layer, one set after the third layer and one set after the fourth layer of the specimen. Each target shall be inserted at the edge of the specimen and radially spaced 120 degrees apart.

d After specimen compaction has been completed, the compaction water content of the remaining material should be verified. The specimen shall be carefully removed from the mold. If the compacted specimen does not have the desired length, the surface shall be trimmed and flatted.

e Hydrostone paste shall be uniformly spread on top of the specimen in order to obtain a thickness no greater that 3 mm of paste. Then, the excess paste shall be squeezed out by pressing the top cap on top of the specimen. The levelness and alignment of the top cap shall be checked and corrected if necessary, by using a water bubble level and by softly tamping the top cap. Any excess hydrostone paste shall be removed from the specimen.

f The hydrostone paste consists of potable water and hydrostone cement mixed in a 0.40 ratio. Once the water is mixed with the hydrostone cement, the hydration of the paste begins, and its consistency is rapidly obtained. A minimum of 120 minutes (counting from the moment water is added to the hydrostone cement) is recommended as a curing time; this ensures that the grout will be strong enough to withstand the M_R test without risking the accuracy and reliability of the measurements.

g The specimen shall be removed from the mold. The sides of the end caps shall be cleaned, and a film of vacuum grease shall be applied at their sides to facilitate the adherence of the membranes with the end caps.

h A rubber membrane shall be placed in position into the membrane expander. A low vacuum pressure shall be applied to ensure contact between the membrane and the expander. Disconnect the vacuum and unfold the membrane to fully embrace the specimen and its end caps. Then, seal the membranes with O-rings.

i Determine the weight, length and diameter of the specimen, and compute the wet and dry densities of the specimen. The weight of the end caps, O-rings, membrane and hydrostone paste should have been determined prior to specimen preparation.

PLACEMENT OF THE SPECIMEN INTO THE TRIAXIAL CHAMBER & FINAL ASSEMBLY

1 The specimen with the end caps shall be carefully placed and properly aligned into the triaxial chamber. The bottom cap of the specimen shall be connected to the base plate of the triaxial chamber through the bottom cap screw. The O-rings and gaskets shall be properly placed in avoid any leakage.

2 The internal targets should be located by carefully presenting the magnets. One magnet will be assigned to each target (a total of nine). The magnets should be 12 mm in diameter. Bonded rare earth magnets are easier to machine. A pull load rate of 10 N is required to ensure strong contacts with the targets and to eliminate any possibility of slippage during the test.

3 The external targets shall be placed on top of the magnets as shown in Figure 1 and shall be carefully adjusted to leave a prudent gap between them and the non-contact probes.

4 Guided by the steel rods, the three positioning rings shall be fixed at the proper working level; that is, nearby one-third of the length from the top, mid-length and one-third of the length from the bottom of the specimen. The positioning rings allow the non-contacts probes to be close to their corresponding measuring levels and to the targets.

5 The non-contact probes shall be firmly screwed and secured to the probe clamps, whereas the probe clamps shall be firmly secured to the positioning rings. At this stage, it is generally necessary to re-adjust the location of the external targets to ensure that the non-contact probes will not run out of working range during the test.

6 A steel ball shall be placed on top of the top cap so that the axial loadings can be transferred uniformly and concentrically to the specimen. The tub shall then be carefully fit over the base, after applying vacuum grease at the circumferential groove of the base plate of the triaxial chamber ,where the acrylic tube will rest on.

7 The wires of the transducer shall be untangled and fit inside the chamber, so that they do not affect the measurements. After applying vacuum grease a the circumferential groove of the cover plate of the triaxial chamber, the top plate should be placed on the steel rods and acrylic tube and shall be securely tightened with the head screws.

8 The loading piston of the triaxial chamber shall then be released from its secured position, so that the steel rod (or an internal load cell attached to it) contact the steel ball. The piston of the actuator shall then be lowered and attached to the loading piston of the triaxial chamber. Proper alignment of the piston of the actuator with the loading piston of the triaxial chamber is very crucial; as such, the entire assembly (triaxial chamber) may need to be moved sideways, so that perfect alignment can be achieved. Once aligned, the entire testing assembly shall be tightly secured to the testing frame.

9 The triaxial chamber shall then be slid into position under the axial loading device. The loading device shall be lowered and coupled to the piston of the triaxial chamber. Then, a seating pressure of no more than 7 kPa shall be applied to the specimen.

TESTING PROCEDURE

The procedure described in this section is used for undisturbed and laboratory compacted specimens and requires a minimum of 30 minutes of testing time. At least two replicate specimens should be tested as representative of each one of the field conditions to be simulated in the laboratory.

1 A confining pressure of 35 kPa shall be applied to the test specimen. The material shall be stabilized to such confinement for at least 5 minutes.

2 Five repetitions of each one of the following deviatoric stresses shall be applied: 35 kPa, 70 kPa and 105 kPa. During the application of each deviatoric stress the actual applied compressional force and the induced resilient axial deformation of the 5 cycles shall be recorded and averaged. The actual confining pressure, the actual applied deviatoric stress, the induced resilient axial and lateral strains, and the calculated resilient modulus and Poisson's ratio shall be reported on a form similar to one shown in Figure 3. Other

parameters - including the seating stress and the cumulative permanent deformations - can also be reported.

3 The confining pressure shall be increased to 70 kPa following the process mentioned in item 1. Deviatoric stresses described in item 2 shall be applied; furthermore, an additional deviatoric stress of 140 kPa shall be applied.

4 The confining pressure shall then be increased to 105 kPa following the process mentioned in item 1. Deviatoric stresses described in item 2 shall be applied; furthermore, additional deviatoric stresses of 140 kPa and 210 kPa shall then be applied.

5 Generally, if the resilient axial and lateral strains fall below the 0.01 percent (minimum reliable strain estimate) that particular result shall be excluded in further analysis. If the total axial strain is greater than 1 percent, the M_R test shall be stopped.

6 Upon completion of the M_R test, the confining pressure shall be reduced to zero and a load at a rate of 0.5 mm per minute shall be applied to drive the specimen to failure. During this test, the applied axial stress and axial and lateral strains shall be recorded in order to calculate the static Young's Modulus and Poisson's ratio. The triaxial chamber shall then be disassembled.

7 The membranes shall be removed from the specimen. A piece from the core of the specimen shall be used to determine its water content after testing to compare this value with the initial water content.

REPORT

The M_R testing report consists of three parts: (1) the basic information of the test specimen; (2) the testing results and plots of the variations of the moduli and Poisson's ratio; and (3) an analysis of results Figure 3 illustrates a typical M_R testing report.

1 Data sheets shall include the basic information of the material, (e.g., its origin, and Atterberg limits) as well as, information related to the specimen (e.g., its age at the time of testing, its dimensions, its water content, and its dry density). In addition, the following test results should be included: the confining pressures, the seating pressures, the deviatoric stresses, the resilient axial and lateral strains, the permanent deformations, and the calculated resilient moduli and Poisson's ratio of each specimen at each one of the stress states of the test.

2 Four plots are recommended. Two arithmetic plots showing the variation of the resilient modulus and Poisson's ratio with deviatoric stress for a given confining pressure, and two semi-logarithm plots showing the variation of the resilient modulus and Poisson's ratio with logarithm of the resilient axial strain for a given confining pressure.

3 The analysis of results consists of developing a linear regression equation to predict the resilient modulus and Poisson's ratio of the material, and suggesting one M_R and Poisson's ratio value for design. Use all the results obtained from the testing of the replicate specimens in the statistical analysis.

a A regression model accompanied by both its coefficient of determination, R^2, and the standard error of the estimate, SEE, should have the following form:

$$Ln(\varepsilon_a) = a + b * \ln(\sigma_d) + c * \ln(\sigma_3),$$

$$\varepsilon_a = e^{a} * \sigma_d b * \sigma_3 c \qquad (2)$$

By definition:

$$M_R = \sigma_d / \varepsilon_a$$

Thus, The modulus can be expressed in two similar equations, in terms of either the deviator stress or the axial strain:

$$M_R = e^{-a} * \sigma_d^{(1-b)} * \sigma_3^{-c},$$

$$M_R = K_1 * \sigma_d^{K2} * \sigma_3^{K3} \qquad (3)$$

$$M_R = N_1 * \varepsilon_a^{N2} * \sigma_3^{N3}$$

$$M_R = e^{-a/b} * \sigma_d^{(1-b)/b} * \sigma_3^{-c/b}, \qquad (4)$$

b The Poisson's ratio to be reported will simply consist of obtaining the average of all the Poisson's ratio values obtained from the testing of the replicate specimens.

c Based on either stress or strain criteria, the pavement engineer can estimate a unique resilient modulus value for use as an input in the AASHTO pavement design guide.

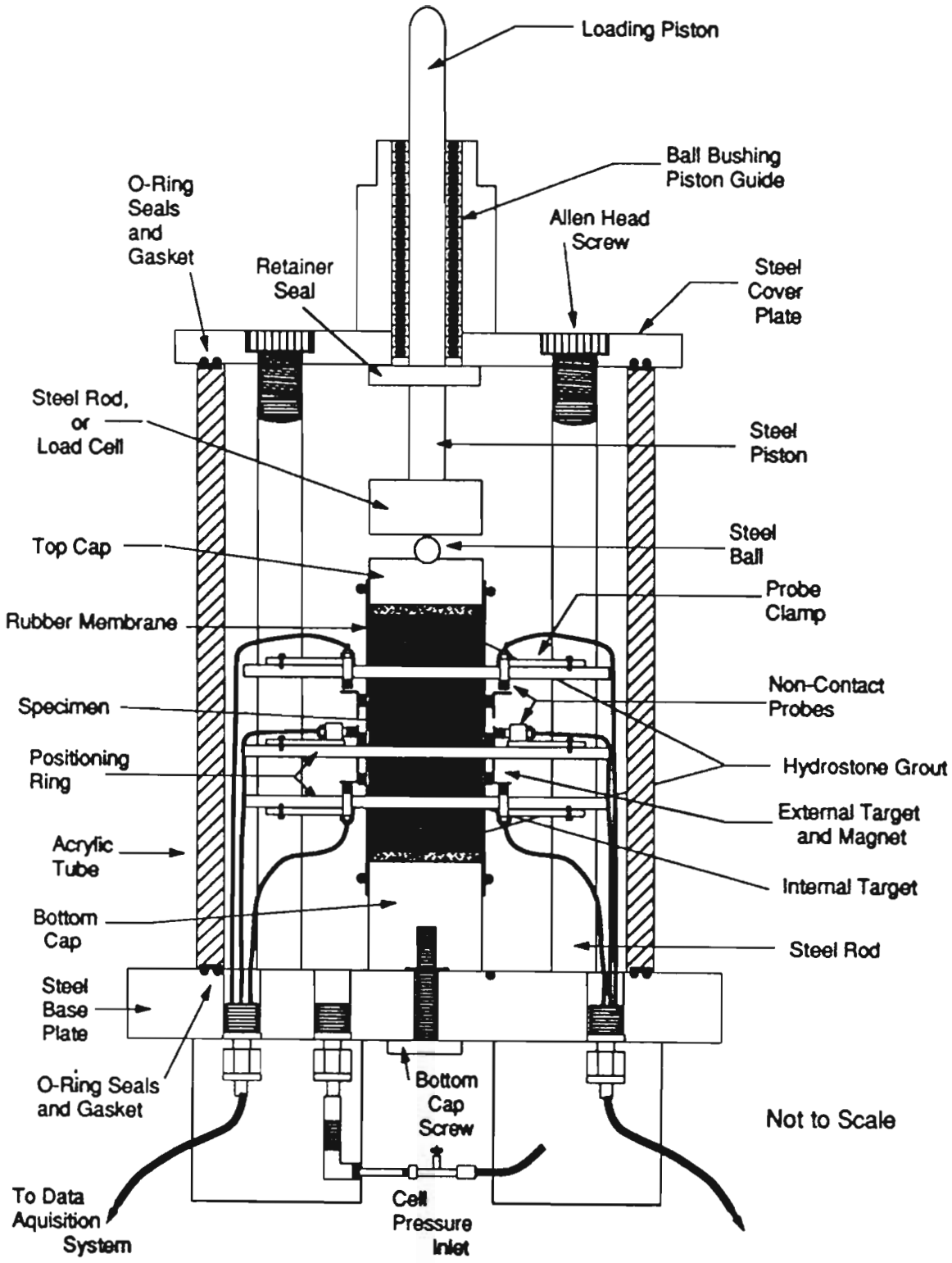

Figure 1. Triaxial Chamber

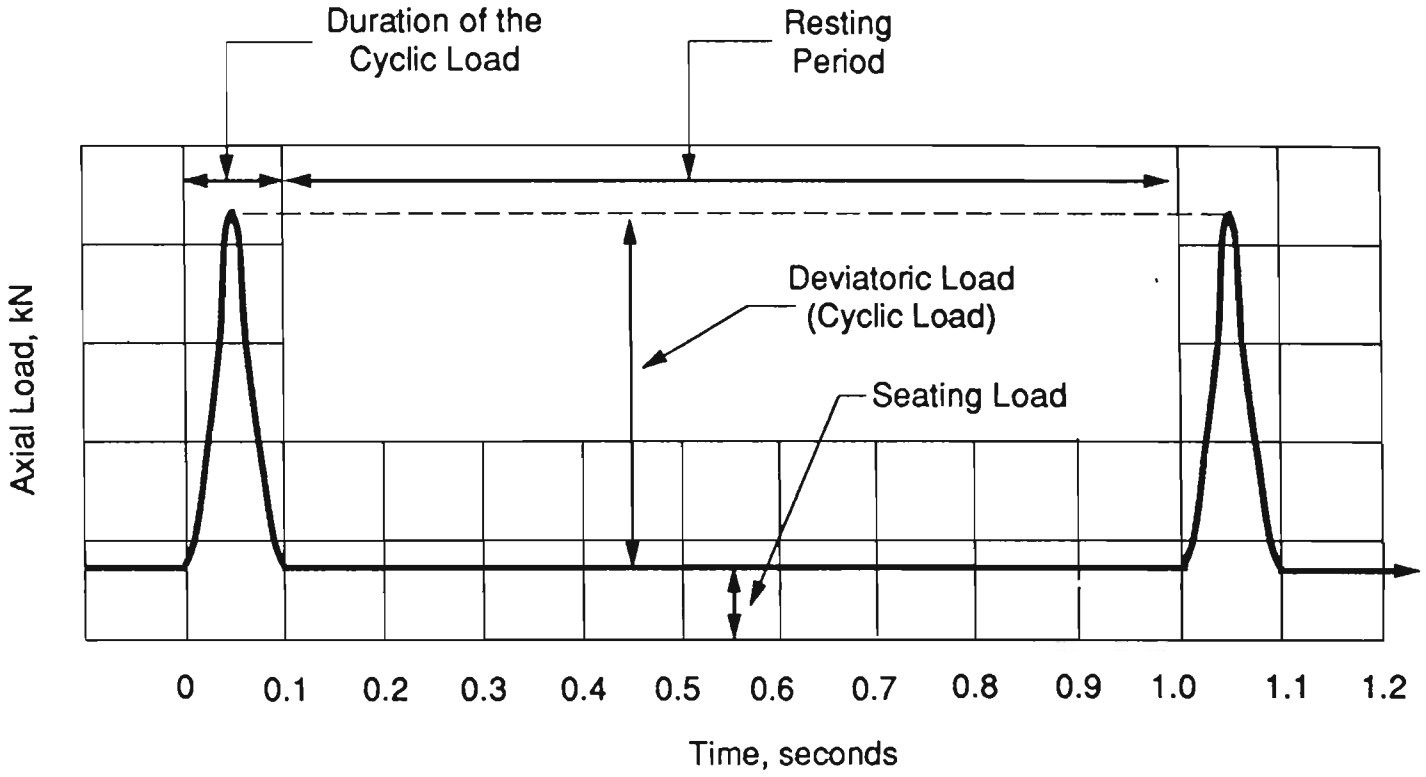

Figure 2. Definition of the Loading Rate, Wave Form and Terms

Example.out RESILIENT MODULUS (MR) TEST RESULTS

SPECIMEN IDENTIFICATION = 1 - Limestone - Grade 4
DESCRIPTION = SAN ANGELO DISTRICT - Tom Green County - R.W. McKinney Alexander Pit
ROAD SOURCE = US67 - Frontage Road - Section 1582 - Outside Lane - 150-mm depth
PLASTIC LIMIT = 3.40 percent
LIQUID LIMI = 16.60 percent
MOISTURE CONTENT = 3.80 percent
DRY DENSITY = 23.30 kN/cm3
SPECIMEN HEIGHT = 308.750 mm
SPECIMEN DIAMETER = 151.250 mm
GAGE LENGTH = 100.600 mm

CONFINING (kPa)	SEATING (kPa)	DEVIATORIC. (kPa)	AXIAL DEF (mm)	LAT. DEF. (mm)	LAT. STR (mm/mm)	AXIAL STR. (mm/mm)	POISSON RATIO	RES. MODULUS (MPa)
34.6	6.95	37.81	0.016700	0.004390	0.000058	0.000166	0.35	227
34.8	5.78	61.10	0.027270	0.007100	0.000094	0.000270	0.35	226
35.4	5.67	83.24	0.036560	0.009300	0.000123	0.000362	0.34	230
69.7	5.49	36.19	0.011310	0.002880	0.000038	0.000112	0.34	322
69.4	5.32	60.86	0.018980	0.004840	0.000064	0.000188	0.34	323
69.9	5.91	84.97	0.026860	0.006660	0.000088	0.000266	0.33	319
70.8	5.87	104.63	0.032920	0.008170	0.000108	0.000326	0.33	321
102.6	5.76	40.86	0.010580	0.002650	0.000035	0.000104	0.33	387
102.9	5.62	61.72	0.016060	0.003930	0.000052	0.000159	0.33	389
103.1	5.44	83.48	0.021920	0.005600	0.000074	0.000217	0.34	385
103.4	7.14	102.15	0.026560	0.006660	0.000088	0.000263	0.33	388
104.2	7.03	188.33	0.049490	0.012250	0.000162	0.000490	0.32	384

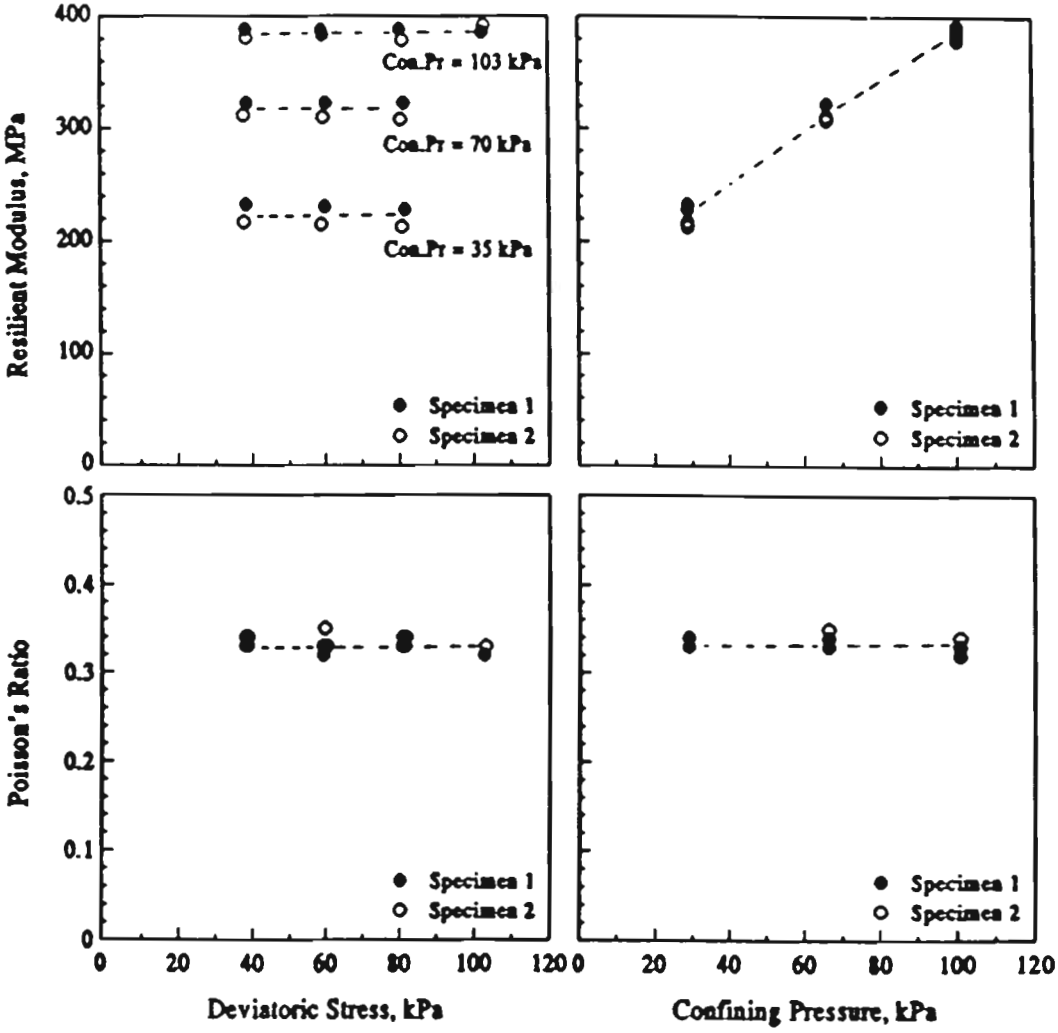

Figure 3. Testing report

APPENDIX B

Questionnaire

QUESTIONNAIRE

District No.: Odessa - 06 Date: 10-15-92

Name of Contact: Stephen G. Smith, P.E. Telephone: (915) 332-0501 Ext. 216

1.- Give a rough estimate of the total centerline miles of your district: 3200

2.- Identify the types of base materials used the most (*up to five*), and give a rough estimate of the percentage of total centerline miles constructed in your district with each one of those base types.

2.a.- Granular Base (Flexible) 90 %

2.b.- Lime-stabilized Base ____ %

2.c.- Cement-stabilized Base ____ %

2.d.- Asphalt Treated Base 10 %

2.e.- Other: ____ %

2.f.- Other: ____ %

3.- Only for the granular bases (up to five), identify their souces, type of aggregates, grades, and types; and, give a rough estimate of the percentage of their use over the road mileage of your district.

Base Code	Source Company name - Pit name	Type of Aggregate (limestone, sandstone, etc)	Grade	Type	%
1B	Roadside - Adjacent to project	Limestone	2	A	80%
2B	Roadside - Adjacent to project	Limestone	1	A	20%
3B					
4B					
5B					

4.- Refer to the codes for the granular materials used in Question # 3. List some of their properties.

Base Code	Max. Particle Size (inch)	Retain. # 4	Retain. # 40	Pass. # 200	LL low-high	PI low-high	Texas Triaxial Class	Wet Ball Mill Increase	Optimum Moisture Content	Actual Density D_A
1B	1½	60	78	N.A.	23-27	8-10	I	15	8-10	135-139
2B	1½	55	80	NA	23-27	8-10	5-40 15-15	15	8-10	135-139
3B										
4B										
5B										

5.- Will you like us to perform Resilient Modulus tests on your granular materials? Yes X No ____

If Yes, we need to receive at least 400 lbs of each sample for testing, no later than January 31, 1993. Also, test results (e.g., Moisture-Density, PI, Triaxial Class, etc, if available) obtained on samples submitted should be attached.

6.- In a sequential way (e.g., 1, 2, 3, and so on), prioritize the factor(s) that determine the use of a typical type of granular material as a base layer in your district, and briefly explain.

FACTORS	PRIORITY	EXPLANATION
Subgrade type	2	Subgrade type would determine thickness
Climate		
Traffic	1	Wheel loads would dictate thickness
Pavement type		
Land use		
Availability		
Other:		

Figure 5.1 A Copy of the Questionnaire received from TxDOT-District 6.

7.- From the types of subgrades that are found the most in your district, give a rough estimate of their availability in terms of a percentage of the total centerline miles of your district, and briefly explain.

SUBGRADE TYPE	%	EXPLANATION
A	30%	Sandy Loam
B	10%	Rocky Loam
C	60%	Sandy Caliche

8.- List some of the properties of your subgrades. (rough values)

Subgrade type	Actual Density D_A	Opt. Molding Moisture	LL	PI	Pass. # 200	Texas Triaxial Class	Heave & Swell Potential	Other
A	125	10%	NA	12	NA	2	NA	
B	130	8-10%	NA	8	NA	1	NA	
C	122	8%	NA	8	NA	2	NA	

9.- Give a rough estimate, in percentage of the total centerline miles of your district, of the types of pavements and their classifications used the most in your district.

9.a.- Rigid Pavement 1 %

[R1] Jointed Concrete Pavement 0.5 %

[R2] Continuously Reinforced Concrete Pavement 0.5 %

[R3] Other: ____ %

9.b.- Flexible Pavement 99 %

[F1] Asphalt Concrete Pavement 15 %

[F2] Asphalt-Rubber Concrete Pavement ____ %

[F3] Surface Treatment 84 %

[F4] Other: ____ %

10.- Refer to the surface layers codes used in Q # 9. List some of their properties. (rough values)

Surface Code	Aggregate type	Density	fc	Modulus of Rupture	Stability Value	Percent of Binder	Percent of Voids
R1							
R2							
R3							
F1	Type D	125 pct			45	6%	3.4%
F2							
F3	Grade 4	N.A.			N.A.	N.A.	N.A.
F4							

11.- Refer to the codes for the surface layers (Q # 10) and the codes of the bases (Q # 3). Include the layer codes, rough estimates of the layer thicknesses, and any other information. Aditionally, give rough estimates, in percentage of the road mileage of your district, of the pavement arrangements used the most in your district.

#	Layer Code	Thickness	General Information	%
1.-	F3	5/8"	2 Course Surface Treatment limestone rhyolite	
	1B	6"-10"	Flexible Base	77%
2.-	F1	1.75"	Type D HMAC	
	1B	6"-10"	Flexible Base	10%
3.-	F1	1.75"	Type D HMAC	
	BB	5"-10"	Type B HMAC or Black Base	3%
4.-	F1	3"-5"	Type D over Type C	
	2B	10"-18"	Flexible Base	10%

Figure 5.1 A Copy of the Questionnaire received from TxDOT-District 6. (Continued)

APPENDIX C

Variations in Modulus and Poisson's Ratio

Tyler (District 10)
Specimen No: 1 Gage Length = 101mm OMC

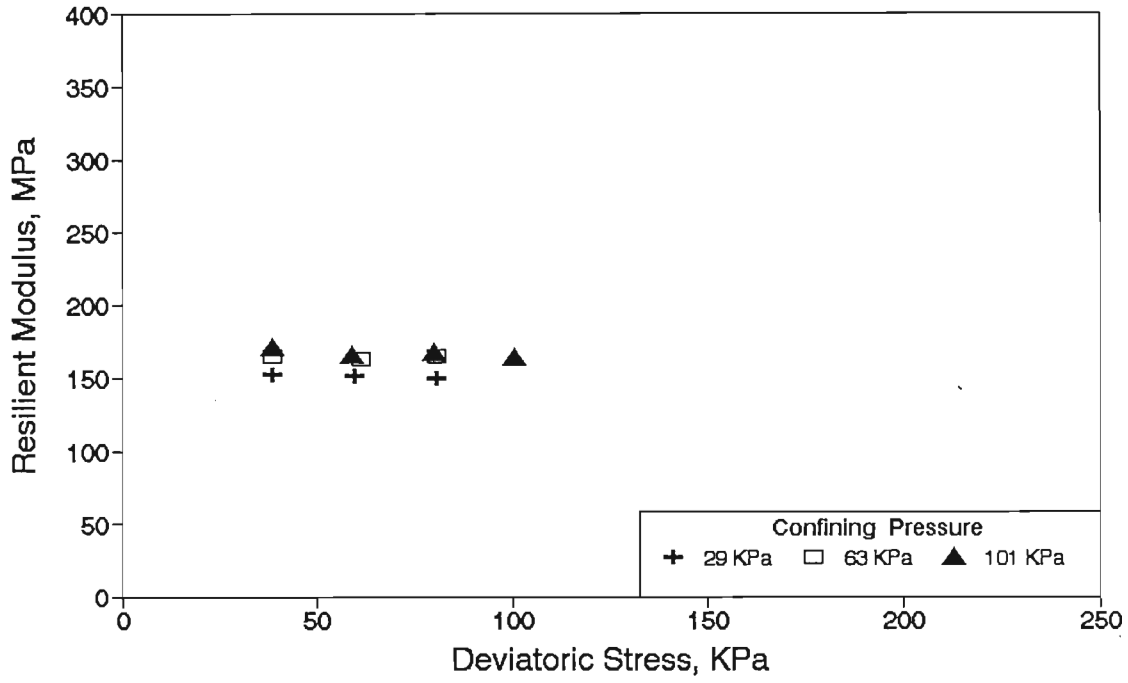

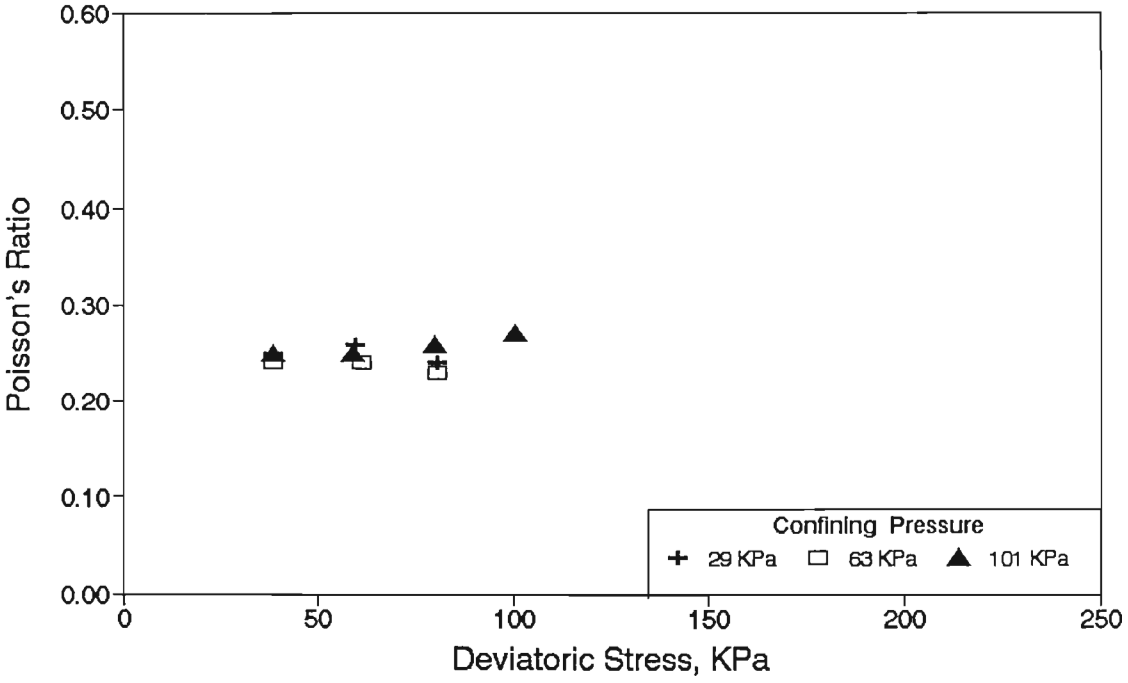

Project-1336/Specimen tested by Sriram/Data reduced and plotted by MRK Reddy

Tyler (District 10)
Specimen No: 2 Gage Length = 101mm OMC

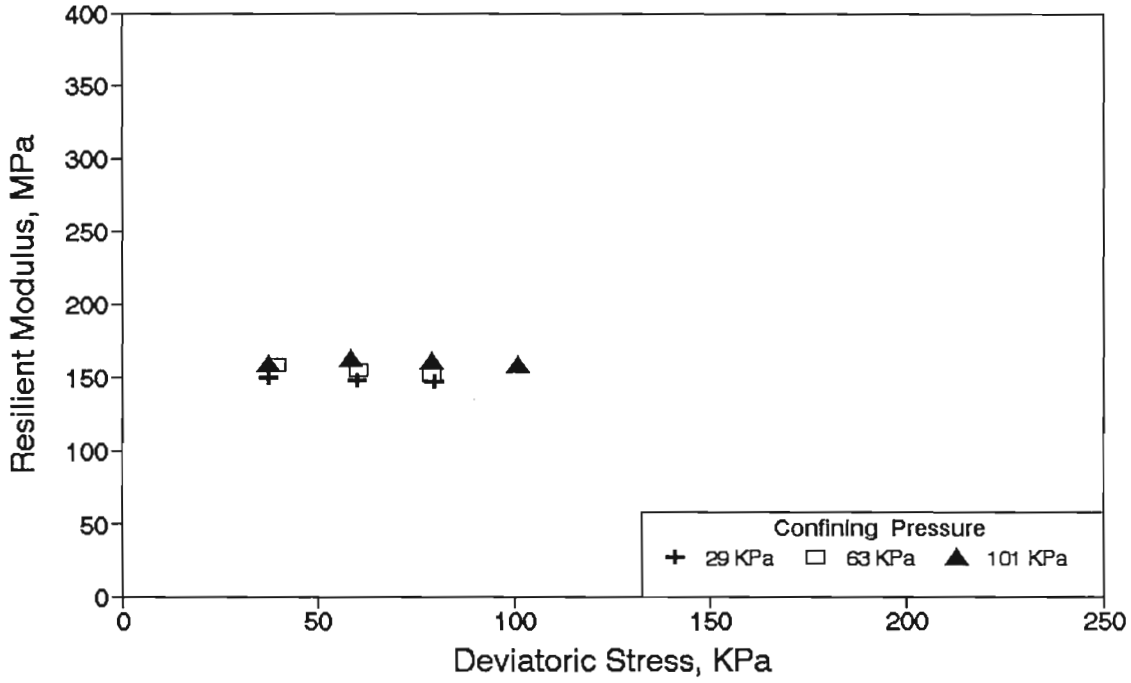

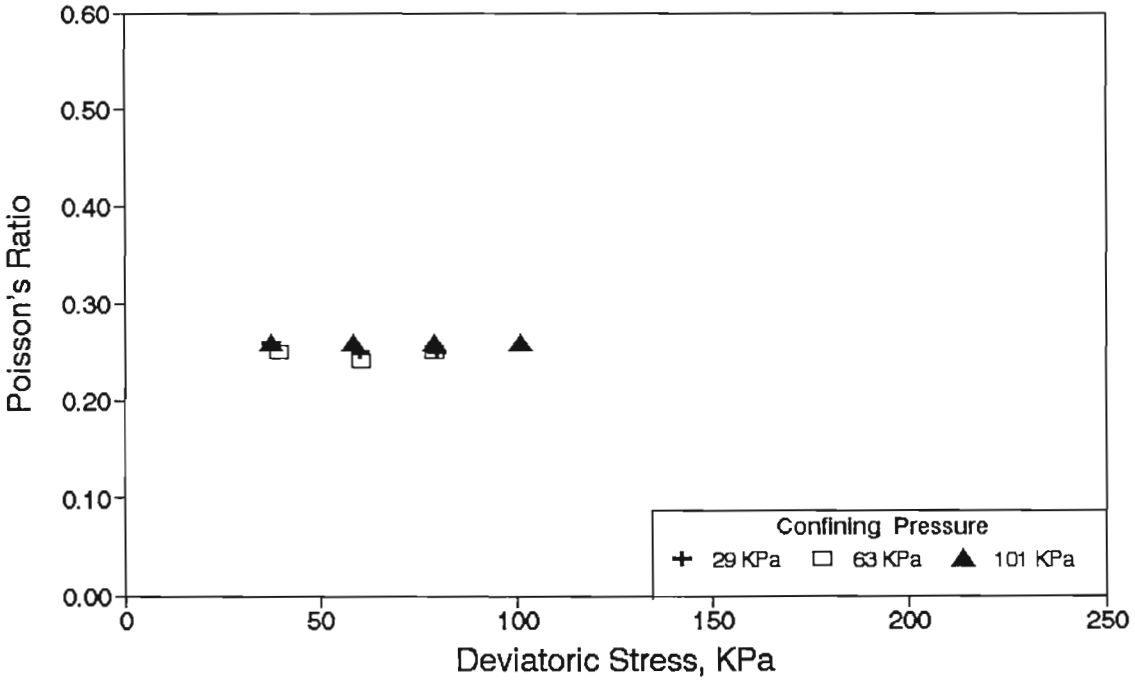

Tyler (District 10)
Specimen No: 1 Gage Length = 101mm Dry of OMC

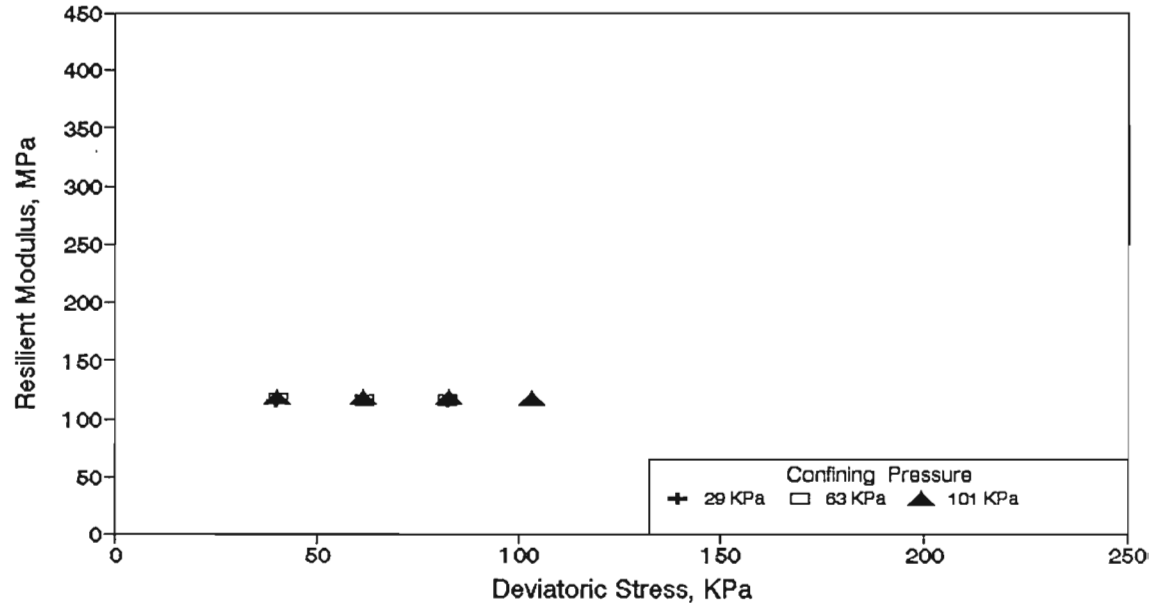

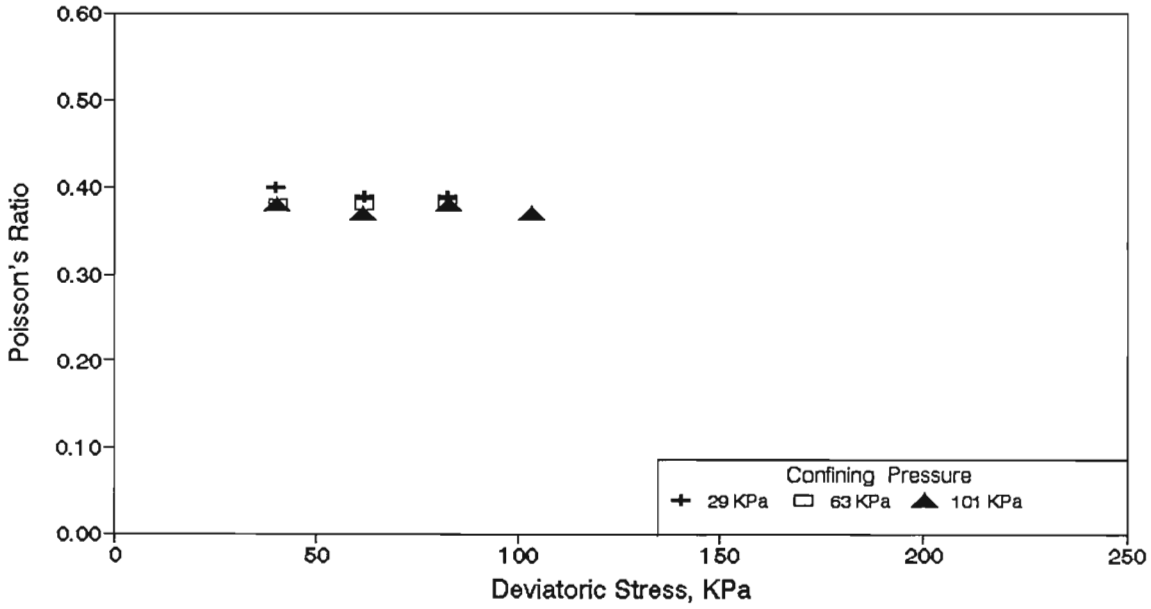

Project-1336/Specimen tested by Sriram/Data reduced and plotted by MRK Reddy

Tyler (District 10)

Specimen No: 2 Gage Length = 101mm Dry of OMC

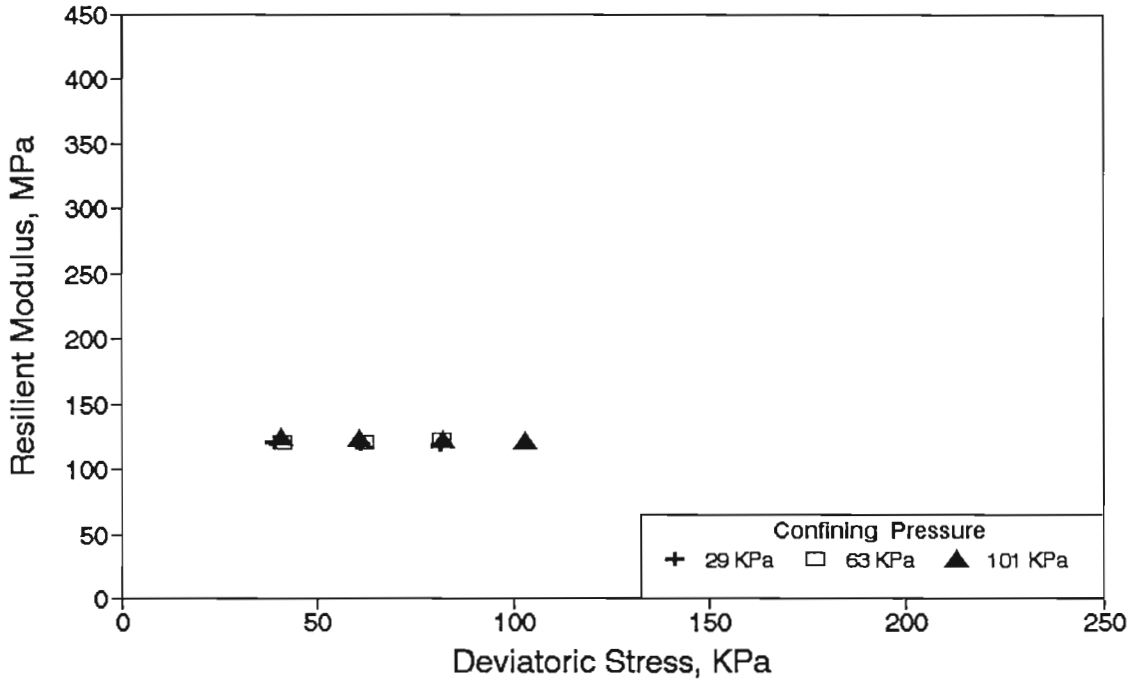

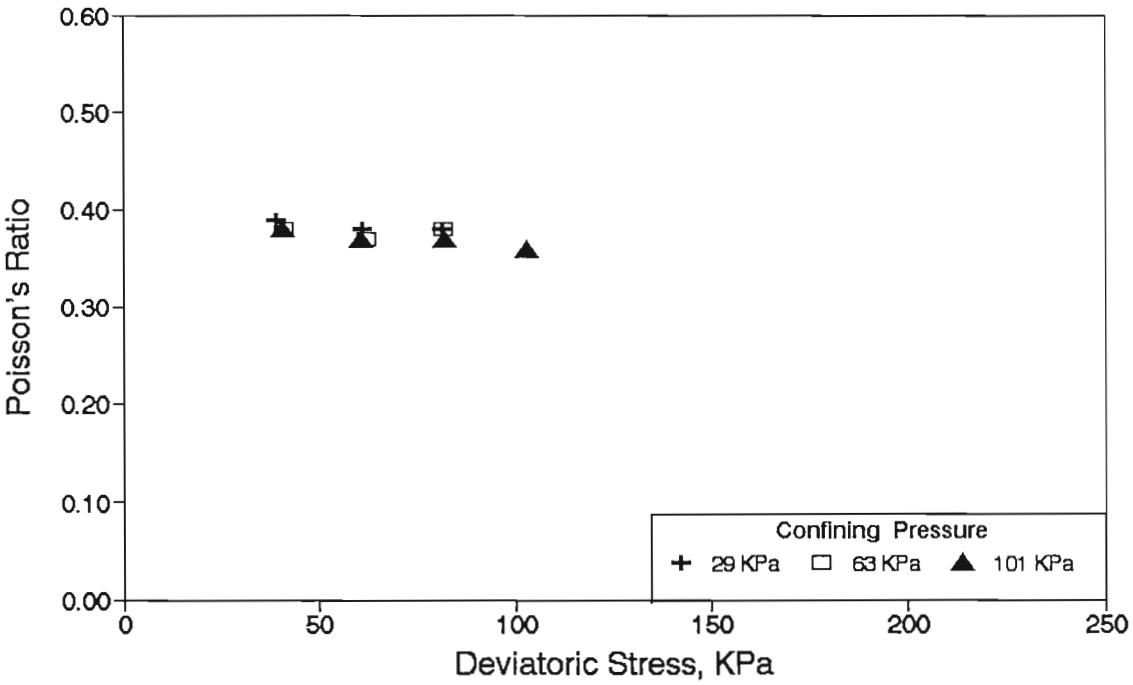

Project-1336/Specimen tested by Sriram/Data reduced and plotted by MRK Reddy

Tyler (District 10)
Specimen No: 1 Gage Length = 101mm Wet of OMC

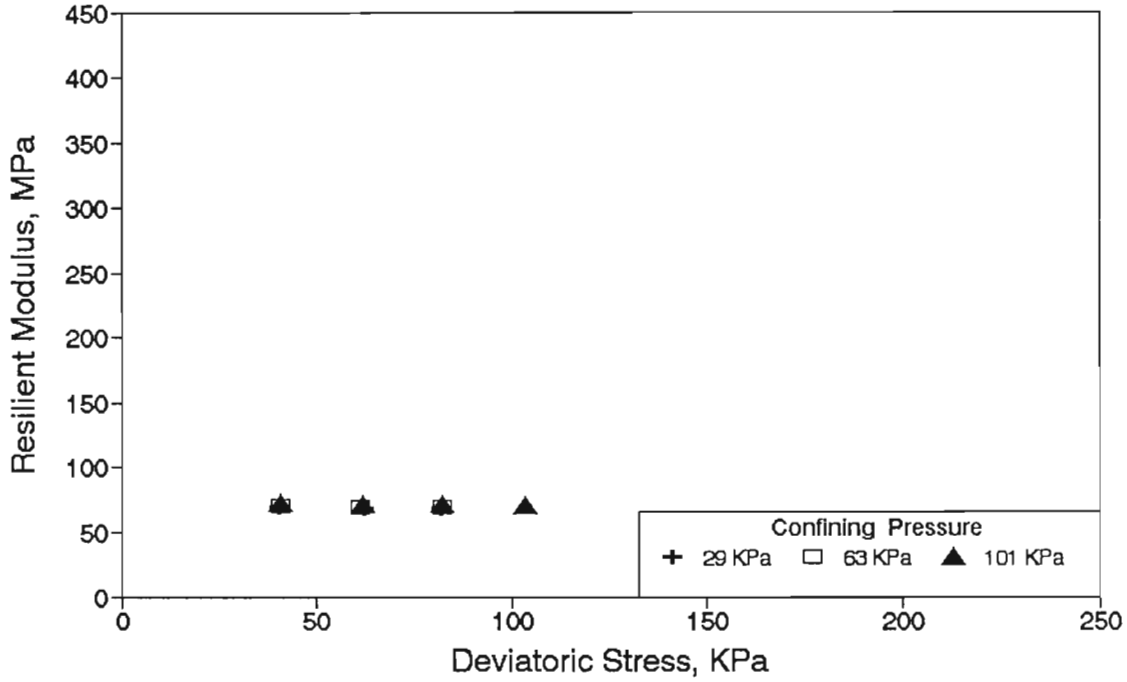

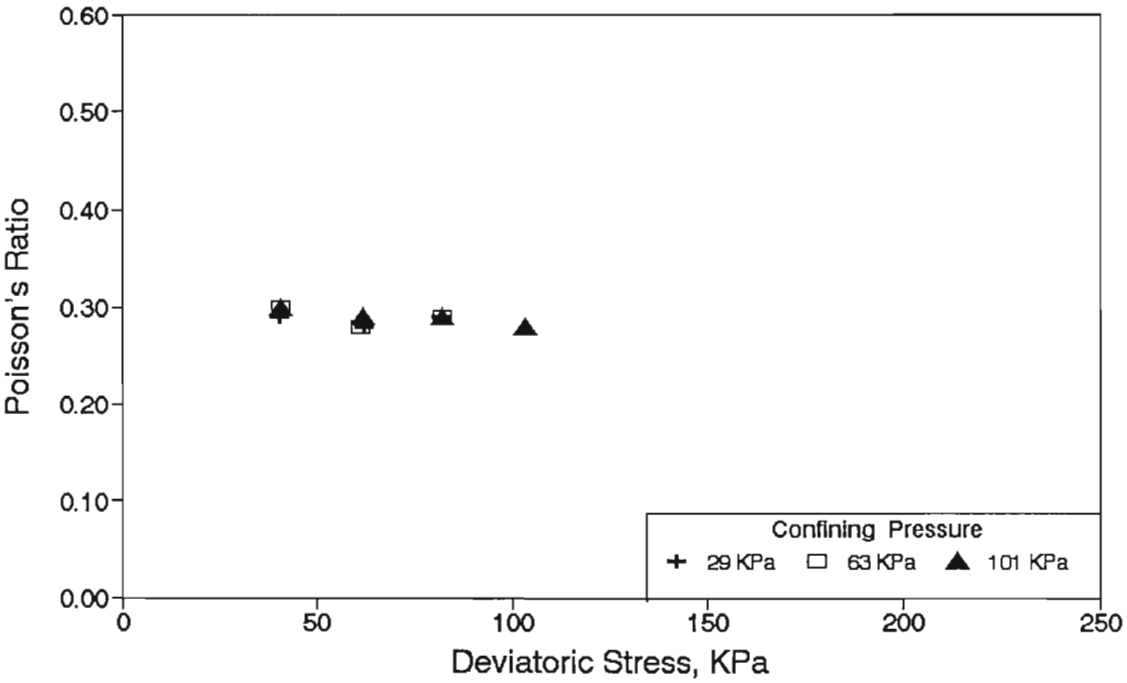

Project-1336/Specimen tested by Sriram/Data reduced and plotted by MRK Reddy

Tyler (District 10)
Specimen No: 2 Gage Length = 101mm Wet of OMC

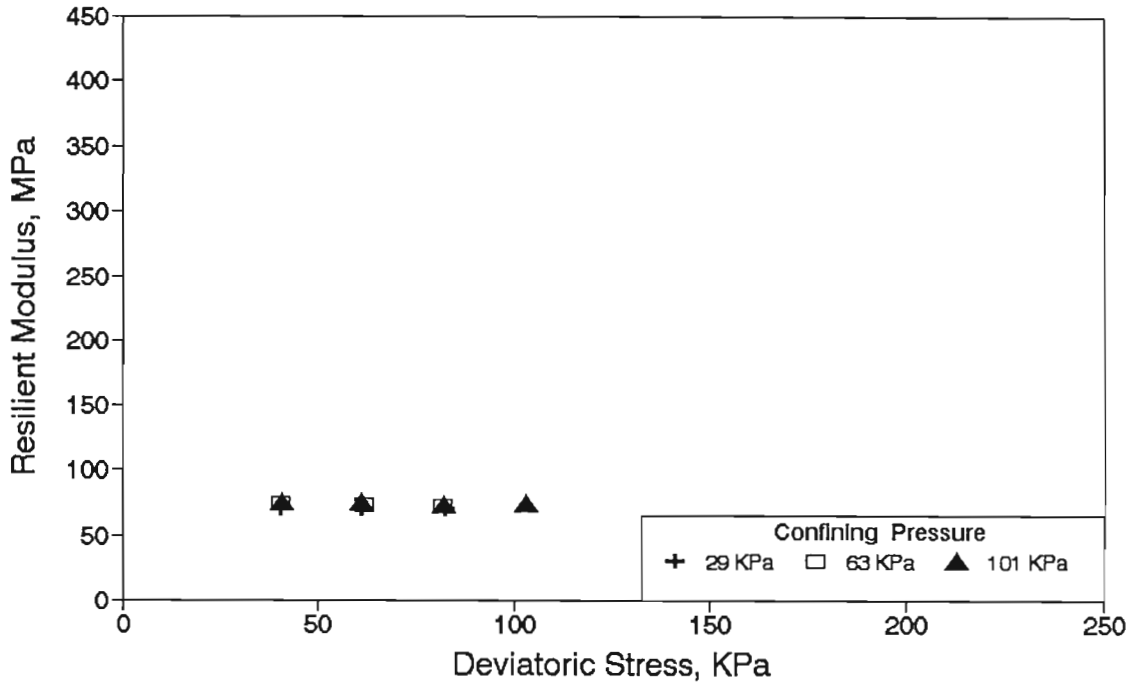

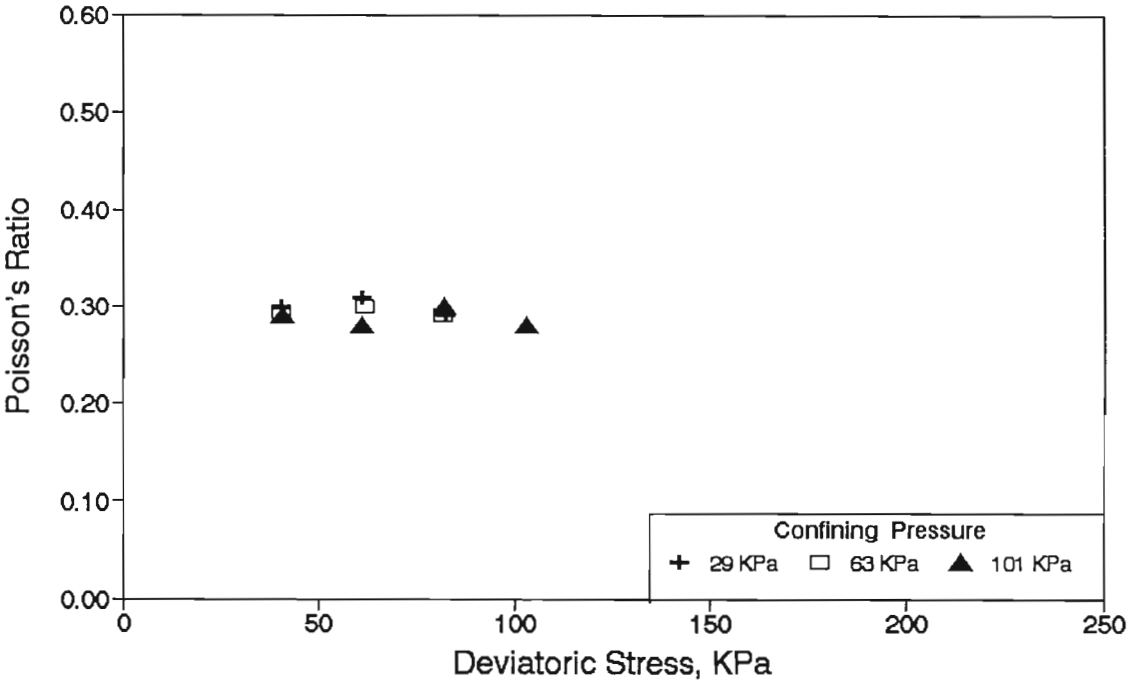

Project-1336/Specimen tested by Sriram/Data reduced and plotted by MRK Reddy

El Paso (District 24)
Specimen No: 1 Gage Length = 101mm OMC

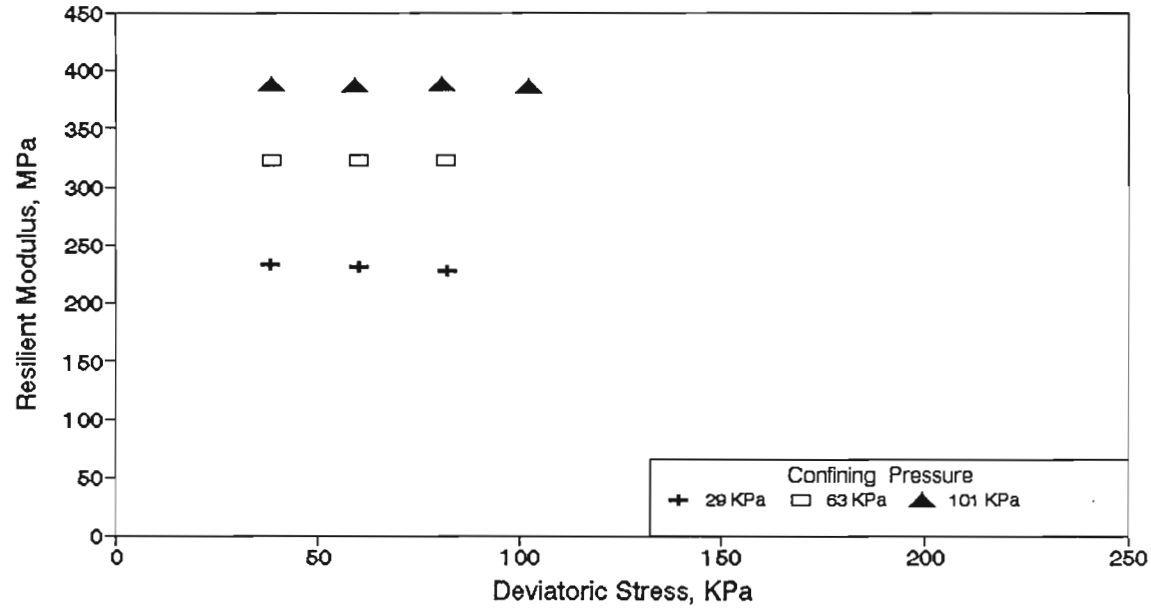

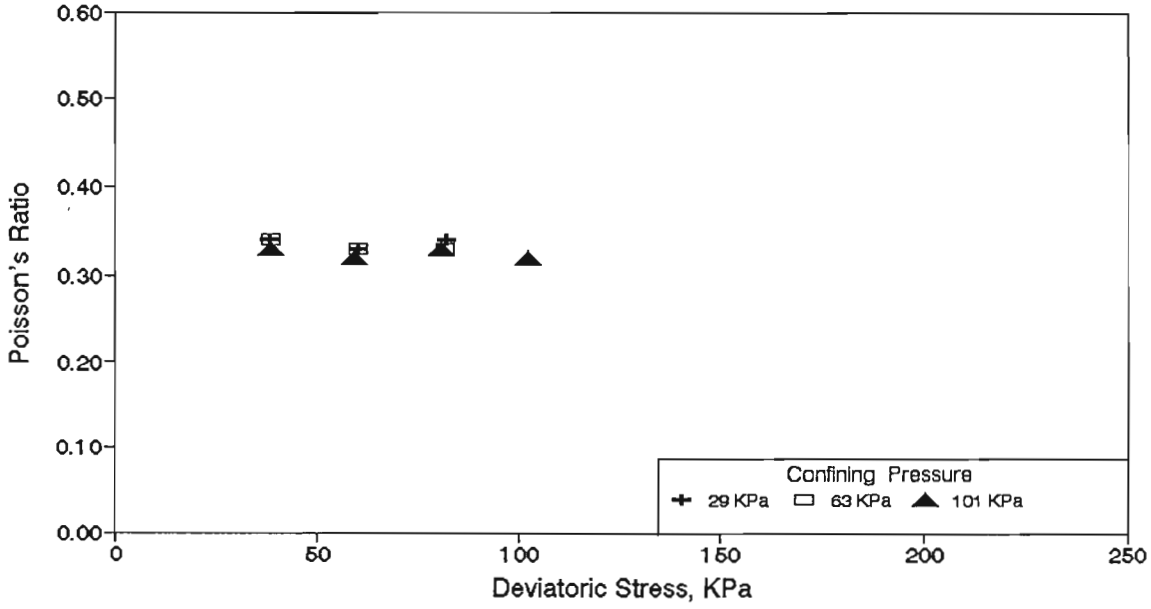

Project-1336/Specimen tested by Sriram/Data reduced and plotted by MRK Reddy

El Paso (District 24)
Specimen No: 2 Gage Length = 101mm OMC

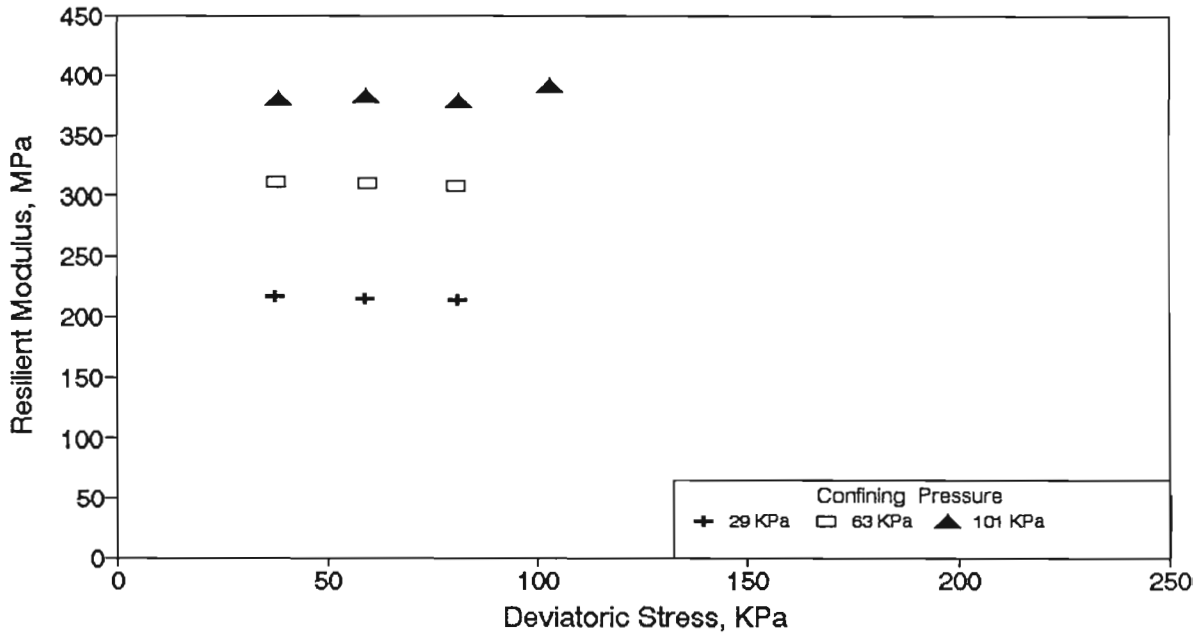

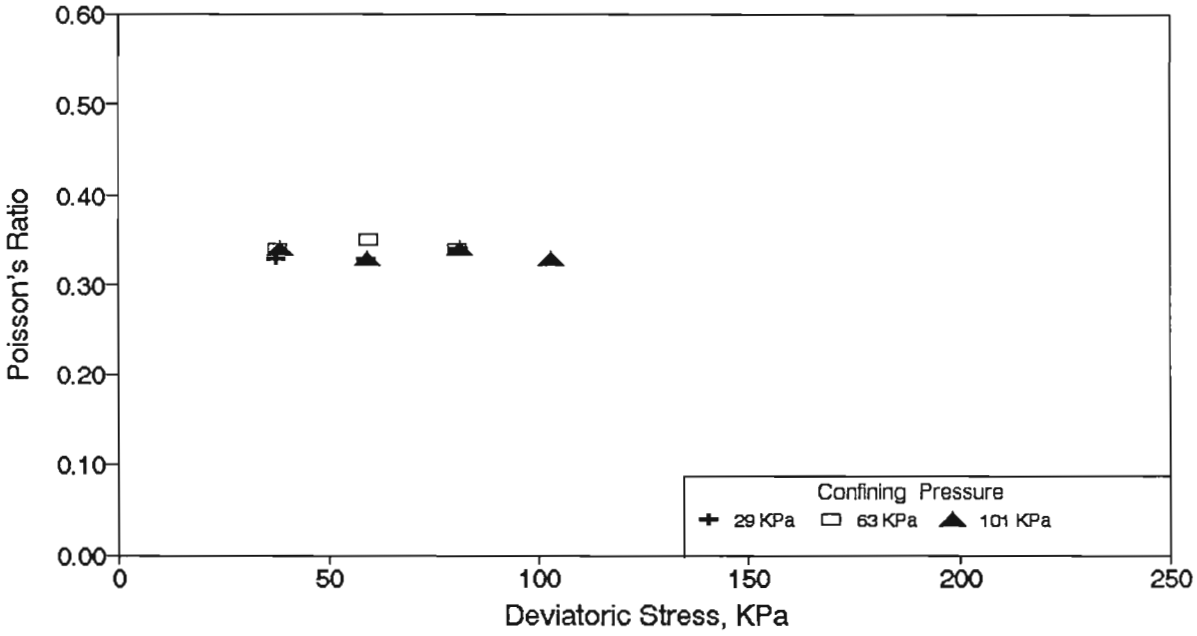

Project-1336/Specimen tested by Sriram/Data reduced and plotted by MRK Reddy

El Paso (District 24)

Specimen No: 1 Gage Length = 101mm Dry of OMC

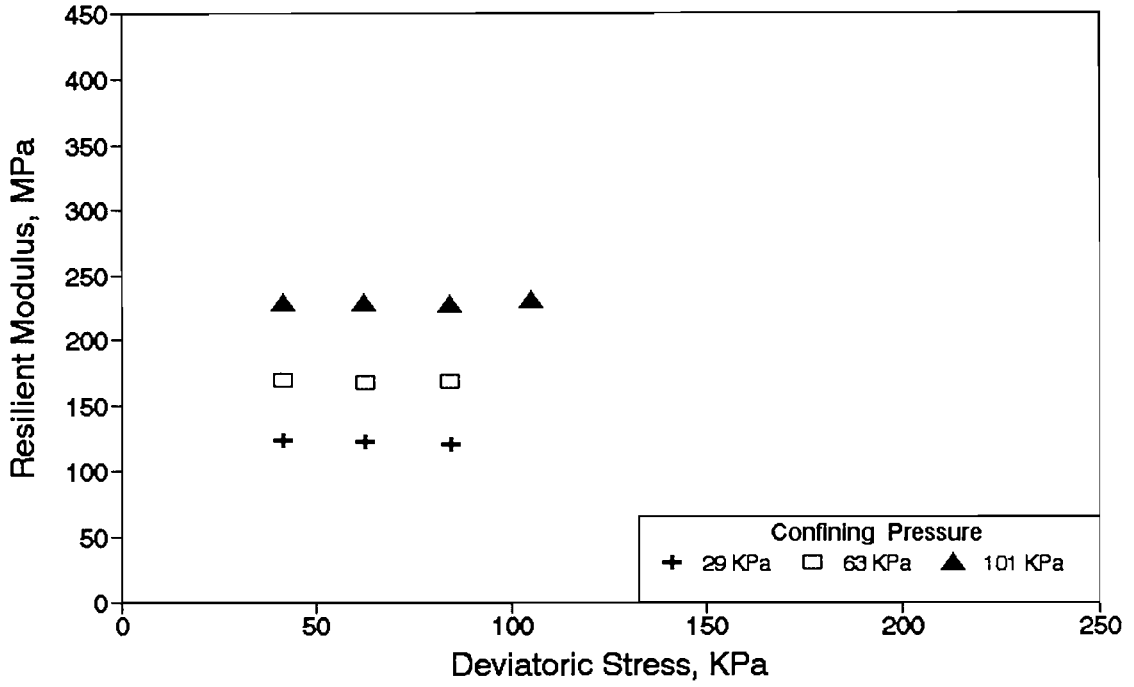

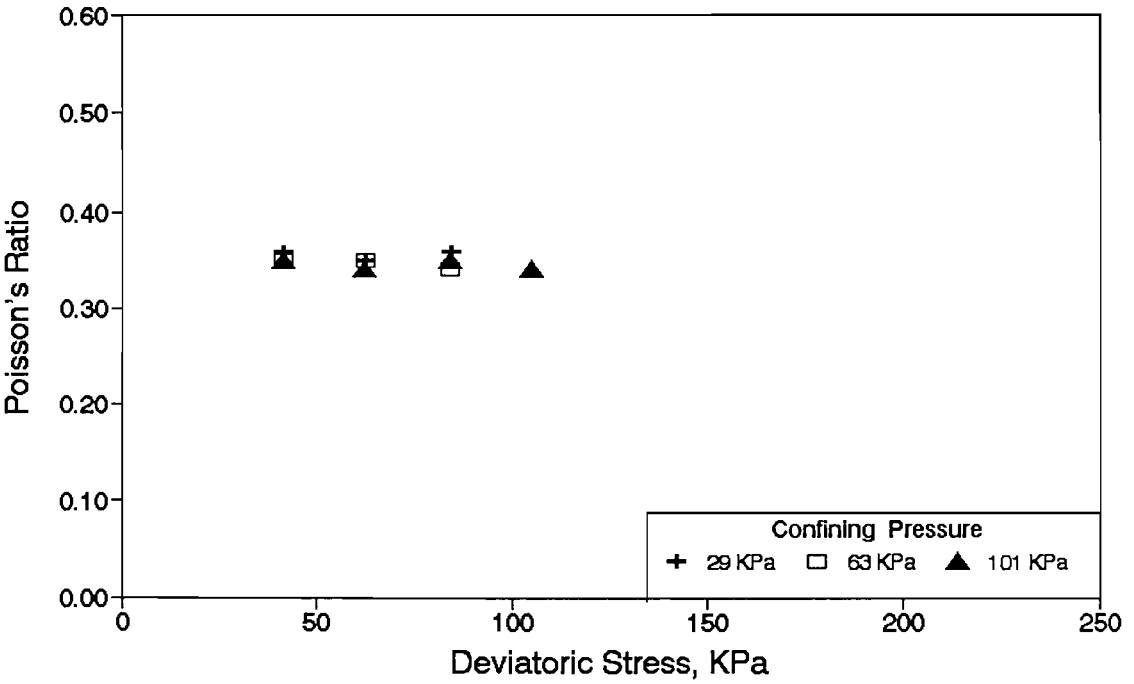

Project-1336/Specimen tested by Sriram/Data reduced and plotted by MRK Reddy

El Paso (District 24)

Specimen No: 2 Gage Length = 101mm Dry of OMC

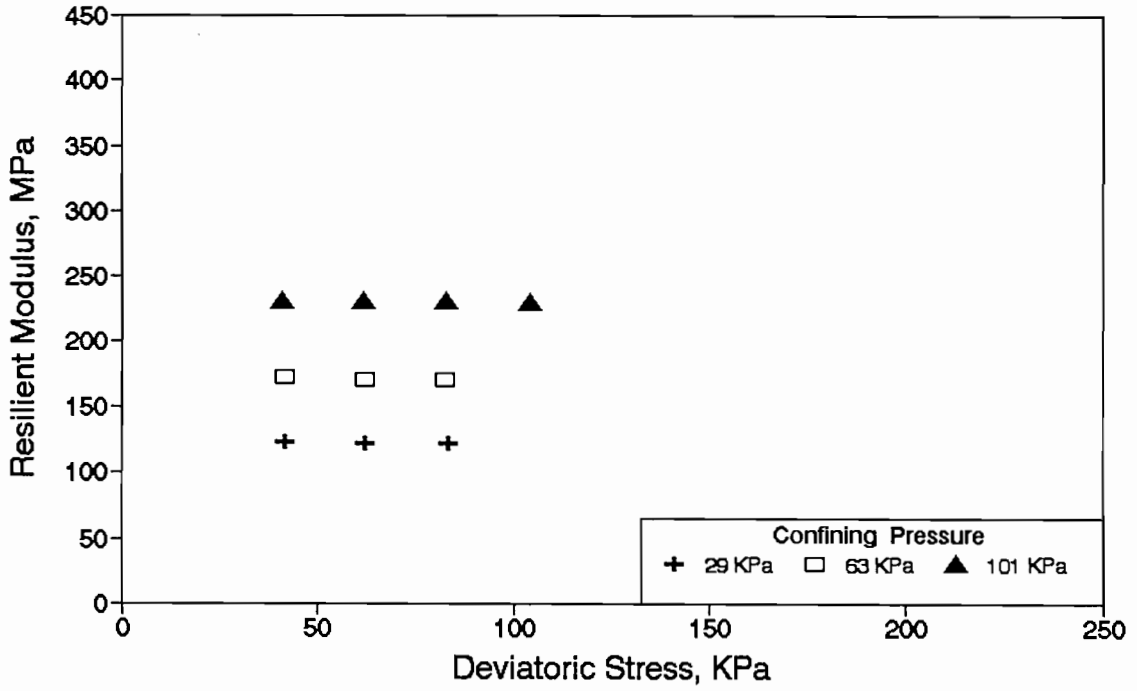

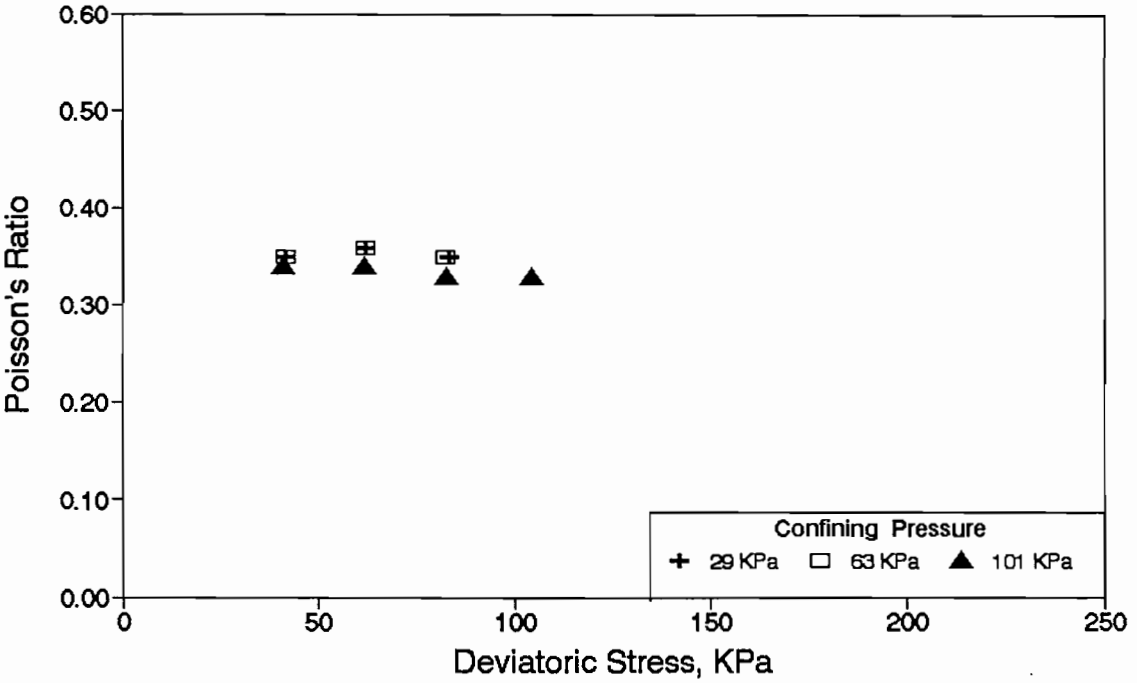

Project-1336/Specimen tested by Sriram/Data reduced and plotted by MRK Reddy

Brownwood (District 24)

Specimen No: 1 Gage Length = 101mm Wet of OMC

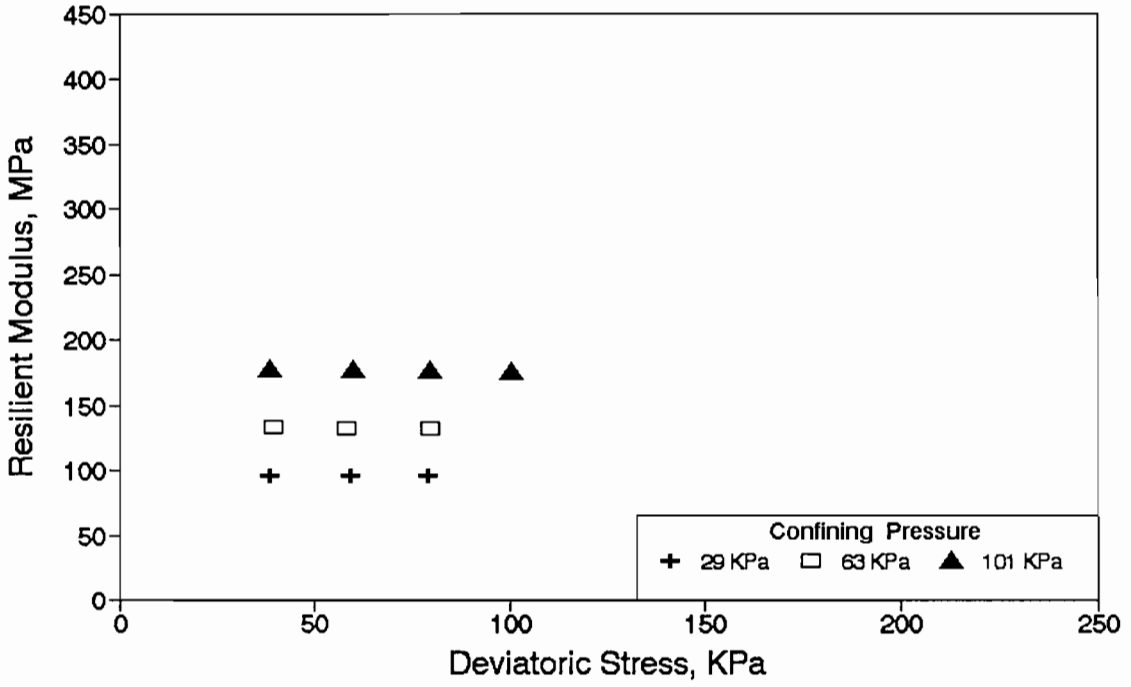

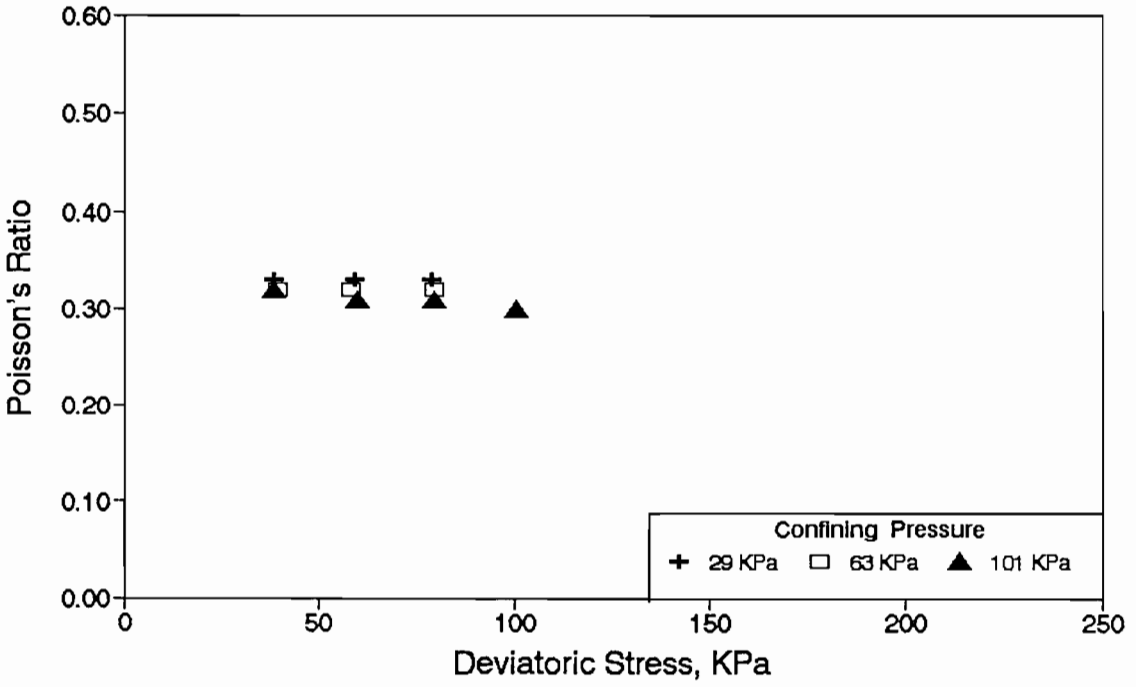

Project-1336/Specimen tested by Sriram/Data reduced and plotted by MRK Reddy

El Paso (District 24)

Specimen No: 2 Gage Length = 101mm Wet of OMC

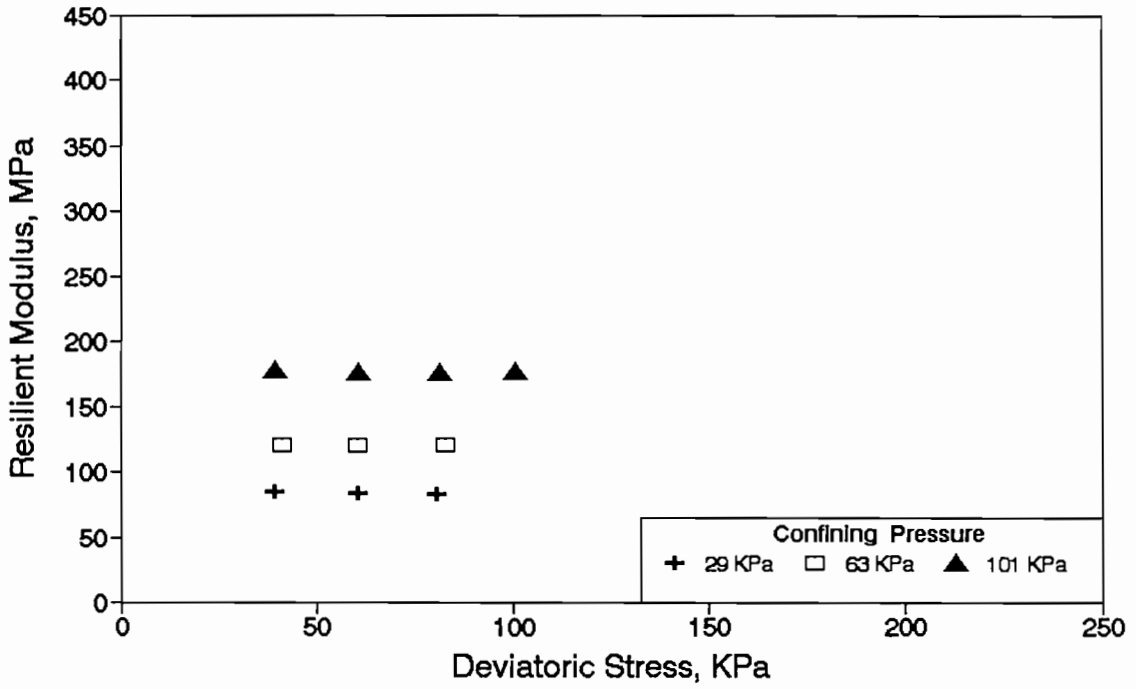

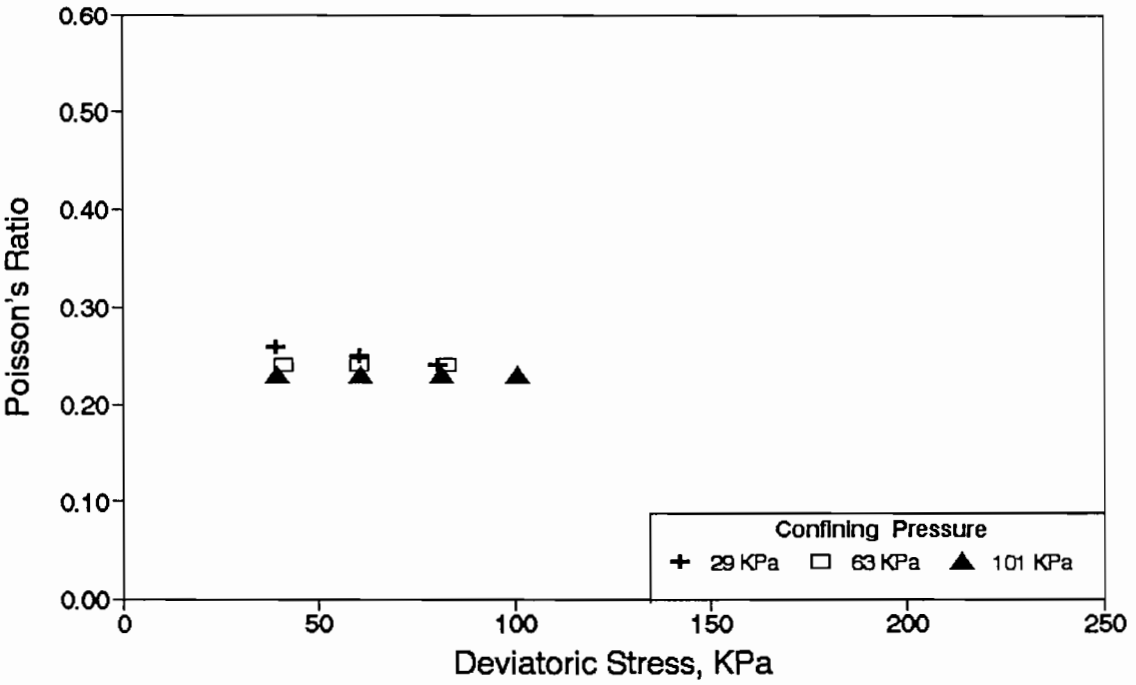

Project-1336/Specimen tested by Sriram/Data reduced and plotted by MRK Reddy

Corpuschristi (District - 16)
Specimen No. 1 (Gage Length = 102 mm) OMC

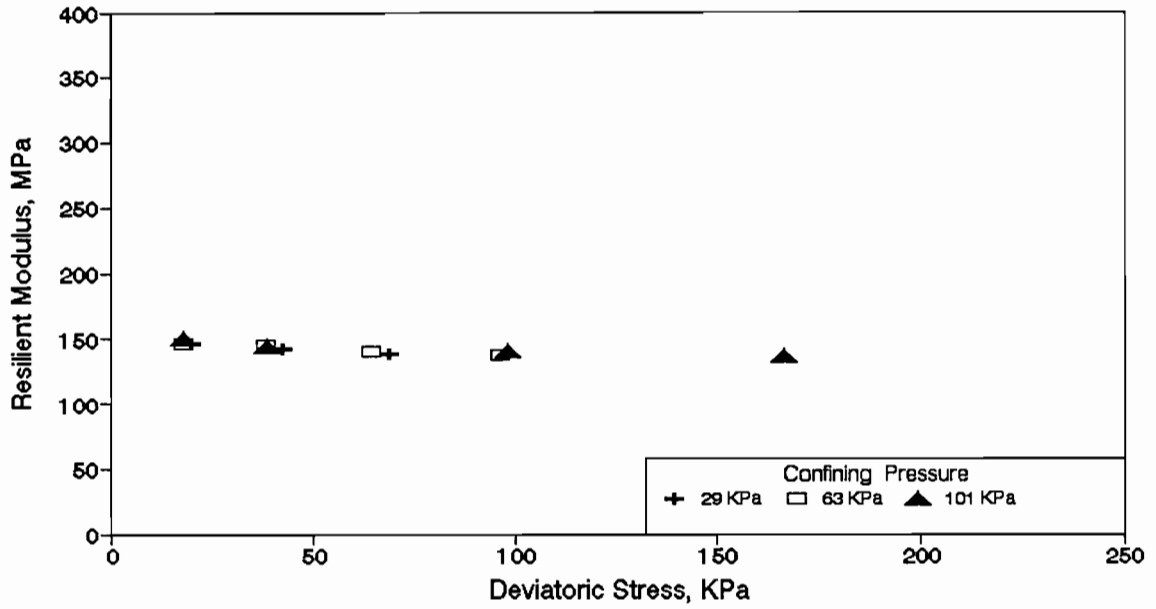

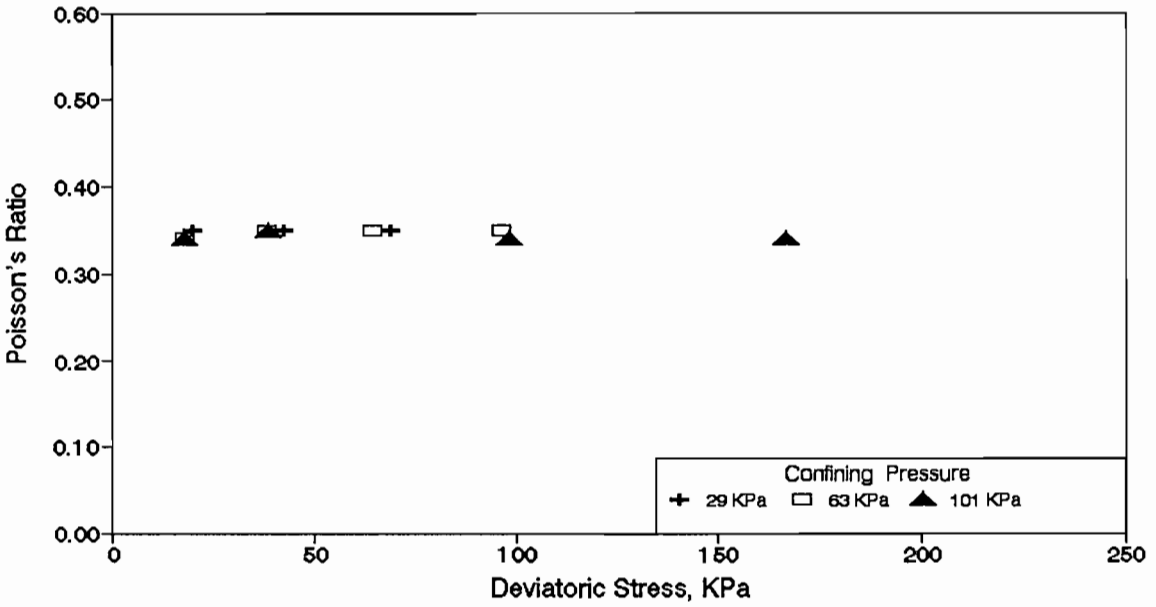

Specimen tested by Sriram

Data reduced and plotted by MRK Reddy

Corpuschristi (District - 16)
Specimen No. 2 (Gage Length = 102 mm) OMC

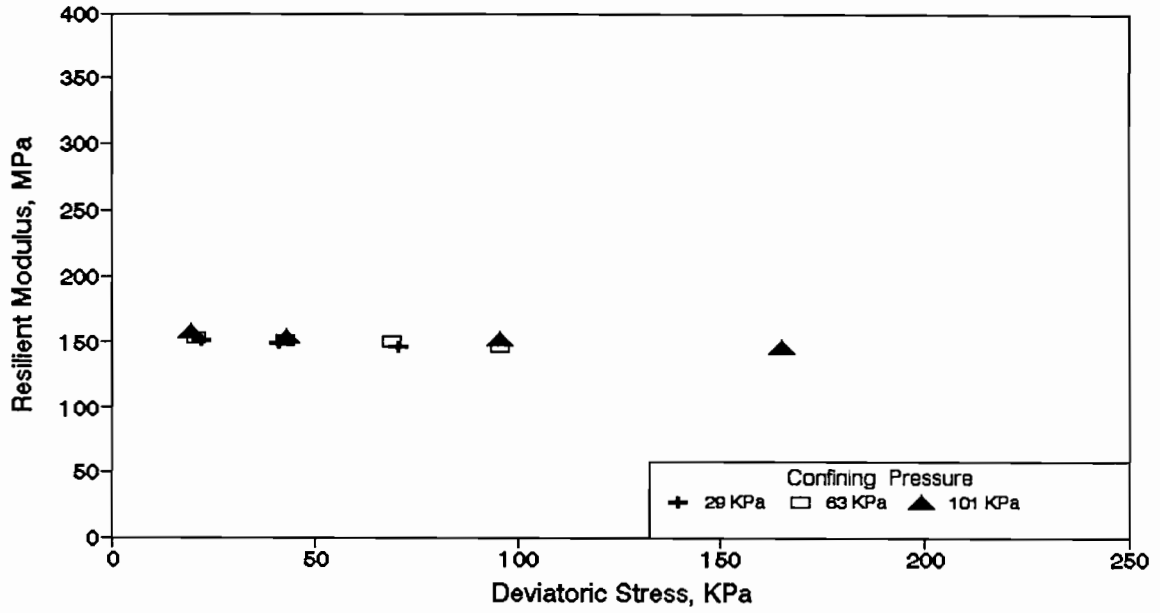

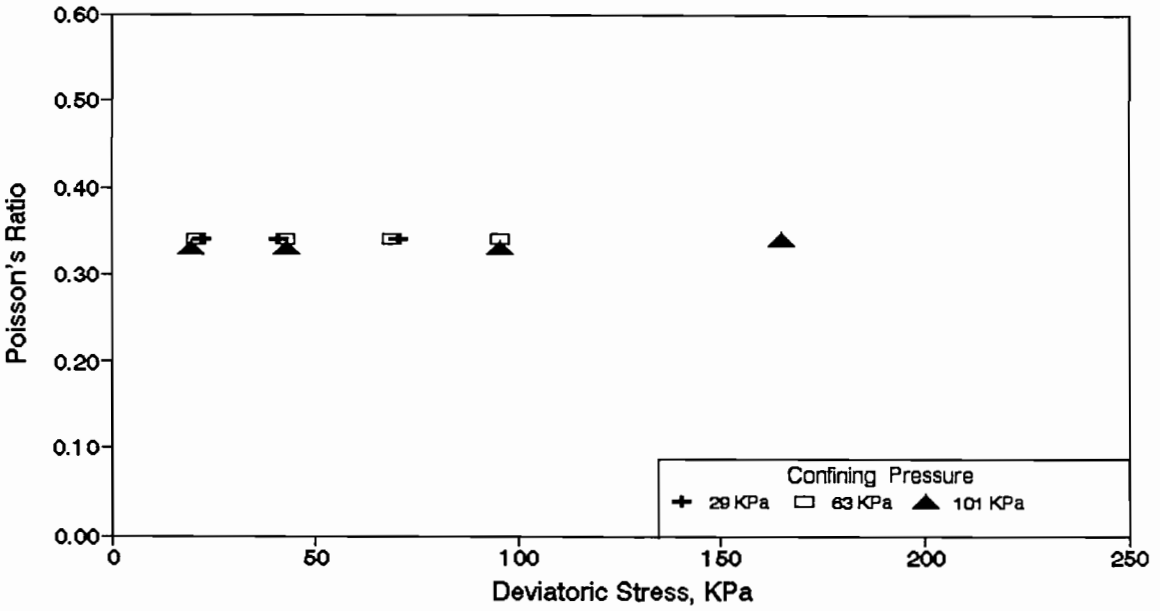

Project-1336/Specimen tested by Sriram/Data reduced and plotted by MRK Reddy

Corpus Christi (District 16)
Specimen No: 1 Gage Length = 101mm Dry of OMC

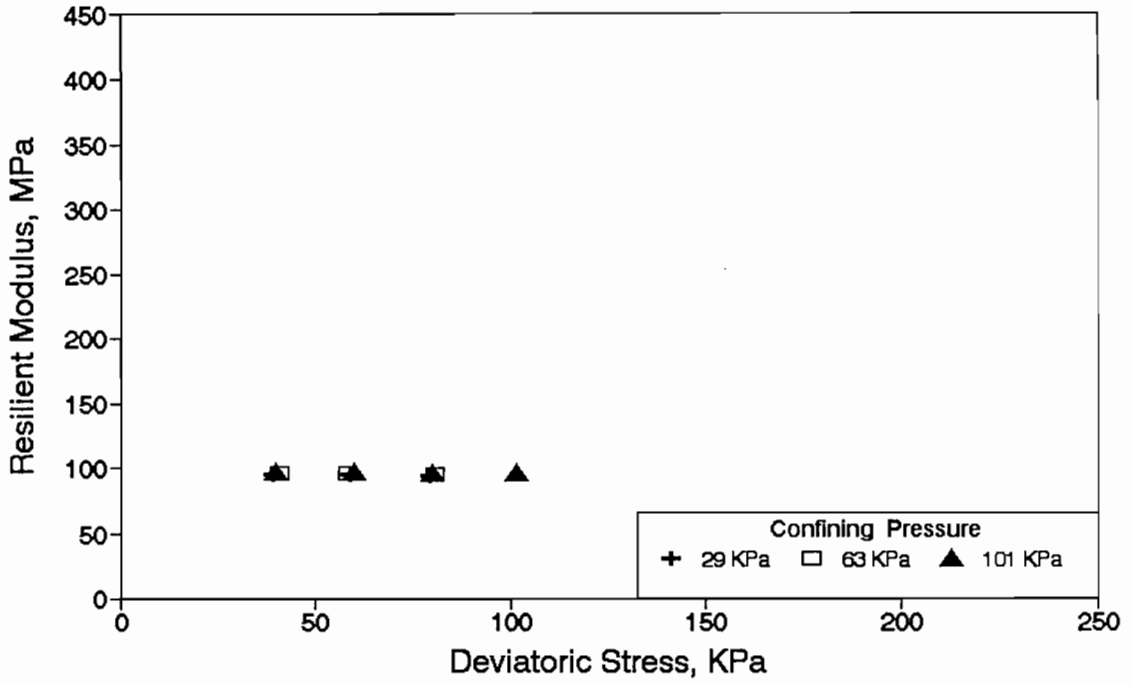

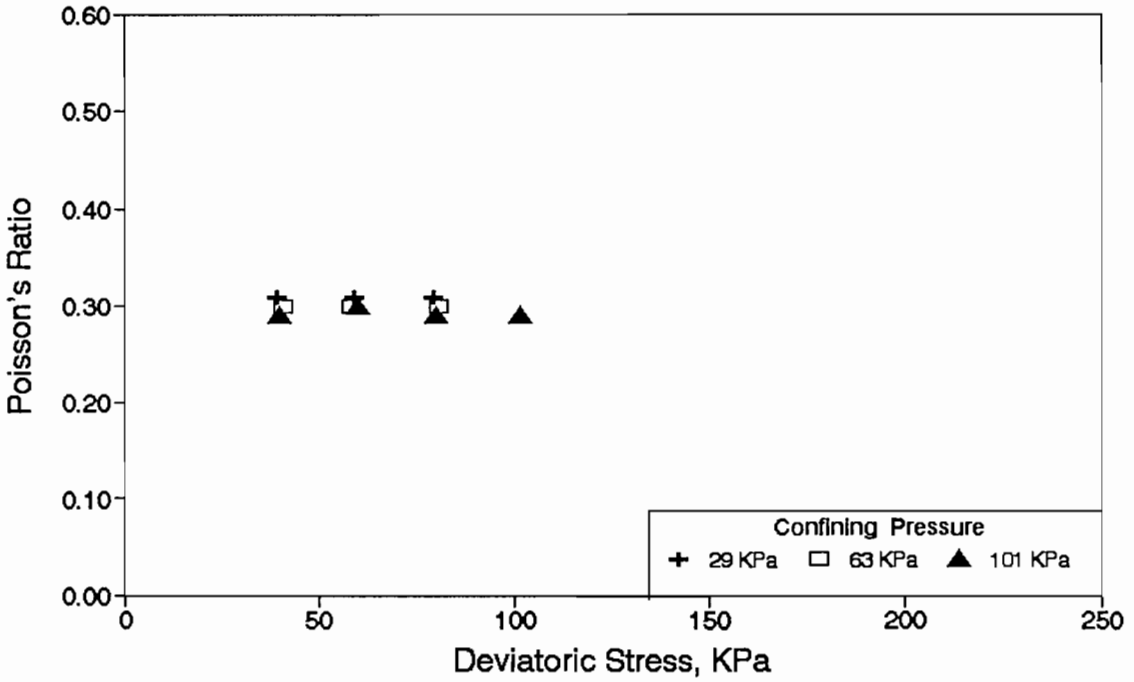

Project-1336/Specimen tested by Sriram/Data reduced and plotted by MRK Reddy

Corpus Christi (District 16)
Specimen No: 2 Gage Length = 101mm Dry of OMC

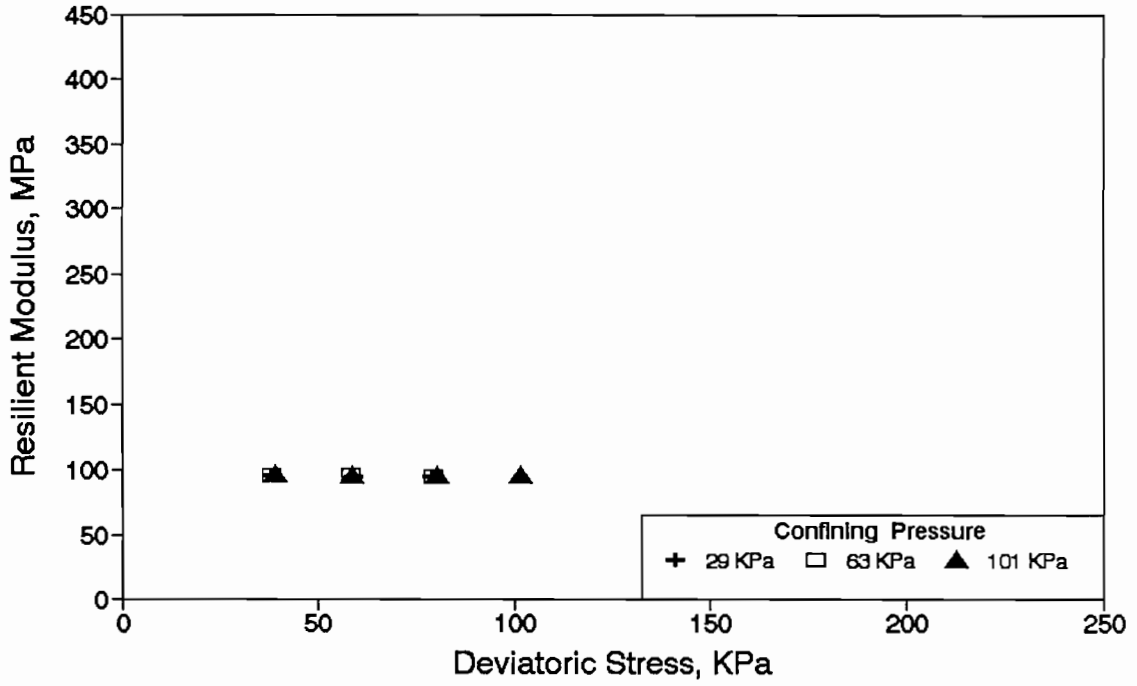

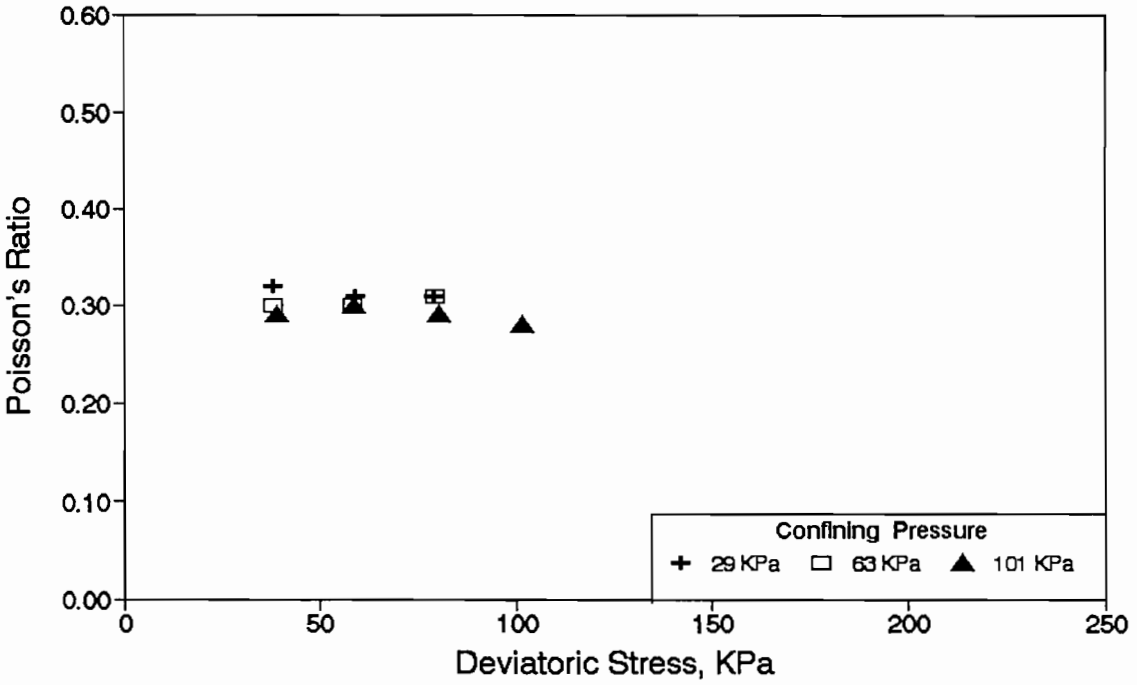

Project-1336/Specimen tested by Sriram/Data reduced and plotted by MRK Reddy

Corpus Christi (District 16)
Specimen No: 1 Gage Length = 101mm Wet of OMC

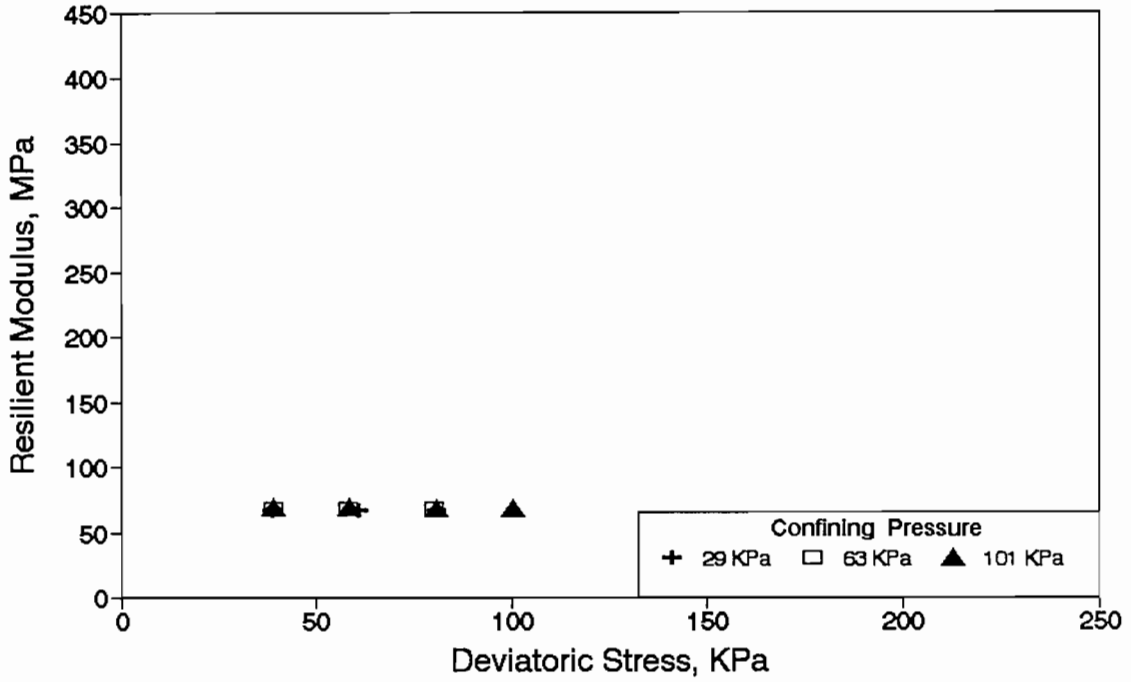

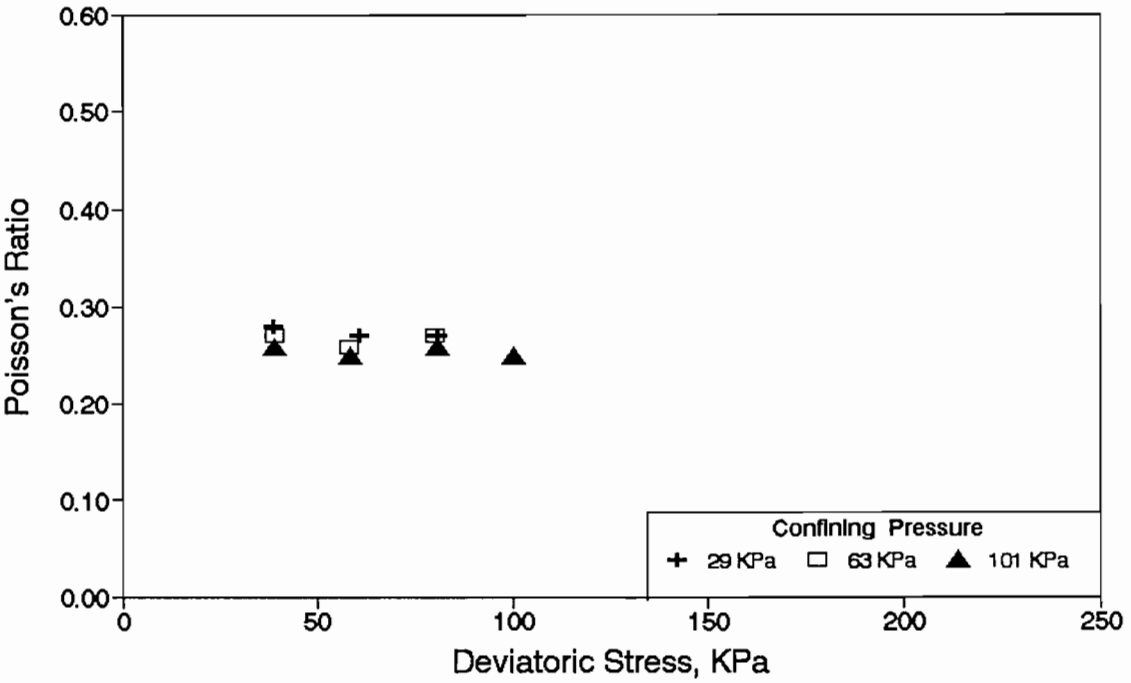

Project-1336/Specimen tested by Sriram/Data reduced and plotted by MRK Reddy

Corpus Christi (District 16)
Specimen No: 2 Gage Length = 101mm Wet of OMC

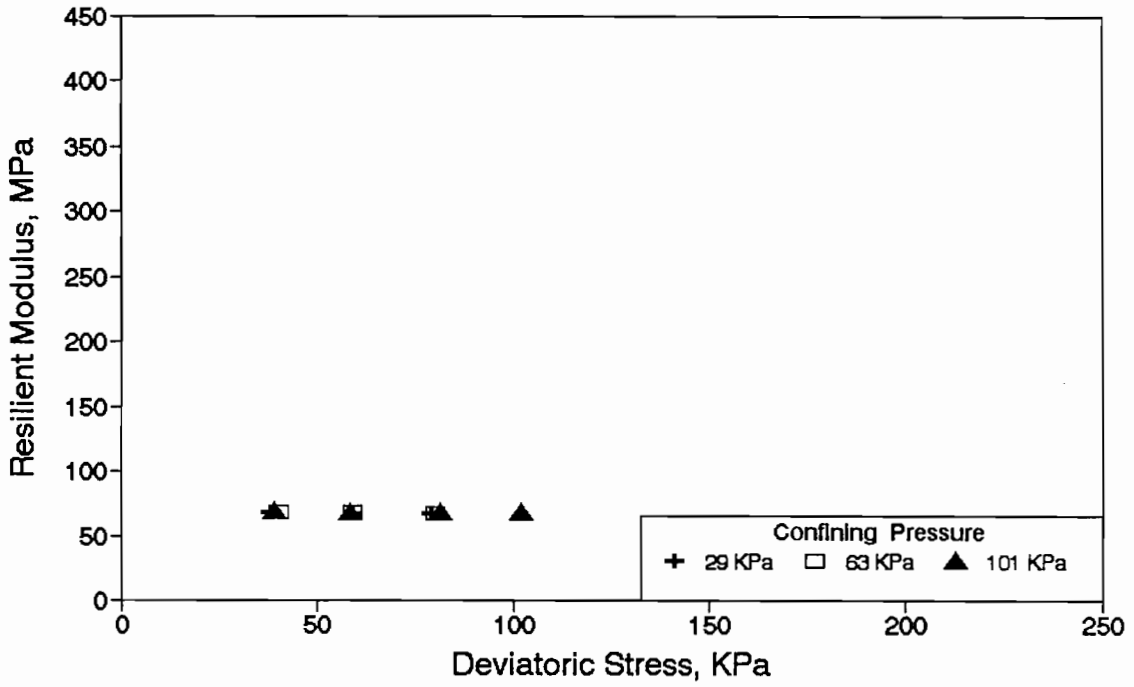

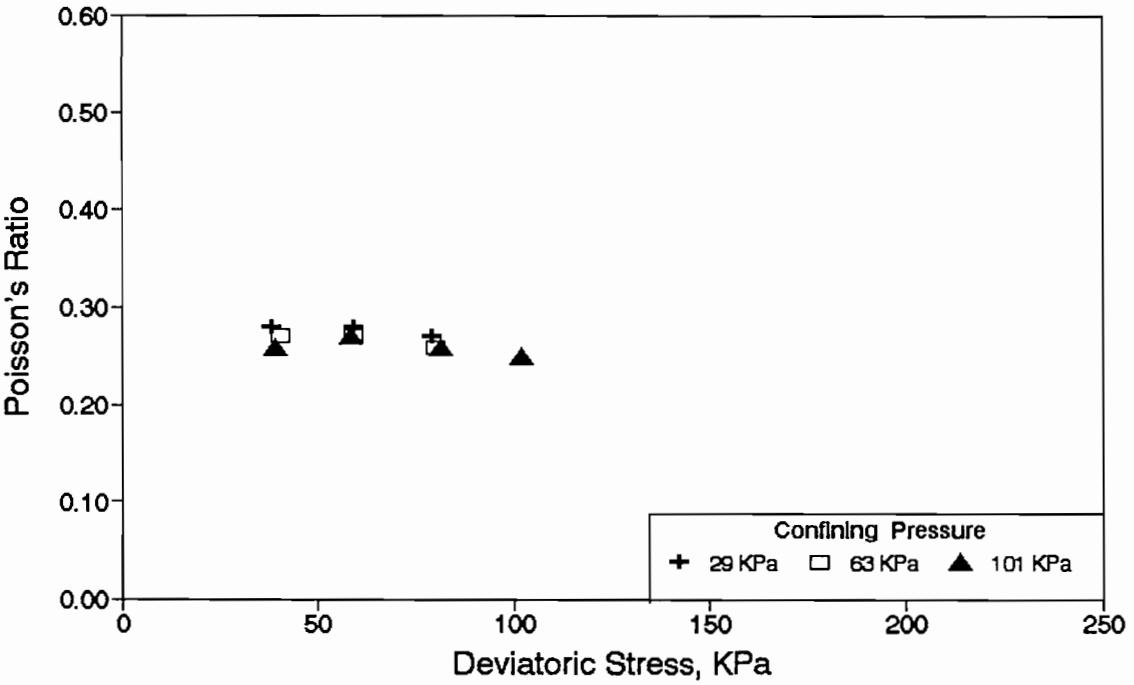

Project-1336/Specimen tested by Sriram/Data reduced and plotted by MRK Reddy

San Antonio (District 14)
Specimen No: 1 Gage Length = 101mm OMC

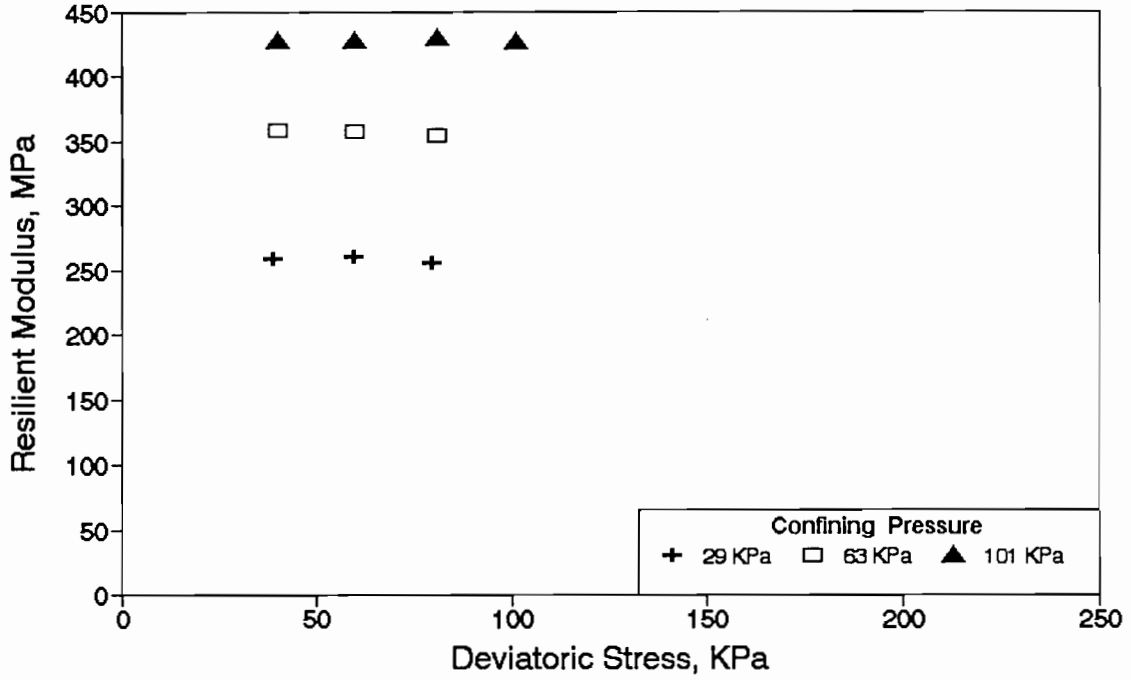

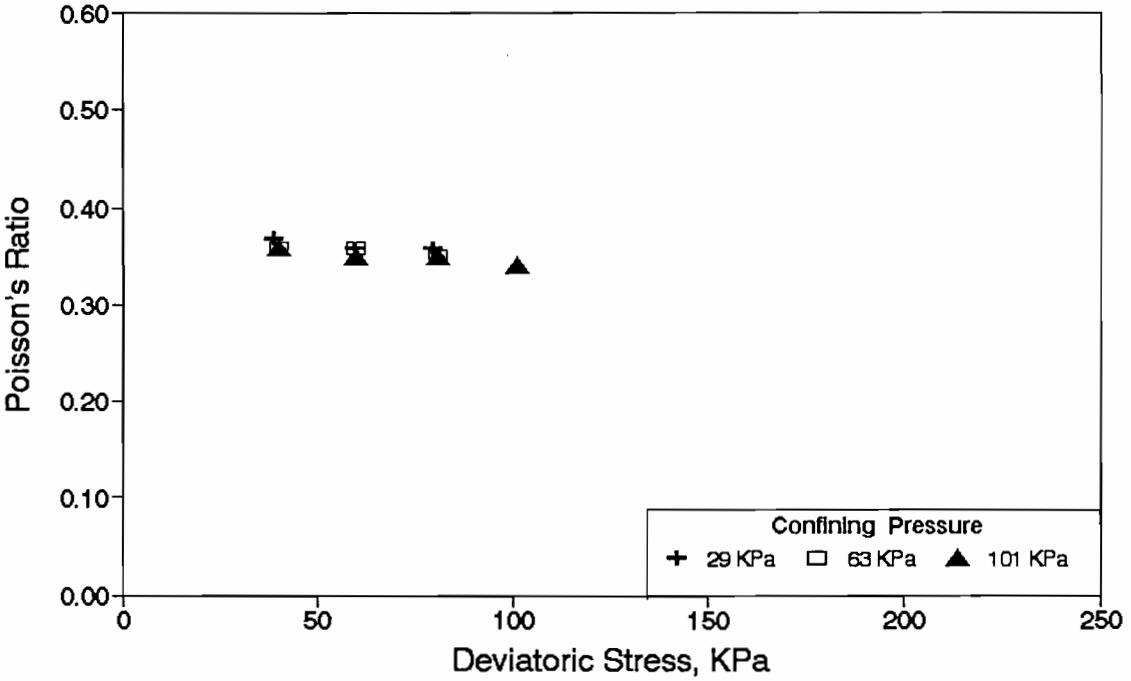

Project-1336/Specimen tested by Sriram/Data reduced and plotted by MRK Reddy

San Antonio (District 14)
Specimen No: 2 Gage Length = 101mm OMC

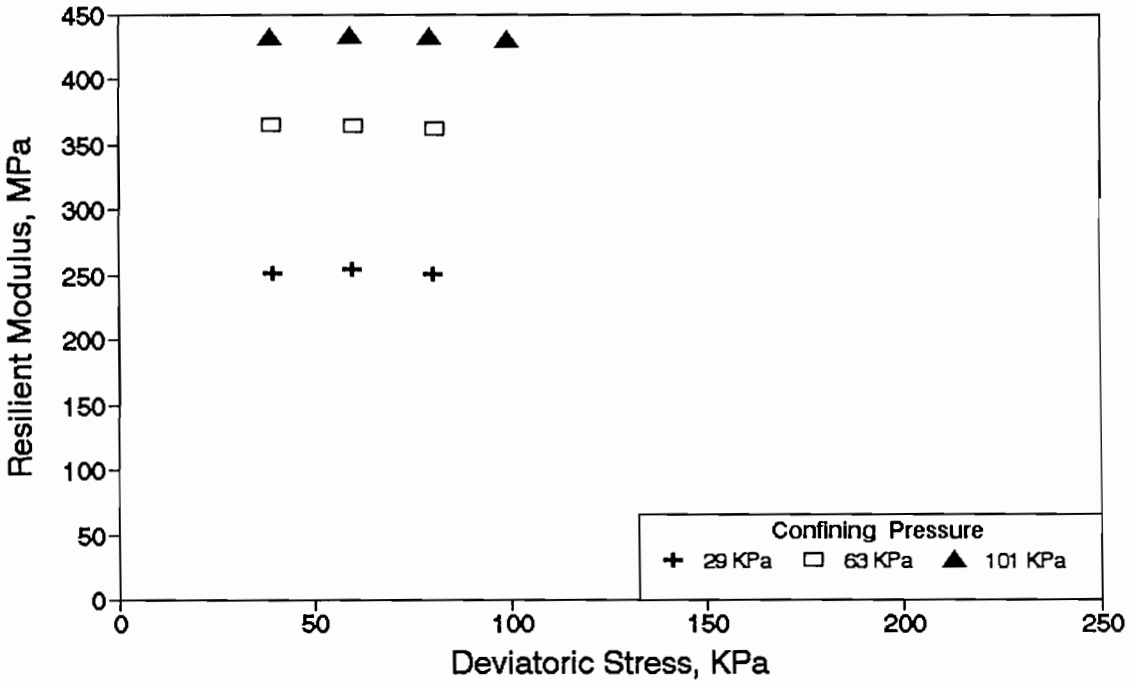

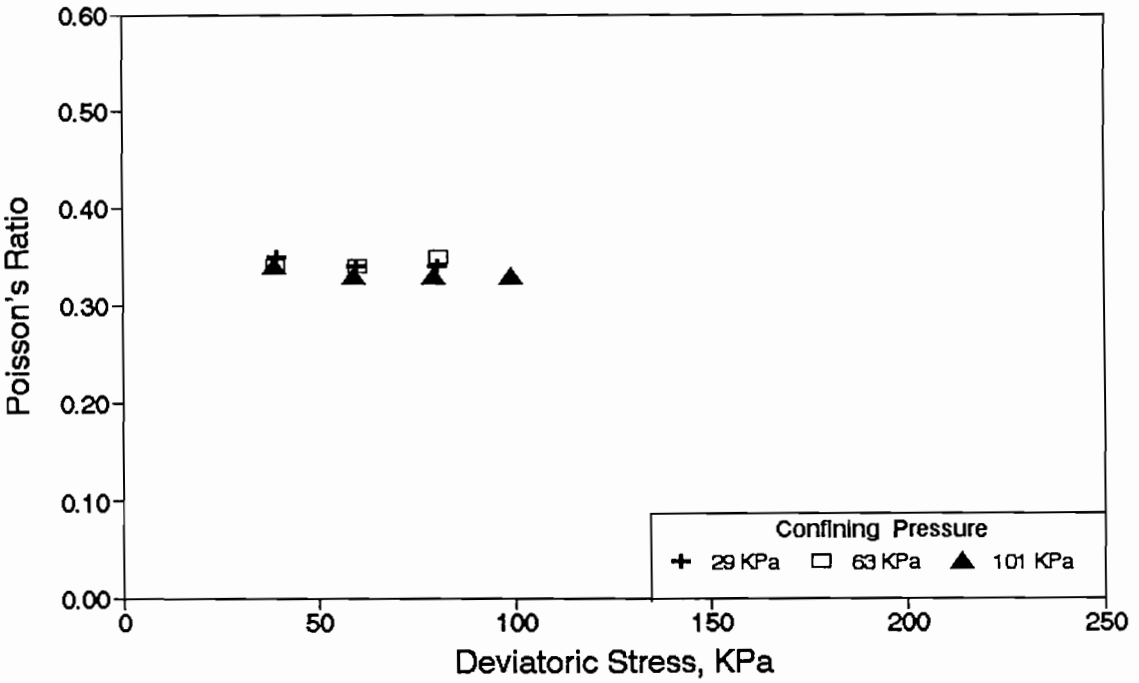

Project-1336/Specimen tested by Sriram/Data reduced and plotted by MRK Reddy

San Antonio (District 14)

Specimen No: 1 Gage Length = 101mm

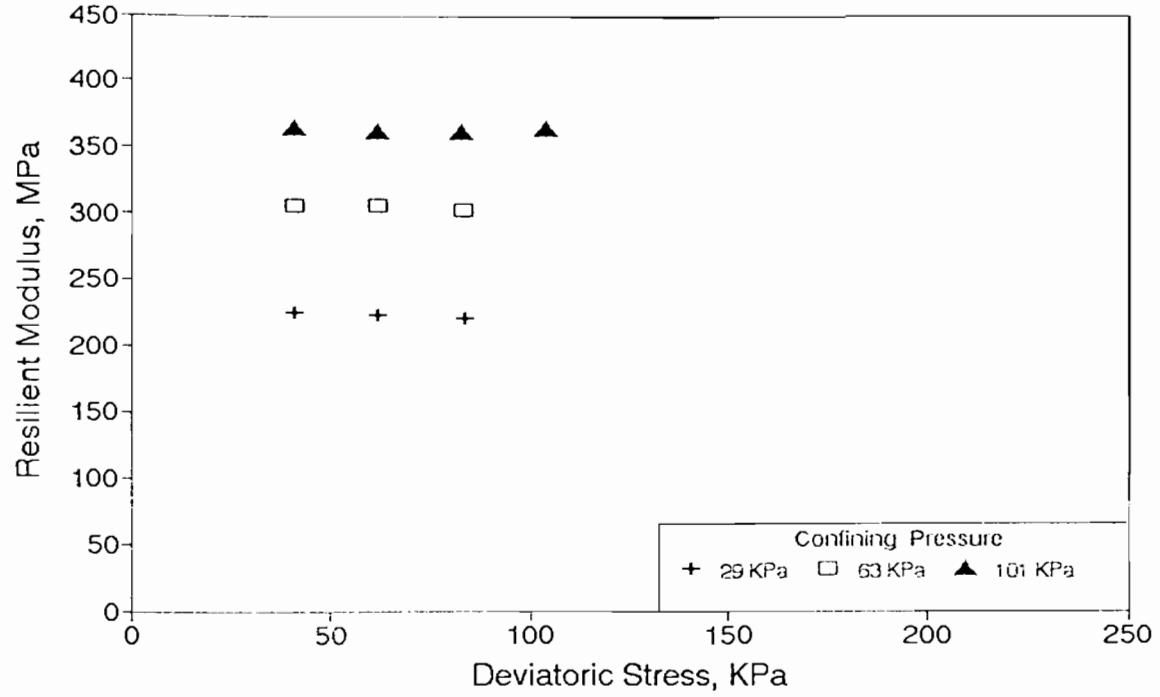

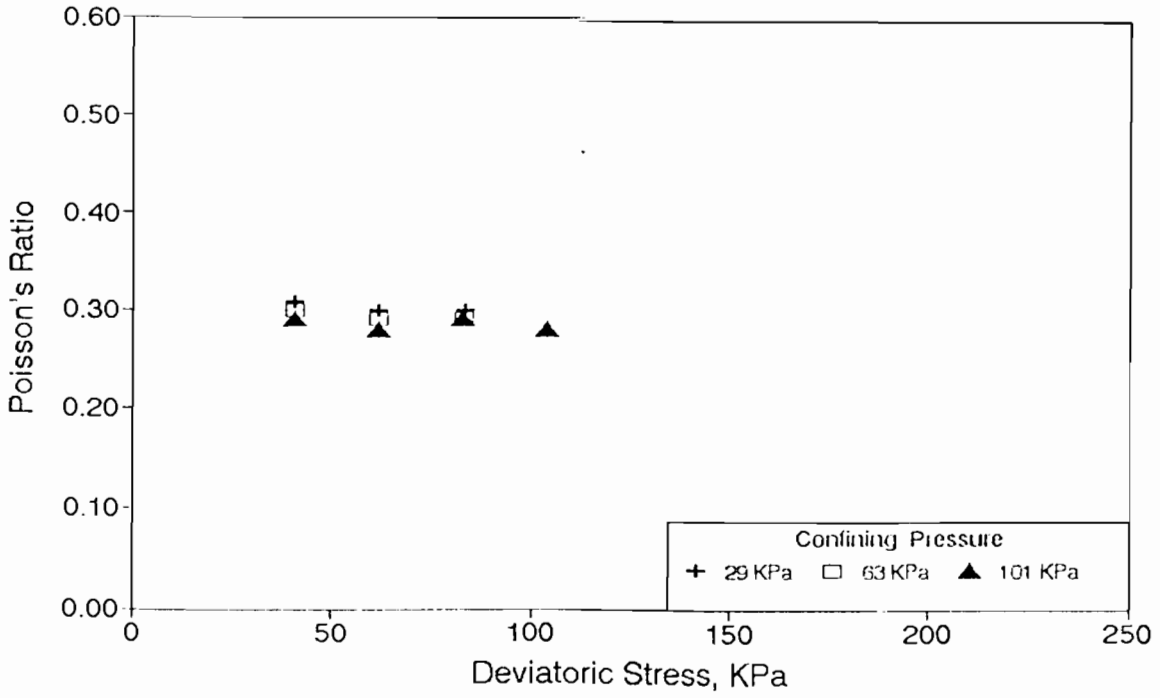

San Antonio (District 14)

Specimen No: 2 Gage Length = 101mm

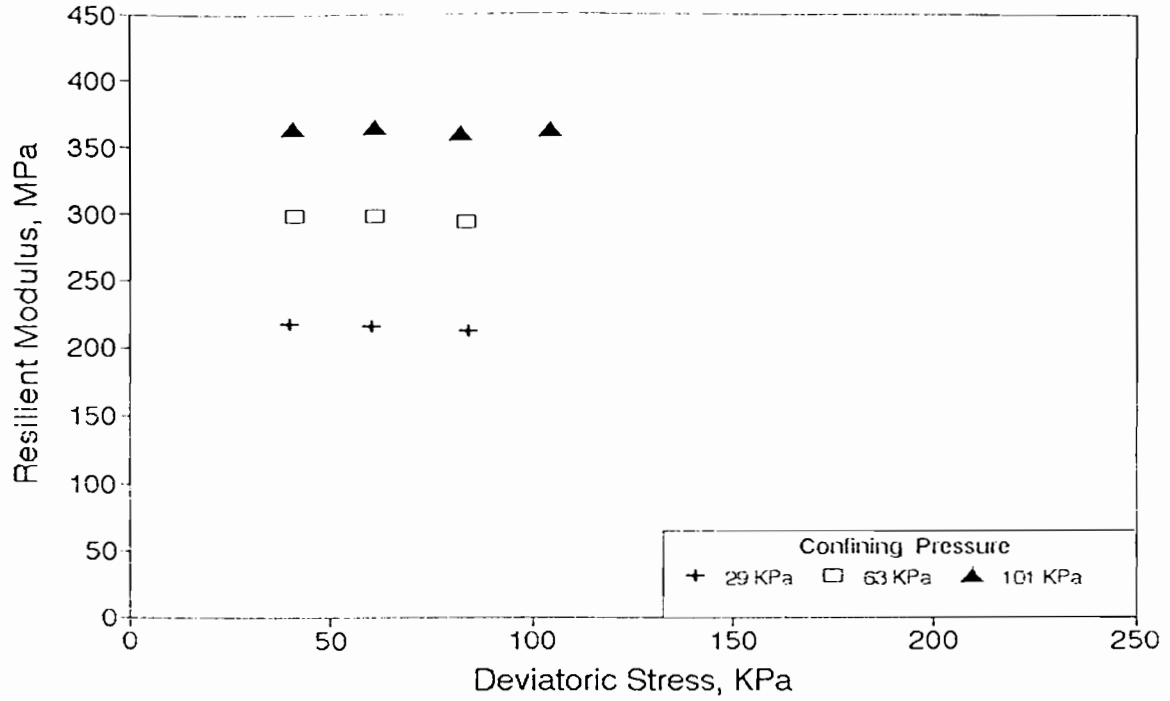

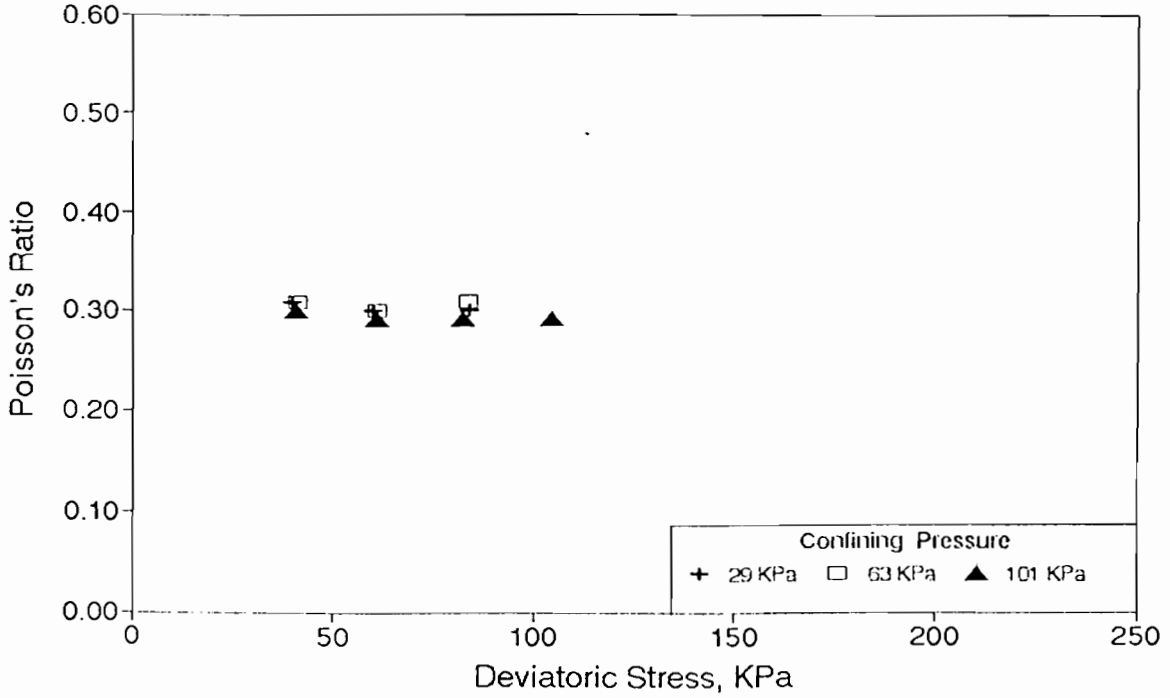

Project-1336/Specimen tested by Sriram/Data reduced and plotted by MRK Reddy

San Antonio (District 14)

Specimen No: 1 Gage Length = 101mm Wet of OMC

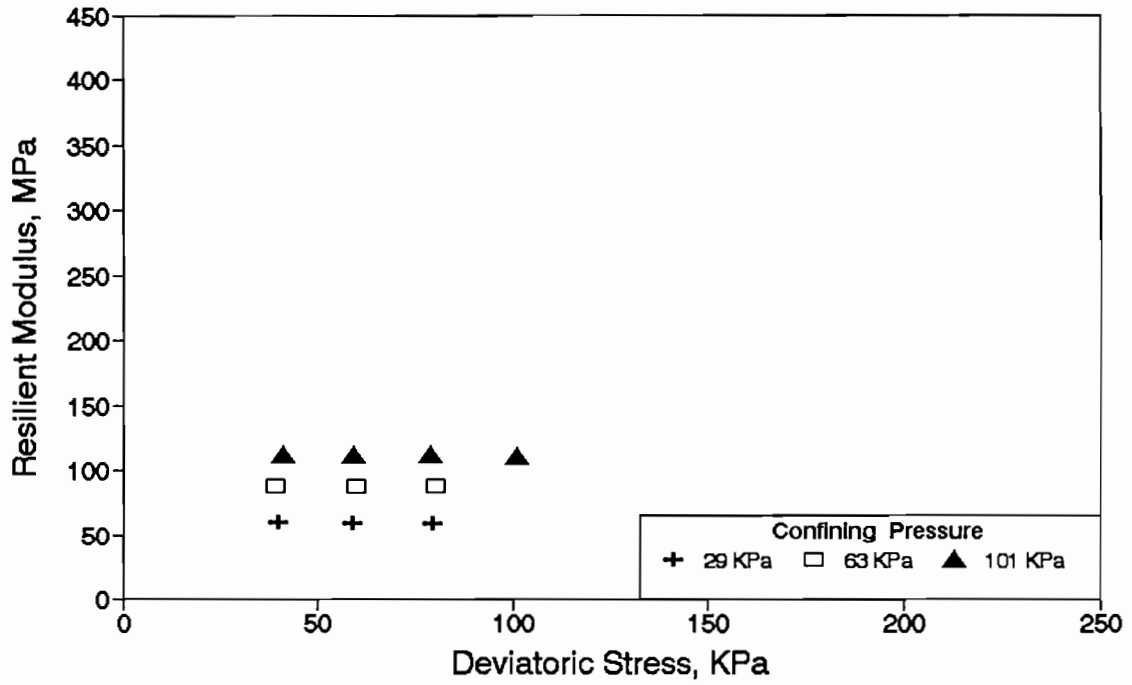

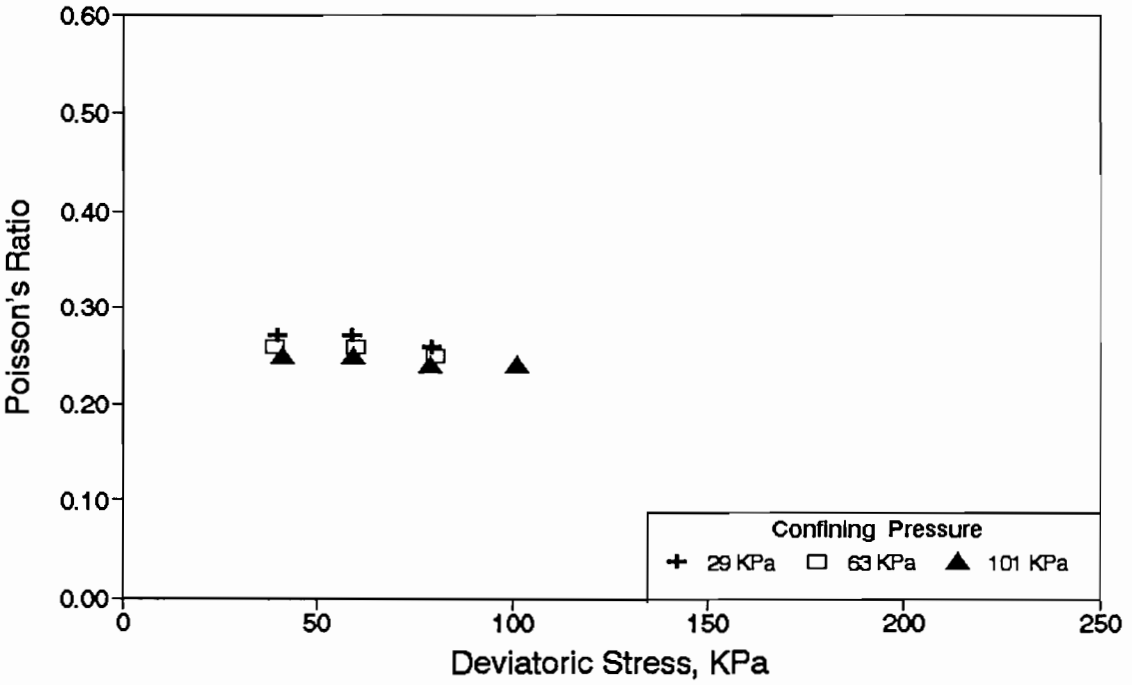

Project-1336/Specimen tested by Sriram/Data reduced and plotted by MRK Reddy

San Antonio (District 14)
Specimen No: 2 Gage Length = 101mm Wet of OMC

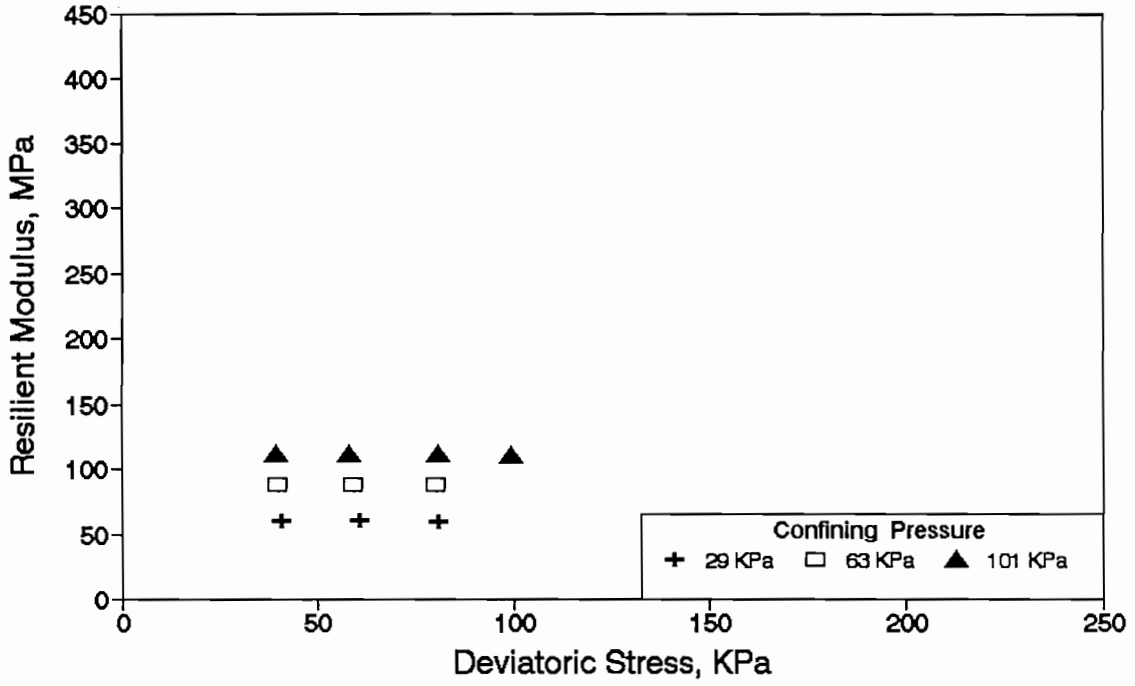

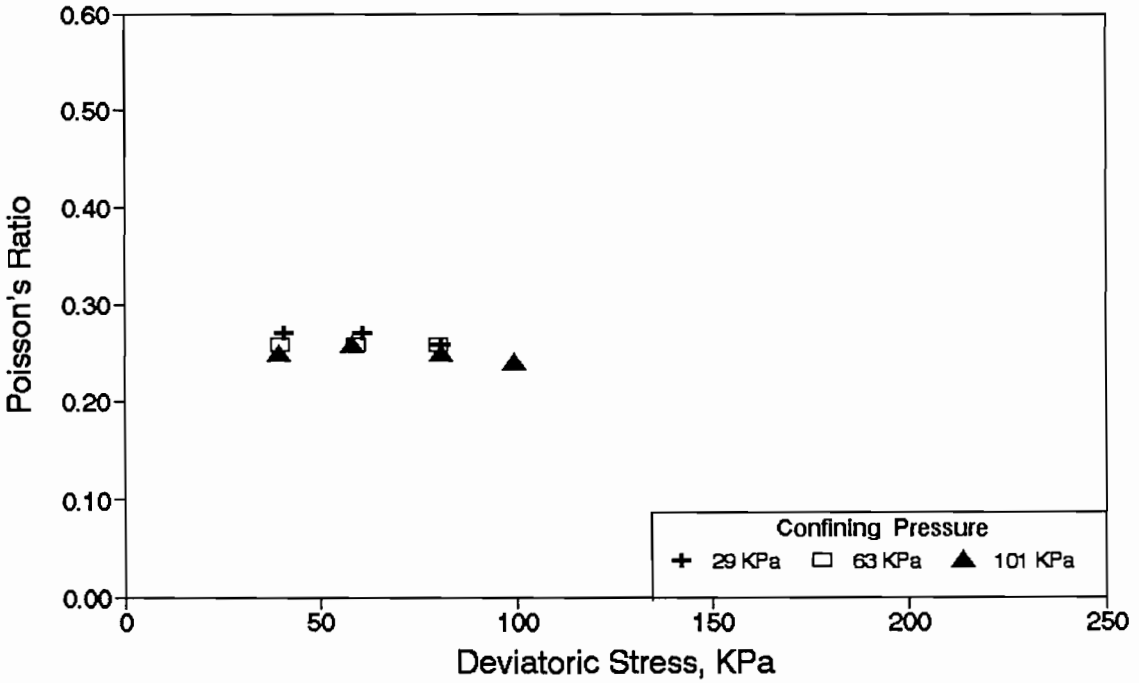

Project-1336/Specimen tested by Sriram/Data reduced and plotted by MRK Reddy

Brownwood (District - 23)
Specimen No. 1 (Gage Length = 101 mm) OMC

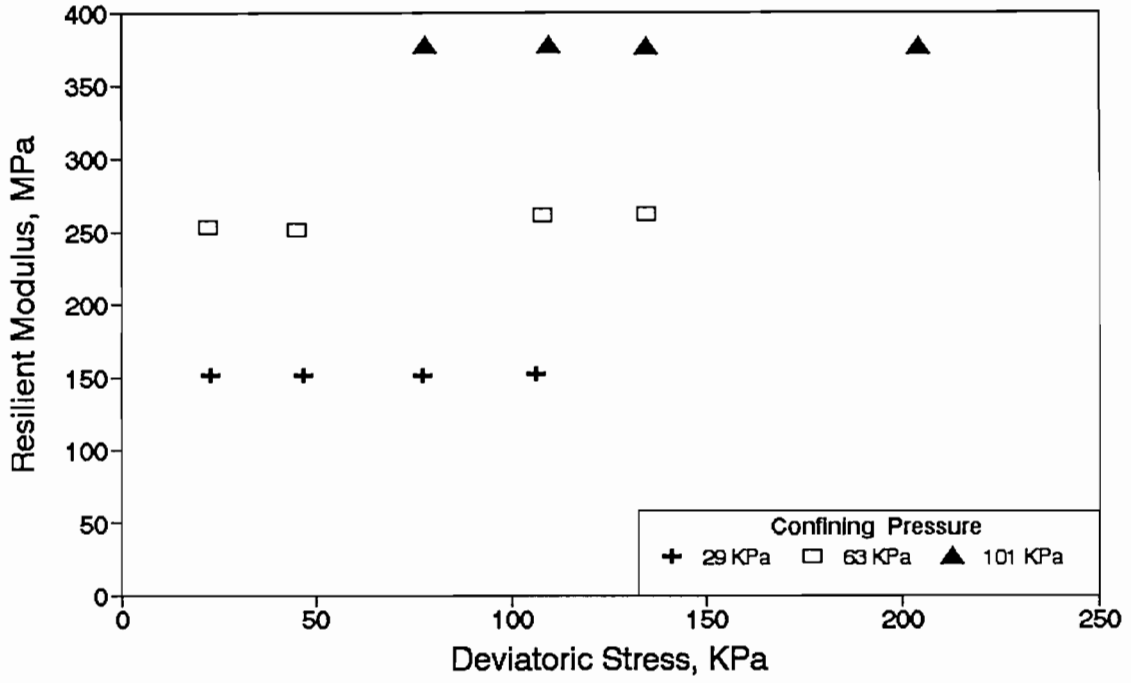

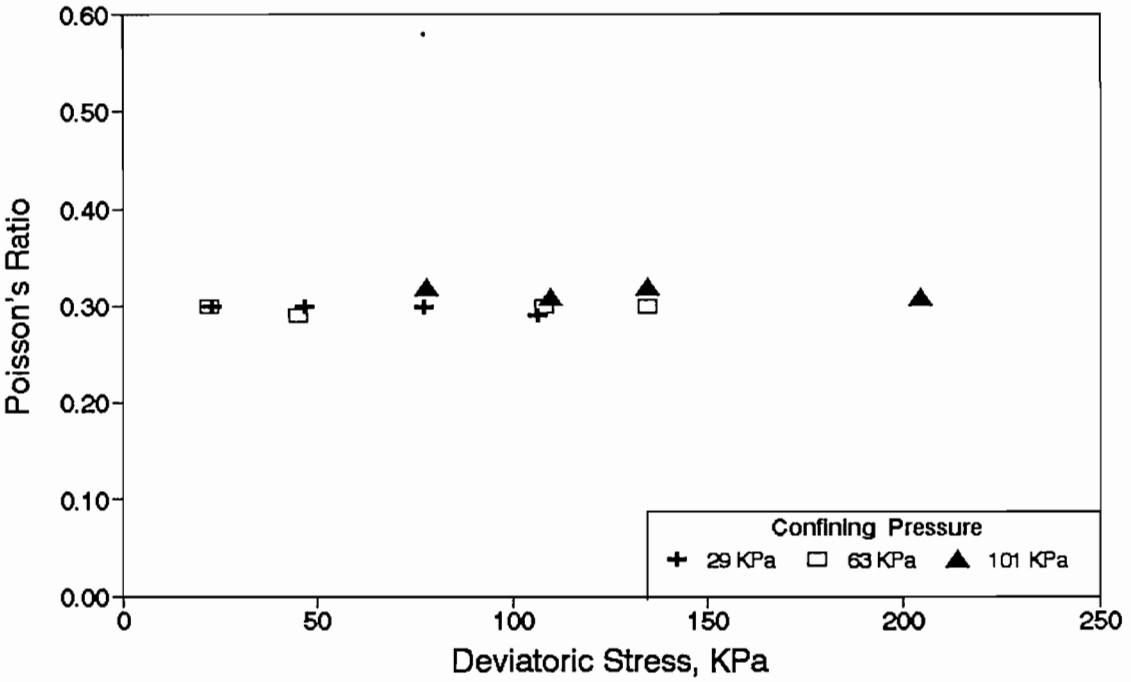

Specimen tested by Sriram

Data reduced and plotted by MRK Reddy

Brownwood (District - 23)
Specimen No. 2 (Gage Length = 101 mm) OMC

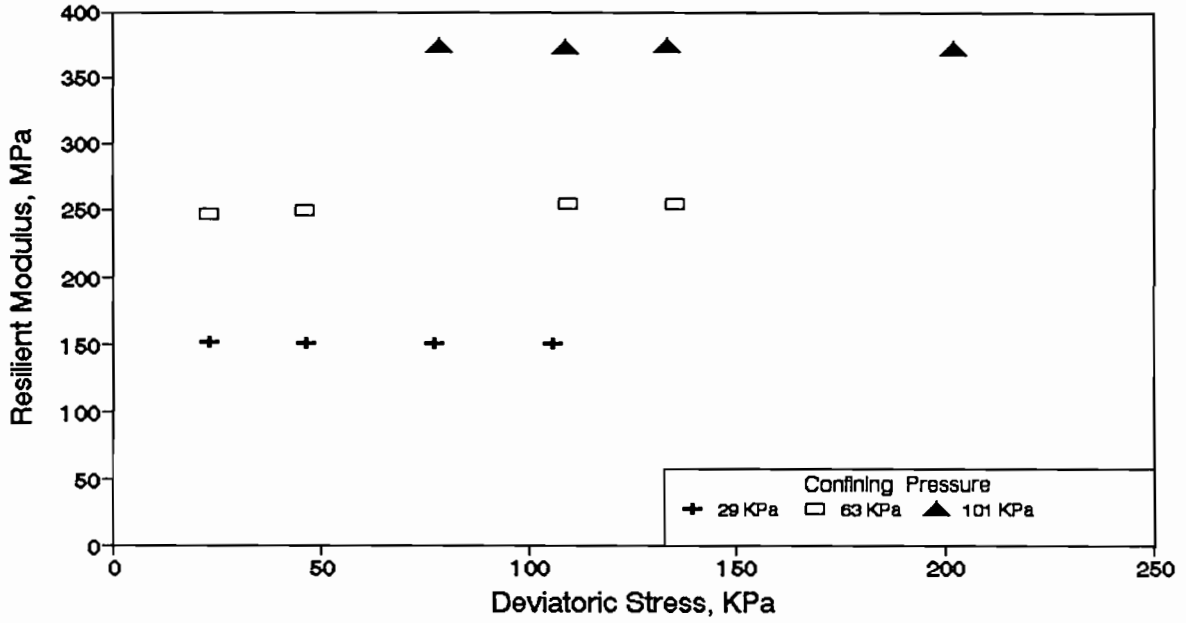

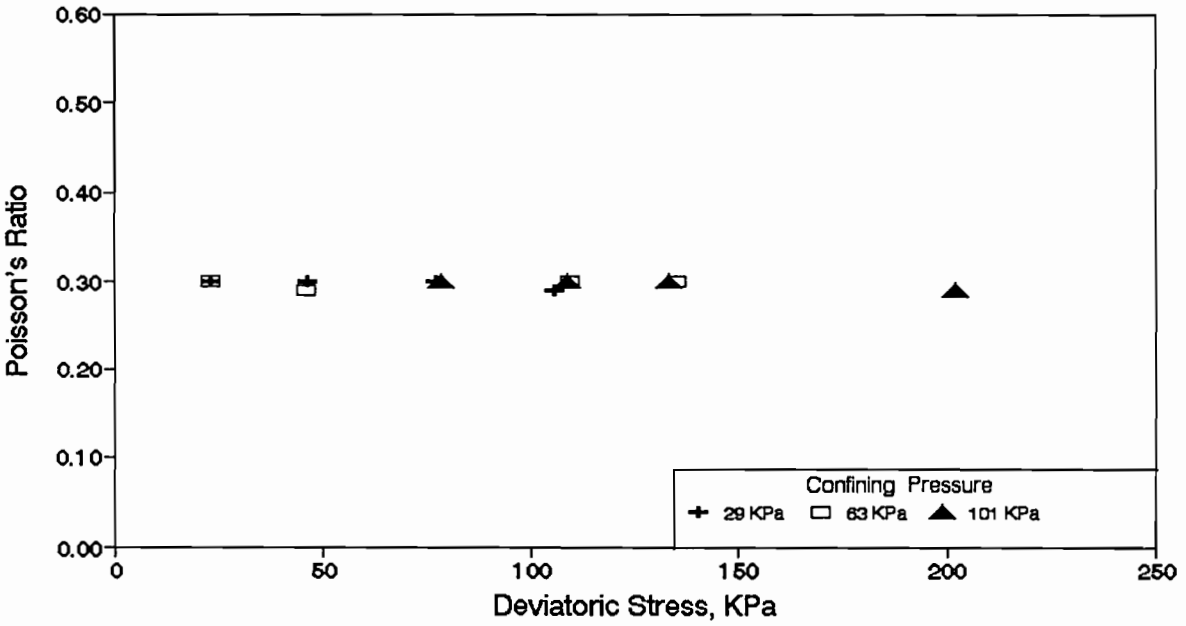

Specimen tested by Sriram

Data reduced and plotted by MRK Reddy

Brownwood (District 23)

Specimen No: 2 Gage Length = 101mm Wet of OMC

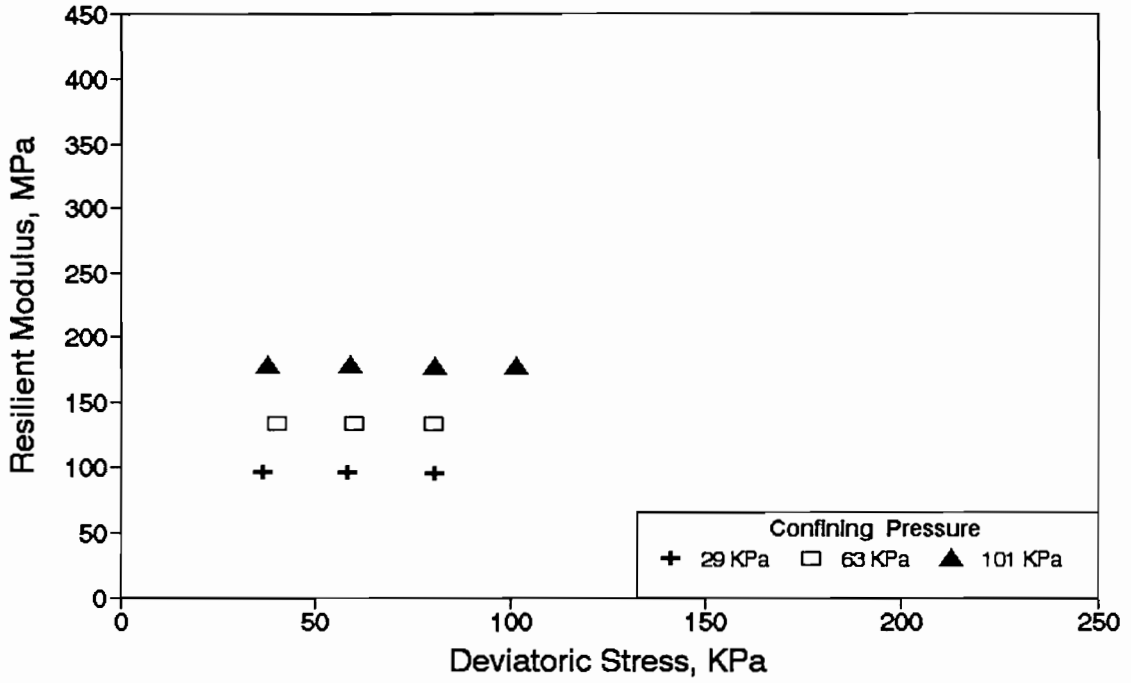

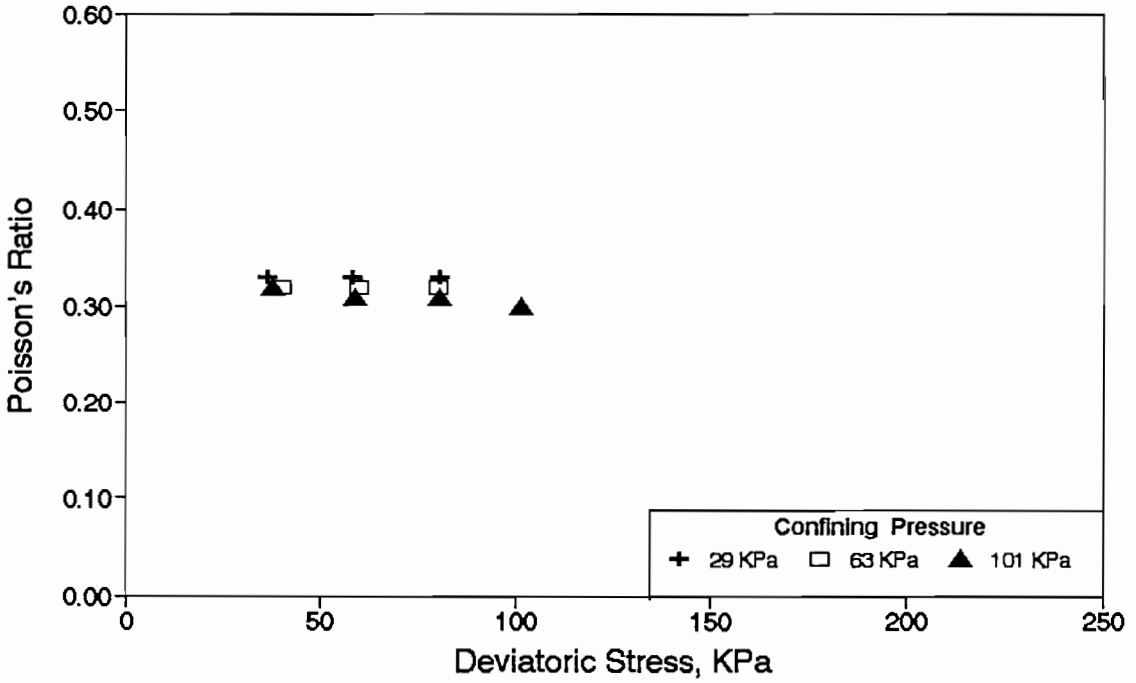

Project-1336/Specimen tested by Sriram/Data reduced and plotted by MRK Reddy

Brownwood (District 23)

Specimen No: 1 Gage Length = 101mm Dry of OMC

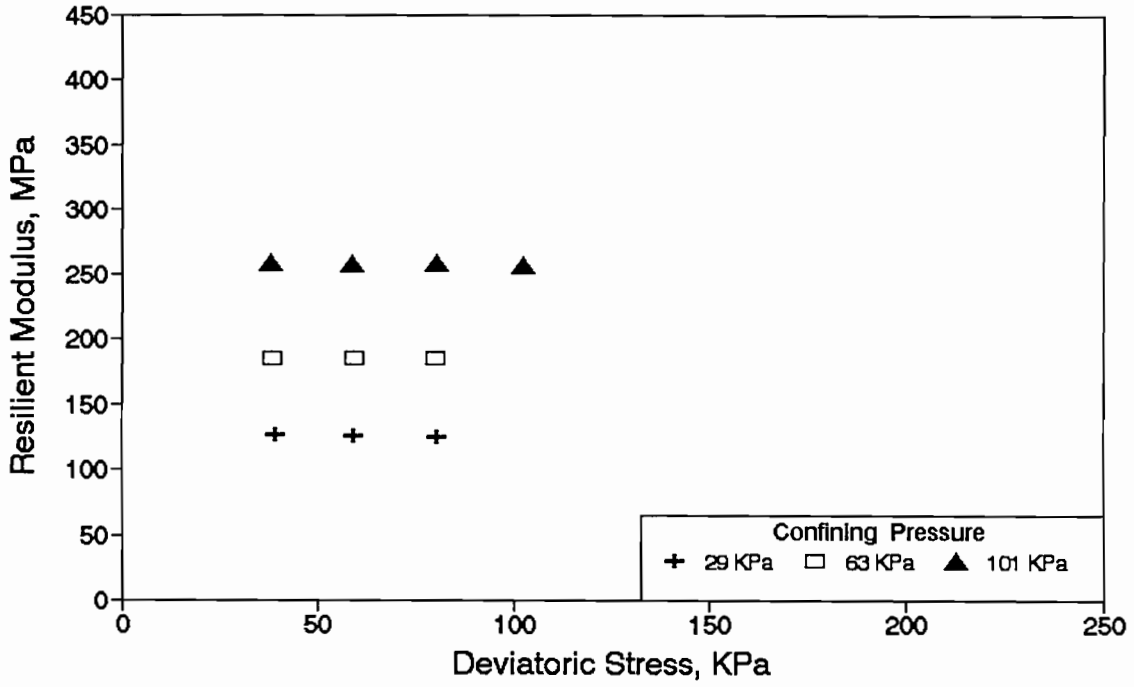

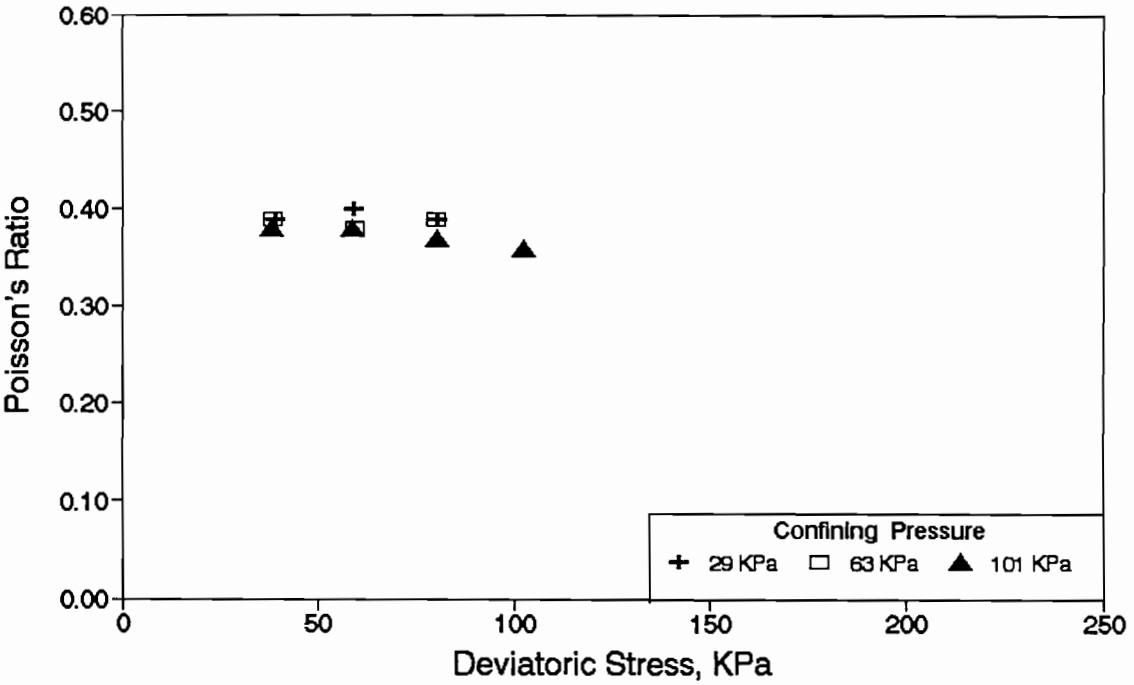

Project-1336/Specimen tested by Sriram/Data reduced and plotted by MRK Reddy

San Angelo (District 07)
Specimen No: 1 Gage Length = 101mm Dry of OMC

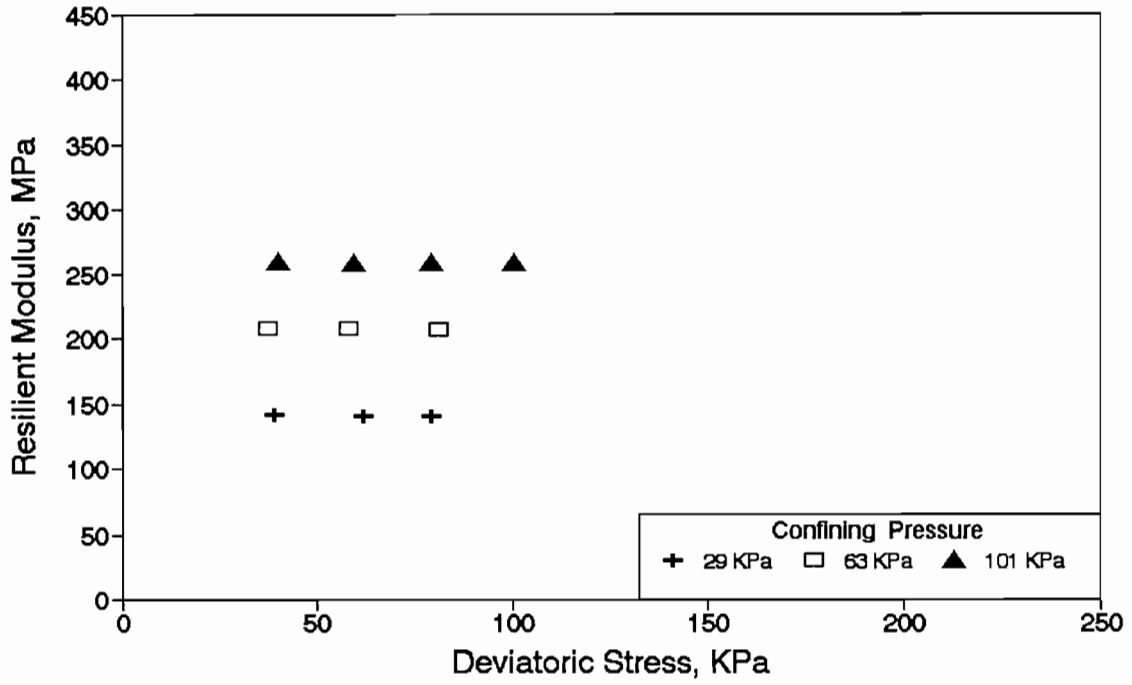

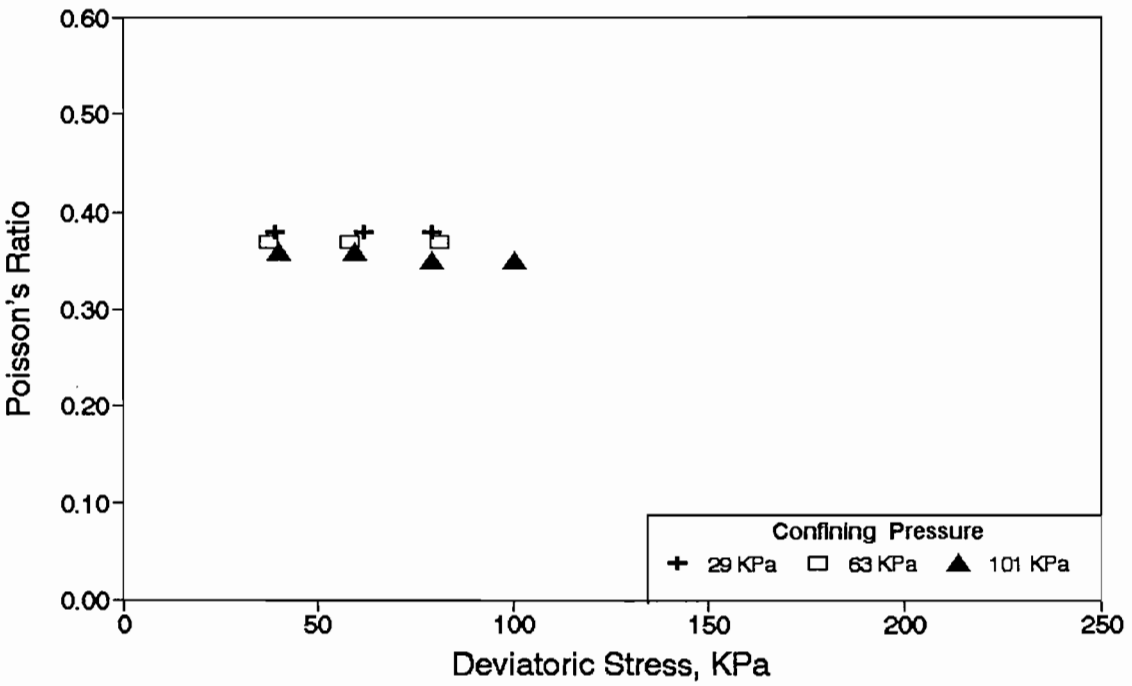

Project-1336/Specimen tested by Sriram/Data reduced and plotted by MRK Reddy

San Angelo (District 07)
Specimen No: 2 Gage Length = 101mm Dry of OMC

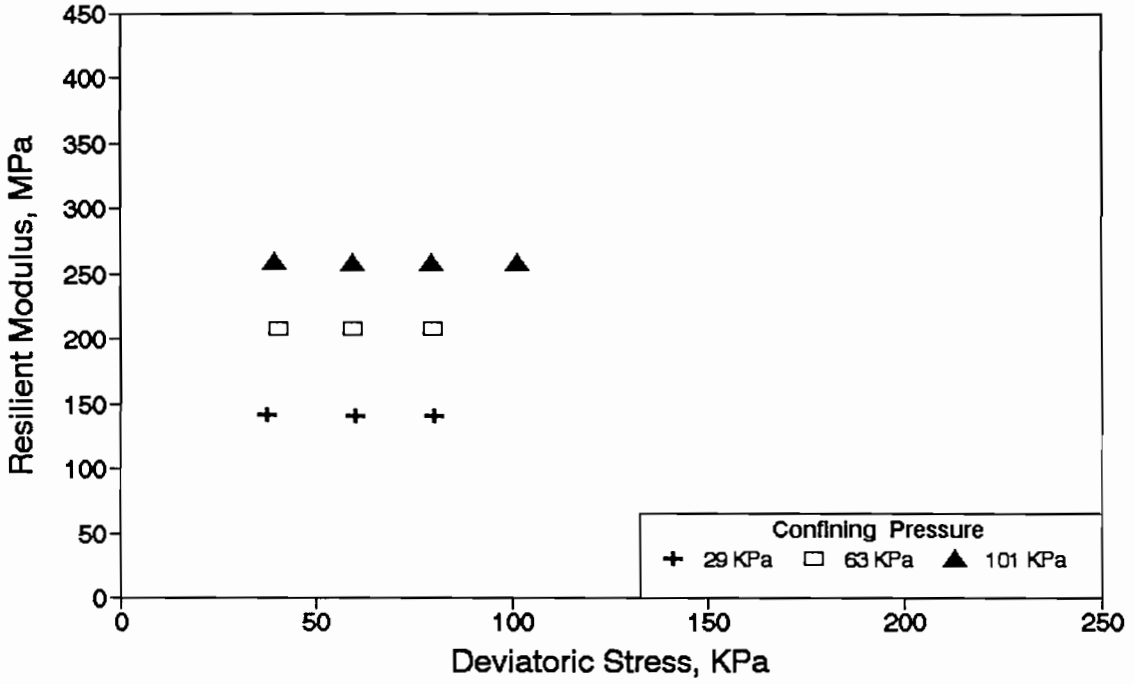

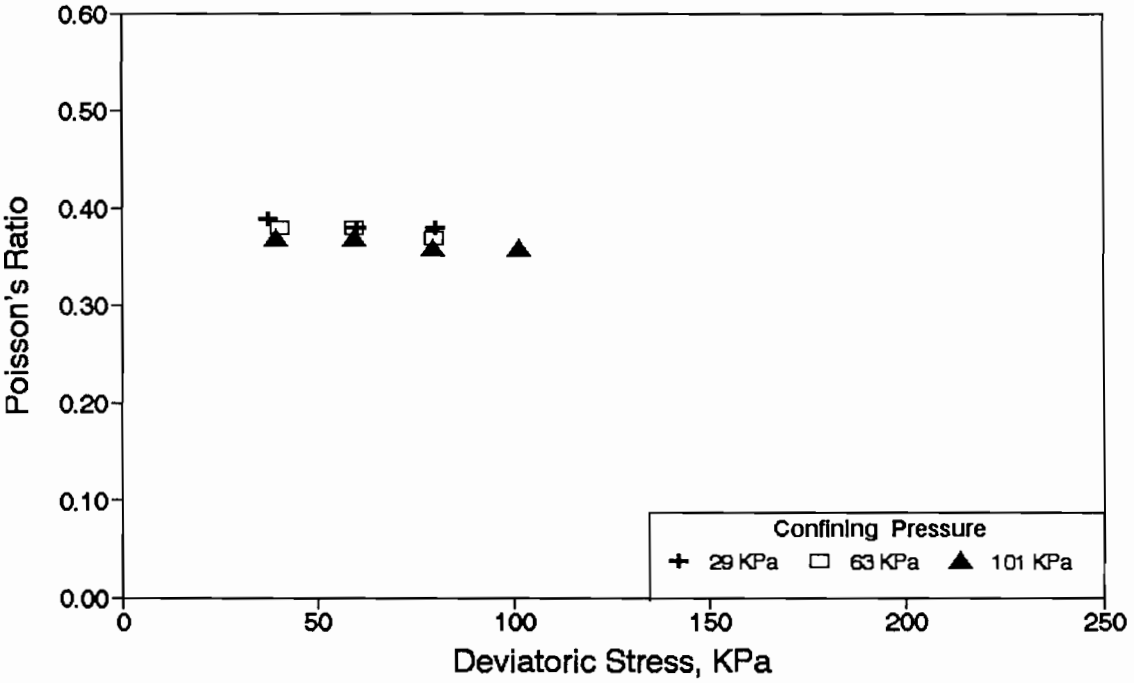

Project-1336/Specimen tested by Sriram/Data reduced and plotted by MRK Reddy

San Angelo (District 07)
Specimen No: 1 Gage Length = 101mm OMC

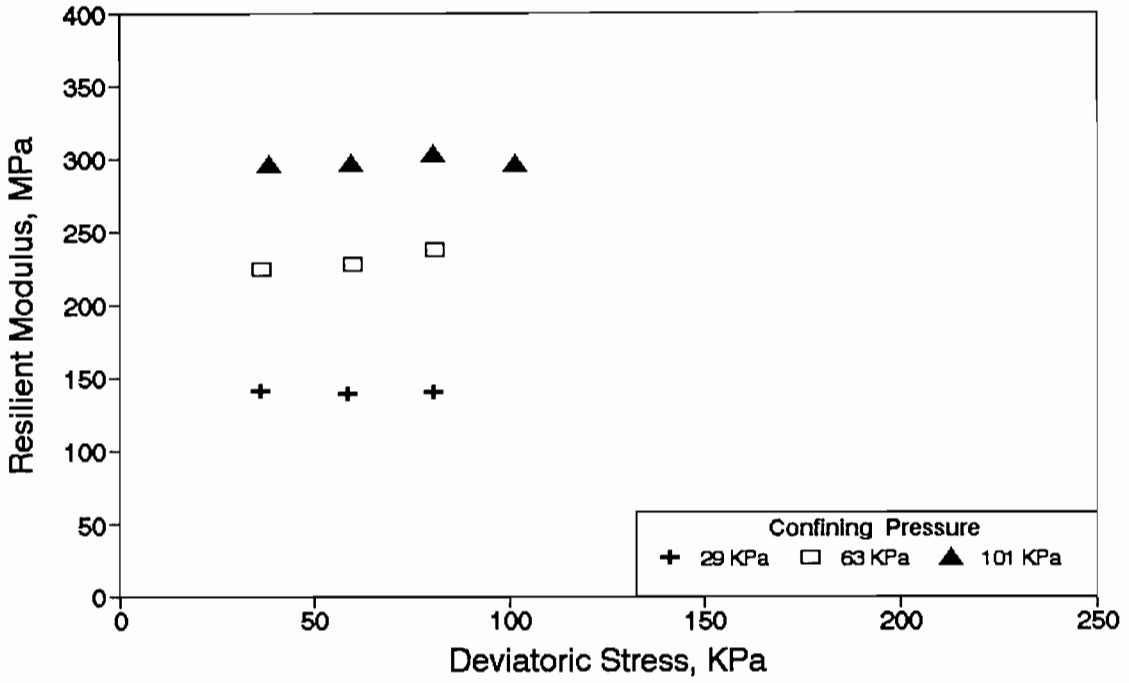

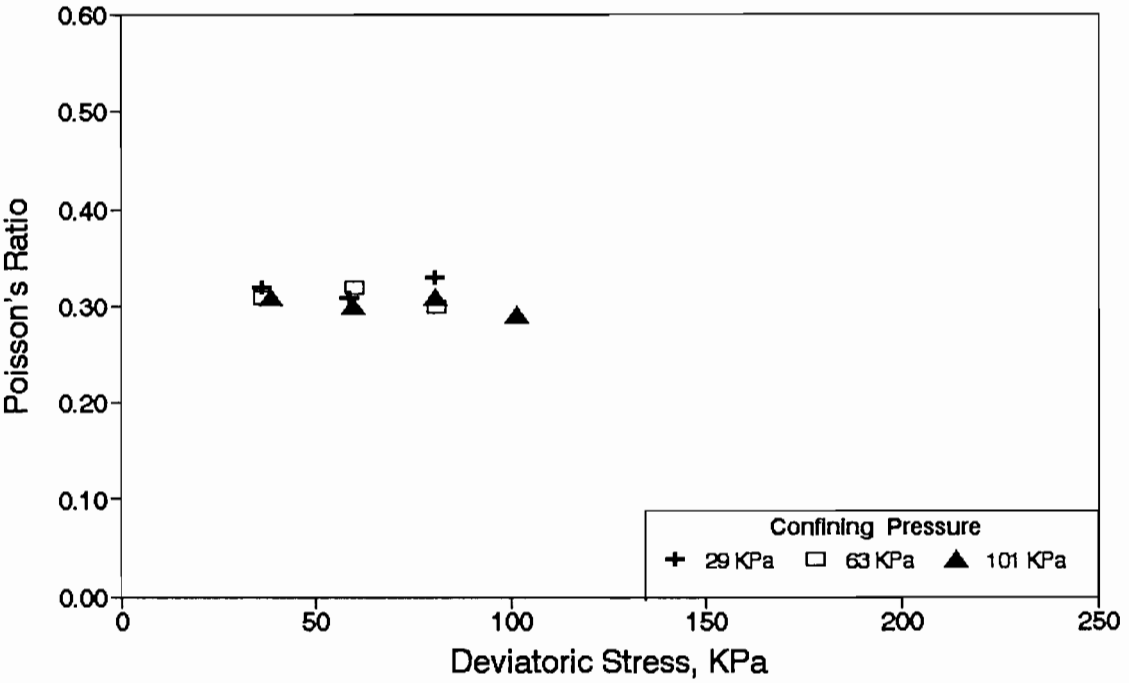

Project-1336/Specimen tested by Sriram/Data reduced and plotted by MRK Reddy

San Angelo (District 07)
Specimen No: 2 Gage Length = 101mm OMC

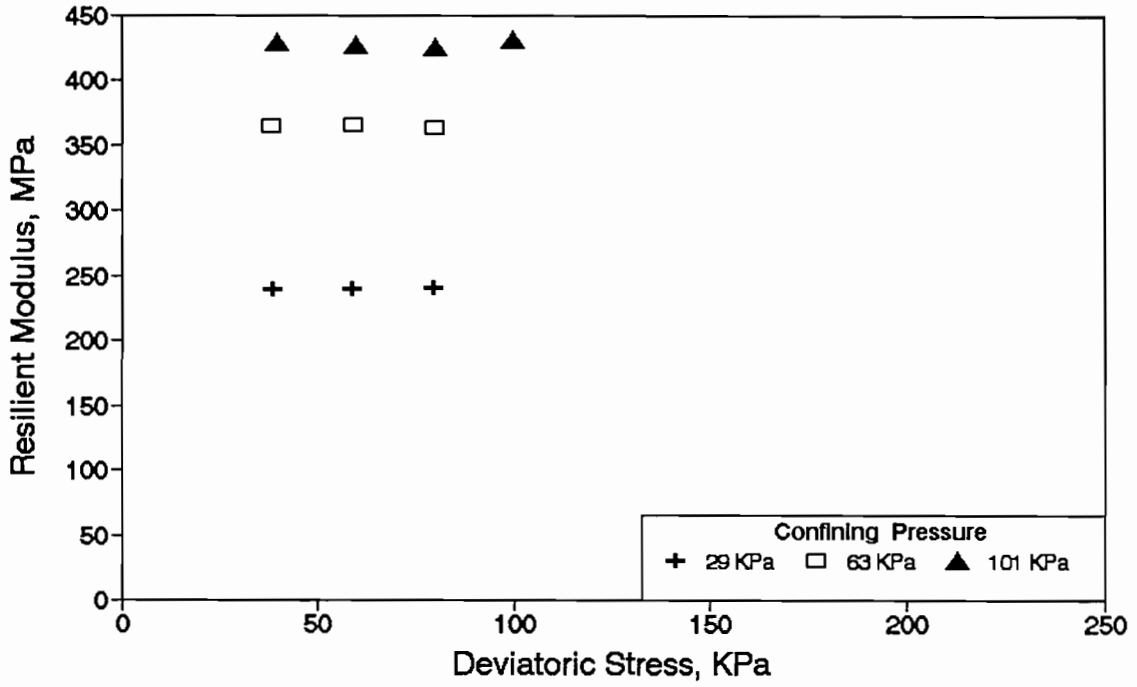

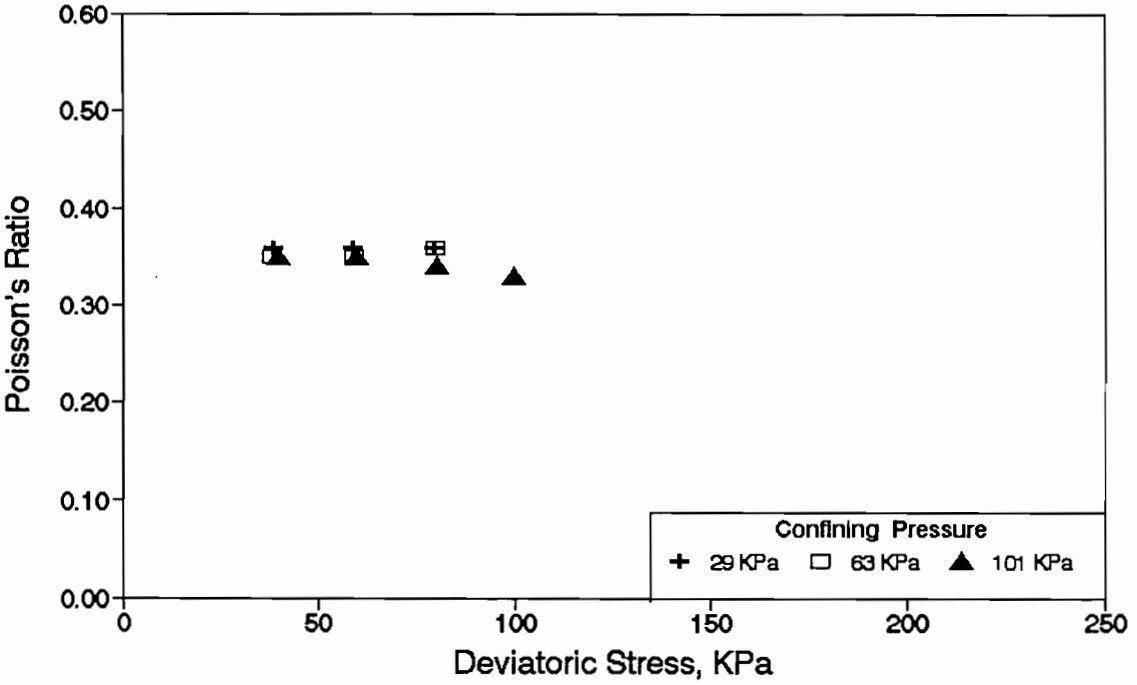

Project-1336/Specimen tested by Sriram/Data reduced and plotted by MRK Reddy

San Angelo (District 07)

Specimen No: 1 Gage Length = 101mm Wet of OMC

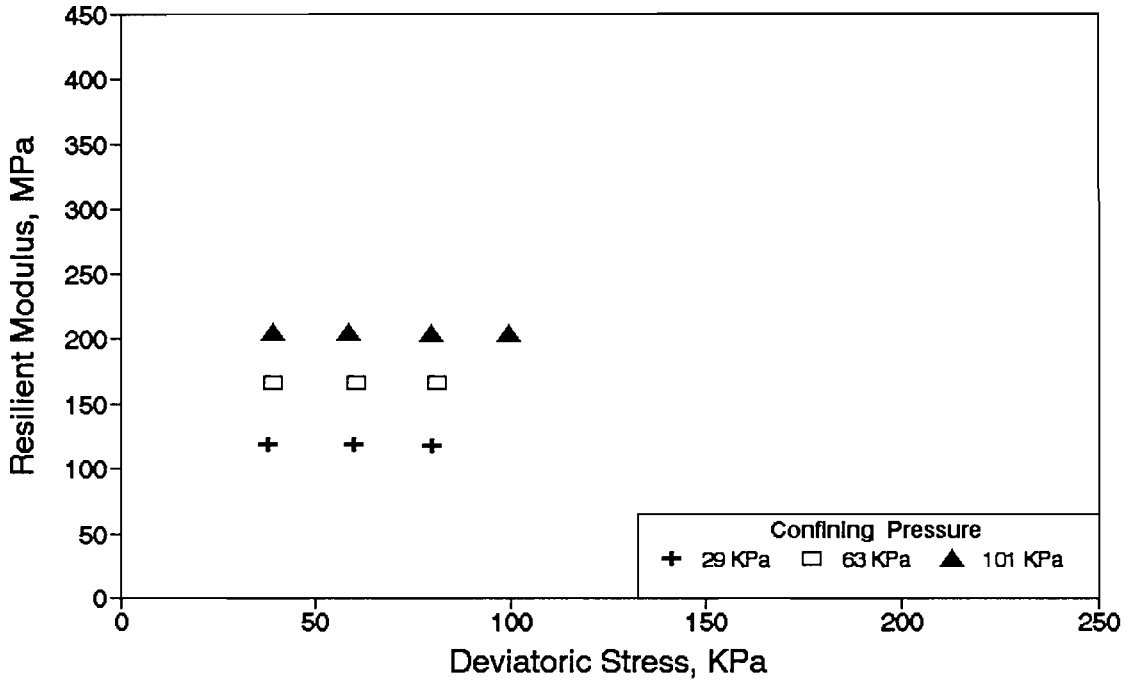

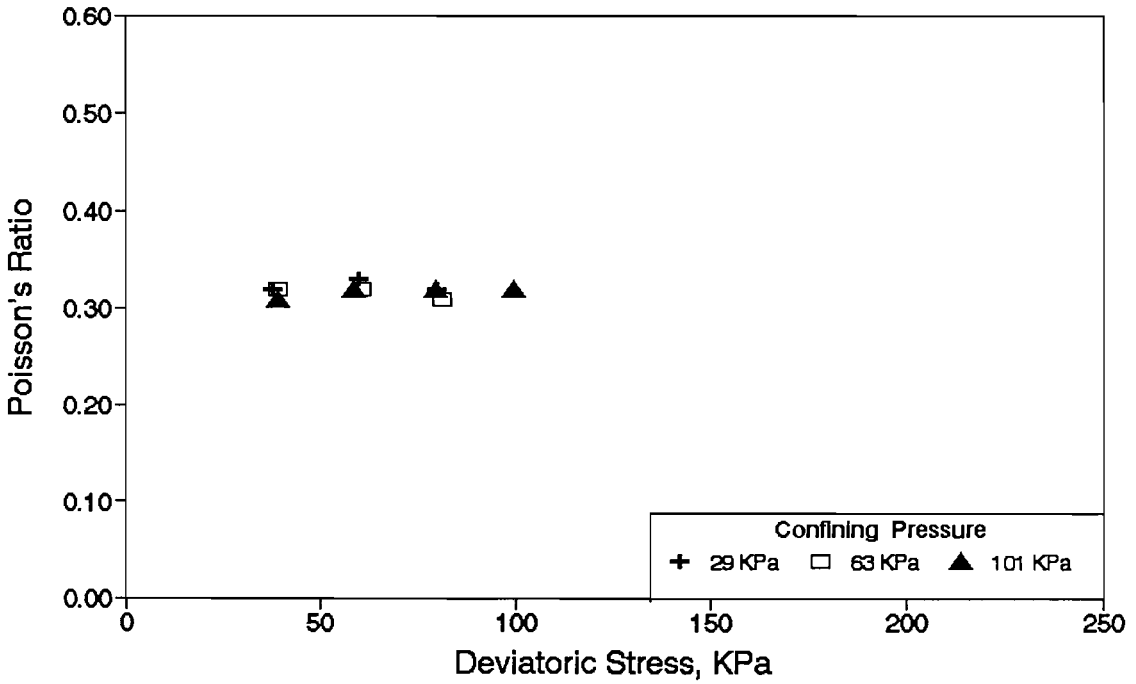

Project-1336/Specimen tested by Sriram/Data reduced and plotted by MRK Reddy

San Angelo (District 07)

Specimen No: 2 Gage Length = 101mm Wet of OMC

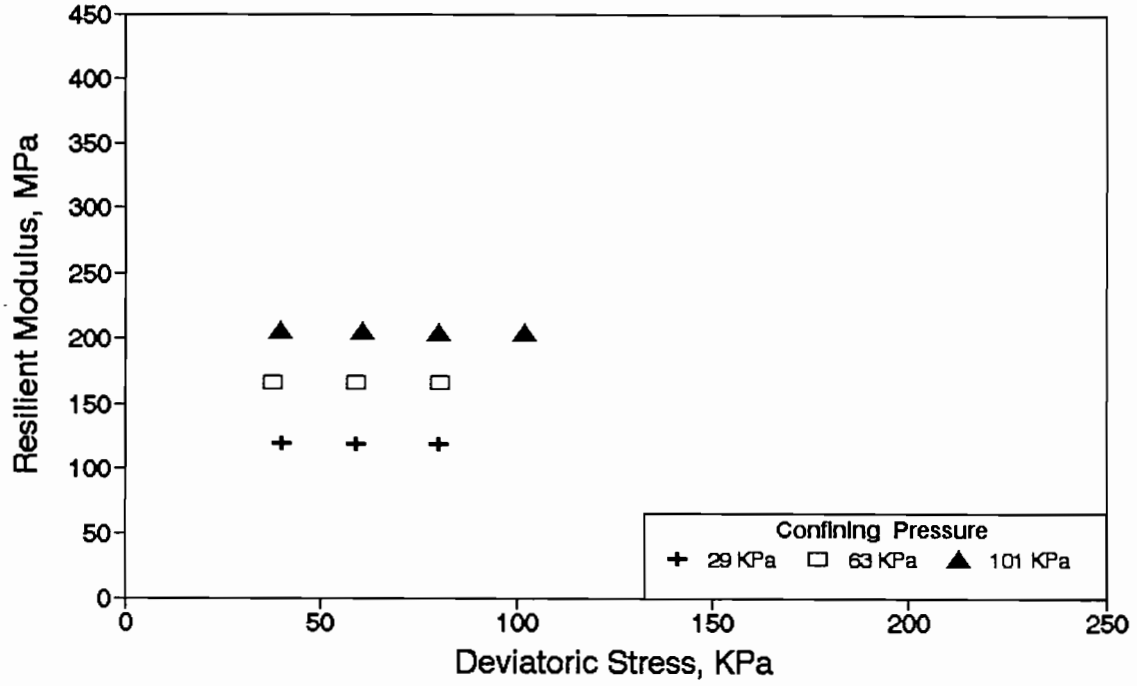

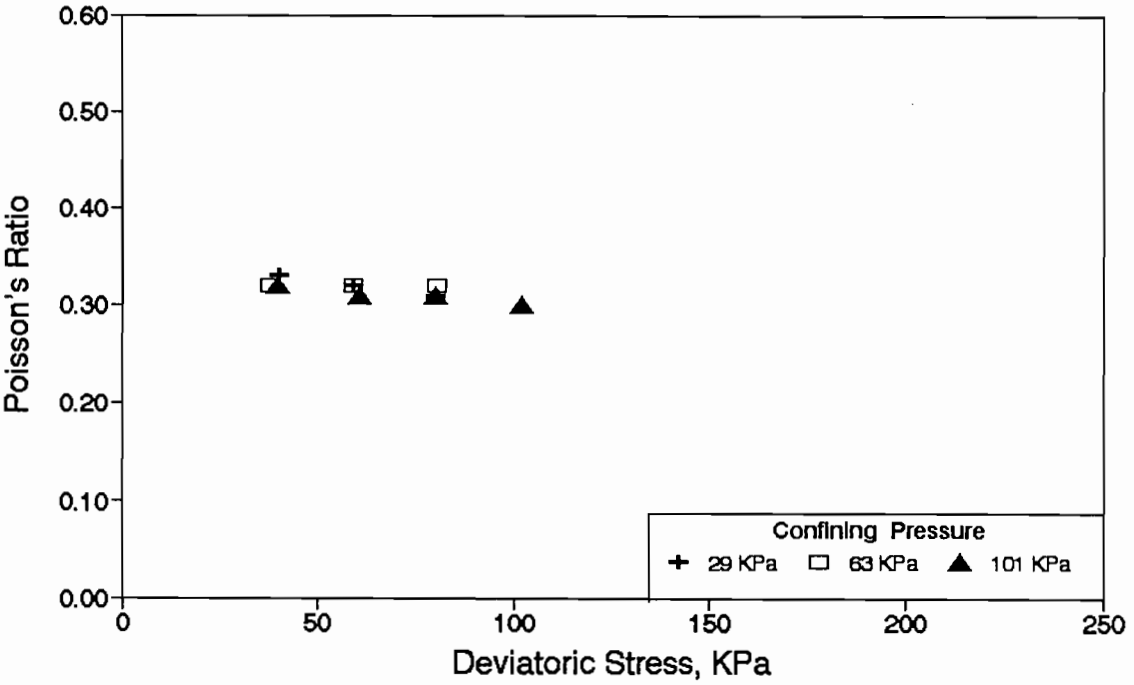

Project-1336/Specimen tested by Sriram/Data reduced and plotted by MRK Reddy

Paris (District - 01)
Specimen No. 1 (Gage Length = 101 mm) OMC

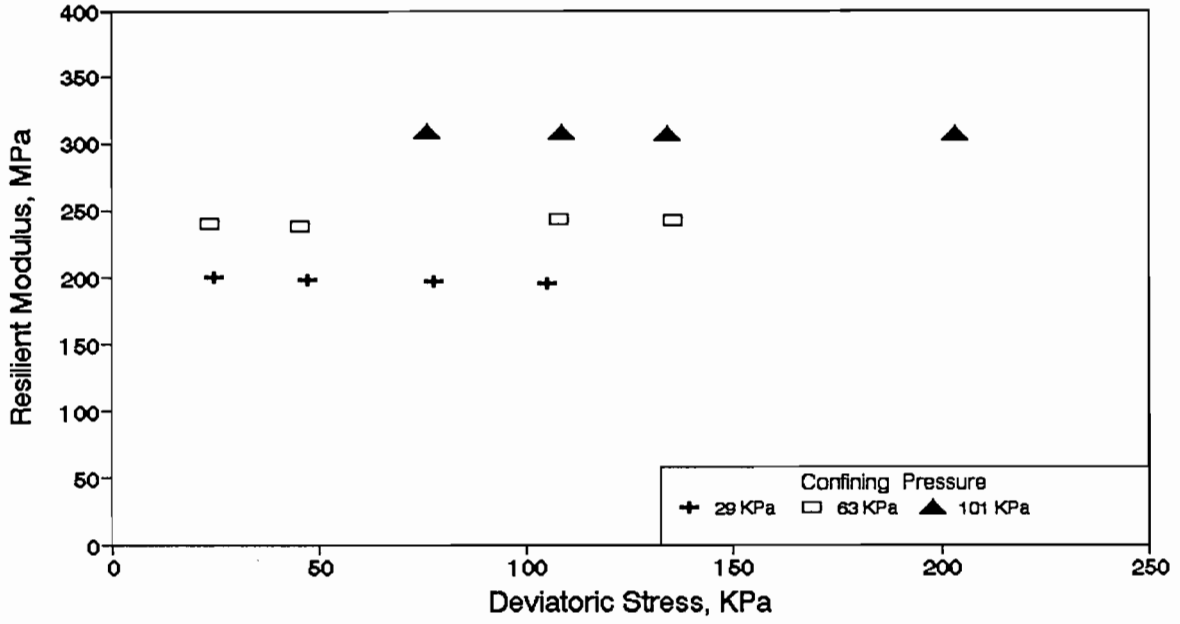

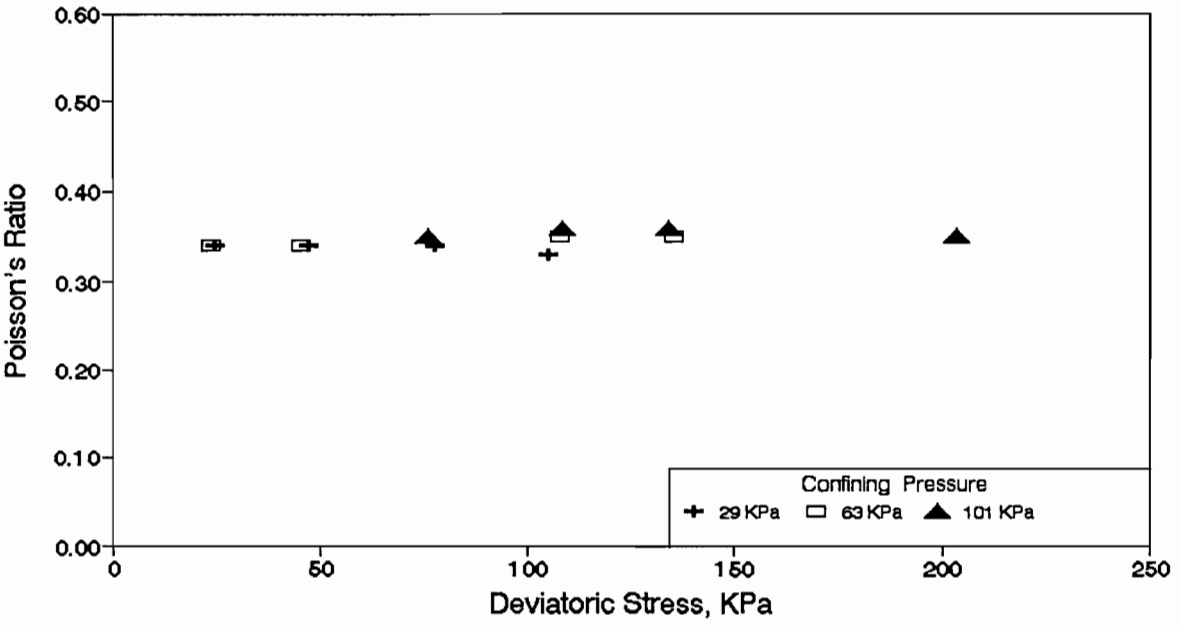

Specimen tested by Sriram

Data reduced and plotted by MRK Reddy

Paris (District - 01)
Specimen No. 2 (Gage Length = 101 mm) OMC

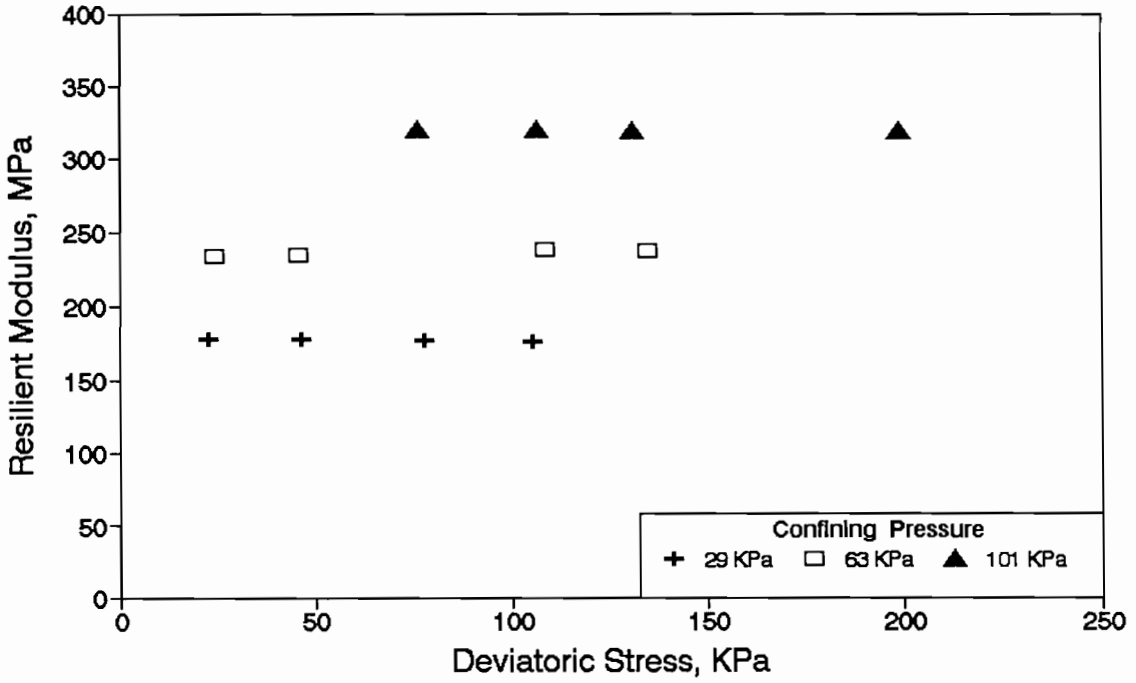

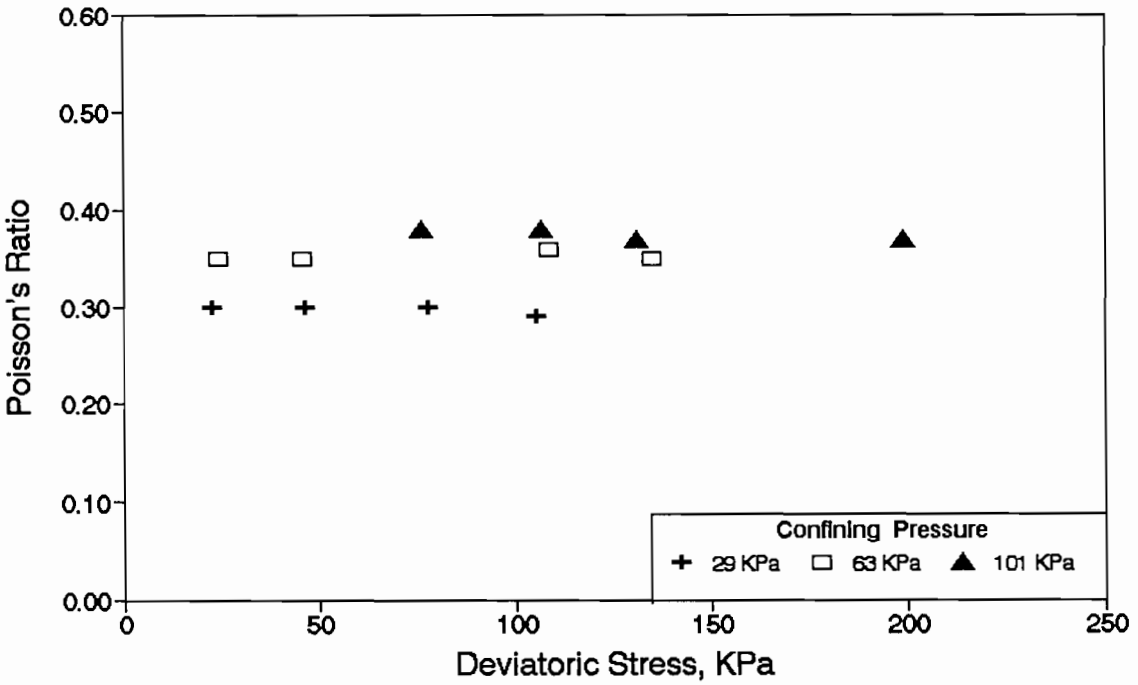

Specimen tested by Sriram

Data reduced and plotted by MRK Reddy

Paris (District 01)

Specimen No: 1 Gage Length = 101mm Dry of OMC

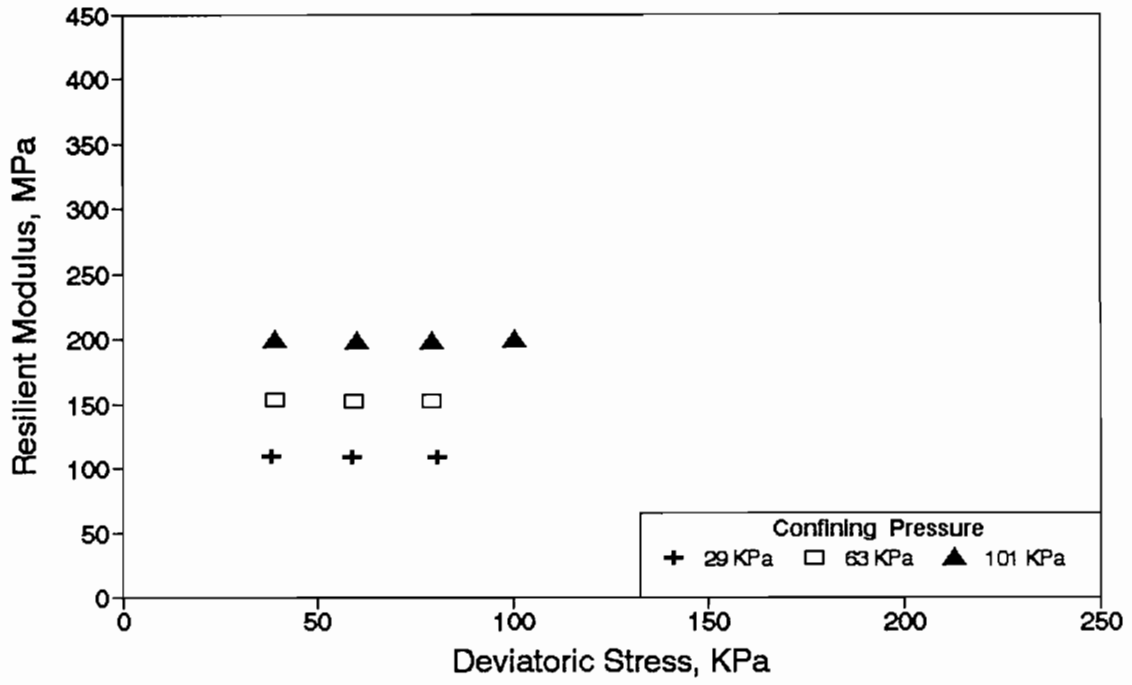

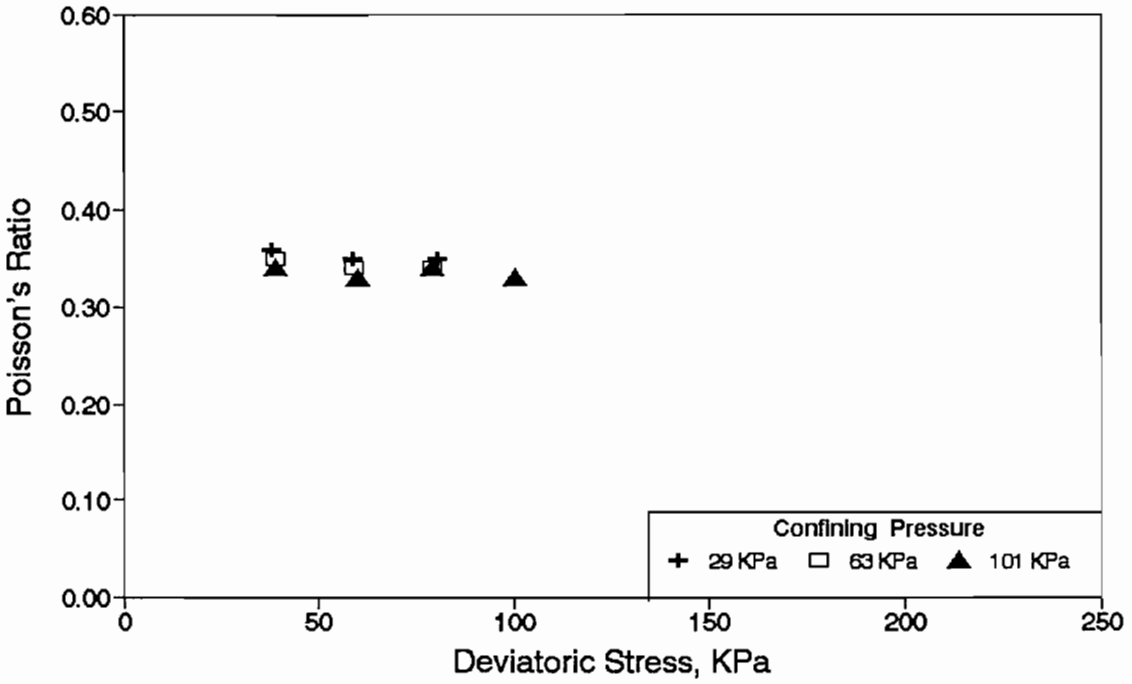

Project-1336/Specimen tested by Sriram/Data reduced and plotted by MRK Reddy

Paris (District 01)

Specimen No: 2 Gage Length = 101mm Dry of OMC

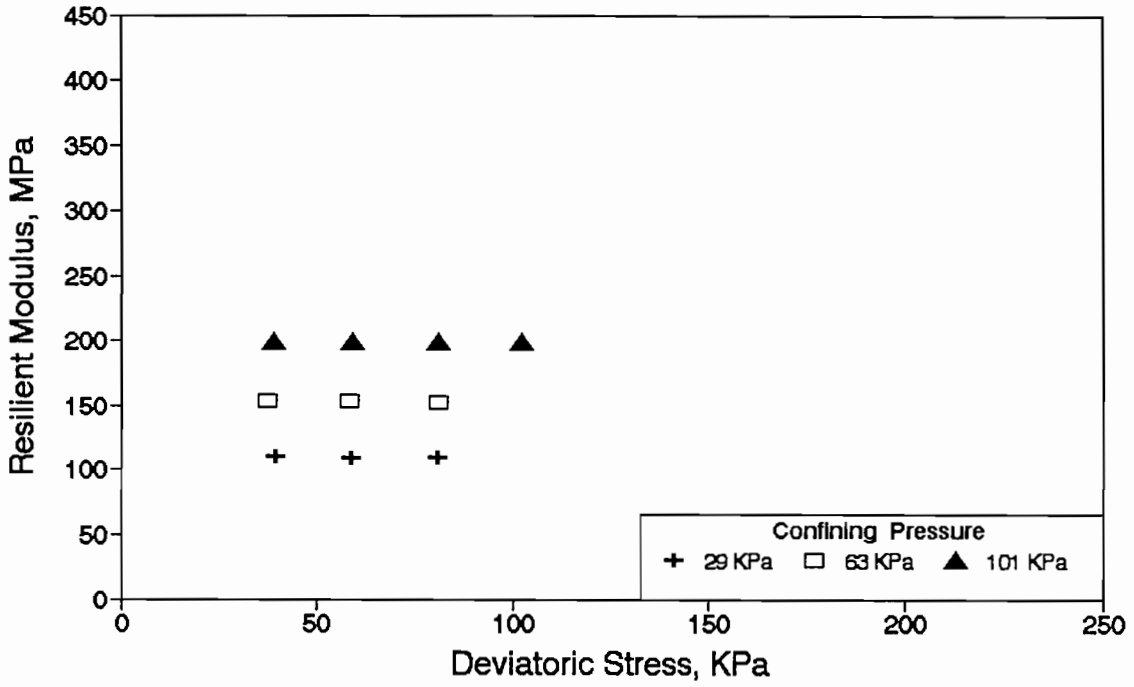

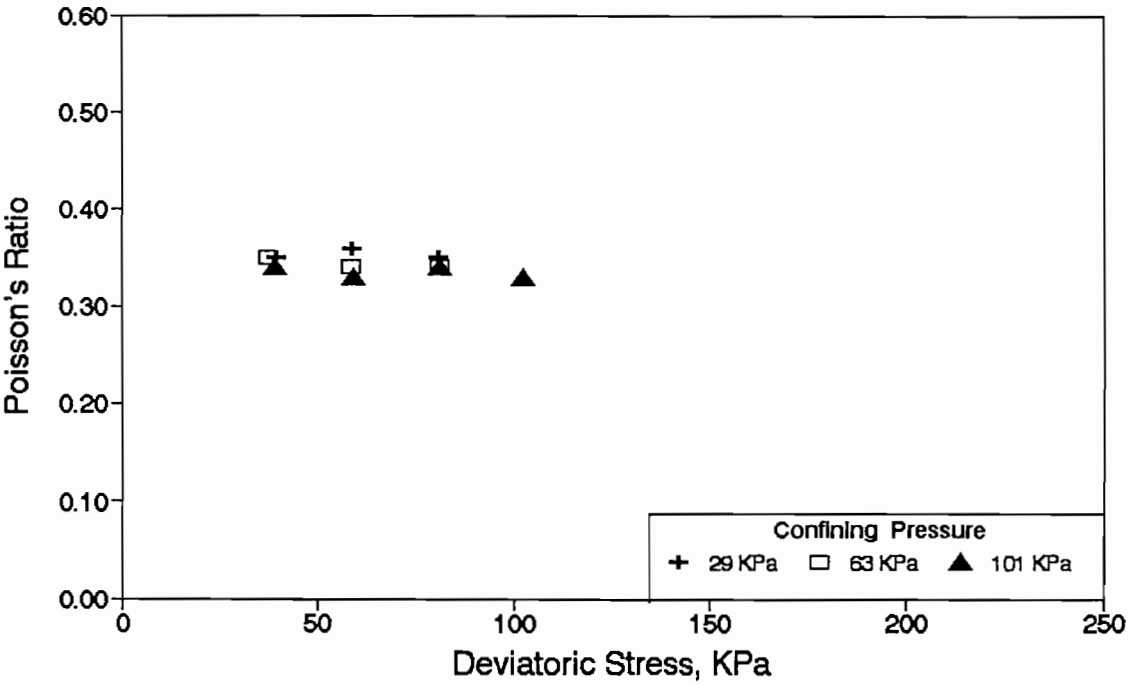

Project-1336/Specimen tested by Sriram/Data reduced and plotted by MRK Reddy

Paris (District 01)

Specimen No: 1 Gage Length = 101mm Wet of OMC

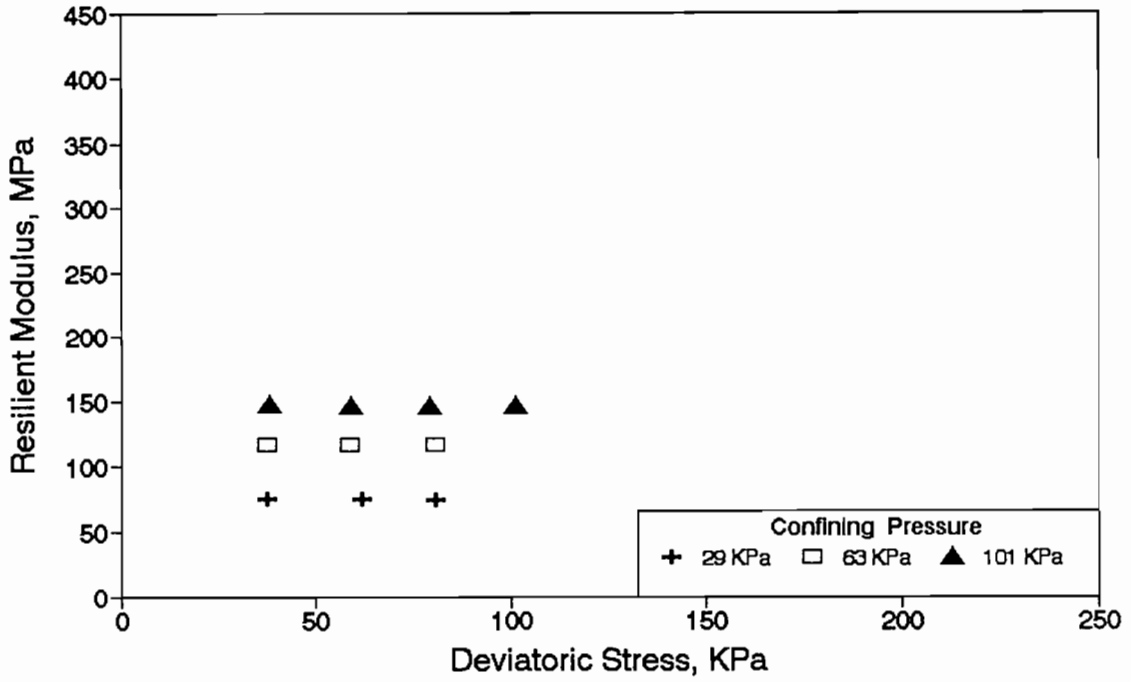

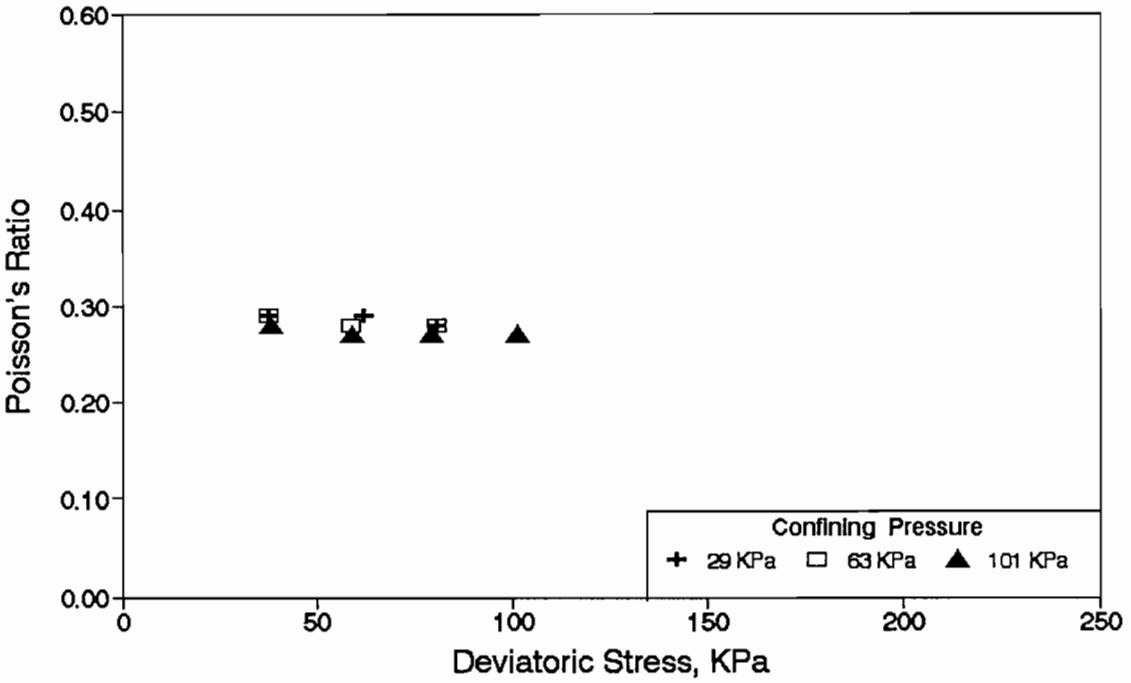

Project-1336/Specimen tested by Sriram/Data reduced and plotted by MRK Reddy

Paris (District 01)

Specimen No: 2 Gage Length = 101mm Wet of OMC

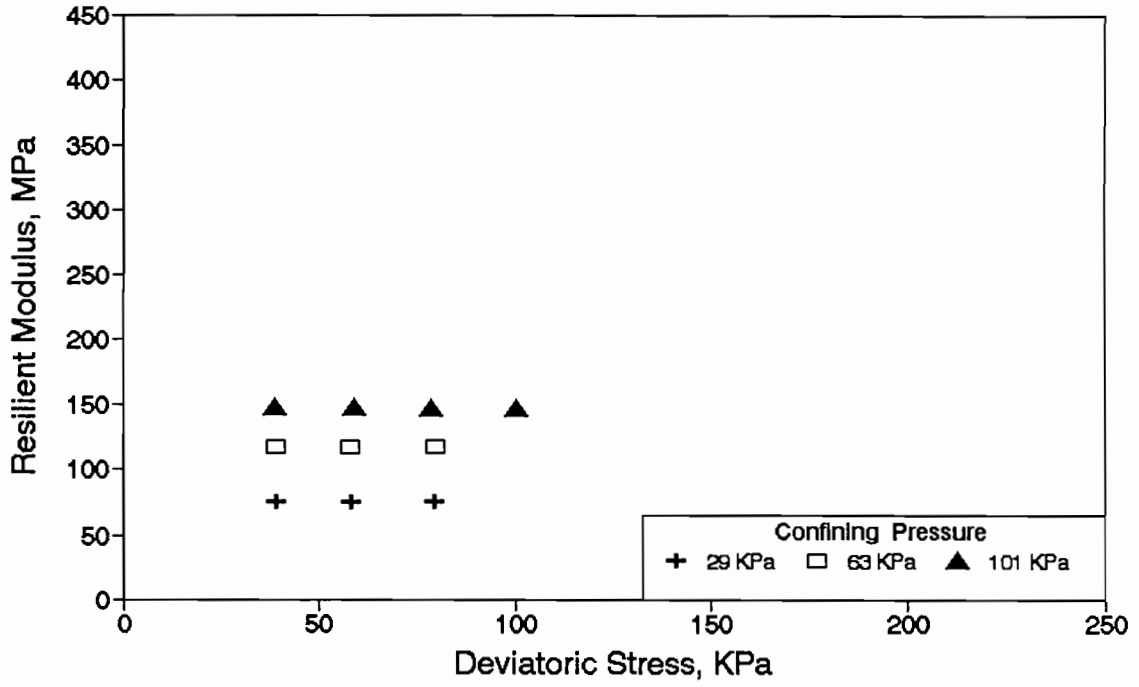

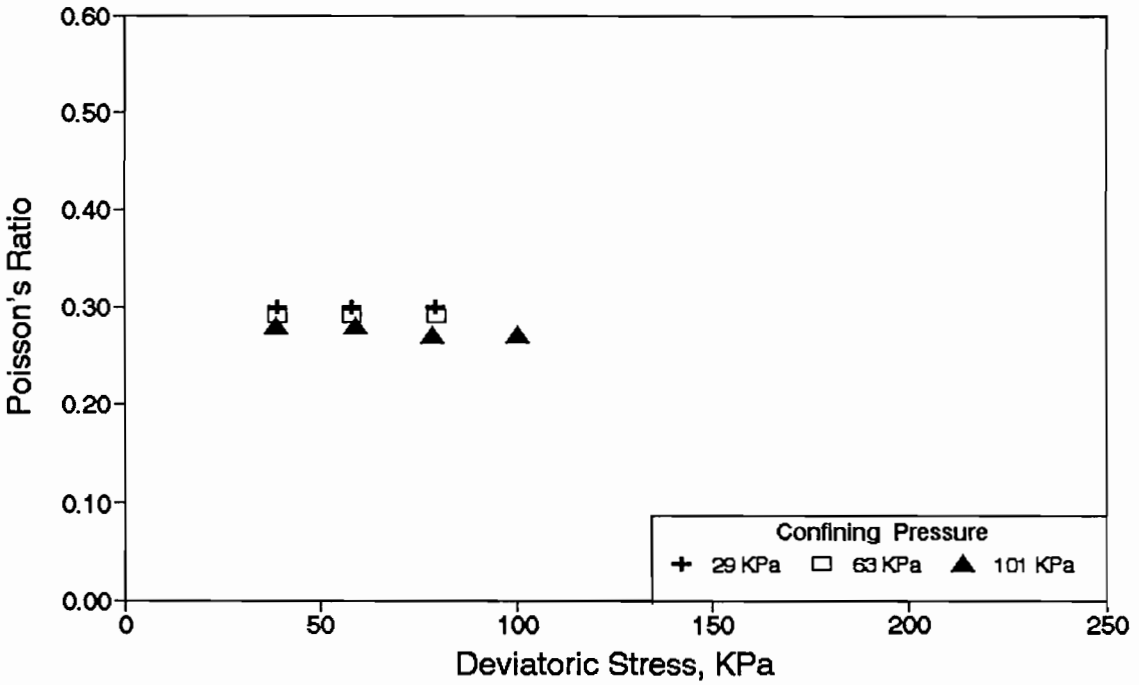

Project-1336/Specimen tested by Sriram/Data reduced and plotted by MRK Reddy

Childress (District 25)

Specimen No: 1 Gage Length = 101mm OMC

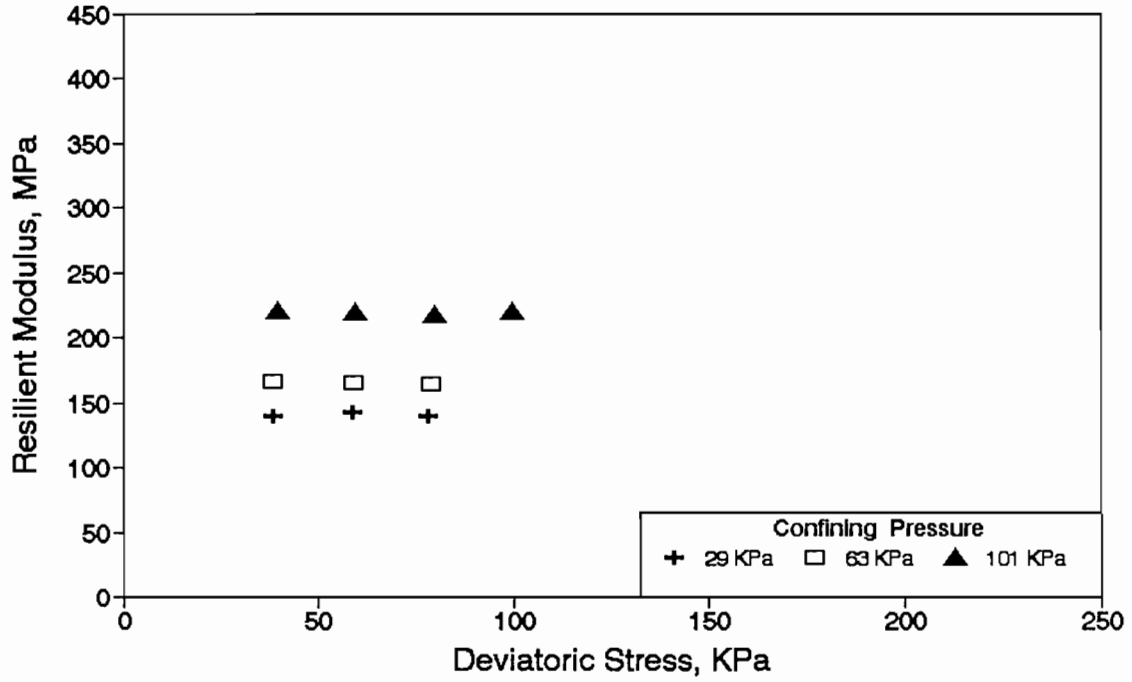

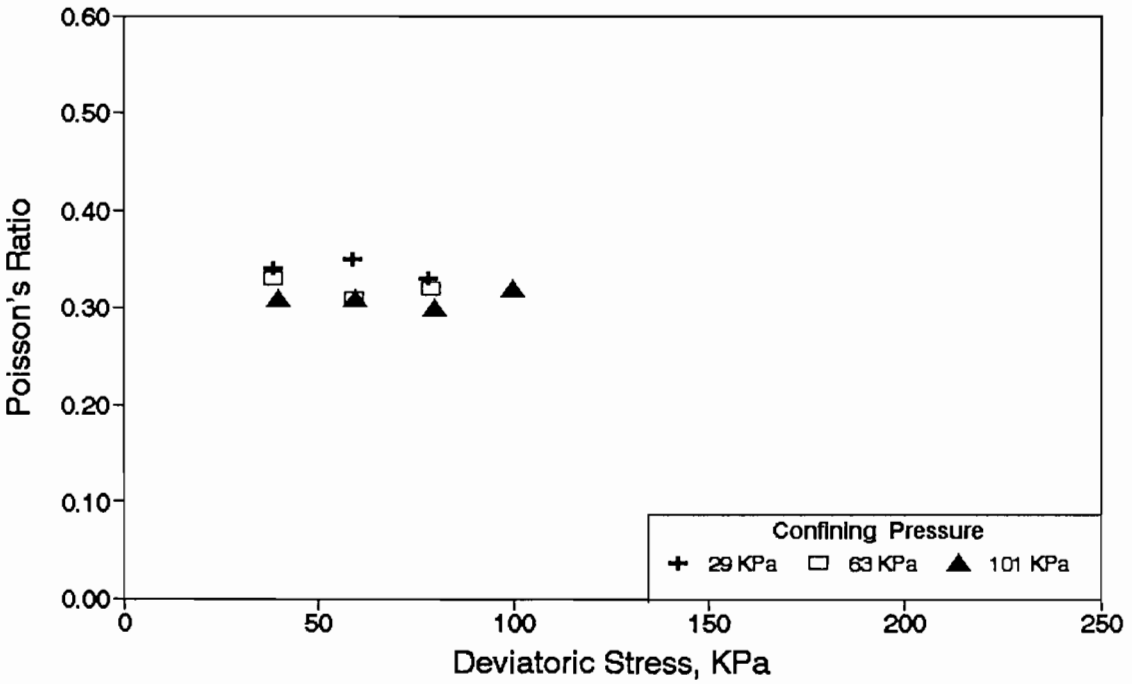

Project-1336/Specimen tested by Sriram/Data reduced and plotted by MRK Reddy

Childress (District 25)

Specimen No: 2 Gage Length = 101mm OMC

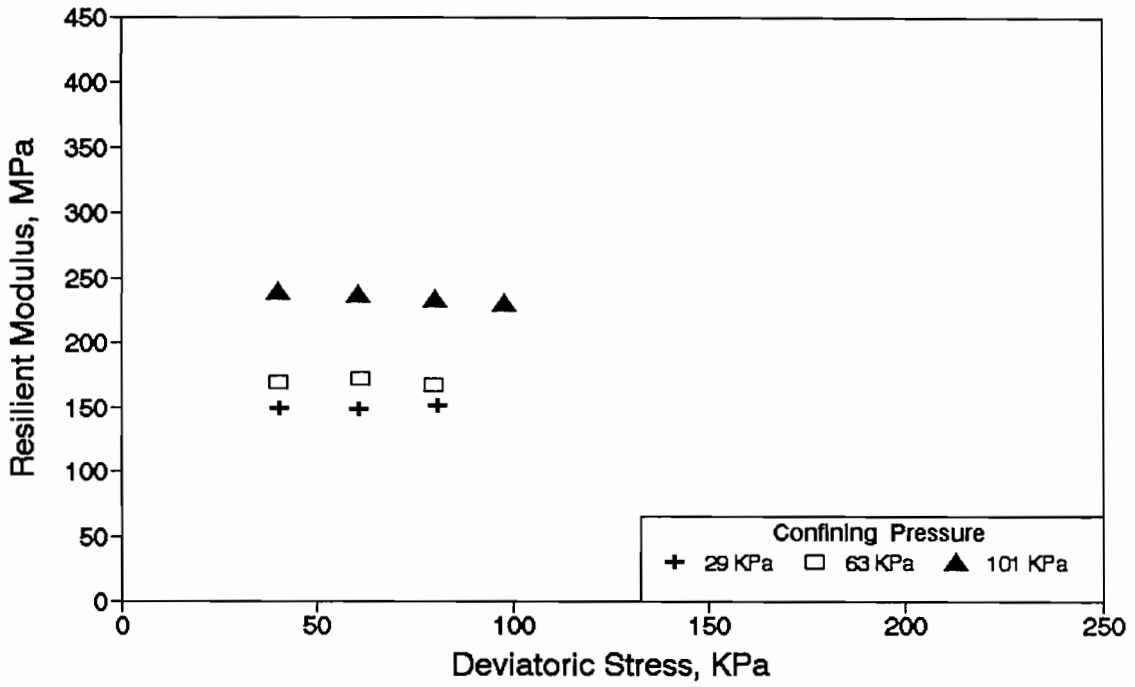

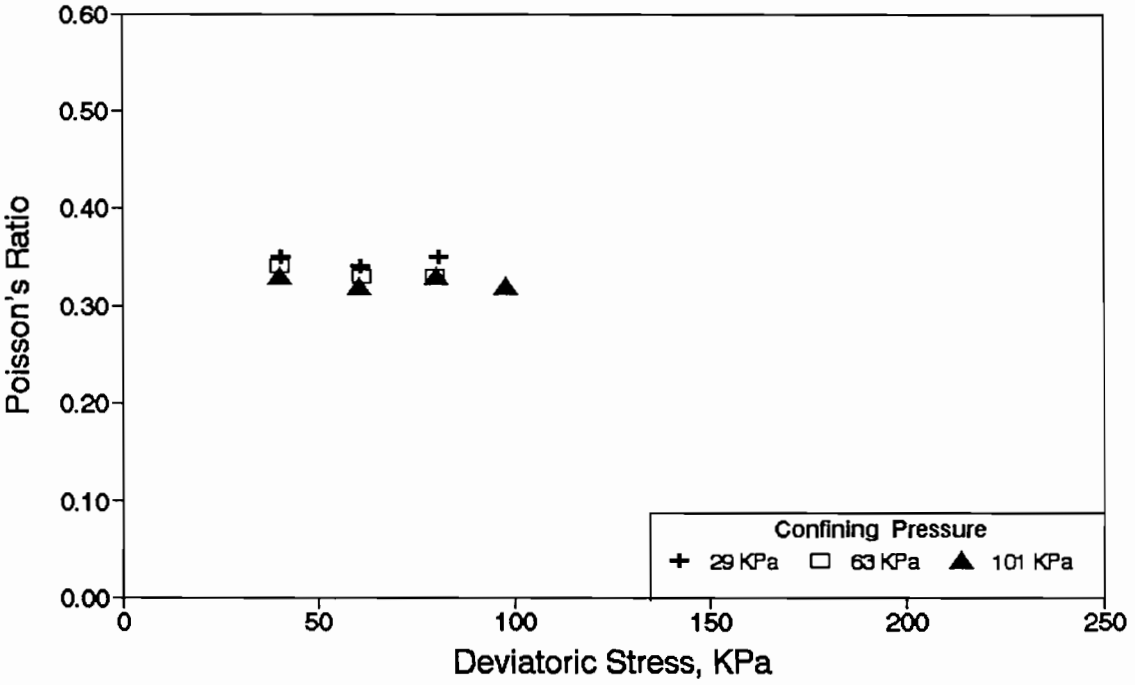

Project-1336/Specimen tested by Sriram/Data reduced and plotted by MRK Reddy

Childress (District 25)
Specimen No. 1 (Gage Length = 305mm) Dry of OMC

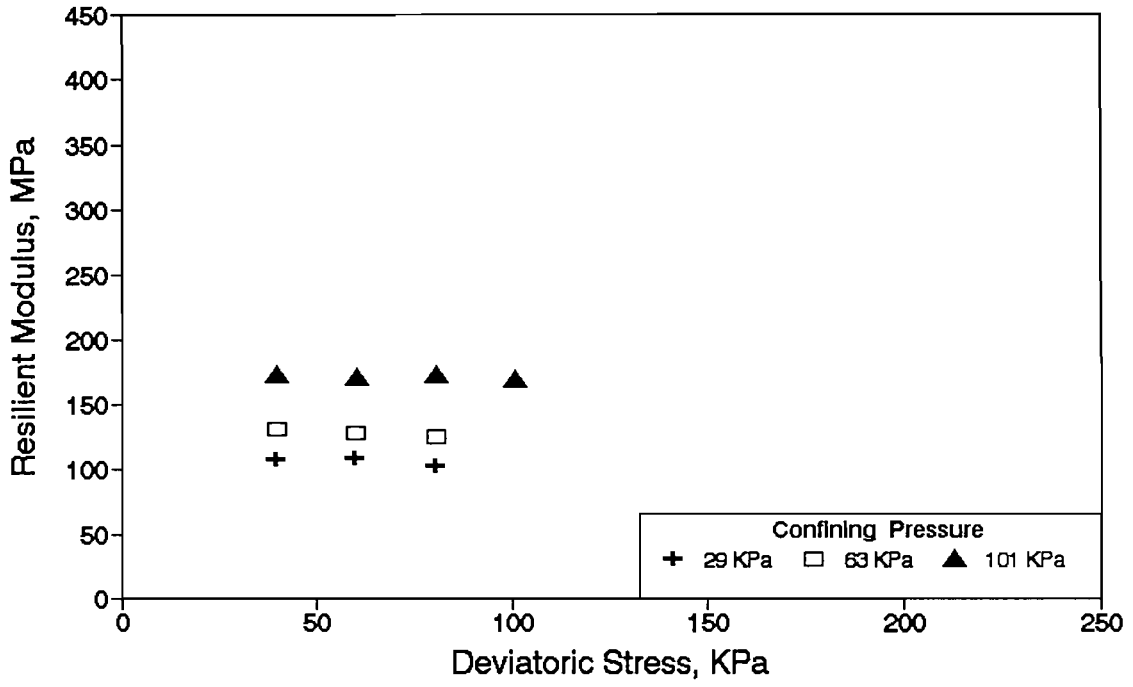

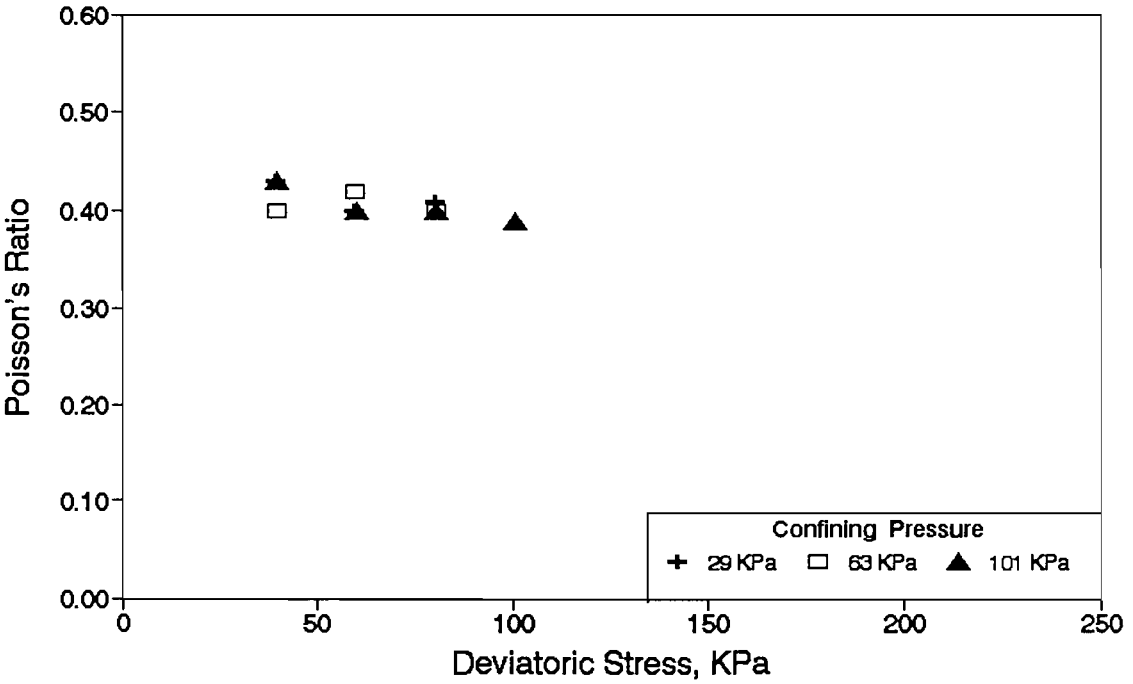

Project-1336/Specimen tested by Sriram/Data reduced and plotted by MRK Reddy

Childress (District 25)

Specimen No: 2 Gage Length = 101mm Dry of OMC

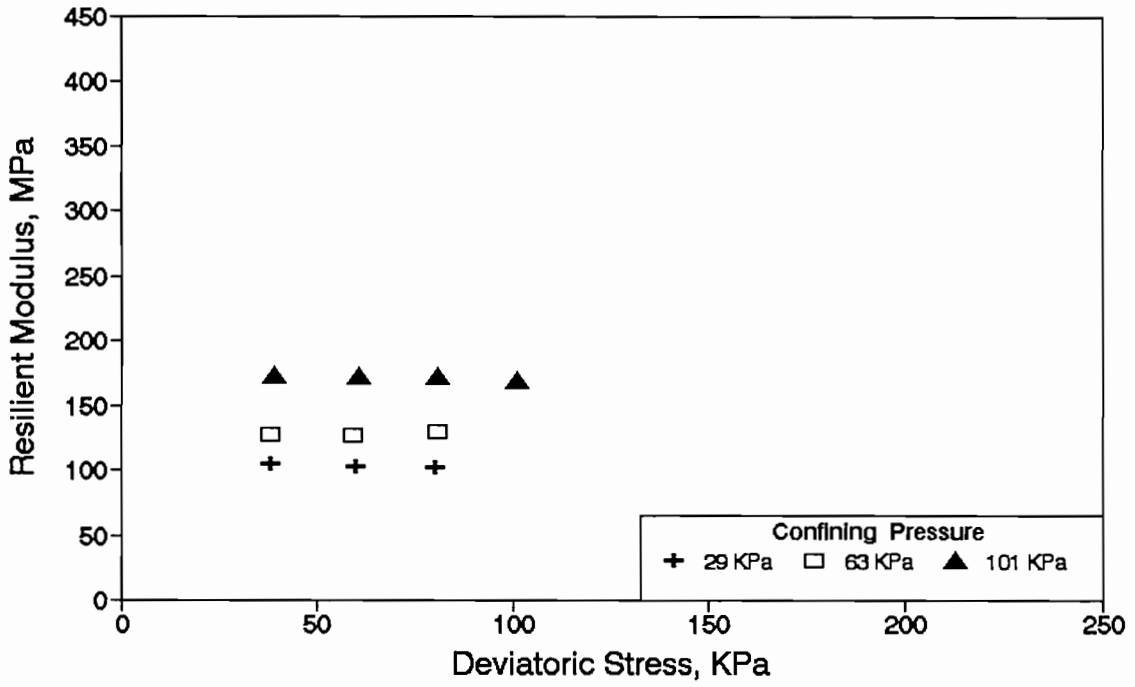

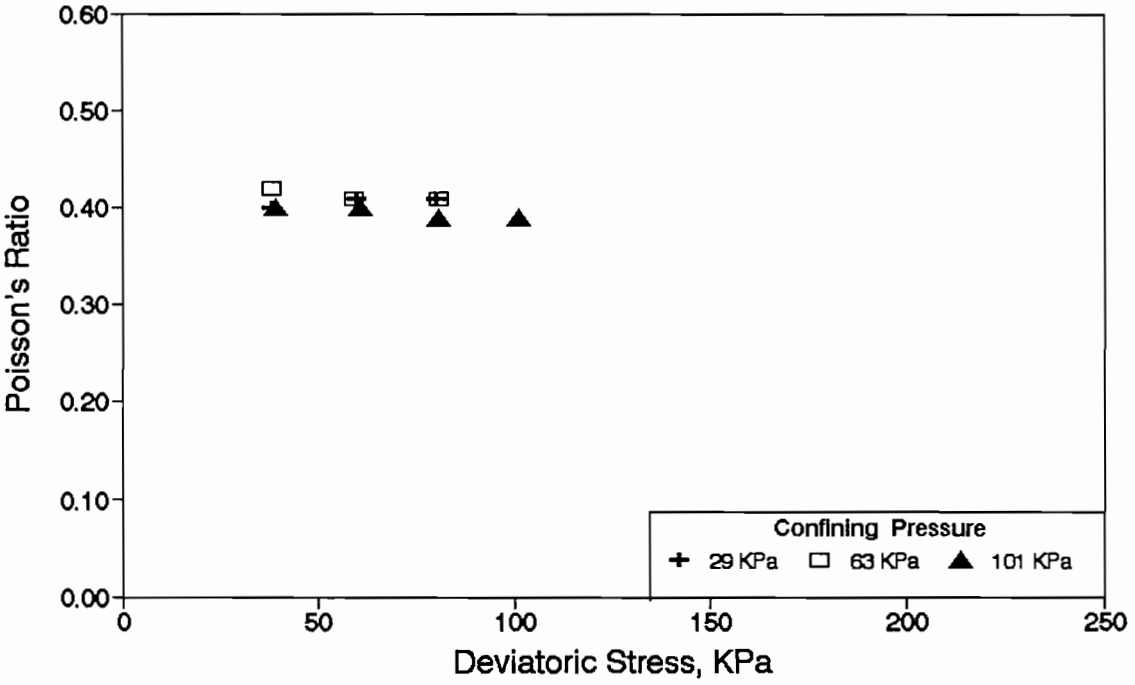

Project-1336/Specimen tested by Sriram/Data reduced and plotted by MRK Reddy

Childress (District 25)

Specimen No. 1 (Gage Length = 101mm) wet of OMC

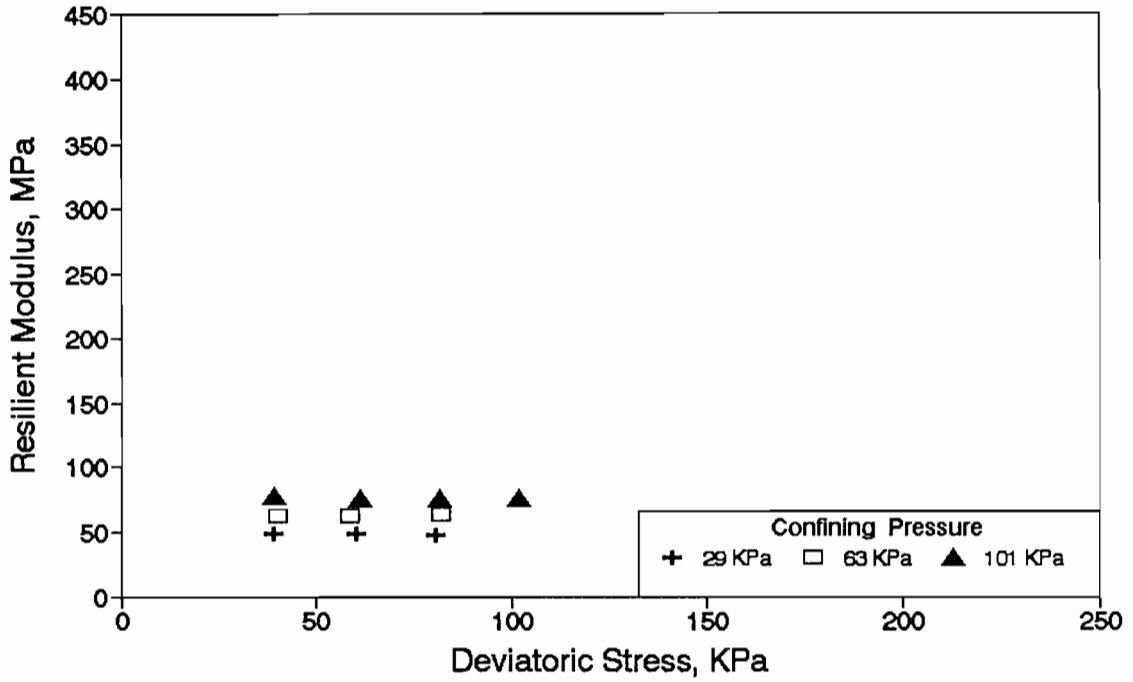

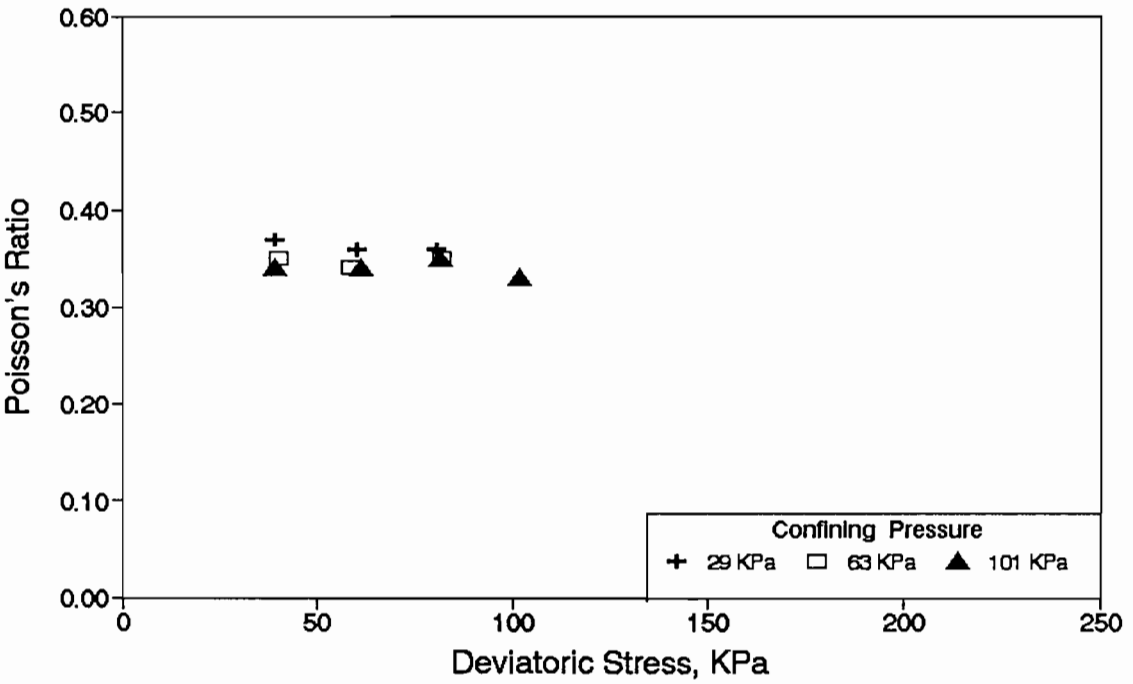

Project-1336/Specimen tested by Sriram/Data reduced and plotted by MRK Reddy

Childress (District 25)

Specimen No: 2 Gage Length = 101mm Wet of OMC

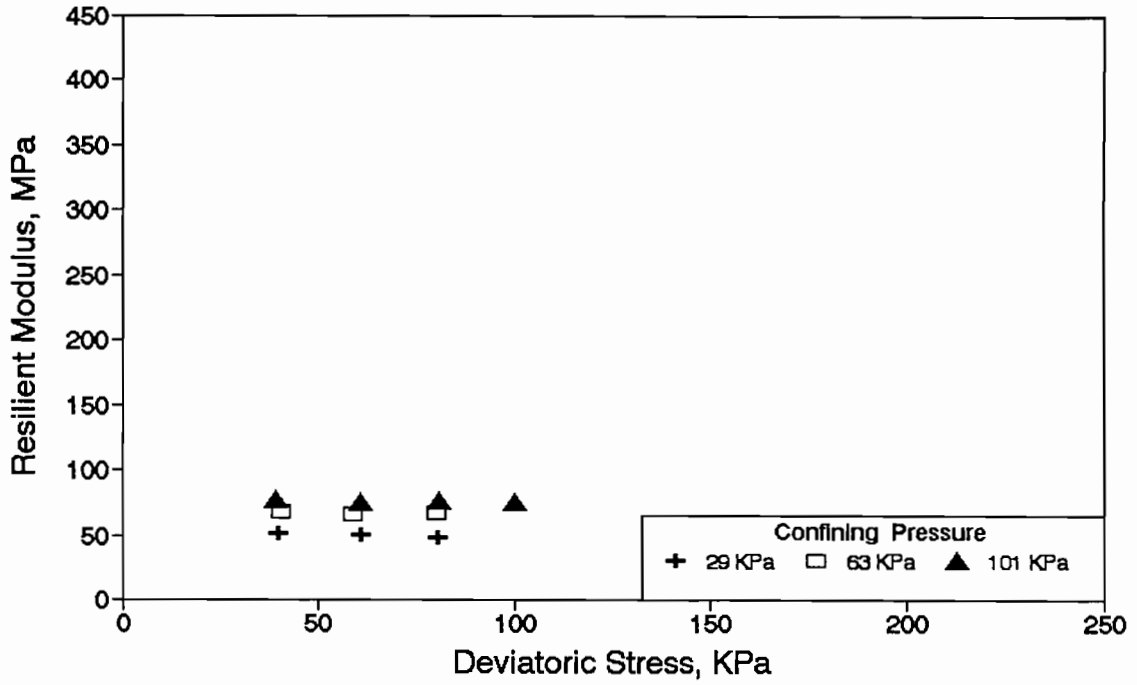

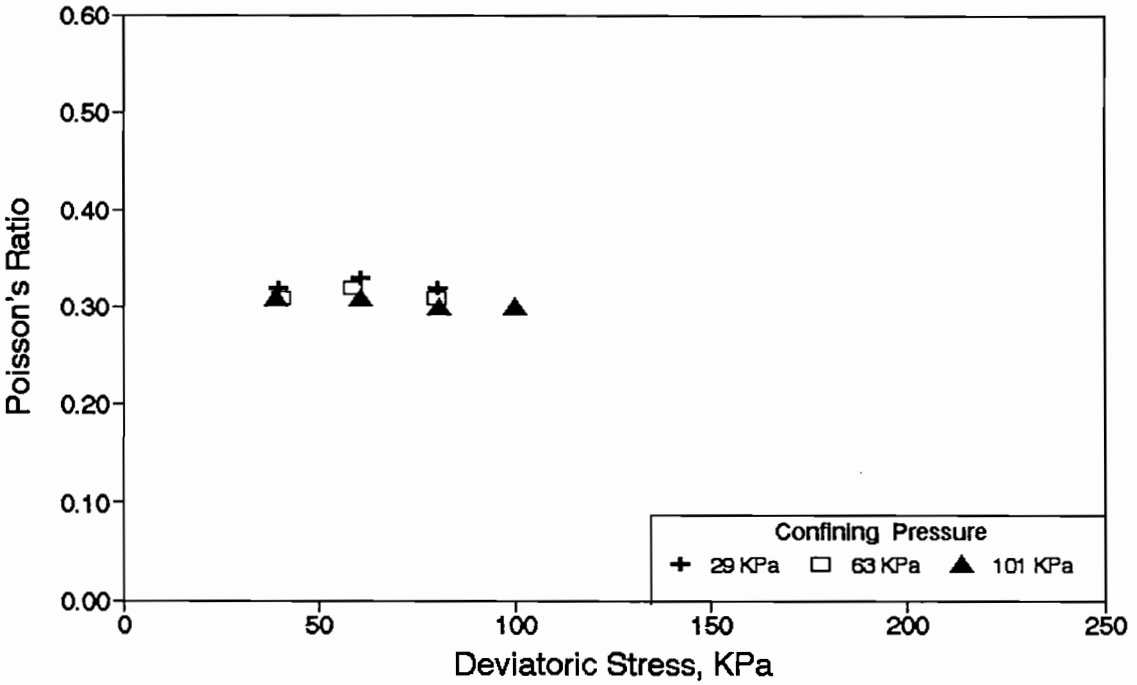

Odessa (District - 06)
Specimen No. 1 (Gage Length = 102 mm) OMC

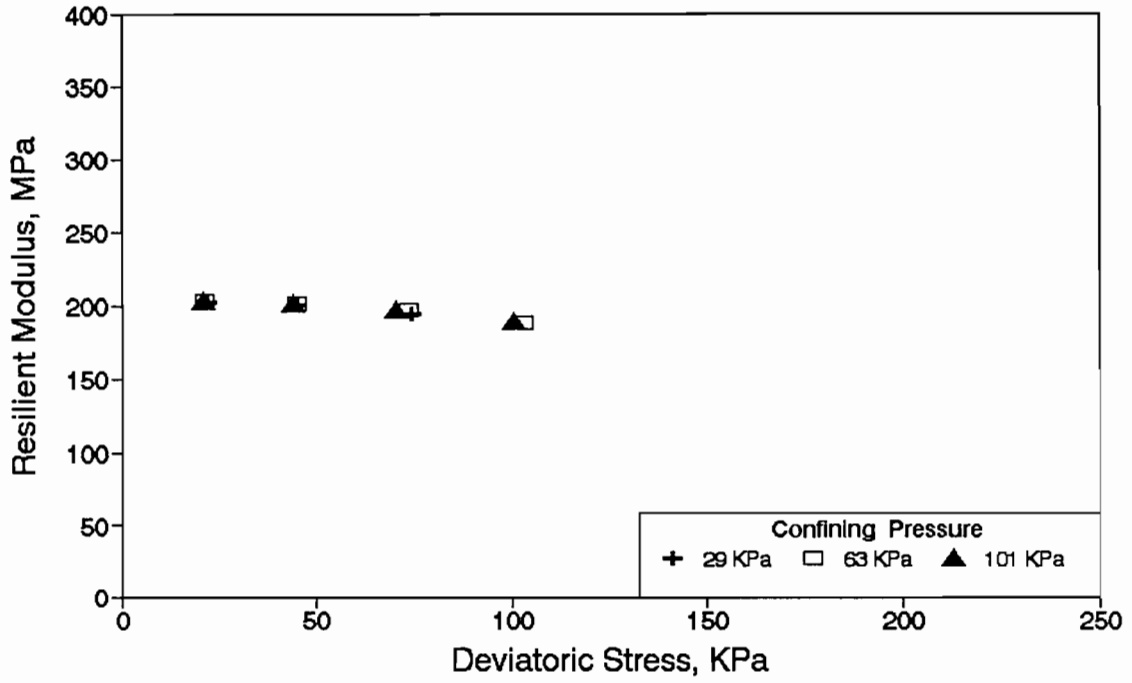

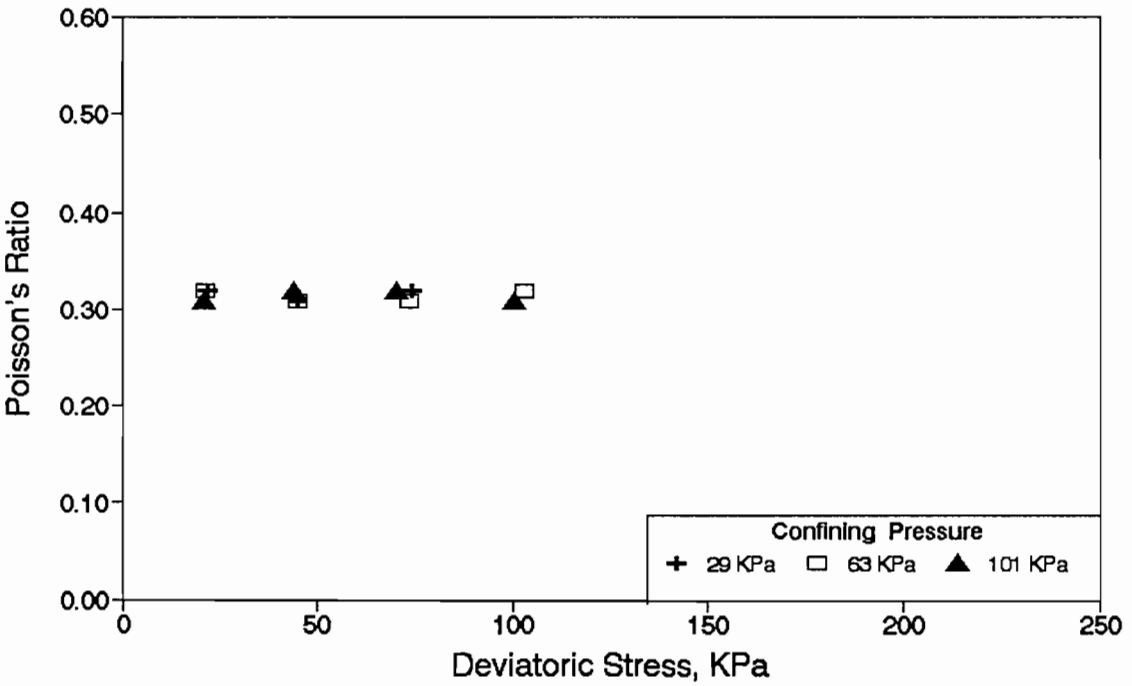

Specimen tested by Sriram

Data reduced and plotted by MRK Reddy

Odessa (District - 06)

Specimen No. 2 (Gage Length = 102 mm)

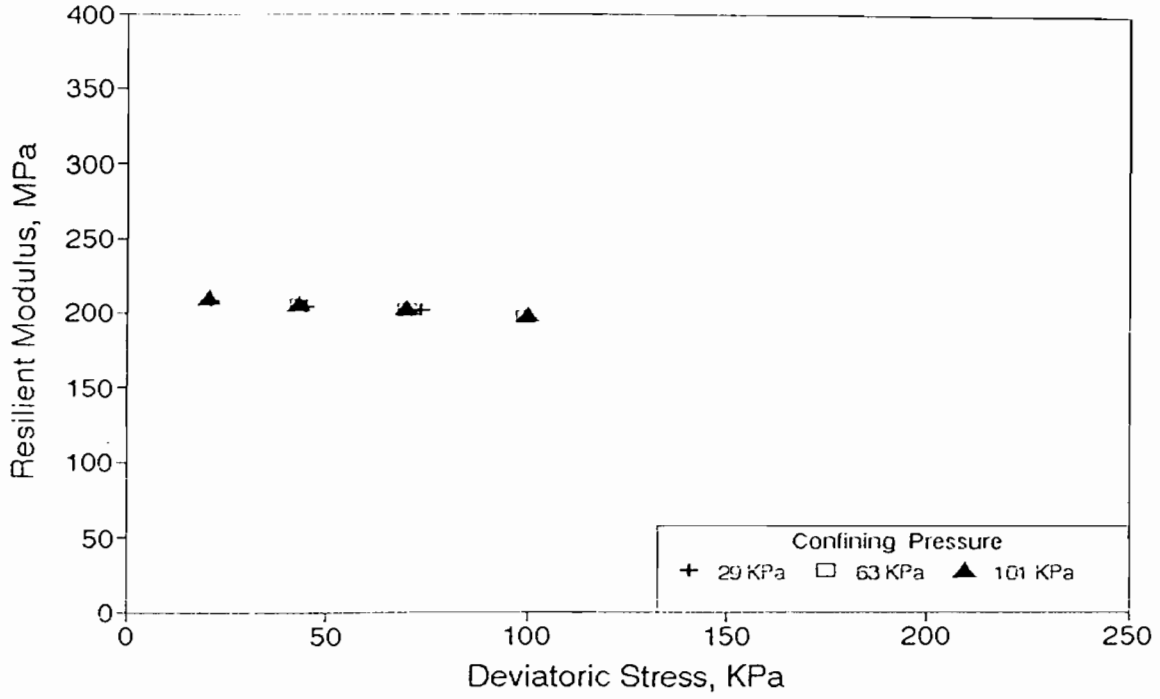

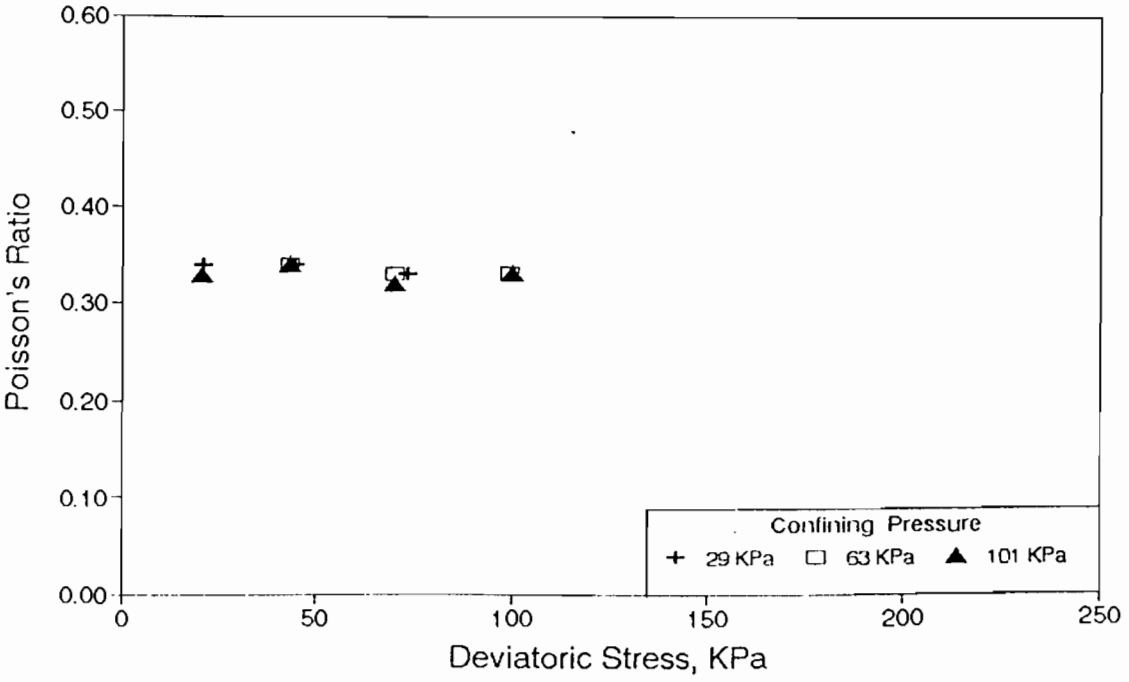

Project-1336/Specimen tested by Sriram/Data reduced and plotted by MRK Reddy

Odessa (District 06)

Specimen No: 1 Gage Length = 101mm Dry of OMC

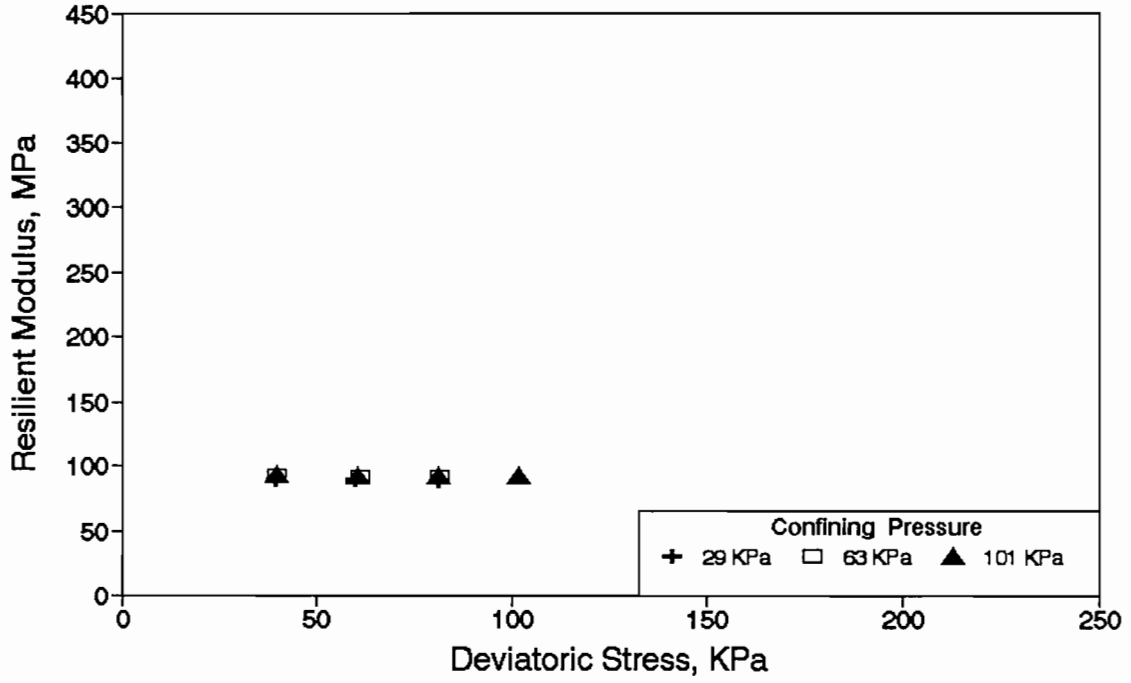

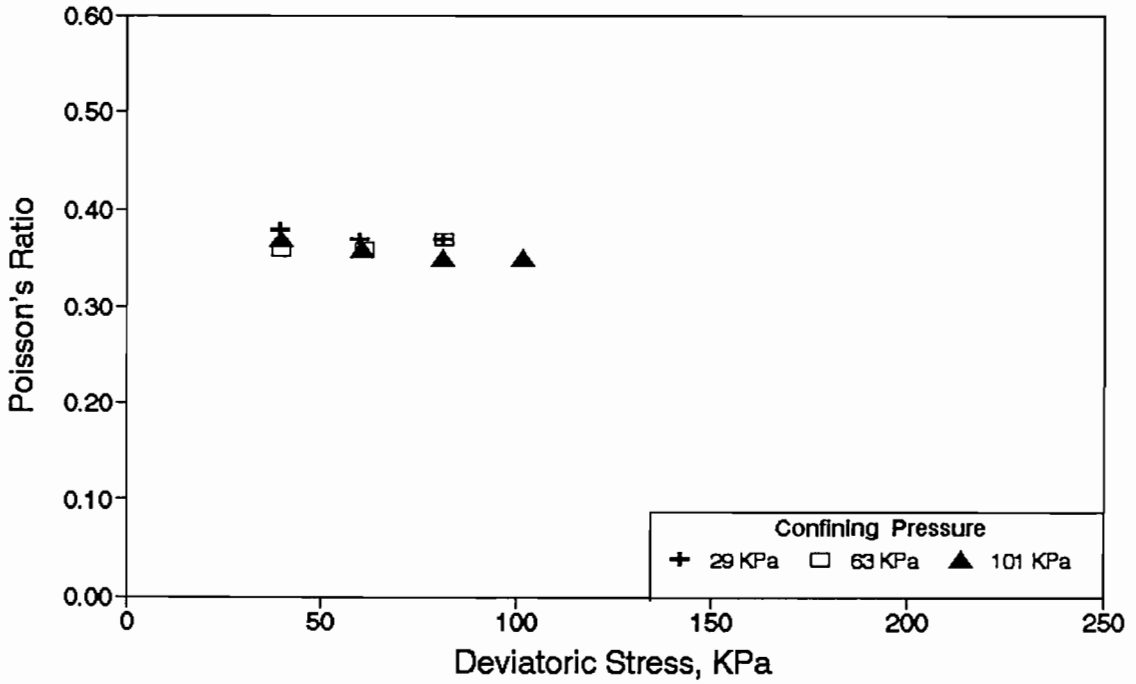

Project-1336/Specimen tested by Sriram/Data reduced and plotted by MRK Reddy

Odessa (District 06)

Specimen No: 2 Gage Length = 101mm Dry of OMC

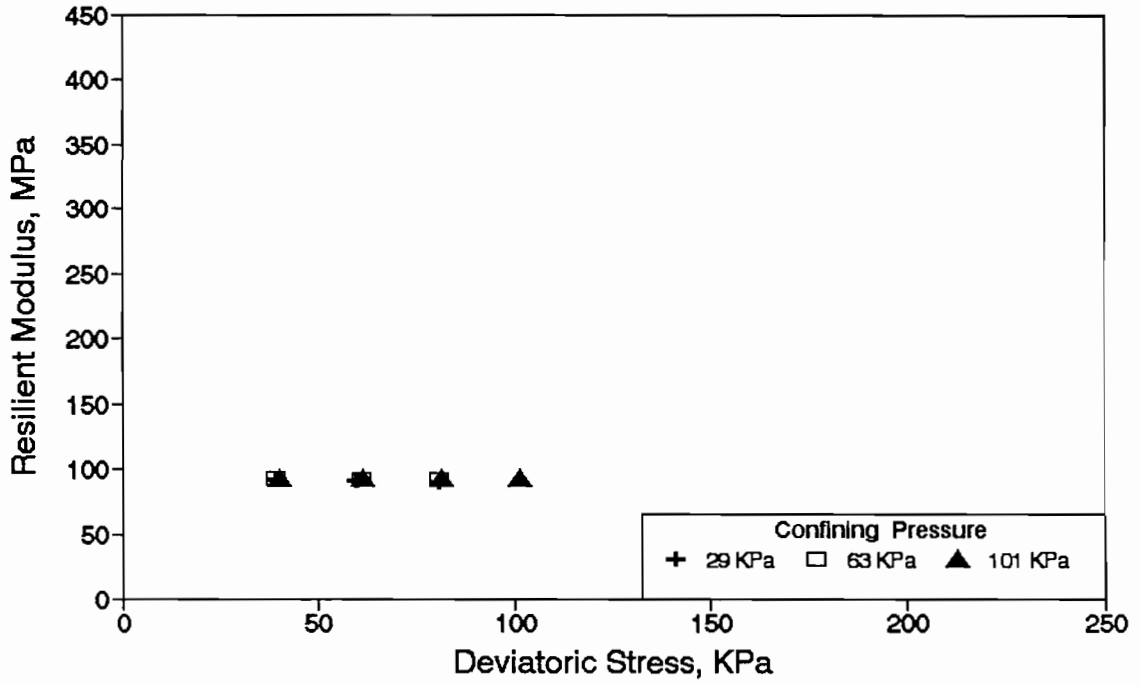

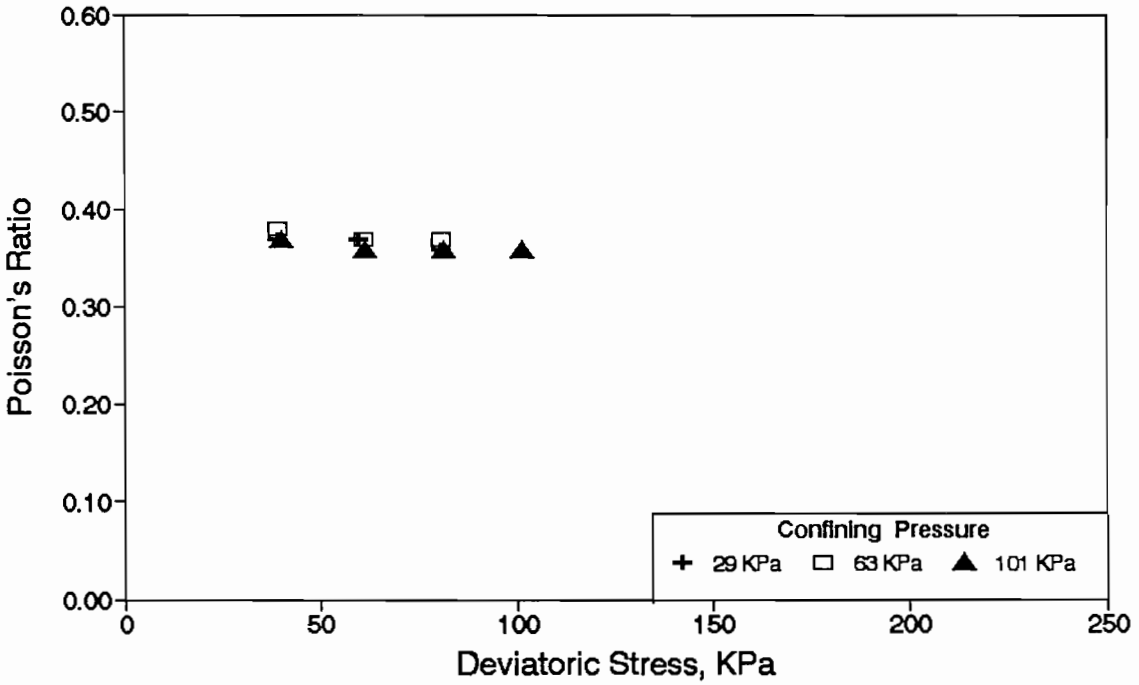

Odessa (District 06)

Specimen No: 1 Gage Length = 101mm Wet of OMC

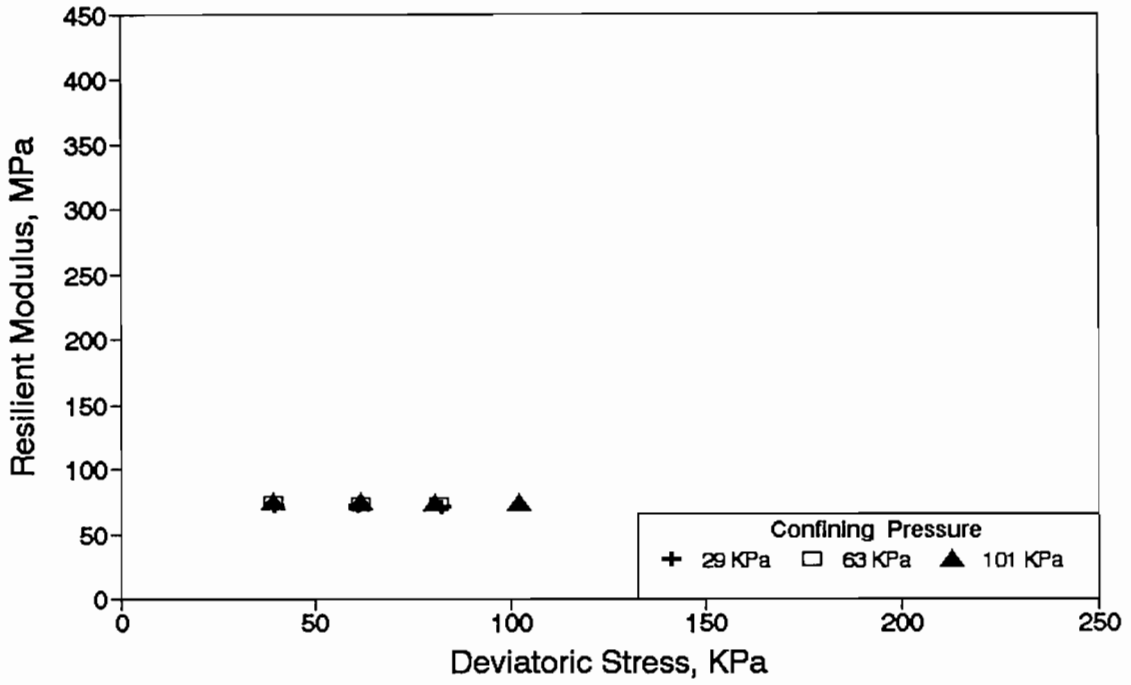

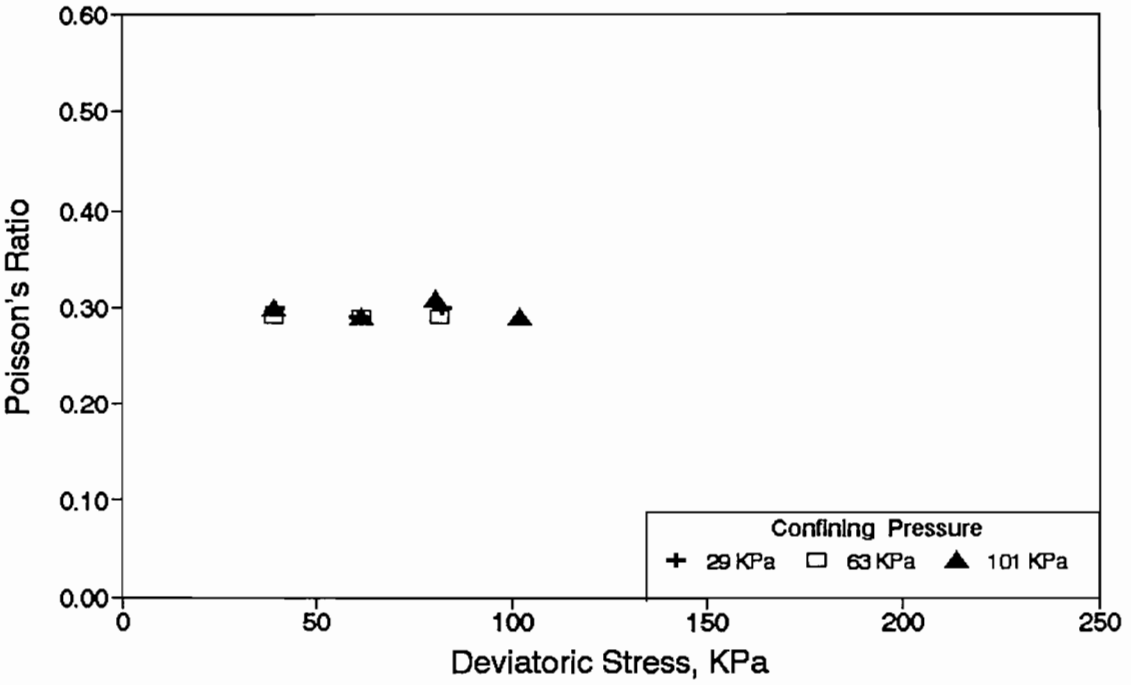

Project-1336/Specimen tested by Sriram/Data reduced and plotted by MRK Reddy

Odessa (District 06)

Specimen No: 2 Gage Length = 101mm Wet of OMC

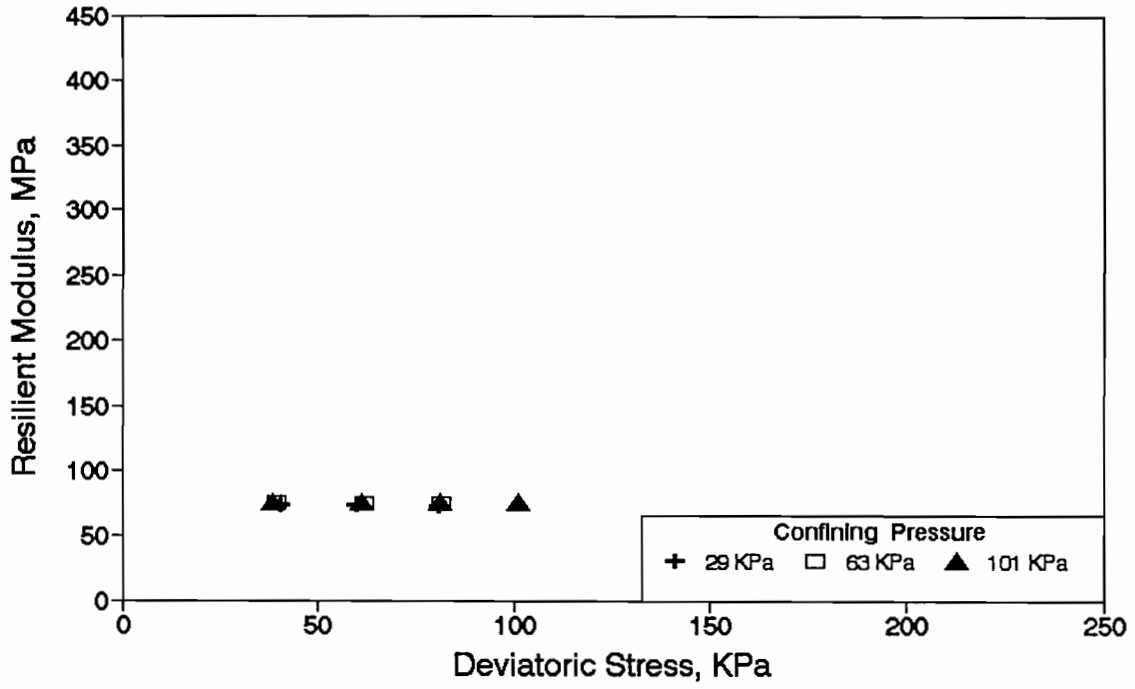

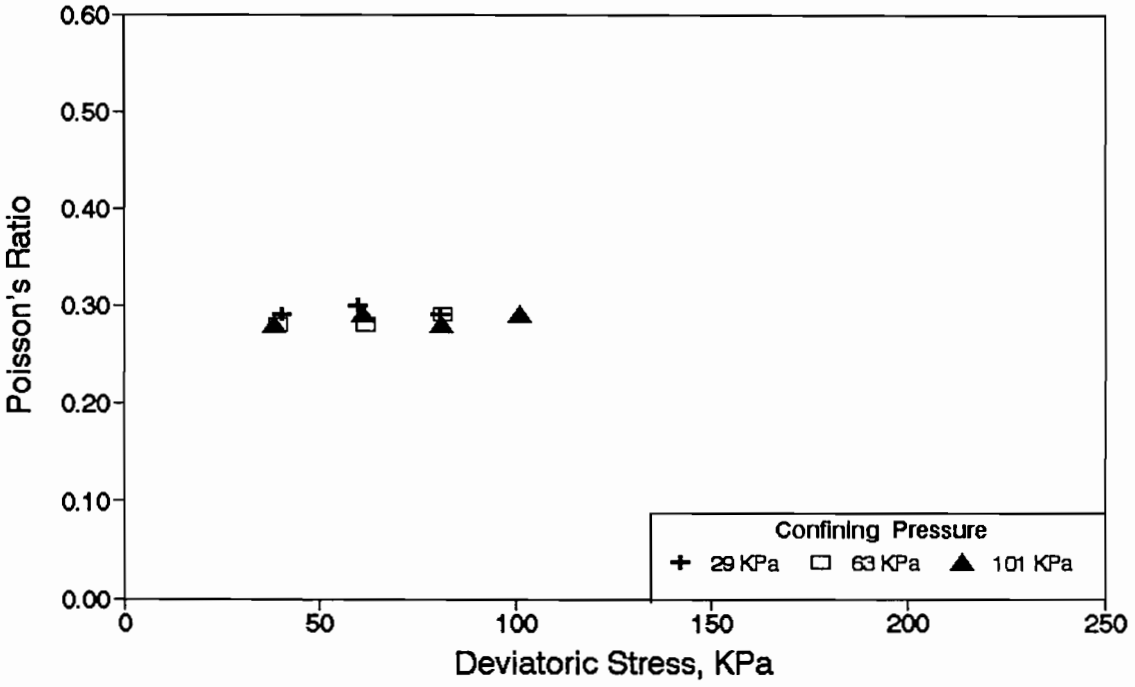

Project-1336/Specimen tested by Sriram/Data reduced and plotted by MRK Reddy